Impulse Measurements in Earthing Systems

by

Deepak Lathi

A Thesis submitted in partial fulfillment

of the requirements for the degree of

Doctor of Philosophy

November 2012

School of Engineering

Cardiff University

Acknowledgements

I am very much thankful to my supervisors, Prof. A. Haddad and Dr. H. Griffiths, for providing me an opportunity to work on this project. I am highly indebted to them, for their valuable guidance and encouragement during the course of this project.

My special thanks are due to Megger Ltd., for sponsoring this project and providing the earth tester and kit for use during the laboratory measurements and the field tests. I am grateful to Mr. Graham Heritage, Mr. Daniel Hammet and Mr. Clive Pink of Megger Ltd., for the useful discussions we had during the project progress meetings held at regular intervals.

I am highly obliged to Dr. Dongsheng Guo for his constant support during the laboratory measurements and the field tests. The fruitful discussions which I had with him all along the project duration helped me expedite to achieve the deliverables of the project. I am also thankful to Dr. Noureddine Harid for his valuable support during the experiments and useful discussions on the experimental results.

Last but not the least I would like to thank my wife Mitali, for her patience and continued support and motivation during my studies at Cardiff.

Impulse Measurements in Earthing Systems

Table of Contents

List of Figures

List of Tables

Abstract

The behaviour of earth electrodes at power frequency conditions is well known. Several studies are going on at present, to understand the behaviour of earthing systems at transient impulse and high frequency conditions. The study of impulse measurements in earthing systems was carried out during this project, to understand the soil electromagnetic behaviour towards high frequency and variable AC/DC/impulse current magnitudes. Several measurement techniques and instrumentation used for the measurement of the earthing systems were surveyed. The limitations and the advantages of each approach have been identified, and the range of application determined. Extensive experiments were performed on the practical earth electrodes at the Cardiff University test site at Llanrumney, and at the Dinorwig power station earthing facilities. These experiments have revealed that there is reduction of impedance of earth electrodes over the frequency range 20Hz to 120kHz. Moreover, a pronounced effect of DC current magnitude was observed on the earth resistance of the electrodes over the range of 1mA to 500mA. The numerical modelling of the test configurations did not show the reduction in earth impedance over the frequency range 20Hz to 120kHz. To understand the different trends shown by the experiments and simulation, and the effect of frequency and current magnitude, a geological literature survey was carried out. This survey revealed that when the soil water electrolyte solution is subjected to high frequency electrical currents, it exhibits conductivity dispersion phenomenon. Conductivity dispersion is a phenomenon where conductivity of the clay water electrolyte solution increases by about 30% over a frequency range 20Hz to 100kHz. The geological literature survey also revealed that the polarisation effect in the soil water electrolyte is responsible for the non-linear current effect.

Moreover, during this project, a new technique of FFT from impulse, was proposed to measure the earth electrode impedance, over a frequency range which is an inherent

component of the impulse signals. The FFT from impulse signals, showed a good agreement of the measured earth impedance of the earth electrodes, with the measured earth impedance using the variable frequency scan method. FFT from impulse technique has an advantage over the variable frequency scan method, from the point of view of the time required for the measurement and the simplicity of the test source, for the measurement of the earth electrode impedance. Such a technique, could have impact on the testing at high current magnitudes, where impulse generation is much easier. Finally, the future scope of work is presented to explore the measurement of earth electrode impedance above the frequency of 120kHz and current magnitudes above 5A.

Chapter 1: Introduction

Contributions of thesis

1. Surveyed the measurement techniques and instrumentation used for earthing systems measurements. The limitations and advantages of each approach have been identified and the range of application determined.
2. Variable frequency AC, DC and impulse tests have been conducted on several full scale earth electrodes at the University earthing test site at Llanrumney and the Dinorwig power station earthing test facility.
3. The extensive experimental data has been analysed and compared with numerical modelling of the test electrode configurations.
4. In particular, the measured earthing impedances of various electrodes were found to be frequency dependent, over the range 20Hz to 120kHz. The impedances of the practical earth electrodes reduced up to 30% when the frequency of injected current was increase from 20Hz to 120kHz. The effect of frequency was attributed to the conductivity dispersion phenomenon revealed by the geological literature survey. Furthermore, the measured earth electrode impedances were also found to be AC / DC current dependent for injected current magnitudes below 100mA, with a pronounced effect for DC currents. The current dependence was attributed to soil polarisation phenomena observed in the geological literature survey.
5. A new FFT analysis of impulse test data was proposed and applied in this work. Good agreement was obtained between the frequency dependence determined by the FFT approach and the results from the direct injection of variable frequency current. Such approach could have important significance for testing of high current magnitudes, where impulse generation is much easier.

1.1 Power system safety requirements

The demand for electrical power has been rising due to rapid economic development in the last century. In order to meet this increased demand, the size and capacity of power stations and substations continue to increase. This growth in capacity and greater interconnection has led to a continued increase in fault current levels. It is desired to have zero tolerance protection system for compact gas insulated substations which are characterised by fast transients and proximity to the public utilities. The tall wind power installations are prone to lightning strikes. The interconnected high and medium voltage power systems require limitation of the step, touch and transferred earth potentials to the permissible values. The high voltage transmission systems close to the public access areas demand heightened safety of equipment and personnel. The proximity of high voltage transmission systems to communication circuits demands very high reliability of power system protection. It is also important to limit the back flashover voltages during direct lightning strike. One of the key factors to provide the heightened safety and reliable means of protection lies in the efficient design and maintenance of low impedance earthing systems. The role of electrical earthing systems is also crucial in maintaining the continuity of service of the power supply. In the event of fault, the resulting high-magnitude currents have to be interrupted as fast as possible in order to protect the electrical equipment and personnel working in the vicinity. These conditions necessitate an efficient earthing system which helps with effective and fast discrimination of the fault currents from the load currents. Efficient earthing systems in co-ordination with the protective relays also help in discriminating the locations of the faulty zones and thereby isolating them effectively before the fault spreads to a wider area. The advanced electronic equipment installed for protection and control purpose in the modern power installations are susceptible to the dangers due to the rise of earth potential [1]. Effective earthing systems keep the rise of earth potential within safety limits. The

telecommunications circuits running adjacent to the power lines may get subjected to earth potential rise due to transferred earth potentials and thereby get damaged. If the earthing impedance is low, the earthing system will be able to absorb high currents without the earth potential rising to dangerously high levels during lightning strikes. If the earthing impedance is high, the lightning strike can cause back flashover directly involving a phase conductor. To obtain safety from direct lightning strikes, an essential aspect is to adopt adequate earthing system, with the eventual need for additional measures such as shielding and overvoltage limiting equipment. It is important to limit the current amplitude of lightning strikes incident in protected zones to be carried by the power circuits by appropriately diverting it to the earthing circuits. However, in the case of power system short circuit faults, the currents are inherently originating from the power circuits which will have to be interrupted by the protective relays in the shortest possible time period. Low impedance earthing systems help with faster determination of the fault currents by the protective relays which operate on the combination of sensing the rate of change of current with time and absolute magnitude of the fault current. The magnitude of earth impedance is an important performance indicator of the earthing system.

1.2 Human Safety

The tolerance of human beings subjected to shock scenarios depends on the amount of current passing through the human body, which in turn depends on the earth potential rise. Dalziel et al. [2, 3] and Beigelmeier et al. [4] suggested that the electric currents below 5mA can be safely conducted by human body. Electric currents above 5mA can cause effects on the human body depending on the individual weight, duration of exposure and magnitude of the current. However, electric currents above 200mA to 300mA for more than 1 second duration [4] can be severely harmful to human beings as it causes ventricular fibrillation

(heart muscles resulting in interference with rhythmic contractions of the ventricles and possibly leading to cardiac arrest).

1.3 Functions of Earthing system

Earthing systems are required to manage the transfer of fault energy in such a manner as to limit the risk to people, equipment and system operation to acceptable levels. An earthing system is required to perform this function for the life of the electrical network for which it is installed, for the range of configurations of the network and nearby infrastructure that are foreseeable. The earthing system may need to be augmented over time so as to continue to fulfil this function. The earthing system is required to limit the level of transient voltage and power frequency voltage impressed on electrical equipment. It is also required to provide appropriate current paths for fault energy in such a manner that those fault energies do not impair equipment or equipment operation. System events/disturbances may otherwise cause extensive damage to equipment and associated ancillary equipment such as insulation breakdown and thermal or mechanical damage from arcing, fires or explosions. The earthing system is required to ensure proper operation of protective devices such as protection relays and surge arresters to maintain system reliability within acceptable limits. It is intended to provide a potential reference for these devices and to limit the potential difference across these devices. The earthing system is required to achieve the desired level of system reliability through facilitating the proper and reliable operation of protection systems during earth faults. This entails reliable detection of earth faults and either clearing the fault or minimising the resulting fault current. In order to meet the foregoing operational requirements earthing systems need to be adequately robust and able to be monitored.
Robustness - The earthing system, its components and earthing conductors shall be capable of conducting the expected fault current or portion of the fault current which may be applicable and without exceeding material or equipment limitations for thermal and mechanical stresses.

Ongoing monitoring – The earthing system shall be designed and configured to enable the system to be tested at the time of commissioning and at regular intervals as required, and to enable cost effective monitoring of the key performance parameters and/or critical items.

1.4 Earthing System Safety requirements

The safe earthing system is expected to meet the following objectives,

a) Provide means to carry electric currents into the earth under normal operating conditions, fault conditions, switching transients and lightning strike without the rise of earth potential exceeding the safe limits and to maintain continuity of the service [5].
b) Provide safety of the operating personnel in the vicinity of the earthing system by limiting the amplitude of the step, touch and transferred earth potentials during power system fault conditions and transient phenomenon such as lightning.

A transmission line surge arrester conducts a lightning surge to a low impedance earthing systems to protect the surrounding insulators from the excessive flashover voltages which would have otherwise developed. It is desired that the earthing system provides least impedance path to the flow of lightning impulse currents, transient surge fault currents and power frequency fault currents to limit the rise of earth surface potentials within the permissible values. It is, therefore, required to study the behaviour of the earthing systems under these different conditions to predict its effectiveness. The impedance of an earthing system depends on various factors such as the soil resistivity and permittivity of the general mass of the earth carrying the surge currents, the geometry of the earthing electrode and the magnitude and wave front rise time of the current surge. The aging of earthing conductor system as a result of corrosive action of the soil also affects the impedance of earthing system. These aspects pose many challenges in designing an effective earthing system such as to cope with the seasonal changes in the resistivity of soil and the aging effects due to

corrosion properties of various soil will have to be adequately predicted during the design phase. In addition to verifying the design of earthing systems at new stations to meet the requirements, the adequacy of the earthing system performance at existing stations, especially at the very old stations where the earthing grid design is unknown, has to be monitored periodically to ascertain its efficiency.

Lightning protection of transmission lines has attracted a lot of attention of electrical engineers in the past. Initial efforts were in the direction of reducing the induced voltages due to lightning strike on the transmission lines. But later on, it was observed that it was the direct lightning strike which resulted in outages of high voltage power transmission circuits. Efforts were then made to shield the overhead open wires with an earth wire running on the top of the transmission towers. Lightning earths are expected to have least possible impedance to high frequency currents. Lightning surge characteristics of an earthing system have an influence on electromagnetic transient behaviours in low-voltage and control circuits. The lightning surge phenomena are important factors for determining the insulation level of the power transmission equipment. Hideki Motoyama [12] conducted experiments on earth mesh to evaluate the lightning surge characteristics by analysis of transient potential rise at various points in the earth mesh. The theoretical analysis of lightning surge characteristics by Sunde [13] is well known. The soil resistivity ρ and the electric permittivity ε are frequency dependant [14]. The magnetic permeability μ is in general equal to permeability of free space μ_0. Power transmission line earthing systems are usually assumed as extended earthing systems. Leonid Grcev [15] observed that the propagation effects are dominant in early time in the extended earthing systems, when the earthing systems are subjected to fast front lightning currents. He analysed the dynamic behaviour of such earthing systems taking into consideration the propagation effects. The wavelength of the electromagnetic wave in the soil depends on the soil resistivity. Therefore, the classification of the earthing systems as

concentrated or extended may be quite different in different soils for a particular current impulse.

The first strike of a lightning surge is characterised by the frequency components in the range of few tens of kHz to few hundreds of kHz. Similar-frequency currents exist in switching transients. The frequencies of the order of few MHz are present in the subsequent return strokes of a lightning surge. These phenomena were the motivation behind studying the behaviour of the earthing systems over a high frequency range. Most of the commercial earth resistance testers measure earthing resistance by injecting switched DC signals into the earth electrode. This resistance is an estimate for predicting the behaviour of the earthing system under power frequency conditions. However, the behaviour of earthing systems during lightning strike or transient faults is considerably different from that at power frequency and low currents.

1.5 Recent trends in earthing impedance measurement

Conventional instruments generally inject switched DC signals at low frequency (typically 128 Hz) to measure the resistance of the earthing system. However, in case of the large earthing systems, the DC resistance is quite low while the inductive reactance is generally higher in magnitude, so it becomes relevant to measure the impedance of the earthing system. The measurement of impedance of the large earthing system requires injection of the AC currents at the frequencies close to the power frequencies. On the other hand, if a spectrum of transient surges and lightning surges is observed, then it reveals various components of low and high frequencies. High frequency components are a result of the fast rising wave fronts and the low frequency components are contributed by the wave tail of the surges. In order for the earthing system to be effective, it should be able to control the earth potential rise during the absorption of the power frequency fault currents as well as transient frequency surges.

The impulse behaviour of the wire-type electrodes, buried horizontally, differ quite markedly depending on whether or not electrode length is negligible, in comparison with wavelength of transient phenomena. The distinction between the concentrated and extended electrodes is based on the importance of the inductance terms compared with the resistance terms. Therefore, besides considering the maximum slope of the impulse current front, it is necessary to consider soil resistivity too, because if the soil resistivity is high, it results in increase in resistive drop in relation to the inductive drop. Mazetti et al. [41] presented a mathematical model to analyse the transient behaviour of buried earth wire when fed at one side by an impulse current similar to a lightning stroke. In case of a lightning strike, the earthing has to absorb the lightning energy in a very short duration [30]. Considering that the flow of current (electrons) is at the speed of light, a 0.2 μs rise time (wave front) of lightning restrike phenomenon will result in the length of lightning current flow up to 30 meters (speed of light x rise time) by the time wave front is over. So, a 30 meter rule is being used in the Lightning earthing systems, which shows that the effective length of a lightning earthing system is up to 30 meters, indicating that the earthing system beyond this point will not play any role in absorbing the energy of a lightning restrike. Injecting various frequency current waveforms in the earthing system and analysing the response of earthing to these waveforms provides an order of magnitude impedance of the earthing system over a range of various frequencies. Previous studies [6, 7] have indicated that the behaviour of earthing systems excited by lightning impulse and phase to earth faults considerably differ from that of low frequency injection. Jong-kee et al. [33] experimentally measured the earth impedance of mesh type earth grid in the frequency range from 0.1 Hz to several hundred kHz. The published studies of the transient behaviour of earth electrodes of various forms (horizontal wires, vertical rods and mesh networks) from the theoretical [34-37] or experimental [38-40] point of view helped in improving the knowledge of performance of earthing systems in

lightning conditions. Leonid Grcev and Markus Heimbach [6] did transient analysis of large earthing systems to study the influence of soil resistivity, location of feed point, grid size, depth, conductor separation, earth rods and shape of the lightning current impulse, on the transient performance of earth grids of different sizes.

Rong Zeng et al. [8] developed a new method of measuring earth impedance. According to the theoretical analysis carried out by them, it is proposed that there lies a fixed voltage electrode position between the earth electrode and current electrode position in fall of potential method irrespective of the length of the current electrode from the earth electrode. Based on this analysis they proposed to calculate this position which they named as a compensating position of the potential electrode with the help of a computer programme. Following inputs are required for their programme such as soil resistivity data of various locations in the vicinity of earthing system, earthing system topology, length of current electrode from the earth electrode. The resulting potential distribution profile gives guidance on where the potential probe should be placed, so as to get the value of the true earth resistance. Griffiths et al. [32] used the Lock-in amplifier technique to inject variable frequency signal in the earthing system under test. From the experiments, they found out that injecting the frequencies of 48 Hz and 52 Hz gives the least effect of background noise at a power frequency of 50 Hz. They successfully tested the earthing impedance measurement system based on lock in amplifiers on different substations and transmission environments. Rong Zeng et al. [8] used the swept frequency method to measure the impedance of earthing systems. In their system, the effect of noise at power frequency was eliminated by measuring the impedances at several different frequencies other than the power frequency and then interpolating the earth impedance at the power frequency. The earth impedance was measured over a frequency range of 30Hz to 100Hz and the earth impedance at power frequency was interpolated from these measurements. They [8] used software to evaluate the

compensating position of the voltage electrode by analyzing the soil structure, earthing system and the position of the current electrode.

CIGRE Working Group C4.2.02 [69] showed that the variable high frequency method, used with a strict operational method, or the use of a classical earth tester with a ring current transformer to measure the injected current, appear to be the most accurate methods for making measurements on towers with earth wires, especially on towers which have a high value of earth resistance or are very close to a substation. However, for most towers in a line the widely used method based on the injection of a high frequency current gives sufficient accuracy, taking into account the limitations for towers located very close to a substation.

1.6 Objectives of the project on impulse measurements in the earthing system

The project on impulse measurements on earthing systems aimed at characterising the earthing systems at higher frequencies. The behaviour of earthing systems under the power frequency conditions has been extensively studied in the past. The behaviour of the earthing systems under the lightning frequency and transient surge conditions is of interest in this project to devise new techniques of measuring the impulse earth impedance to predict the behaviour of the earthing systems under high frequency conditions. Megger and Cardiff University jointly funded this project with a view to develop earthing measurement techniques for impulse conditions. In this context, at the start of this project a survey of recent trends in earthing measurement techniques and impulse behaviour of earthing systems was carried out.

1.7 Thesis Outline

This chapter outlined the importance of earthing systems in the power installations and summarized the interest of the researchers in measuring the earthing impedance to lightning and surge currents.

Chapter 2 deals with the literature survey performed to assess the present trends in earthing impedance measurement techniques. Different methods of measurement of earth impedance are discussed in Chapter 2 with a view to understand the applicability of the earthing measurement techniques to various earthing systems such as concentrated and distributed earthing systems. Subsequently, the comparative analysis of the capability and limitations of the commercially available instruments for measuring earth impedance / resistance is presented.

Chapter 3 outlines the determination of the accuracy of the voltage and current transducers used in the field tests and preliminary laboratory tests performed to calibrate the transducers with the standard resistance. The soil sample impedance and electrolyte water solution impedance measurements made with the AC / DC and variable frequency sources are also reported in Chapter 3.

Chapter 4 describes the test sites and earthing set-ups available at two experimental test sites. The reason for the selection of the Dinorwig test site is explained in Chapter 4 with a view to perform the earthing measurement tests in the uniform resistivity conditions so as to compare with the simulation results. The overview of the Cardiff University Impedance Measurement System, Impulse Generator, RF Generator, Megger make DET 2/2, DET 4TC DC resistance testers and ABEM LUND resistivity measurement systems is provided to introduce the sources used during the field tests of earthing systems. The soil resistivity surveys performed at Llanrumney test site are discussed in details in Chapter 4.

The measurements carried out on various earthing systems at the two test sites are presented in Chapter 5. The core contribution of this thesis is given in Chapter 5. A series of earthing

measurement tests performed during this project are discussed in details along with the test set-up. The test results are discussed at length for each experiment. The effect of current magnitude and frequency on the impedance of earthing systems are elaborated with the experimental observations.

Chapter 6 presents the comparison of the experimental results with the simulations performed on the test set-ups and geometry of the earthing systems represented in the CDEGS software. The soil resistivity obtained from the soil resistivity surveys was used in the CDEGS modelling to predict the earthing impedance. The differences in the experimental and simulation results for the non-homogenous soil conditions are discussed in Chapter 6. The effect of current magnitude and the frequency on the measured earth impedance observed in the field was not displayed by the modelling of earth electrode configurations. Reasons for this difference are discussed in Chapter 6.

Chapter 7 provides the survey of geo-physics literature where the effect of current magnitude and frequency is observed on the resistivity of the soil. The analysis of the geo-physical literature provides an insight into the experimentally observed phenomenon of variation of the earthing impedance with the current magnitude and frequency of the injected signal. The soil electromagnetic behaviour is discussed in Chapter 7.

Chapter 8 presents the conclusions derived from the present project and proposes the feasibility of the different techniques for the impulse measurements in the earthing systems. The advantages and limitations of different impulse measurement techniques are presented in Chapter 8. Finally suggestions for future work are presented.

Chapter 2: Literature review of earthing measurement techniques

This chapter comprises literature review on earthing measurement techniques, a comparative study of commercially available earth testers and detailed description of smart ground meter (SGM) developed by EPRI and recent trends in earthing impedance measurements for power frequency and impulse conditions.

2.1 Introduction

Three phase power systems are earthed by connecting one or more selected neutral points to buried earth electrode systems. Such earths are referred to as system earths. According to the way the neutral is connected to the earth, electrode systems are categorised as solidly earthed or impedance earthed. Impedance earthed systems can be classified as resistance, reactance or resonant types. In the UK power system, solid earthing has been adopted on networks operating at 66 kV up to 400 kV [16]. At the transmission level 275 kV / 400 kV, the power system is multiple earthed and is operated as a mesh system. This practice reduces transformer capital costs, where graded insulation can be used and surge arresters of lower temporary over-voltage rating can be employed. At voltage levels from 6.6 kV to 66 kV, the system is normally radial configured and earthed at a single point corresponding to the neutral or derived neutral of the supply transformer. On networks at 33 kV and below, low resistance earthing is used. Reactance earthing and resonant earthing have the disadvantage of high transient over voltages and hence are rarely used. A system is classified as effectively earthed when the single phase to earth fault current is more than or equal to 60 % of the magnitude of three phase short circuit current. Generally, when the earth impedance value is greater than 1 Ω the reactive component of the impedance may be negligible, and the earth impedance can be termed as earth resistance. However, this may not be the case always as for

example the chain earth impedance of the towers for high voltage overhead lines may have earth impedance value greater than 1 Ω and simultaneously have a significant value of the reactive component. In other words, it may be considered that for the concentrated earthing systems if the earth impedance is greater than 1 Ω then it can be safely treated that the reactive component of the earthing impedance is negligible and the earth impedance is mainly contributed by the earth resistance. The reactive component is generally taken into account when ohmic value of the earthing under test is less than 0.5 Ω.

Usually the approach to building an earthing installation for a power station or substation is 'do what they did last time' [31]. It has been observed that the old earthing installations may not be adequate enough to handle high fault currents or not sufficiently robust and configured to maintain the safety of the power system. As continuous monitoring of the earthing systems is not always feasible, the deterioration in the earthing system over time may go unnoticed. This fact demands extra care during design and installation stages. Periodical measurement of earthing system performance is required by ENATS 41-24 to account for the seasonal changes as well as the operational integrity.

2.2 Methods of measurement of earth impedance

The impedance of an earthing system is usually determined with alternating current of power frequency to avoid possible polarization effects when using direct current [5]. When the power frequency current is injected into the earthing system under test, care has to be taken to avoid the interference in measurement system due to the power system leakage currents. It is generally considered to inject the current signal at the frequency close to the power frequency such as either close to 48Hz or 52Hz but not exactly at 50Hz (when the power system frequency is 50Hz) to avoid the power frequency signal interference which can distort the measurement results. Commercially available earth testers tend to inject the switched DC

signal at a frequency of 96Hz to 128Hz to avoid the interference with the fundamental component and the third harmonic component of the power frequency signals of 50Hz or 60Hz power system frequency.

The generally used methods for measurement of earthing resistance as described by various authors [10], [18], [20], [23], [25] are fall of potential method, two-point method, three-point method, ratio method, staged fault test, single clamp earth resistance testing, double clamp earth resistance testing and attached rod technique. These methods are briefly described in the following text. The three point method and the ratio method are derived from the analytical calculations related to the fall of potential theory. The two point method and clamp method of measuring earth resistance should be limited to small earthing systems. It should be noted that the measured ohmic value is called resistance. However, when the measured ohmic value of the resistance is generally less than 0.5Ω, there is a reactive component that should be taken into account if the earthing system is of a relatively large extent.

2.2.1 Fall of potential method

This method involves passing a current in the earth electrode whose resistance is to be measured and recording the influence of this current in terms of potential between the earth electrode under test and an electrode P as shown in the Figure 2.1. Prior to the conduction of the fall of potential test, the earth electrode may be disconnected if possible from the system to which it is providing protection. However, the fall of potential method of measuring earth impedance can also be carried out with the earth electrode connected to the power system provided that the earth leakage current from the power system is measured appropriately. As shown in the Figure 2.1, current ‘I’ is passed through the test electrode E and the current electrode C.

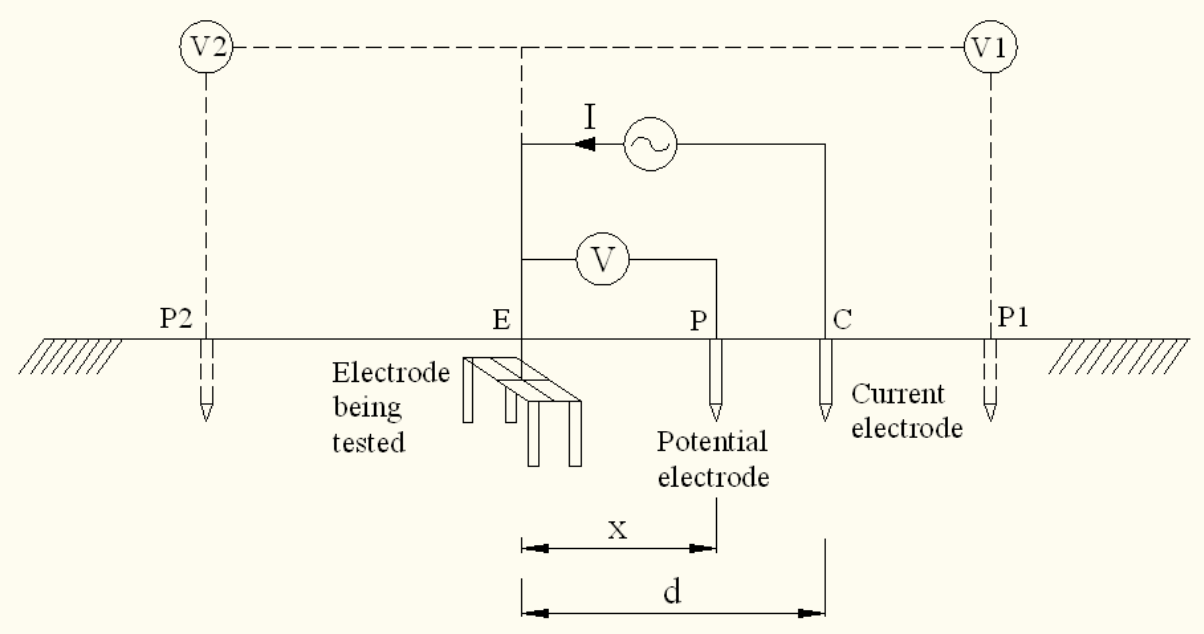

Figure 2.1 Typical set up of fall of potential test

This causes distribution of earth surface potential along the surface of the earth. The earth surface potential profile along the electrodes C, P and E will have a curve as shown in the Figure 2.2. Potential is measured with respect to the earth test electrode E. The ratio of V / I = R (apparent resistance) is then plotted as a function of probe spacing. The potential electrode is gradually moved away from the electrode under test in steps. A value of resistance is obtained at each step. This resistance is plotted as a function of distance, and the value in ohms at which this plotted curve appears to level out is taken as the true resistance value of the earthing system under test. In order to obtain a flat portion of the curve, it is necessary for the current electrode to be placed outside the influence of the earth to be tested as shown in Figure 2.2. For large earthing systems, the spacing required may be impracticable and other methods of interpretation can be used. A theoretical analysis of the fall of potential technique [18] shows that placement of potential probe P at the opposite side with respect to electrode C i.e. (P_2) will always result in a smaller measured apparent resistance compared with the true resistance.

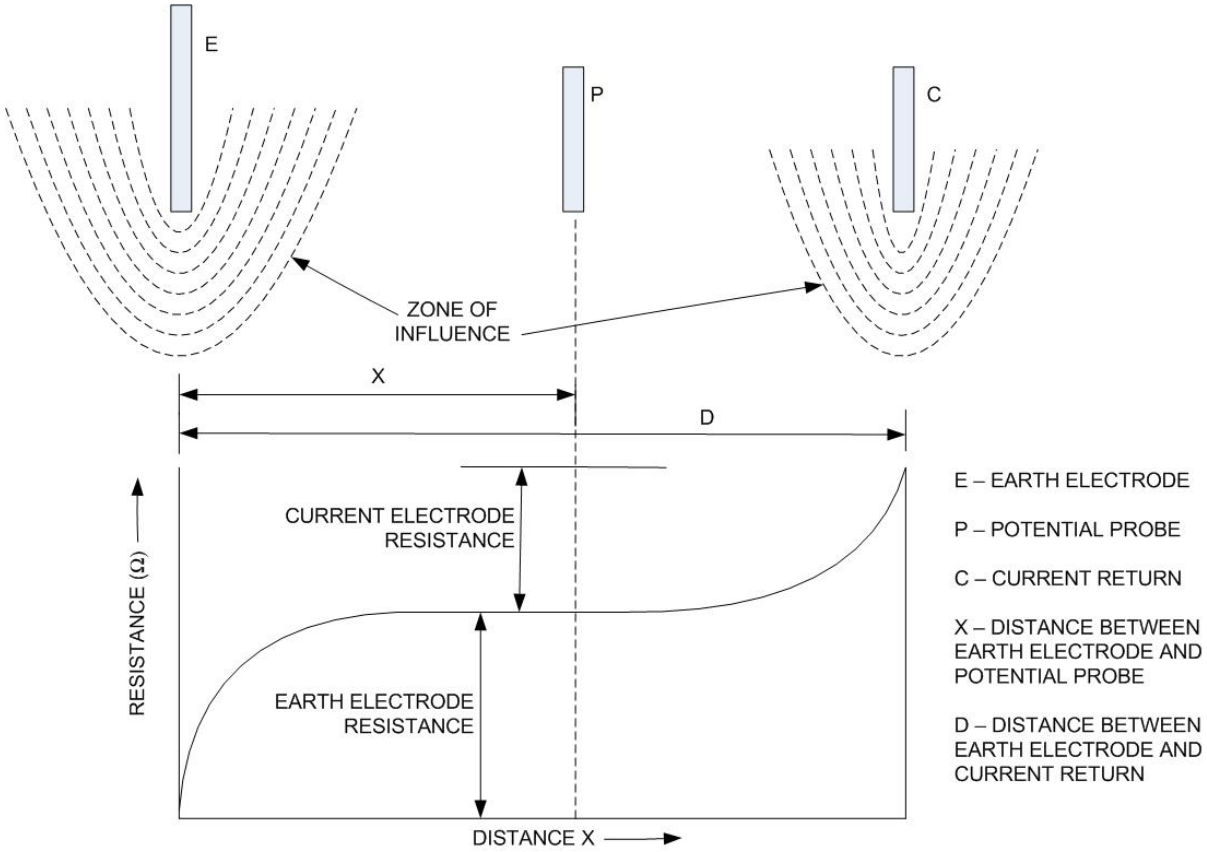

Figure 2.2 Fall of potential profiles

However, the arrangement of P_2 as shown in Figure 2.1 has the advantage of reducing the mutual coupling between test leads. If reasonably large distances between P_2 and C are achieved (with respect to the electrode E under test), then according to [19] it is possible to use this method to obtain a lower limit for the true resistance of electrode E. When P is located on the same side as electrode C and away from it (P_1), there is a particular location which gives the true resistance.

The correct spacing may be very difficult to determine, especially if the earth grid has complex shape [19]. The correct spacing is also a function of soil configuration [21]. The required potential probe spacing x when the probe is between E and C and when the soil is uniform, is such that the ratio x/d = 0.618. This was first proved by E.B. Curdts [20] for small hemispherical electrodes. From the above statements, it is clear that the following conditions should be met to apply the 61.8 % rule.

- The soil has to be uniform
- A large spacing should be maintained between the electrodes E and C

The reference origin for the measurement of spacing must be determined. For large earthing systems, some authors introduced the concept of electrical centre and the method of determining the impedance of extensive earth systems embedded in uniform soils is described in a paper by Tagg [23]. It should be noted, however, that there is no proof that the electrical centre is a physical constant (such as a centre of gravity) which is not influenced by current electrode location and its characteristics.

2.2.2 Two-point method

In this method as shown in Figure 2.3, the total resistance of the unknown and an auxiliary earth are measured [11].

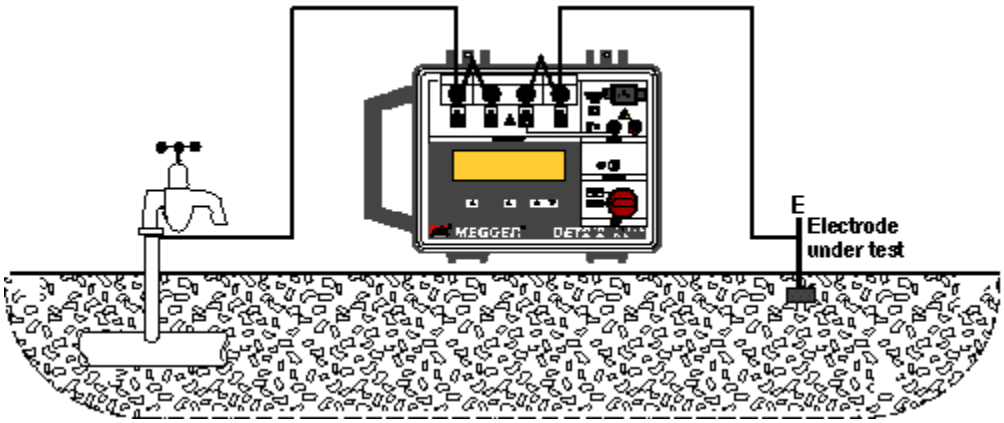

Figure 2.3 Two-point method [11]

This method is generally used to measure the resistance of a single rod driven earth which has metallic water pipes in close vicinity and which can be used as an auxiliary earth. The earth resistance of metallic water pipes without insulating joints is assumed to be of the order of 1 Ω which is low in relation to the driven earth resistance which is usually of the order of 25 Ω. The resistance of the auxiliary earth (metallic water pipes) is assumed to be negligible in comparison with the resistance of the unknown earth, and the measured value of the resistance is taken as the resistance of the unknown earth. This method is not suitable for low

resistance earths. This method can be used for driven earths where a rough estimate of earth resistance is required.

2.2.3 Three point method

This method [11] involves the use of two test electrodes with the resistance of the test electrodes taken as R_2 and R_3. The resistance of the earth electrode under test is taken as R_1. The resistance between each pair of electrodes is measured and designated as follows

R_{12} – Resistance between earth electrode and test electrode 1

R_{13} – Resistance between earth electrode and test electrode 2

R_{23} – Resistance between test electrode 1 and test electrode 2

We know

$$R_{12} = R_1 + R_2 \quad \text{---------} \ (2.1)$$

$$R_{13} = R_1 + R_3 \quad \text{---------} \ (2.2)$$

$$R_{23} = R_2 + R_3 \quad \text{---------} \ (2.3)$$

Solving the simultaneous equations, (2.1), (2.2) and (2.3) we get

$$R_1 = \frac{R_{12} + R_{13} - R_{23}}{2} \quad \text{--------} \ (2.4)$$

Thus, by measuring the series resistances of each pair of earth electrodes and substituting the resistance values in to (2.4), the value of earth resistance can be calculated. If the magnitude of the resistance of two test electrodes is comparatively higher than the earth electrode, then this method will not give accurate results. The spacing of the test electrodes for driven earths should be more than 5 meters. This method is not suitable for large area earthing systems [11].

2.2.4 Ratio method

In this method [11], the resistance of the electrode under test is compared with a known resistance, usually by using the same electrode configuration as in the Fall of Potential Method. As this method is a comparison method, the ohmic readings are independent of the test current magnitude. The test current magnitude can be kept high enough (few tens of milli-amps) to give adequate sensitivity.

2.2.5 Staged fault test

The most representative measurement of the earth impedance of an installation is the staged fault test [11]. This test produces realistic fault current magnitudes and by using the remote voltage reference the rise of earth potential and earth impedance can be calculated. The staged fault test is seldom performed due to economic penalties and the system operational constraints. Staged high current tests may be required for those cases where specific information such as the integrity of the earthing system is desired on particular earthing installation.

2.2.6 Single clamp earth resistance testing method

In this method [24], the auxiliary test probes for injecting current and measuring the voltages are not needed when measuring the earth resistance. Earth resistance can be measured without disconnecting the connections between the earthed body and the metal work of the electrical plant. This means that there is no need to turn off the equipment power or disconnect the earth rod. The clamp-on methodology is based on Ohm's Law (R=V/I). Figure 2.4 shows the typical set-up of the clamp-on earth tester.

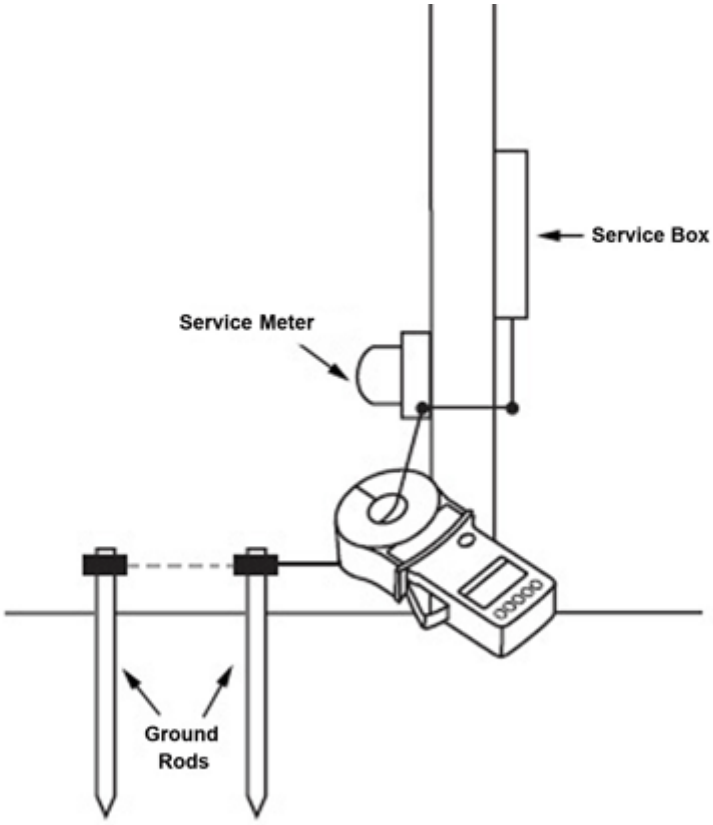

Figure 2.4 Clamp on earth resistance testing

A known voltage is inductively applied to a complete circuit with the help of the source coil inside the clamp of the earth tester inducing the voltage. The resulting current flow in the earthing circuit due to the induced voltage is measured by the current coil installed in the same clamp of the earth tester. The resistance of the circuit can then be calculated by taking the ratio of the induced voltage and the circulated current in the earthing circuit. It has to be ensured that the earthing system under test is included in the current circulation loop. The clamp-on earth tester measures the resistance of the path traversed by the induced current. All elements of the loop are measured in series. This method assumes that only the resistance of the earthing system under test contributes significantly.

According to the manufacturer (Megger), this method has the following disadvantages,

- If the frequency of AC current injected into the earth by the tester happens to be of the same as that of disturbance current in the earth, then the accuracy of the readings are seriously affected.

- The mutual inductance between the voltage and current loops of the clamp tester has some effect on the measurement accuracy.
- The clamp-on method is only effective in situations with multiple earthing electrodes are in parallel and a closed circuit is available for the current circulation. It cannot be used on isolated grounds, as there is no return path, thus making it in-applicable for installation checks or commissioning new sites.
- Measurement of low earth resistance of the order of 0.5 Ω is difficult with this method.
- The internal diameter of the clamp is usually small of the order of 25 mm which prevents the measurement of earth rods greater in size.

2.2.7 Double clamp earth resistance online tester [25]

This method is slightly different to the single clamp earth resistance measurement method in the sense that it uses two separate clamps instead of one to avoid the effect of mutual coupling between the two coils installed in the same clamp. This system can be used without isolating the earth conductor or turning off the power. The tester uses a variable low frequency AC voltage generator, two separate clamps [25] for voltage and current. Figure 2.5 shows the double clamp online earth tester.

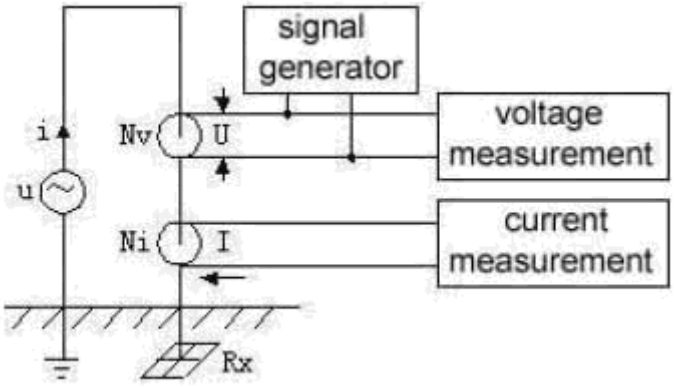

Figure 2.5 Double clamp online earth tester [25]

The frequency of injected current can be automatically adjusted so as to eliminate the effects of earth disturbance current frequency. As shown in Figure 2.5, 'V' is the voltage applied to the voltage clamp by the signal generator. By electromagnetic induction, voltage 'v' will be induced in the earth loop. This voltage is given by the equation

$$v = \frac{V}{N_v} \quad \text{--------- (2.5)}$$

Where N_v is the number of turns on the voltage clamp.

The induced voltage 'v' produces an electric current 'i' in the earth loop. This current is given by the equation

$$i = \frac{v}{R_x} \quad \text{--------- (2.6)}$$

where R_x is the Resistance of the earth path.

The current measured by the current clamp can be expressed as $I = \frac{i}{N_i}$

Where N_i is the number of turns on the current coil.

We know $R_x = \frac{v}{i}$ --------- (2.7)

$$R_x = \frac{V / N_v}{I \times N_i} \quad \text{--------- (2.8)}$$

$$R_x = \frac{V}{I \times N_v \times N_i} \quad \text{--------- (2.9)}$$

If the value of N_v and N_i are set as 1, then the earth resistance can be worked out as

$$R_x = \frac{V}{I} \quad \text{--------- (2.10)}$$

In order to improve the anti-interference ability of the tester, the frequency of the AC voltage produced is kept variable and typically can be chosen automatically from four values as 94

Hz, 105 Hz, 111 Hz and 128 Hz. These frequencies avoid the interference from the fundamental power frequencies of 50Hz or 60Hz and their third harmonics.

2.2.8 Attached rod technique (ART) by Megger [24]

The Attached Rod Technique (ART) method of testing [24] provides some of the advantages of clamp-on testing (not having to disconnect the ground electrode) while remaining true to the theory and methodology of fall-of potential testing. A fall-of-potential measurement can be made without disconnecting the ground electrode if additional measurements were made with an earth leakage clamp meter (milliamp meter). In case of an interconnected earthing system if the fall of potential test is carried out, it will measure the effective resistance of the interconnected earthing systems. If the earthing resistance of the individual earthing system is of interest, then it is necessary to know the current carried by the individual earthing system during the test conditions. This is accomplished with an additional clamp-on meter used in the ART as shown in Figure 2.6.

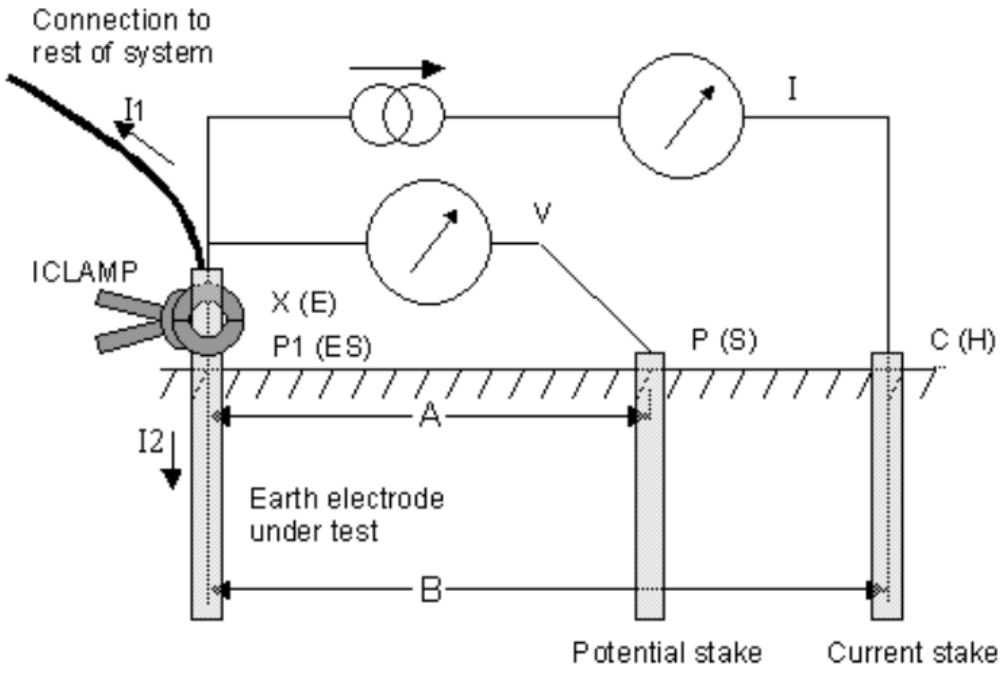

Figure 2.6 Attached rod technique (ART) measurement (Megger) [24]

It involves three steps. (a) The first step is to measure the effective resistance (R) of the entire system using a typical fall-of-potential configuration with the applied voltage V, (b) The second step is to measure the total current (I) being injected into the system and (c) The third step is to measure the amount of current (I1) flowing to the rest of the interconnected system other than the earthing under test. The difference of the current (I) and the current (I1) gives the current (Ie) passing through the earthing system under test. Using this current, the resistance of the earthing (Re) system under test can be calculated as follows,

$$R_e = R \times \frac{I}{I_e} \qquad \text{--------- (2.11)}$$

2.3 Comparative study of earth testers

This study was undertaken to understand the features and limitations of some commercially available earth testers.

2.3.1. Commercially available earth testers

The comparison of the features and limitations of the various commercially available earth testers are summarized in the Table 2.1 and Table 2.2

Table 2.1 Summary of the comparison of the commercially available earth testers

Feature: Test current / frequency range and noise rejection capabilities	
Fluke 1625 GEO Earth Tester	Measurement at automatically / user selectable test frequencies of 94, 105, 111, 128 Hz is provided to mitigate the effects of interference due to the power frequency and harmonic noise. It can inject test currents up to 250 mA ac @ 20/48V AC.
AEMC Instruments,	Automatically seeks optimum measurement test current and test

Digital Earth Resistance Tester, Model 6470	frequency from 40 to 513Hz to avoid interference with the power frequency and harmonic noise. It can inject test currents up to 250 mA ac @ 16/32V DC.
Omicron (CPC 100 + CP CU1)	It has automatic / manual frequency selective measurement of the test system that allows testing at typically 30 to 100 Hz. Narrow band digital filtering is provided to mitigate the effect of power frequency and harmonic noise. It is capable of injecting test currents up to 100A AC in the large earthing systems having low earthing impedance in the range of 0.05Ω to 0.2Ω. While test currents of up to 10A AC can be injected in the earthing systems with resistance of 25Ω to 300Ω.
Megger (DET 2/2)	User selectable test frequencies in the range of 105 Hz to 160 Hz. Maximum test current is 50 mA. It is capable of max noise rejection of 40V peak to peak and 14V RMS @ 50/60 Hz sinusoidal.
Megger (DET4TC)	It can inject test current of 4.5 mA @ 25V / 450 µA @ 50V. Noise rejection of 40V peak to peak and 14V RMS is possible. It can measure earth noise voltage/current. Maximum probe resistances allowed are 100kΩ @ 50V range, 50kΩ @ 25V range and 5kΩ for 10mΩ resolution.
ABEM Terrameter SAS 1000	Automatic or user selectable currents of 1, 2, 5, 10, 20, 50, 100, 200, 500, 1000 mA @ voltages up to 400 V (800 V peak to peak) and maximum output power of 100W @ 50% duty cycle. Current pulse length is 0.1 to 4 seconds.
Comments: All the commercially available earth resistance / impedance testers have an adequate power frequency noise rejection capability. Omicron-make instrument has the maximum current injection capability of up to 100A which makes it suitable for measuring	

large earthing systems. Remaining earth testers have a limited current injection capability which makes them suitable only for the small and medium earthing systems. ABEM Terrameter is capable of measuring earth resistance at a wide current range (1mA to 1A) at maximum 100W power level. This feature makes it suitable for use as a DC variable current source of measuring earth resistance to study the effect of current magnitude on the earth resistance.

Table 2.2 Summary of comparison of commercially available earth testers

Feature: Types of measurements performed.	
Fluke 1625 GEO Earth Tester	It can perform two/three/four-terminal method of measurement of earth resistance, fall of potential test and soil resistivity measurements. It is capable of operating at a maximum potential stake and current stake resistances of 100 kΩ. Stakeless measurement is possible with current and voltage clamps. Resolution of earth resistance measurement is up to 1 mΩ. It can also measure earth impedance at 55 Hz AC.
AEMC Instruments, Digital Earth Resistance Tester, Model 6470	Two/three/four-terminal method for measurement of earth resistance, Fall of Potential test and soil resistivity measurements (user selectable resistivity test method: Wenner or Schlumberger) can be performed with this instrument. It indicates individual test electrode resistance, test voltage, current and frequency during measurement to help identify if the test electrode resistance is not excessively high and sufficient test current is injected in to the earthing system under test. Resolution is up to 10 mΩ
Omicron (CPC 100 + CP CU1)	It is suitable for measurement of earth impedances of large substations [16]. It can measure step and touch voltages. Earth impedance measured at high magnitudes of test current to reflect more accurately the earth resistance at fault current levels.
Megger (DET 2/2)	Two/three/four-terminal method for measurement of earth resistance, Fall of Potential test and resistivity measurement can be performed. Touch and Step potential measurement is possible. It can indicate the

	potential probe / current probe resistance or noise interference if they are too high. Resolution is up to 1 mΩ.
ABEM Terrameter SAS 1000	It is capable of measuring earth resistance and performing soil resistivity surveys with an automatic logging of Wenner / Sclumberger configuration measurements using multiple stakes installed in the soil over the area of soil survey.
Comments: All the commercially available earth testers are capable of measuring earth resistances and touch and step potentials. Majority of the earth testers are capable of performing stakeless measurements except the AEMC instruments model 6470 and Omicron earth tester. However, Omicron earth tester is the only instrument capable of performing measurements for the large earthing systems. All the commercially available earth testers measure the earth resistance / impedance at power frequency levels. No instrument is capable of measuring the earth imepdances at lightning frequency levels or transient surge frequency levels. All the commercially available earth testers are capable of measuring soil resistivity. ABEM Terrameter LUND imaging system is especially suitable for carrying out 2D / 3D soil resistivity surveys.	

2.4 Smart ground meter [27]

Smart ground meter (SGM) [27] measures the earth impedance at various frequencies by injecting a pseudorandom signal in the earthing system under test. A sample of pseudorandom signal is shown in Figure 2.7. It is an AC signal of typically 28V peak to peak magnitude and having random frequency components in the range of 0 to 400Hz. The Smart ground meter is an instrument for earth impedance testing with computer based techniques. An electric current as shown in Figure 2.7 is injected for a short duration into the earth electrode under test, and the return current is collected from the current electrode placed at a sufficiently long distance so as to be out of reach of the influence of earth. This instrument integrates the hardware and software to measure the earth impedance, soil resistivity, tower earth resistance, touch, step and transferred earth potentials.

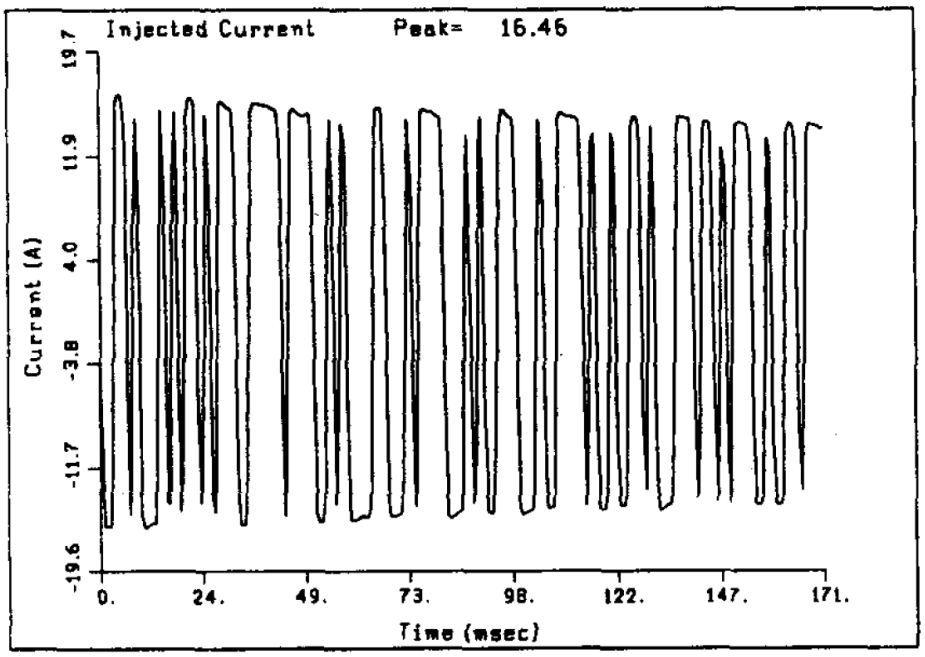

Figure 2.7 Sample waveform of the pseudorandom signal [27]

The earth impedance measurement function can be applied to any existing earthing system of an energised or de-energised facility. It measures the earth impedances of the system consisting of all interconnected earthing electrodes as well as nearby earths connected via shield and neutral wires. The smart ground meter generates a pseudorandom signal across the black and red terminals. As shown in Figure 2.8 the black terminal is connected to the earth under test and the red terminal is connected to an auxiliary current probe. As a result, a current circulates between the earth under test and the auxiliary current electrode. The circulating current generates a potential distribution on the soil.

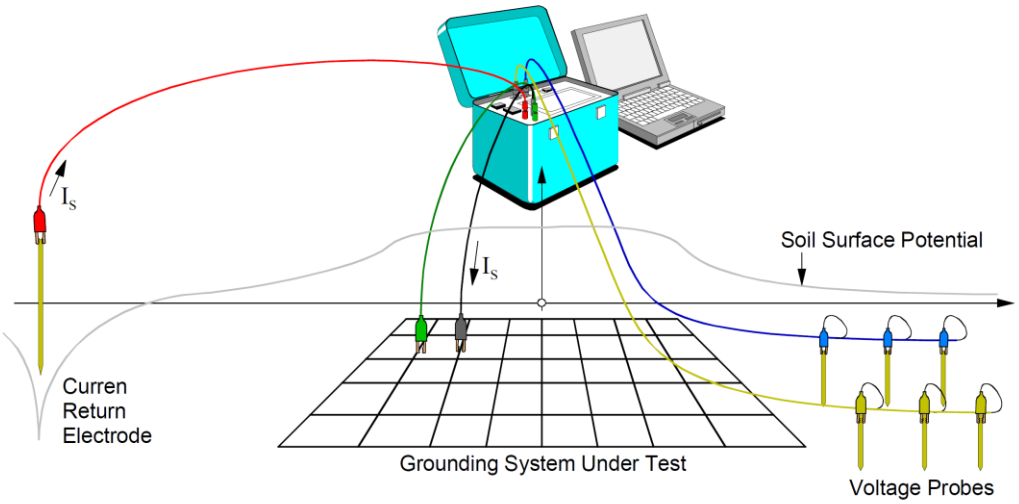

Figure 2.8 Smart Ground Meter [27]

The SGM samples soil potential at six locations via six voltage probes installed at six locations in the vicinity of earth under test as shown in Figure 2.9. In addition, the SGM monitors the injected electric current. The raw measurement data consists of earth potential differences (GPD) between the earthing system under test and six voltage probes due to the current injected by SGM.

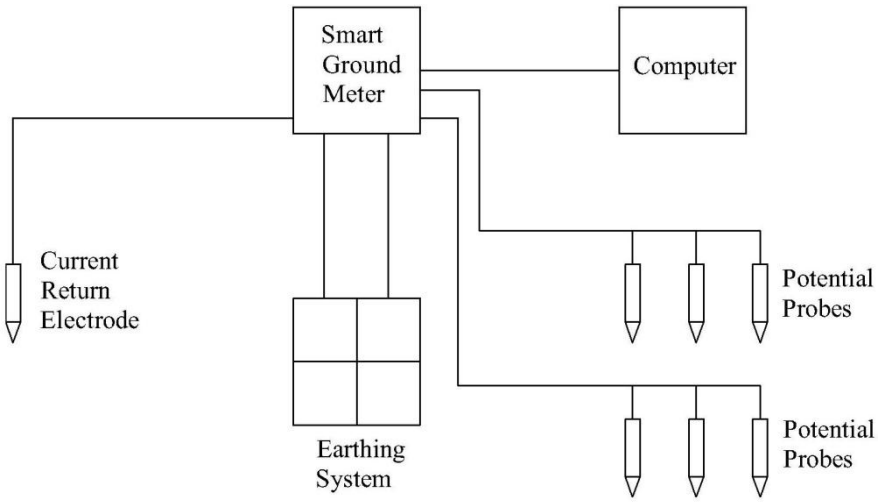

Figure 2.9 Measurement set up for smart earth meter [27]

From these data, the impedance of the earthing system under test is extracted using estimation methods and error correction techniques using the software installed in the SGM.

The measured impedance of the earthing system is obtained as a function of frequency. The estimated impedance is presented as a plot of variation of impedance magnitude and phase with frequency. The measured earth impedance is the combination of the impedance of the earthing system under test in parallel with the impedance to earth of all shield wires, neutral wires and other earthed metallic structures connected to the earthing system under test. The soil resistivity function is based on the extension of the four-terminal method. Specifically, the SGM is capable of taking simultaneous measurements on nine probes uniformly placed along a line on the soil surface. The measurements obtained from the nine probes are processed by error correction and estimation algorithms in order to construct a two layer soil model. The resistivity of the two soil layers and the thickness of the upper soil layer are presented. Soil resistivity measurements are also characterised by an expected error versus confidence level. For soil resistivity measurements, the SGM displays the confidence level for dynamically selected error boundary (based on particular case). The results are displayed in graphical as well as tabular format. Soil in general exhibits complex variations of resistivity even within a relatively small area (several tens of meters). Yet for design purposes a manageable and measurable soil model is required. The two-layer soil model may be taken as a suitable approximation for such applications. The tower earth resistance meter option measures the earth resistance of an energised or de-energised transmission line tower. Shield wires may be connected to the tower earth during measurements. The SGM injects a current into the tower earth and measures the earth potential differences (GPD) between the tower earth and six voltage probes installed around the tower. These data are used to compute the parallel combination of the tower earth resistance and the impedance looking into the transmission line shield wires. However, as the maximum frequency of the injected signal is not more than 400Hz this measurement will tend to highly underestimate the tower earth impedance as the chain impedance of the tower earth with the transmission line shield wires

connected to the other towers. This measurement will provide a significantly lower impedance reading at a frequency of 400Hz. It is shown later in this thesis, in Fig. 5.28, that, to estimate the tower earth resistance, a frequency of injected current will have to be more than 30kHz. This is one of the limitations of Smart Ground Meter while trying to use it to measure the tower earth resistance with shield wires connected. An identification algorithm determines the contribution of the shield wires and eliminates this contribution from the measured total impedance. The algorithm is based on the observation that the shield wire impedance is predominantly reactive while the tower earth impedance is resistive. Moreover, the shield wire resistance and reactance are functions of frequency. The algorithm takes advantage of this frequency dependence to extract the tower earth impedance from the measured data. The algorithm also provides the statistical measures of the measurement accuracy, which is expressed in terms of expected error versus confidence level. The presented results consist of the tower earth impedance plotted as a function of frequency. The touch and step voltage function measures the actual touch and step voltage at a substation as a function of the fault current. The measurement is performed at up to six points near the earthing system. A required input for this function is the fault current available at the location of the earthing system. The data analysis takes into consideration the effect of the proximity of the current return electrode on the measured touch and step voltages. The additional data required for this measurement function are the co-ordinates of the voltage probes, current return electrode and approximate size and shape of the earthing system.

A personal computer is used to compute the values of potential gradients and current at various locations to generate the values of earth impedances at various frequency levels. The signal acquisition unit acquires, filters and attenuates the signals to the suitable level for further processing. There is also a current source unit which circulates the test current into the earth electrode under test. There are six voltage probes with a set of three voltage probes each

in an insulated flexible conduit. These probes are used for recording the potential at various points in relation to the earth under test. It also consists of one assembly of current return electrode.

2.5 Effect of pin spacing on the measured earth impedance

The minimum geographical extent required to measure the earth impedance with sufficient accuracy (linear pin spacing required between the injection electrode and the return current electrode and the orthogonal pin spacing required between the injection electrode and the potential reference electrode) is of interest from the point of view of area constraints faced during the measurement of the large area earth electrodes. The effect of pin spacing on the earth resistance depends on the geometrical extents of the earthing electrode and the soil resistivity pattern of the site of earthing [63]. Wenner 4-pin measurement method is generally used to interpret the layered soil resistivity at the site. It is generally known that larger the Wenner pin spacing, higher the depth of the soil resistivity sensed. To study the effect of pin spacing on the measured earth resistance Southey et al. [63] performed computer simulations based on the measured soil resistivites with different pin spacings and substituted these values in the computer program to estimate the earth resistance. They considered 152m x 152m earth grid and the two double layer soil resistivity models such as a) 100Ωm layer over 5000Ωm and b) 5000Ωm layer over 100Ωm. They computed grid earth resistance as a function of top layer thickness sensed by the resistivity measurements. The % error in the computed grid resistance and safety voltages observed by them is shown in Figure 2.10.

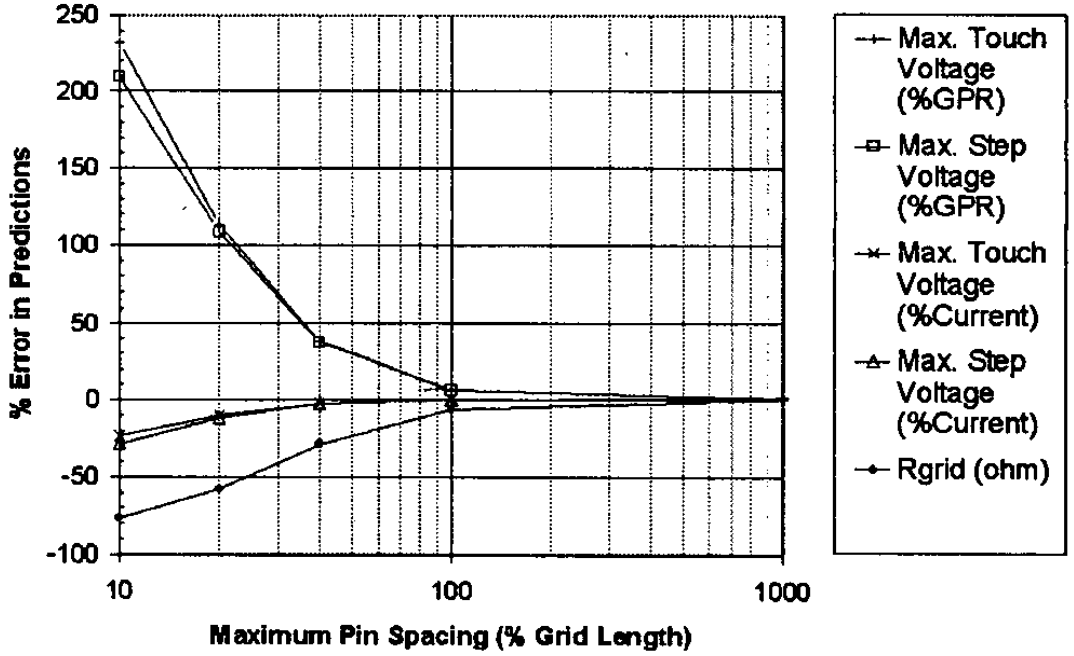

(a) Error in grid perfromance predictions versus maximum pin spacing: 100 Ωm soil layer, 30m (100ft) thick, over 5000 Ωm soil.

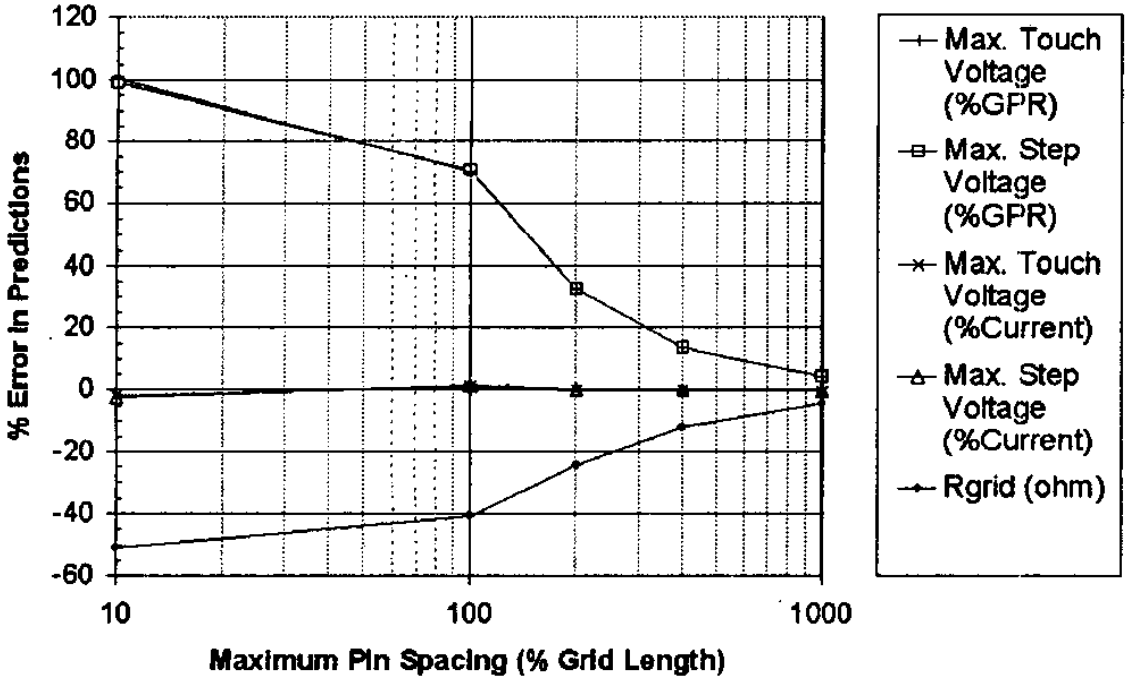

(b) Error in grid perfromance predictions versus maximum pin spacing: 100 Ωm soil layer, 152m (500ft) thick, over 5000 Ωm soil.

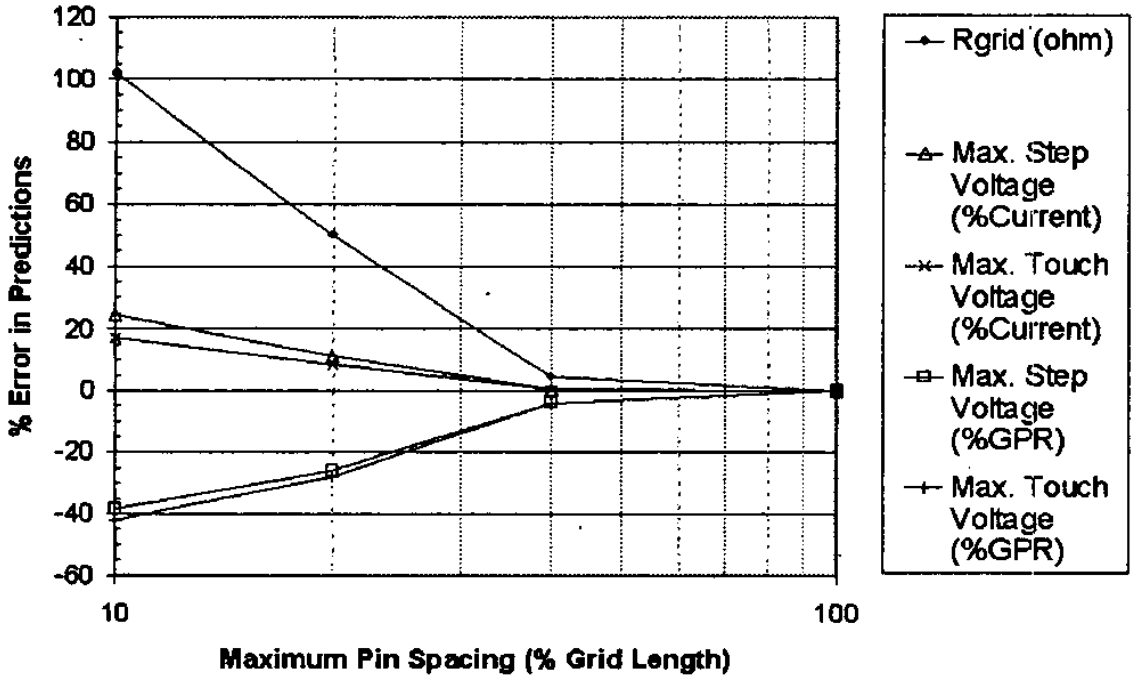

(c) Error in grid perfromance predictions versus maximum pin spacing: 5000 Ωm soil layer, 30m (100ft) thick, over 100 Ωm soil.

Figure 2.10 Percentage error in computed grid resistance as a function of pin spacing [63]

They concluded that with the resistivity ratios varying from 1:50 and 50:1 (extreme cases expected in the field) between two layers, the maximum error in the computed grid resistance depends on the depth of the top layer and maximum pin spacing as shown in Table 2.3.

Table 2.3 Computed grid resistance error range

Maximum pin spacing (% of grid length)	Maximum computed grid resistance error range
40%	-50% to +30%
100%	-33% to +9%
300%	-17% to +(<9%)

From the study conducted by Southey et. al, it can be concluded that for the high over low resistivity layer model, the pin spacing (between the injection current electrode and return current electrode) of more than 3 times the maximum grid length is sufficient to minimise the error within +9% for the computed grid resistance. For the converse resistivity model (low

over high resistivity layer, with deeper top layer), it is desirable to have the pin spacing (between the injection current electrode and return current electrode) close to 10 times the maximum grid length to minimise the error (<-10%) in the computed earth resistance. The pin spacing between the injection electrode and the potential reference electrode is desired to be such that the potential reference electrode is outside the zone of influence of the earth electrode under test.

2.6 Conclusion

The literature review revealed that the most reliable method of measurement of earthing impedance of the practical earth electrodes is the Fall of Potential Method. This method has been widely used by the commercially available earth resistance measurement testers. However it is time consuming and labour intensive. Therefore different other methods of measurements such as three point method, ratio method, clamp-on earth testing method are used to measure the impedance of earthing system. The behaviour of earth impedance measurement at the power frequencies has been studied in considerable details in the past and has led to the development of robust techniques for the measurement of earthing impedance at power frequencies. Several efforts were also made by the authors in the past and are being made at present to characterise the behaviour of earthing systems under high frequency and impulse conditions. However, to know to complete extent, the behaviour of earthing systems under transient impulse and high frequency conditions it would require further investigation. These findings will help us propose the suitable measurement techniques to measure the earth impedances which will be representative at the lightning transient and impulse conditions. It was noted that the Smart Ground Meter will provide underestimation of the values of the tower earth resistance as the injected signal from the Smart Ground Meter is less than 400Hz. This limitation of Smart Ground Meter can be overcome by using a suitable current signal

injection source with a frequency of the order of few tens of kHz. The literature review has also revealed that the effect of electromagnetic coupling between the test leads, interference with the leakage power frequency currents circulating in the earthing system and the spacing between testing electrodes may affect the measurement. Due care is required to be taken to reduce the error introduced by these aspects. Moreover, in this chapter, the survey of earthing measurement techniques was carried out, the limitations and advantages of the commercially available earth testers has been identified and the range of applications of these earth testers have been determined.

Chapter 3: Determination of accuracy of transducers and preliminary laboratory tests

3.1. Introduction

The experimental programme in this thesis required the use of several voltage and current transducers. These transducers were tested in the laboratory with the variable frequency / voltage / current sources to ascertain their accuracy and characterise their response. The objective of this exercise was to verify the suitability of the transducers and apply correction factors if necessary to the values obtained during the experimental campaign. The laboratory tests were performed on the earth resistance testers to measure the standard resistance. Laboratory tests were also performed on the conduction mediums such as dry sand, wet sand, tap water and distilled water to see the behaviour of these mediums to the variable frequency and variable magnitude current signals.

3.2. Voltage transducers

The voltage transducers used in the test were differential voltage attenuators. Differential voltage measurement was required to decouple the electronics measurement systems from the power frequency noise present in the earthing systems under test. Attenuation was necessary to bring the level of the measured signals to sufficiently lower amplitudes compatible with the electronics measurement systems. The technical specifications of SI 9000 and Chauvin Arnoux make DP25 voltage probes are as follows. The accuracies of both the potential transducers is specified as 2%. The selectable attenuation values are 20 and 200 for the SI9000 voltage probe and 20, 50 and 200 for the DP25 voltage probe. The input impedance is 2MΩ/2.5pF for the SI9000 voltage probe and 4MΩ/1.2pF for the DP25 voltage probe. The 3dB bandwidth of SI9000 and DP25 voltage probes is DC to 25MHz and DC to 15MHz

respectively. Both the voltage probes are capable of measuring a voltage signal of fastest rise time up to 24nS. The maximum input to ground voltage capability of SI 9000 is 700V RMS at attenuation setting of 200 and 70V RMS at attenuation setting of 20. DP25 is capable of measuring maximum of 600V RMS between input to ground at all the attenuation settings. Appendix A1 gives the detailed specifications of the voltage probes tested in the laboratory.

The test setup used during laboratory tests on transducers is shown in Figure 3.1 and the test results are shown in the Figure 3.2 and Figure 3.3.

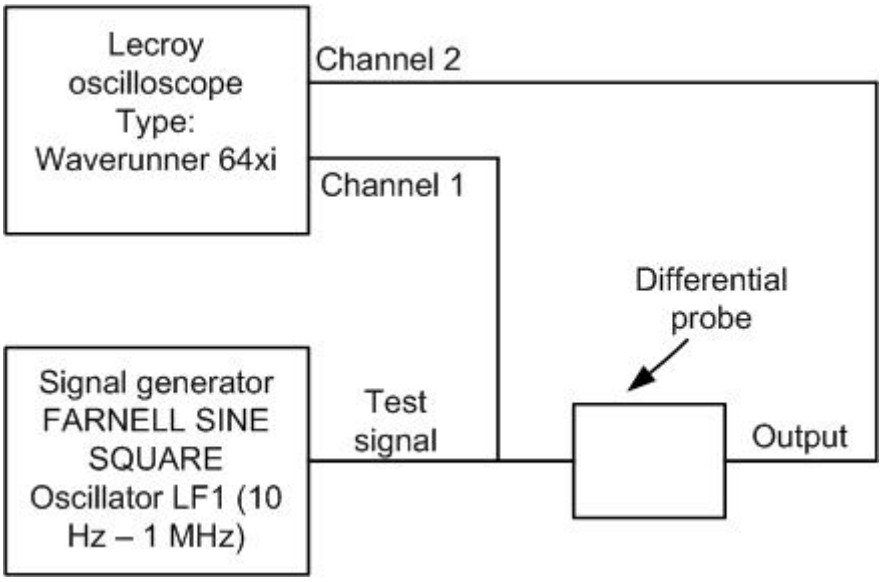

Figure 3.1 Test setup for calibration of differential probes

A standard signal generator was used with test voltages in the range of 0-5V and frequencies over the range 20 Hz to 1MHz as a source. Output of the signal generator was directly fed into a duly calibrated Lecroy oscilloscope (Waverunner 64xi) to measure the input voltage level. The output of the differential voltage attenuator transducer was fed into the channel 2 of oscilloscope. The two signals were compared. Figure 3.2 and Figure 3.3 shows the percentage error of the signal for the output of the transducer compared with the direct signal measurement.

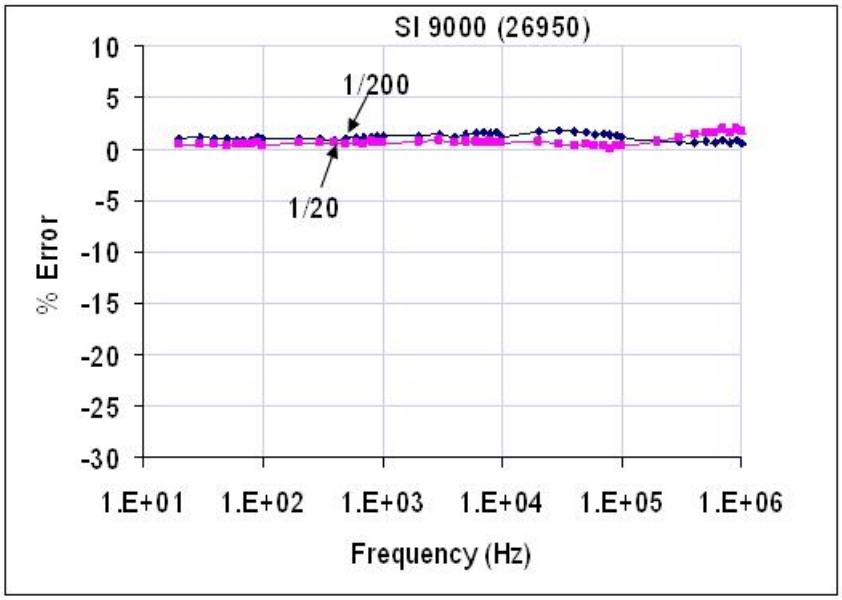

Figure 3.2 Determination of the accuracy of the voltage transducer SI 9000 serial number 26950

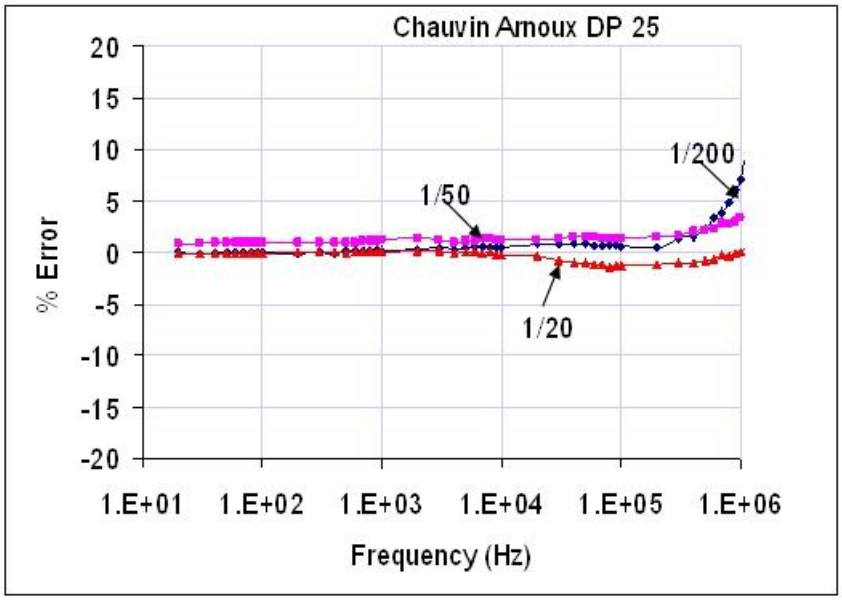

Figure 3.3 Determination of the accuracy of the voltage transducer DP25 serial number 20080843

The transducers were tested over a frequency range 20 Hz to 1 MHz. The different potential transducers tested had a measured error of less than ± 3% over a complete frequency range. These calibration curves obtained were used to apply the correction factors to the values of measured voltages during the experiments.

3.3. Current transducers

A comparison of the frequency response of different current transducers was made. The transducers included LILCO CT, Stanganes current transformers and Tektronix make current probes. In the test set up shown in Figure 3.4 the current transducers to be compared were used for measuring the same current generated by a standard signal generator over the frequency range 20 Hz to 10 MHz.

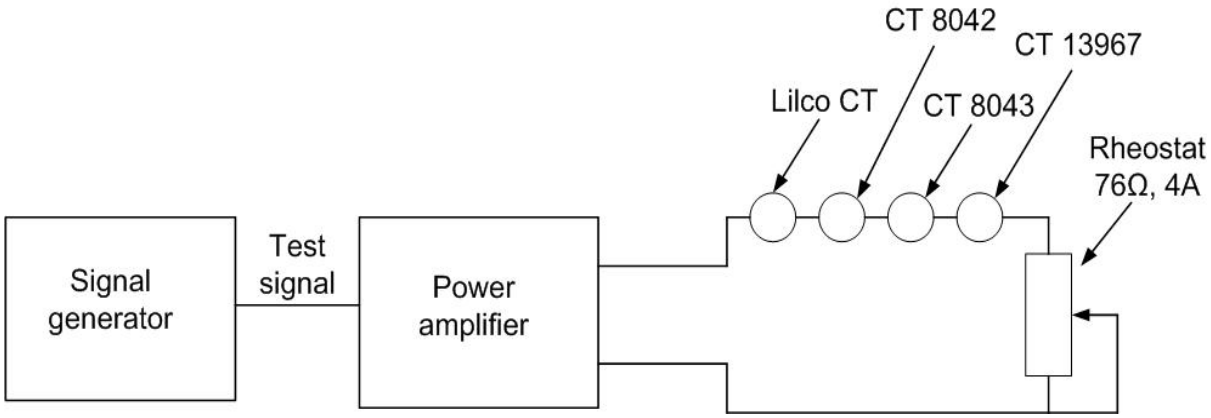

Figure 3.4 Test set up for comparison of current transducers

The current transducers were tested in four groups as shown in the Table 3.1.

Table 3.1 Groups of current transducers formed for testing purpose

Group No.	Current transducers included in the group
Group No. 1	LILCO CT and Tektronix current probe
Group No. 2	Tektronix probe, Stanganes CT serial nos. 12316, 13370 and 13971.
Group No. 3	LILCO CT and Stanganes CT serial nos. 8042 and 8043
Group No. 4	LILCO CT and Stanganes CT serial nos. 8042, 8043 and 13967

The current transducers were grouped to a maximum number of four to facilitate waveform measurements on the four channel Lecroy oscilloscope. Same current was passed through the current transducers in each group to measure their response to current magnitude and frequency. LILCO CT and Tektronix current probes are wide bandwidth transducers while the Stanaganes CT's were the pulsed CT's. The detail specifications of the current transducers is provided in the Appendix A1. The LILCO CT and Tektronix current probe

were tested over a wide band of frequencies 20Hz to 200kHz. The Stanganes CT's were tested over a frequency range of 1kHz to 1MHz. LILCO CT was used to measure the standard cropico resistance for a low frequency response. The accuracy of LILCO CT was found to be highest during the test with the standard resistance measurement. Hence LILCO CT was used as a reference for comparison of the other current transducers.

Output responses of different current transducers is shown in the Figure 3.5. As seen from Figure 3.5, the response of the current transducers was in close agreement over the frequency range 20Hz to 200kHz and 1kHz to 1MHz.

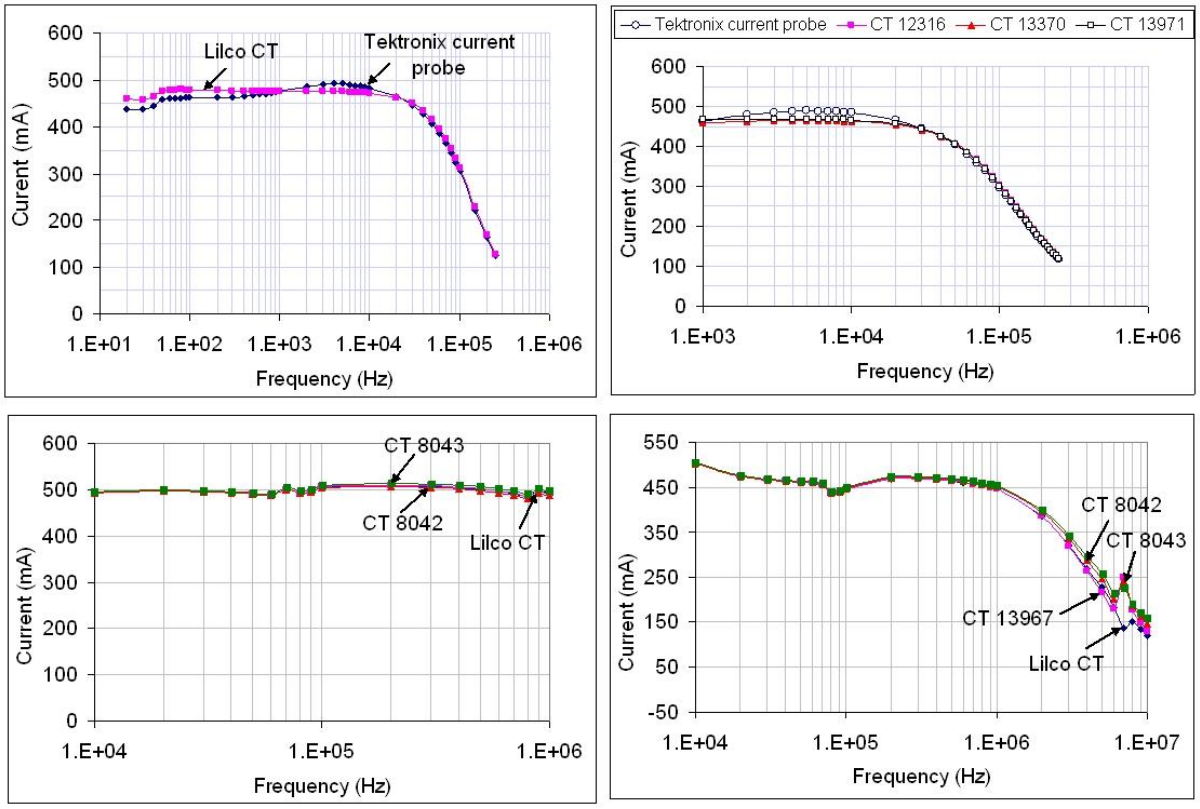

Figure 3.5 Comparison of current transducers

The Stanganes current transformers showed accuracies close to the LILCO CT (less than 2% error was observed), while the Tektronix probes were comparatively less accurate (about 6% error was observed). The majority of the subsequent field experiments were performed using the LILCO CT.

3.4. Laboratory tests of earth resistance meters and earth impedance measurement system (IMS)

Calibrated resistances using a CROPICO make standard resistance were measured with a Megger earth resistance tester DET 2/2, the Cardiff University make Impedance Measurement System (IMS) [42] employing the lock-in amplifiers and the ABEM Terrameter.

3.4.1. DET 2/2 laboratory tests

The Cropico make standard resistance MTS1A at 1Ω, 1.9Ω and 10Ω settings was measured with Megger make DET2/2 earth resistance tester. As seen from Figure 3.6, Figure 3.7 and Figure 3.8, the measured value of resistance was found to be accurate within 0.2 % of the standard value. DET 2/2 has a facility to measure the DC earth resistance at a low DC switching frequencies ranging from 105Hz to 160Hz.

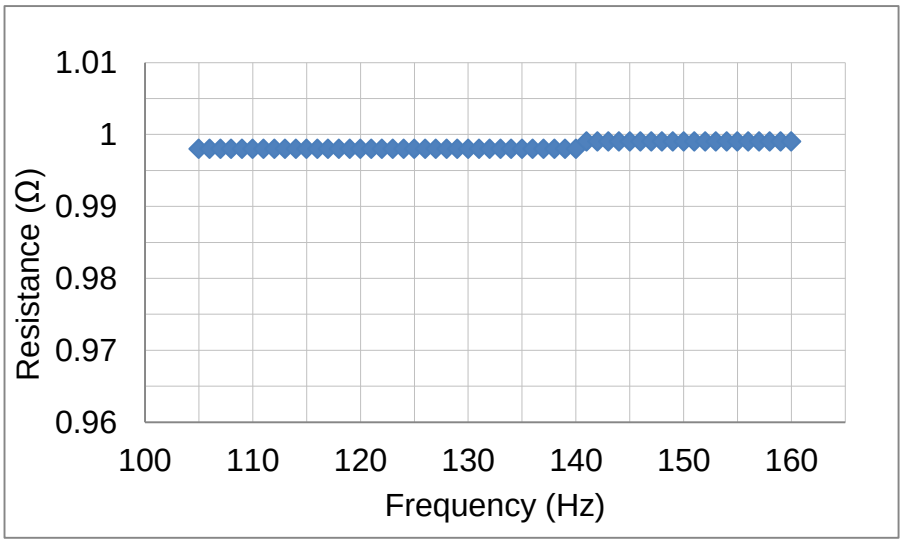

Figure 3.6 Measurement of Cropico MTS1A standard 1Ω resistance with DET 2/2

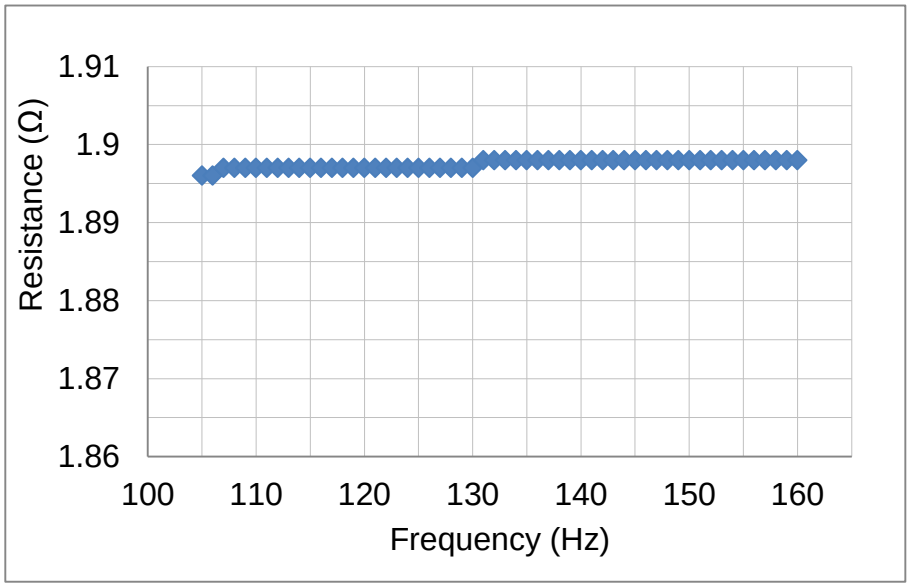

Figure 3.7 Measurement of Cropico MTS1A standard 1.9Ω resistance with DET 2/2

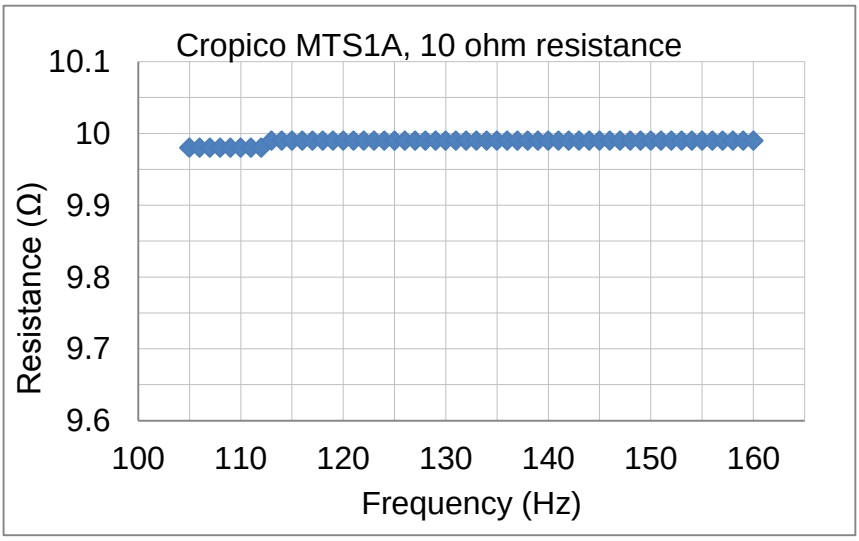

Figure 3.8 Measurement of Cropico MTS1A standard 10Ω resistance with DET 2/2

3.4.1. IMS laboratory tests

Figure 3.9 shows the measurement of 1Ω standard resistance with the Cardiff University make IMS over the frequency range 80Hz to 1kHz. As seen from the Figure 3.9 the measured resistance value is close to 0.9825Ω over the freqncy range 80Hz to 1kHz.

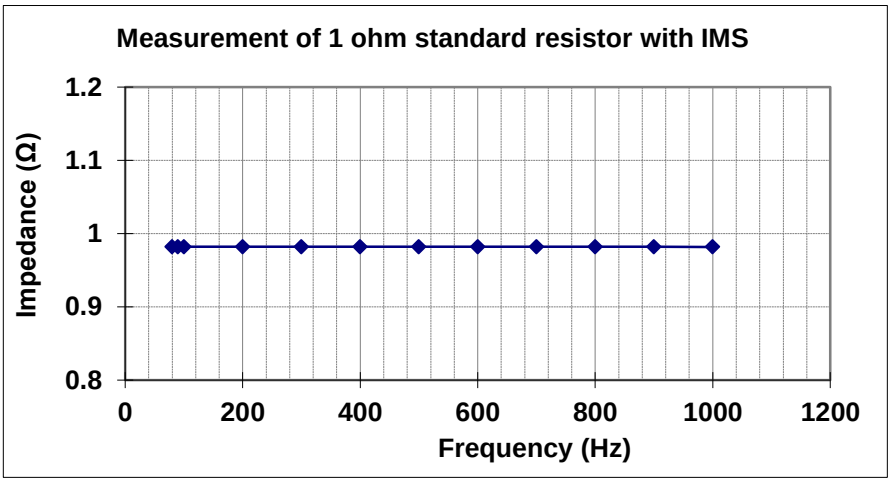

Figure 3.9 Measurement of resistance with Cardiff University Impedance Measurement System

3.4.2. ABEM Terrameter laboratory tests

The cropico standard resistance at 1Ω setting had a maximum current rating of 75mA. So the ABEM Terrameter was used upto a current range of 50mA to be safe within the rating of the resistance. The measured value of the resistance was found to be accurate within 0.2% of the standard value as shown in Figure 3.10.

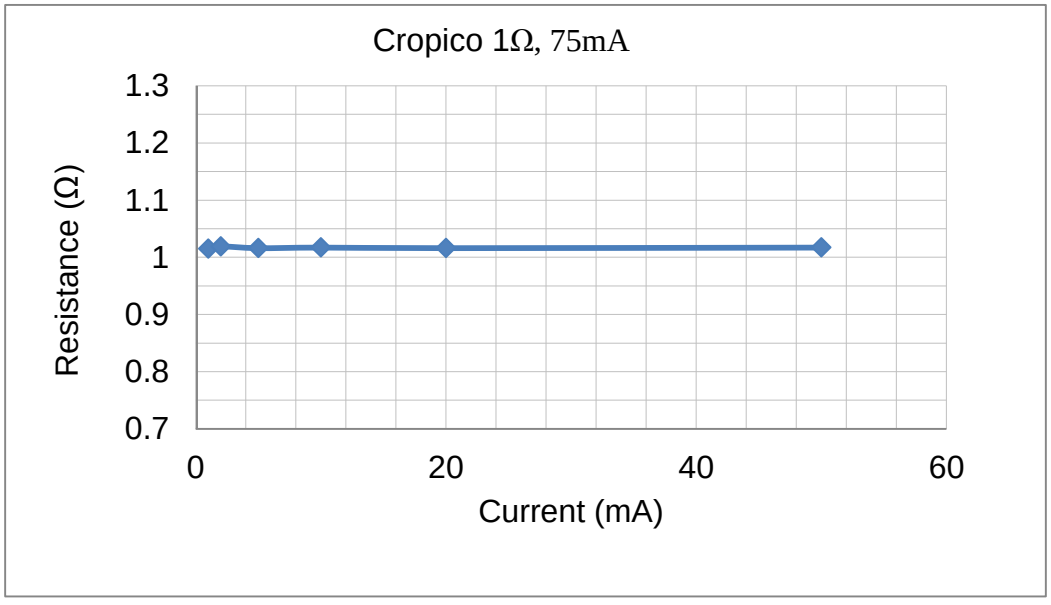

Figure 3.10 Measurement of resistance with ABEM Terrameter

3.1 Laboratory tests of impedance measurements of soil and electrolytes

Figure 3.11 shows the experimental test set up of the impedance measurement tests performed in the laboratory controlled environment.

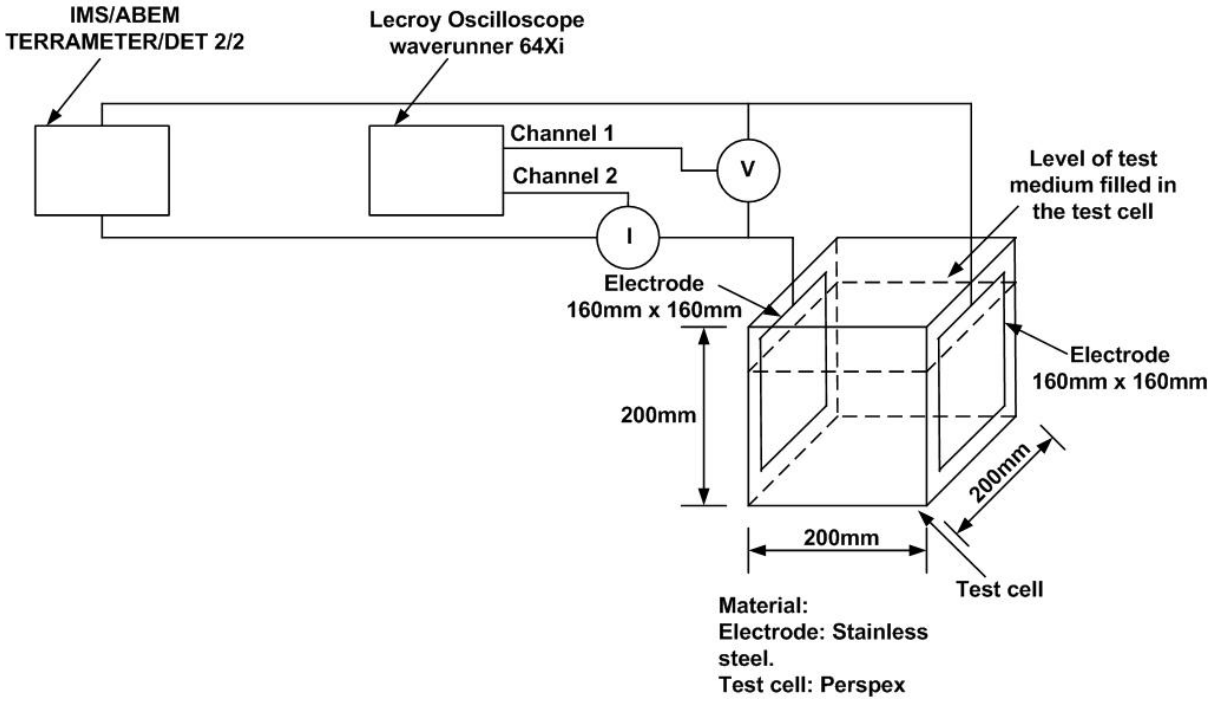

Figure 3.11 Test set-up for laboratory tests on the soil and water.

The objective of these tests were to observe the effect of frequency and current magnitude on the impedance of distilled water, dry sand, wet sand and tap water respectively. The test cell was 200mm x 200mm x 200mm (length x breadth x height). The height of the medium (distilled water / dry sand / wet sand / tap water / electrolyte solution) with which the test cell was filled was 160mm. The space above the level of 160mm would introduce some stray capacitance. However, it was found that this stray capacitance is negligible.

Various conducting mediums such as dry sand, 3.24% wet sand, tap water and distilled water were tested for the measurement of the impedance at frequencies over the range of 20Hz to 100kHz. The current magnitudes were also varied from few milli-amperes to few hundred milli-amperes. The effect of frequency and the AC / DC current magnitudes was studied during the experiments performed on the test cell at the Cardiff University laboratory.

Figure 3.12 shows the effect of frequency on the measured impedance of the 3.24% wet sand filled in the test cell. As seen from the figure there is about 10% reduction in the measured earth impedance over the frequency range 20Hz to 100kHz. The plots in different colours denote the impedances observed over the current range 39mA to 780mA.

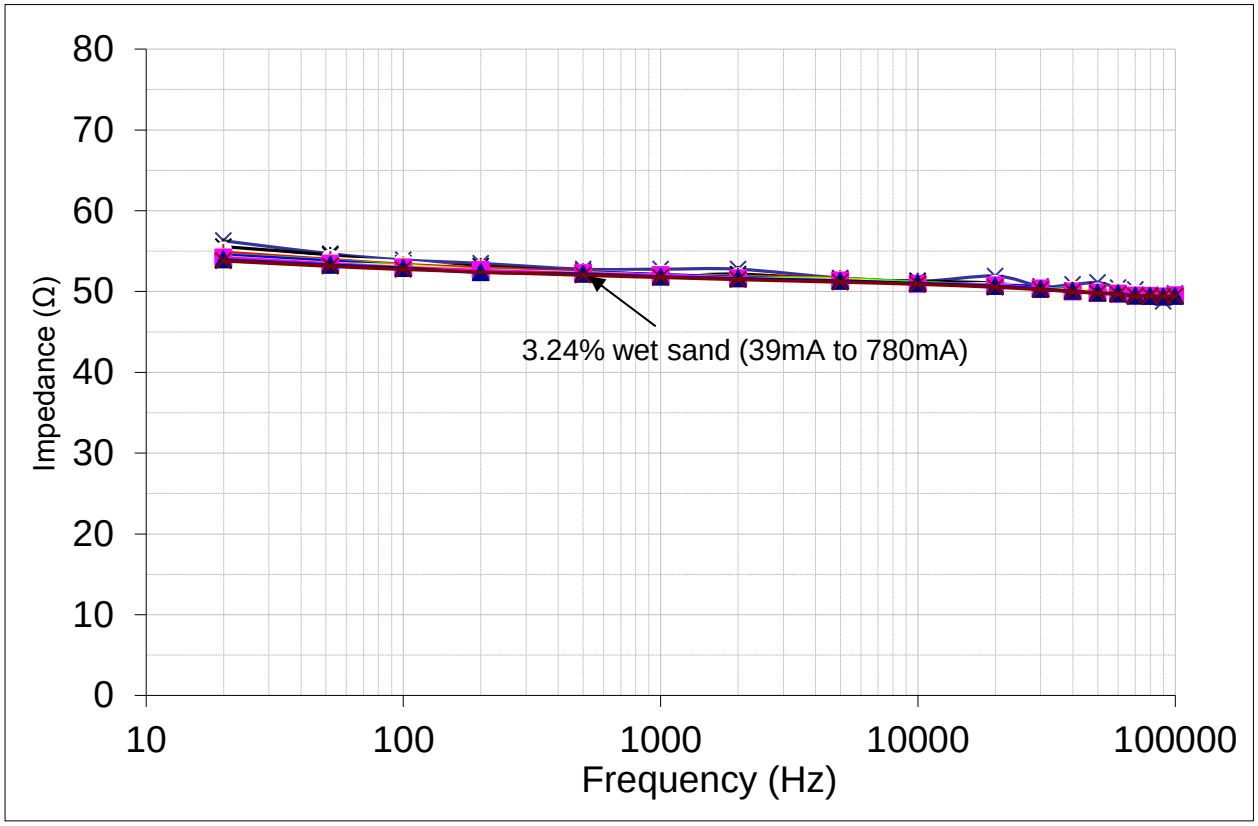

Figure 3.12 Effect of frequency on the impedance of 3.24% wet sand filled in the test cell

Figure 3.13 shows the effect of frequency on the measured impedance of the dry sand filled in the test cell. As seen from the figure there is about 30% reduction in the measured earth impedance over the frequency range 20Hz to 100kHz. The plots in different colours denote the impedances observed over the current range 3.7mA to 84.9mA.

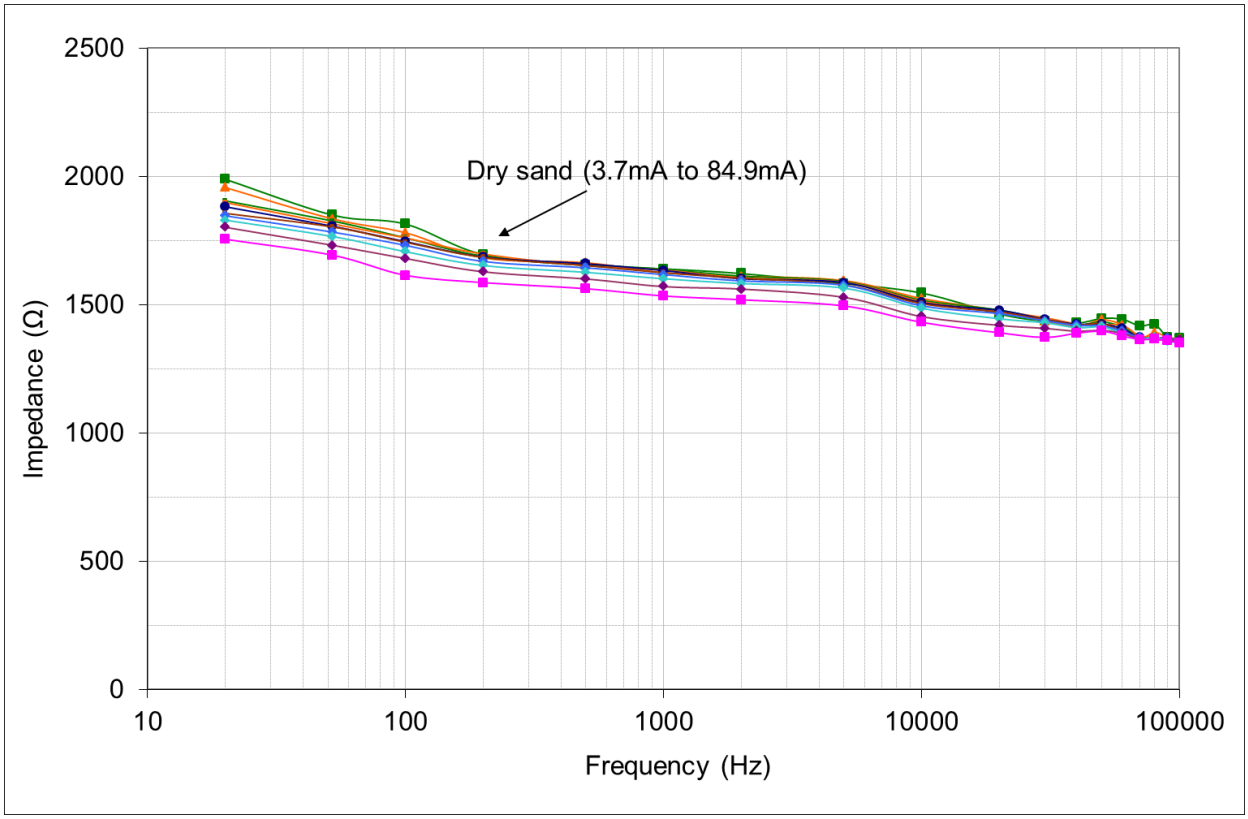

Figure 3.13 Effect of frequency on the impedance of dry sand filled in the test cell

Figure 3.14 shows the effect of frequency on the measured impedance of the tap water filled in the test cell. As seen from the figure there is about 6% reduction in the measured earth impedance over the frequency range 20Hz to 100kHz. The plots in different colours denote the impedances observed over the current range 102mA to 663mA.

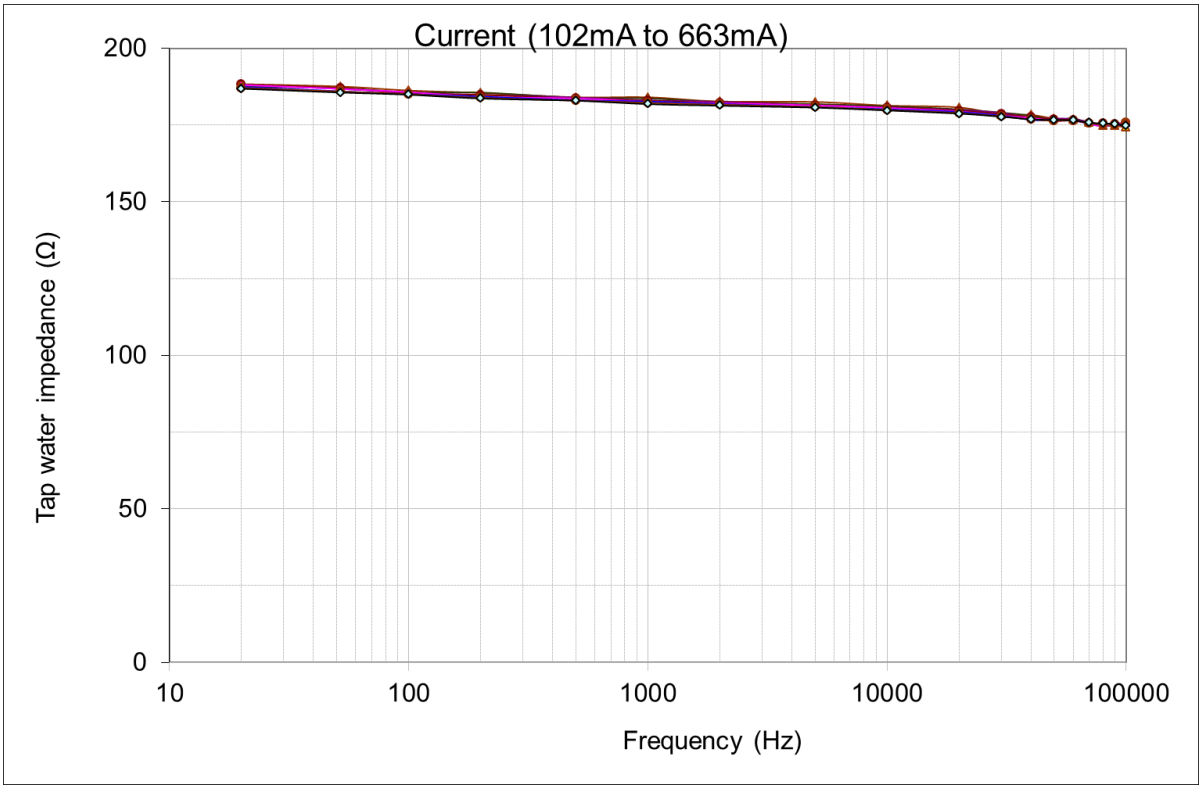

Figure 3.14 Effect of frequency on the impedance of tap water filled in the test cell

Figure 3.15 shows the effect of frequency on the measured impedance of the distilled water filled in the test cell. As seen from the figure there is about 40% reduction in the measured earth impedance over the frequency range 20Hz to 100kHz. The plots in different colours denote the impedances observed over the current range 0.52mA to 11.82mA.

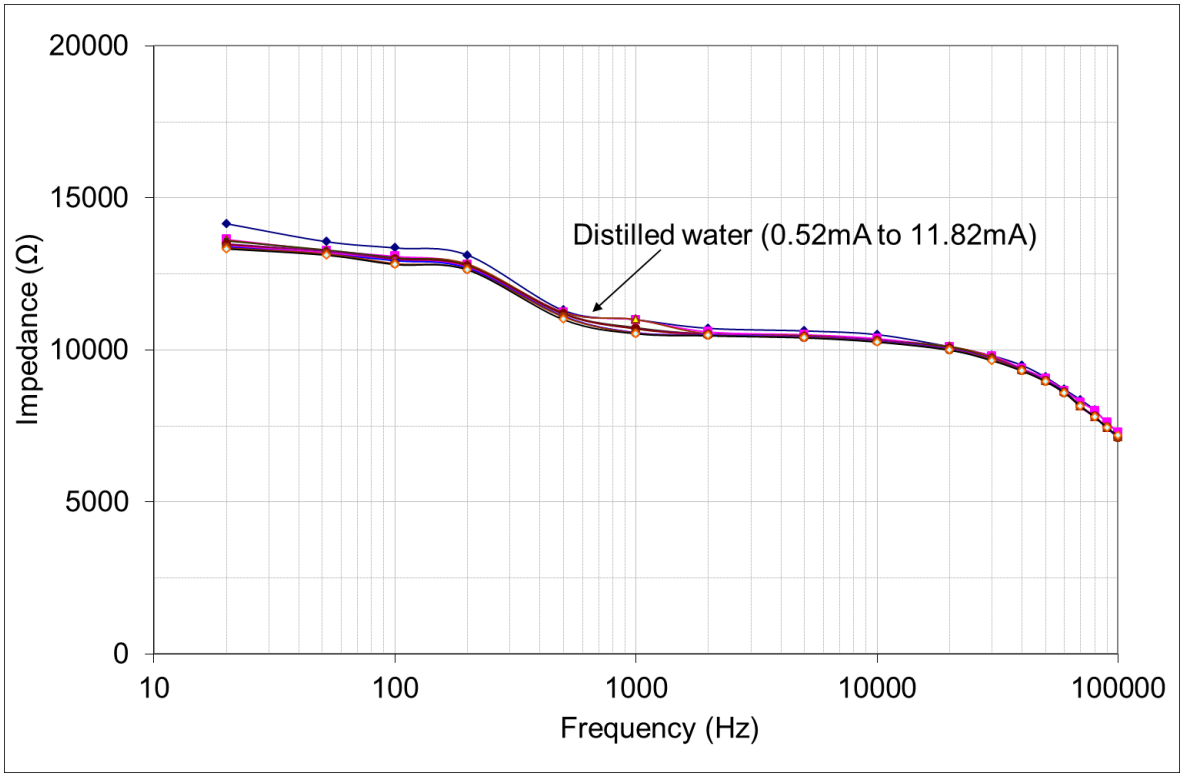

Figure 3.15 Effect of frequency on the impedance of distilled water filled in the test cell

As can be seen from Figure 3.16, there is order of magnitude difference between the measured impedance / resistance of distilled water, dry sand, wet sand and tap water. The impedance was measured at different frequencies with the IMS system while the DET 2/2 was used to measure the resistance of these mediums.

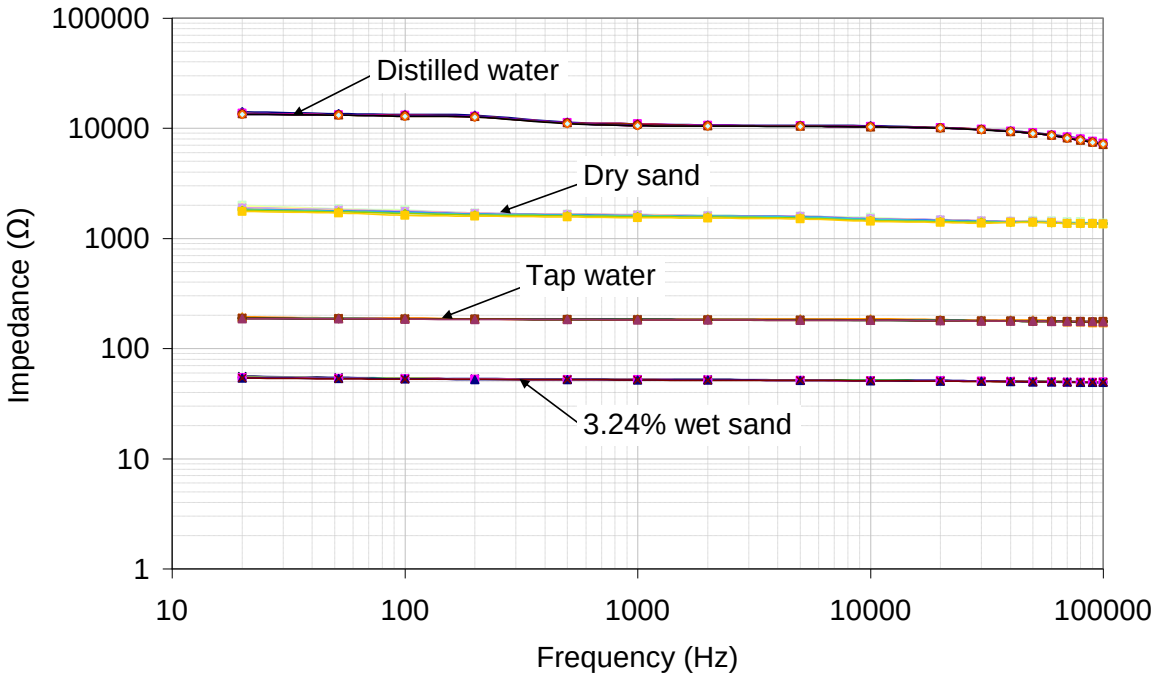

Figure 3.16 Effect of frequency on the impedances of various conducting mediums filled in the test cell

Figure 3.17 shows the effect of AC current magnitude on the measured impedance of the 3.24% wet sand filled in the test cell. As seen from the figure there is about 3% reduction in the measured earth impedance over the AC current range 40mA to 800mA. The plots in different colours denote the impedances observed over the frequency range 20Hz to 100kHz. The effect of AC current magnitude is pronounced at lower frequencies.

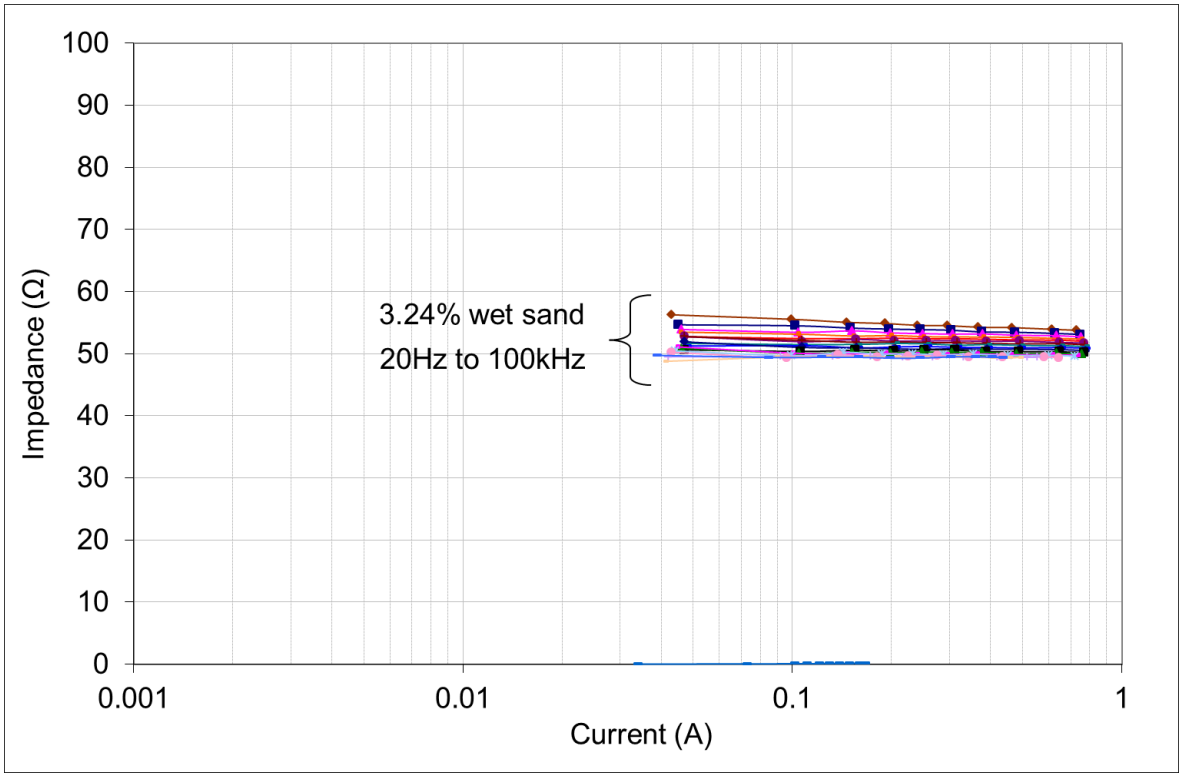

Figure 3.17 Effect of current magnitude on the impedance of 3.24% wet sand filled in the test cell

Figure 3.18 shows the effect of AC current magnitude on the measured impedance of the tap water filled in the test cell. As seen from the figure there is about 6% reduction in the measured earth impedance over the AC current range 40mA to 650mA. The plots in different colours denote the impedances observed over the frequency range 20Hz to 100kHz. The effect of AC current magnitude is pronounced at lower frequencies.

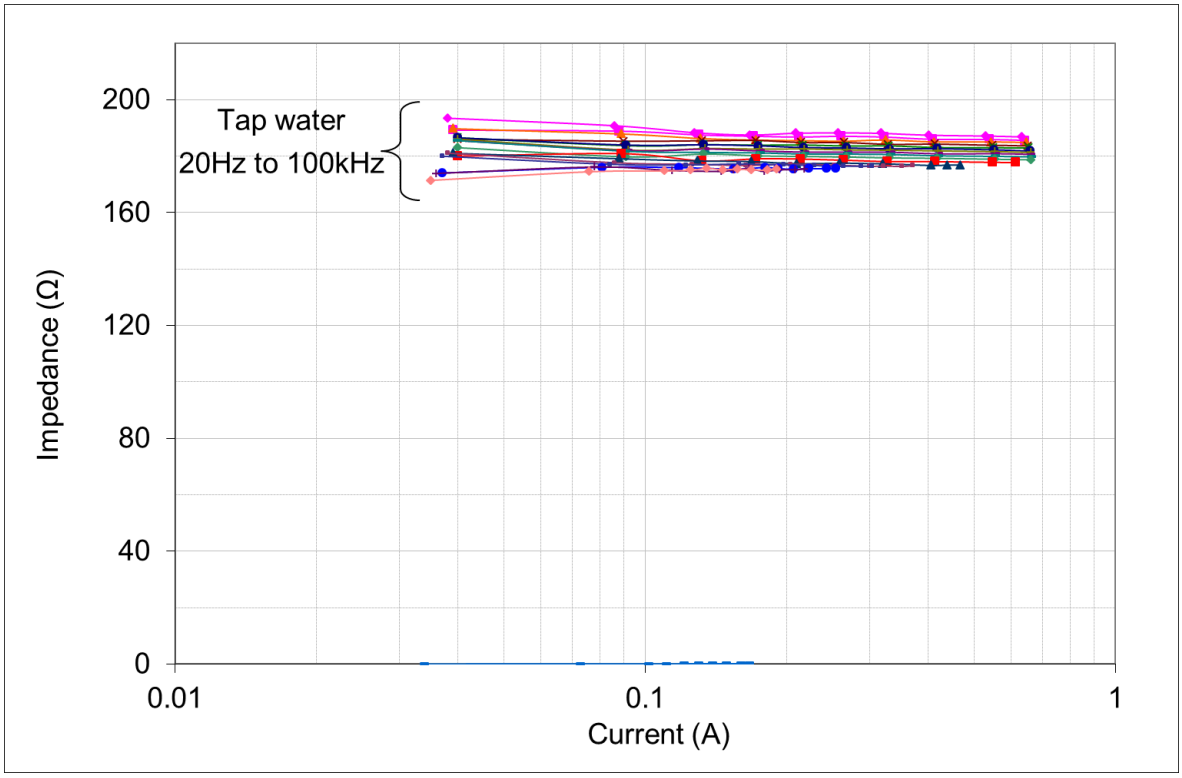

Figure 3.18 Effect of current magnitude on the impedance of tap water filled in the test cell

Figure 3.19 shows the effect of AC current magnitude on the measured impedance of the dry sand filled in the test cell. As seen from the figure there is about 10% reduction in the measured earth impedance over the AC current range 4mA to 80mA. The plots in different colours denote the impedances observed over the frequency range 20Hz to 100kHz. The effect of AC current magnitude is pronounced at lower frequencies.

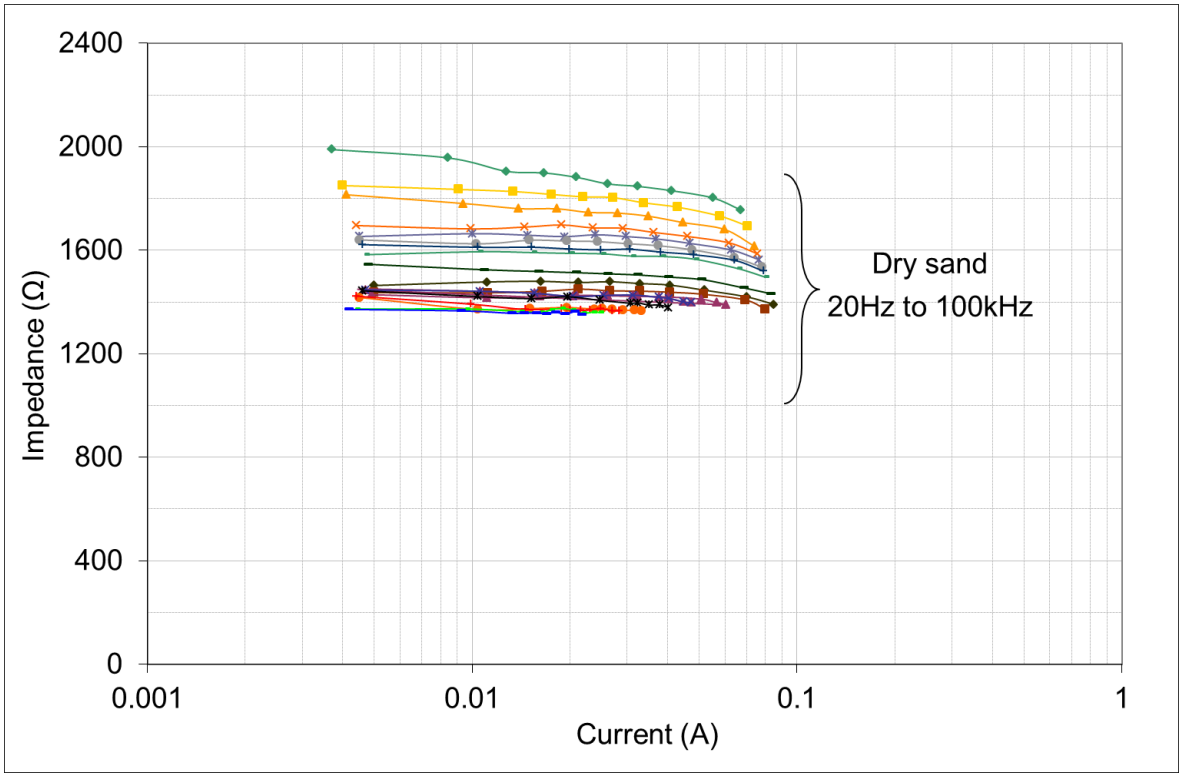

Figure 3.19 Effect of current magnitude on the impedance of dry sand filled in the test cell

Figure 3.20 shows the effect of AC current magnitude on the measured impedance of the distilled water filled in the test cell. As seen from the figure there is about 10% reduction in the measured earth impedance over the AC current range 40mA to 800mA. The plots in different colours denote the impedances observed over the frequency range 20Hz to 100kHz. The effect of AC current magnitude is pronounced at lower frequencies.

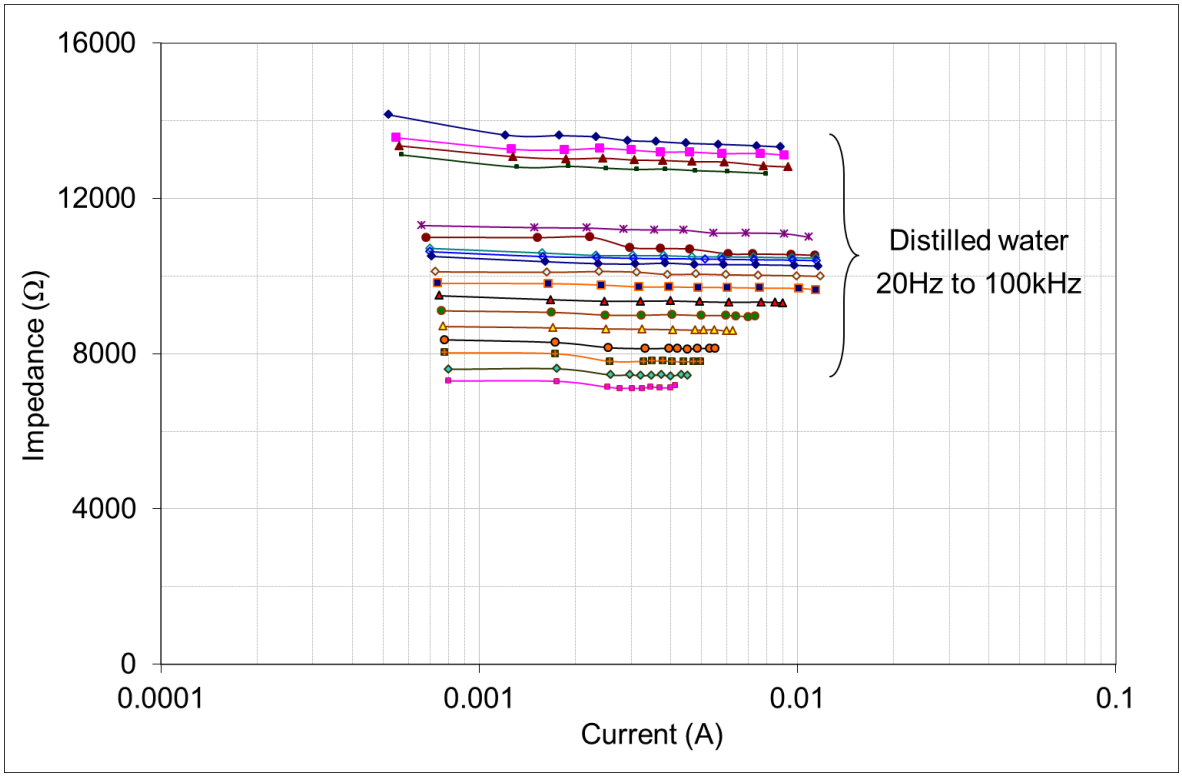

Figure 3.20 Effect of current magnitude on the impedance of distilled water filled in the test cell

Figure 3.21 and Figure 3.22 show the effect of DC / AC current magnitude on the measured values of the impedance / resistance of the various mediums tested in the laboratory at Cardiff University.

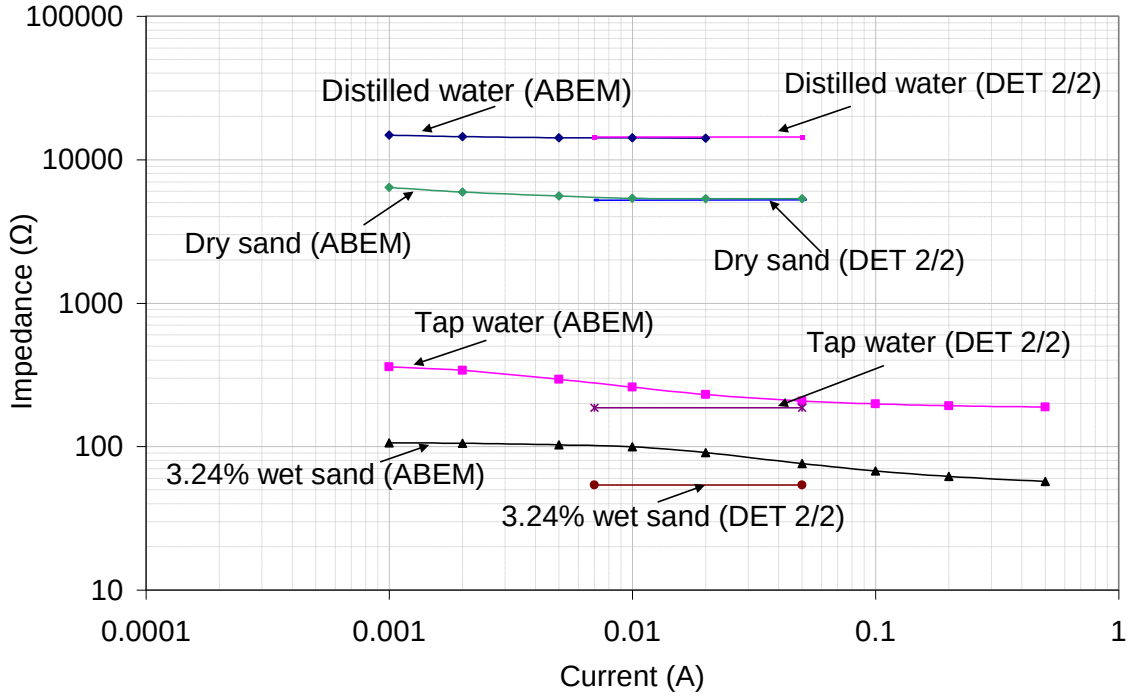

Figure 3.21 Effect of DC current magnitude on the impedance of different current mediums filled in the test cell

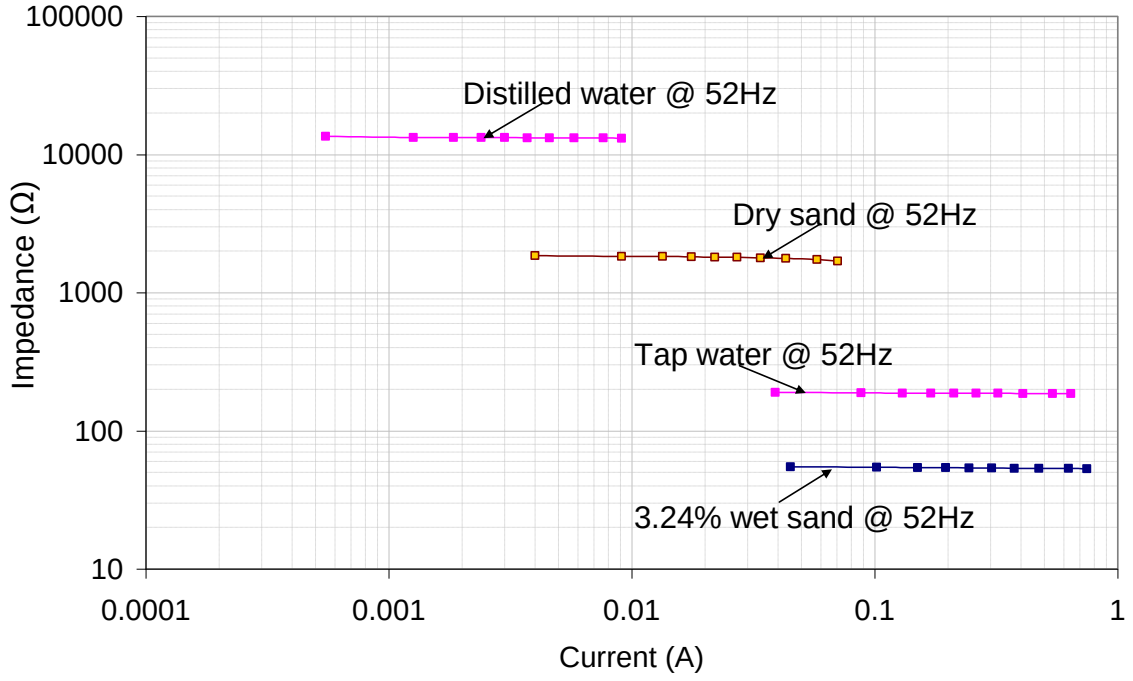

Figure 3.22 Effect of AC current magnitude on the impedance of different current mediums filled in the test cell

It was observed that the effect of current magnitude was higher (close to 20% variation in the impedance of tap water and wet sand over the current range from 1mA to 500mA) in the case of DC currents as seen from the Figure 3.21 (measurement with ABEM instrument).

Figure 3.23 shows the effect of frequency on the measured impedance of distilled water with different electrolyte concentration.

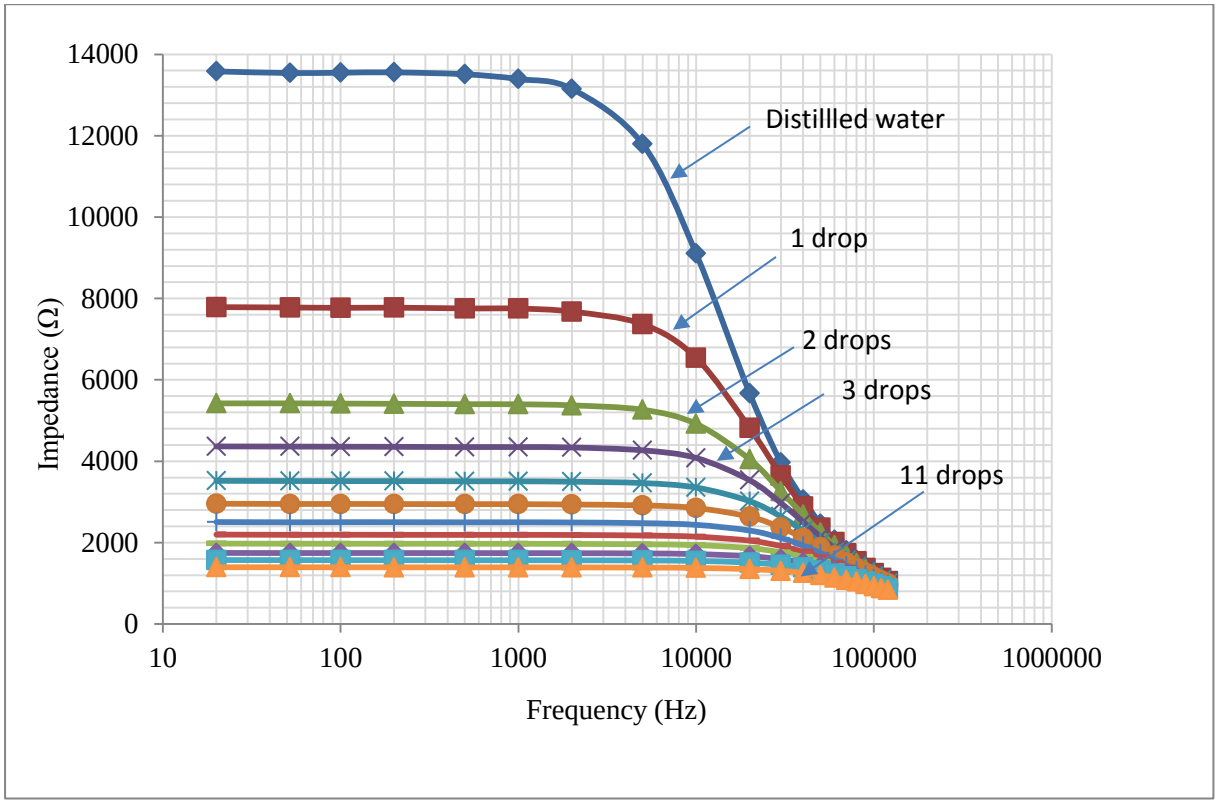

Figure 3.23 Variation of impedance of water with frequency

It was observed that as the frequency increases the capacitive effect dominates and the impedance of distilled water with less concentration of the electrolyte tends to merge towards the resistance value at the higher frequencies of around 120 kHz. The capacitive reactance part of the impedance was calculated from the measured phase angle between the voltage and current for the different frequencies over the range 20Hz to 120kHz. At frequencies close to 120kHz the measured impedance values of the electrolyte solution are close to each other as both the effects (reduction of the capacitive reactance as well as the sharp reduction of the

resistivity with frequency) seems to be playing the role in reducing the measured impedance of the electrolyte solution. The effect of frequency on the resistivity of the water is shown in Figure 3.24.

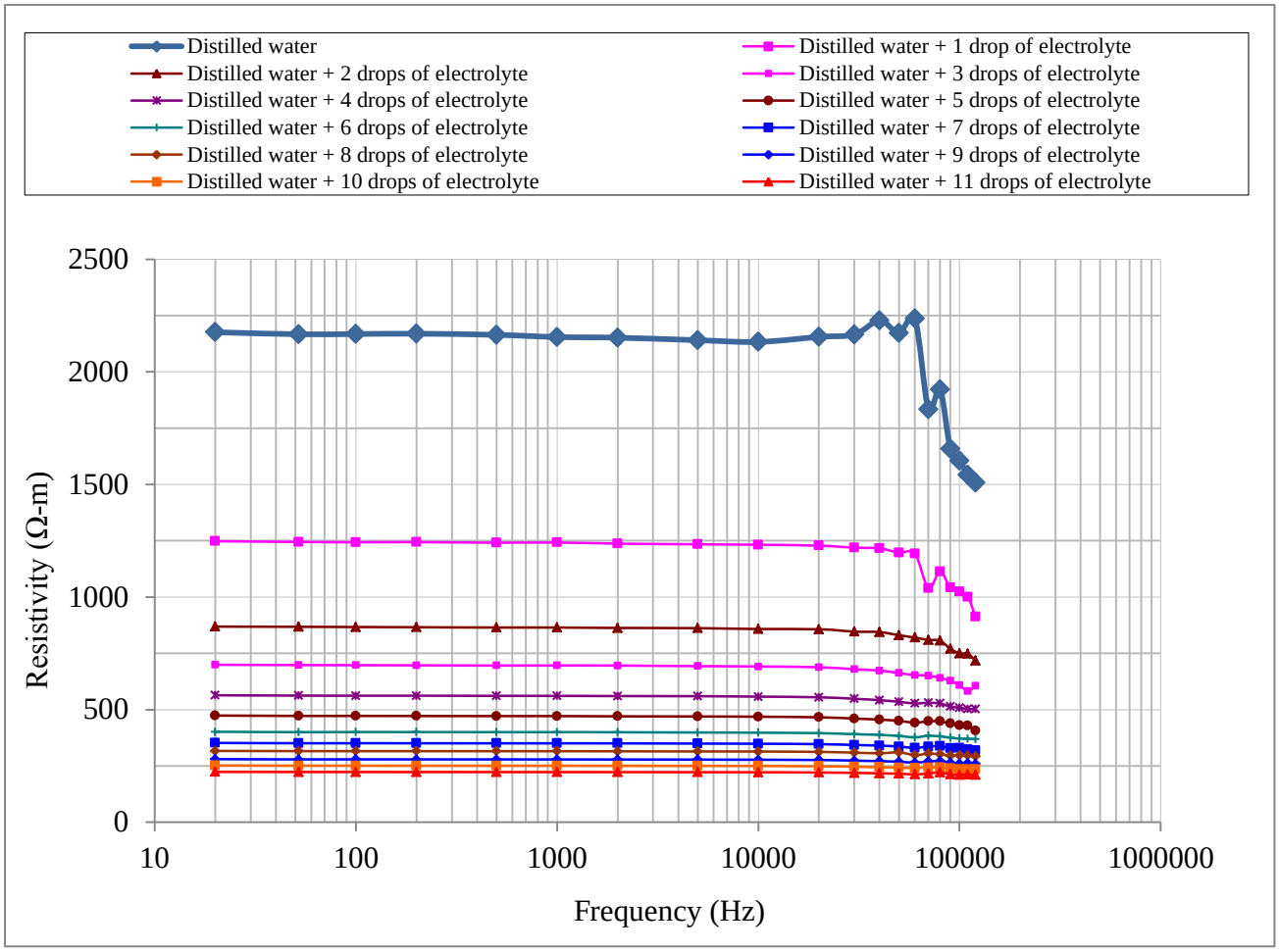

Figure 3.24 Variation of resistivity of water with frequency

The resistive component of the impedance was computed from the phase angles of the measured voltages and currents. It was noted that the resistivity of the distilled water with different electrolyte concentration reduced with increase in the frequency. The effect was more pronounced for the higher resistivity case.

Figure 3.25 shows the percentage change in the resistivity of the distilled water with electrolyte solution when the frequency of the injected current signal is varied from 20Hz to 120kHz. As seen from Figure 3.25 the effect of frequency on the resistivity of electrolyte solution is higher when the concentration of electrolyte is less or in other words it seems from the laboratory experiments with distilled water and electrolyte solution, that the higher impedance medium exhibits higher effect of frequency in the range 20Hz to 120kHz.

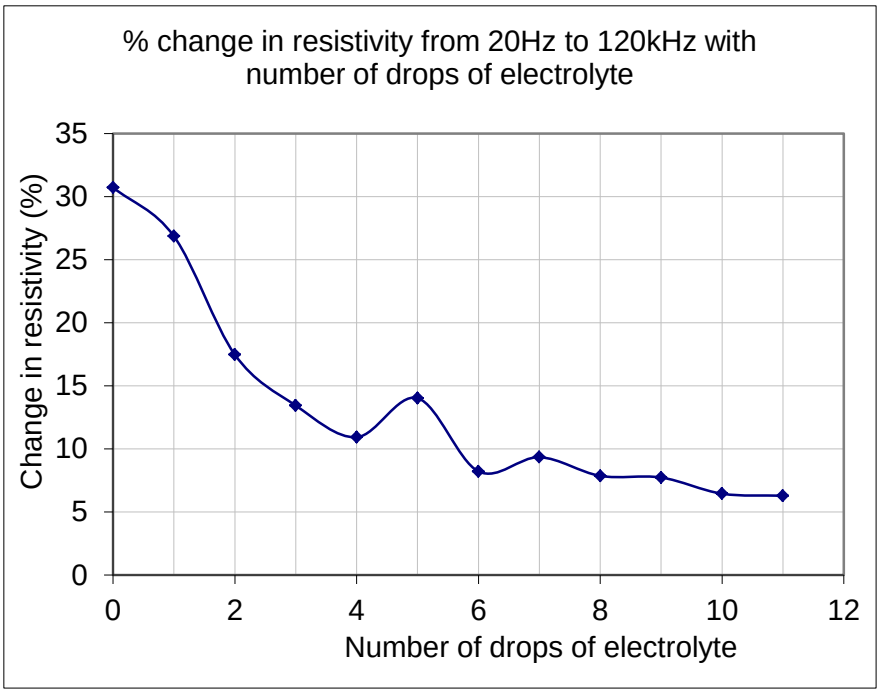

Figure 3.25 Percentage change in resistivity of water with frequency from 20Hz to 120kHz with increasing electrolyte concentration

The impedance / resistance of the distilled water was gradually reduced with addition of the drops of the electrolyte.

The laboratory measurement of the impedances and the calculation of the resistivities of the conducting mediums from the experiments have shown that there is an effect of frequency on the impedance and resistivity of the conducting mediums tested. A small effect of the DC current magnitude was also seen on the resistance of the conduction mediums during the experiments.

3.2 Conclusion

The differential voltage transducers were calibrated over the frequency range of 20Hz to 1MHz in the laboratory and their errors were found to be within the range of specifications.

The output of current transducers were compared and found to be in close agreement over the frequency range 20Hz to 200kHz and 1kHz to 1MHz. The commercially available earth testers such as DET 2/2, ABEM Terrameter were used to measure the Cropico make standard resistance in the laboratory and it was found that the measurement was in good agreement with the standard resistance value. Subsequent to calibration of the voltage and current transducers, and the commercial earth testers, an experimental measurement campaign for soil and water resistance, was carried out in the laboratory environment. The measurement of four different mediums such as dry soil, wet soil, distilled water and tap water was performed over a frequency range of 20Hz to 100kHz. It was found that there was a noticeable decrease (up to 30%) in measured impedance of these four mediums over a frequency range 20Hz to 100kHz. Moreover, the experiments for the measurement of the effect of AC/DC current magnitude on the measured impedance of these four mediums were also performed. It revealed that the effect of AC current on the measured impedance over the range of current magnitude from 1mA to 1A was less than 3%. However, the DC current magnitude of 1mA to 5mA showed a significant reduction (20%) of the measured impedance of the mediums such as wet sand and tap water. Further tests were also performed on the distilled water and distilled water mixed with electrolyte solution gradually increasing the conductivity of the distilled water after each set of measurements of the impedance over a frequency range of 20Hz to 120kHz. These tests revealed slight reduction in the resistivity of the relatively high conductivity water solution over the frequency range of 20Hz to 120kHz. However, a significant reduction in the resistivity of distilled water was observed over the frequency range 20Hz to 120kHz. It is shown in Chapter 7.4 (Figure 7.4) that the conductivity

dispersion observed in the laboratory experiments by Arulanandan [46] and modelled by Oliver de Lima et al. [45] showed about 33% increase in conductivity of the soil water electrolyte solution when subjected to increase in frequency in the range 100Hz to 100kHz. Arulanandan [46] conducted experiments on saturated kaolinite clay-water-electrolyte systems and found that there are two distinct dispersions, one in the low frequency range (0 to 100 kHz) and the other in the high frequency range (1 MHz to 100 MHz). An increase in electrical conductivity has also been experimentally observed for clays by [47], [48], [49], mineralised rocks [50], polymers [51], synthetic membranes [52], ion exchange resins [53] and polystyrene spheres [54]. The conductivity dispersion characteristics were experimentally observed in the frequency range of either 0 to 100 kHz or 1 MHz to 100 MHz.

Chapter 4: Description of test sites and facilities

The Cardiff University-developed earth impedance measurement system injects sinusoidal signal into the earth electrode and captures the earth potential rise to compute the earth impedance. The measurements performed with the sinusoidal signals near power frequencies represent the earth impedance values for the power frequency conditions. However, to measure the earth impedances representative of the lightning frequency and transient surge conditions, a separate set of measurements is required to be performed at sinusoidal currents at higher frequencies. In order to study the response of earthing systems, a series of earth impedance/resistance measurement tests were conducted on different types of earthing systems including rods, rod clusters, grid, tower base, horizontal electrode and tower line. AC/switched DC/impulse energisation sources were used in this work to obtain earth resistance/impedance values of the different systems at different frequency/current magnitudes and impulse wave shapes. Two outdoor test sites were used; (i) Llanrumney fields, where a number of earth test electrodes have been installed and (ii) Dinorwig Power Station lower reservoir.

4.1. Overview of Llanrumney fields test site

Figure 4.1 shows a satellite image of the Cardiff University test field at Llanrumney. As seen from Figure 4.1, the Llanrumney test site has purpose-built earthing systems such as (i) a 3m x 3m earthing grid, (ii) a ring earthing system consisting of 8 single earth rods with a provision to connect them together with a 25 mm^2 bare or insulated copper conductor ring. Each rod has dimensions of 16mm diameter and a length of 2.4m. The bare / insulated copper conductors are buried approximately 20cm in the earth. The test site also includes in the centre of the ring a purpose built tower base and an operational 275kV National Grid

transmission tower VP9 (which is not visible in the satellite image) approximately 100m away from the test tower base.

Figure 4.1 Plan view of University test site at Llanrumney showing outline of installed test electrodes

Figure 4.2 shows the dimensions of the tower footing, the steel reinforcement bars and the surrounding concrete structure. The distance between the leg stubs on the ground surface is 7m. The tower base is located at the centre of the ring electrode as shown in Figure 4.1. Each leg of the tower base is a 'L' cross-section with the dimensions as shown in the section 'A-A' of Figure 4.2. The plan view of four legs of the tower base is shown in Figure 4.3.

The dimensions of the 3m x 3m grid are shown in Figure 4.4. It is made up of a 4 mesh (1m x 1m size) of copper tape with cross section 50mm x 6mm and 2.4m long vertical rods installed at each corner. The horizontal grid conductors are 3m long.

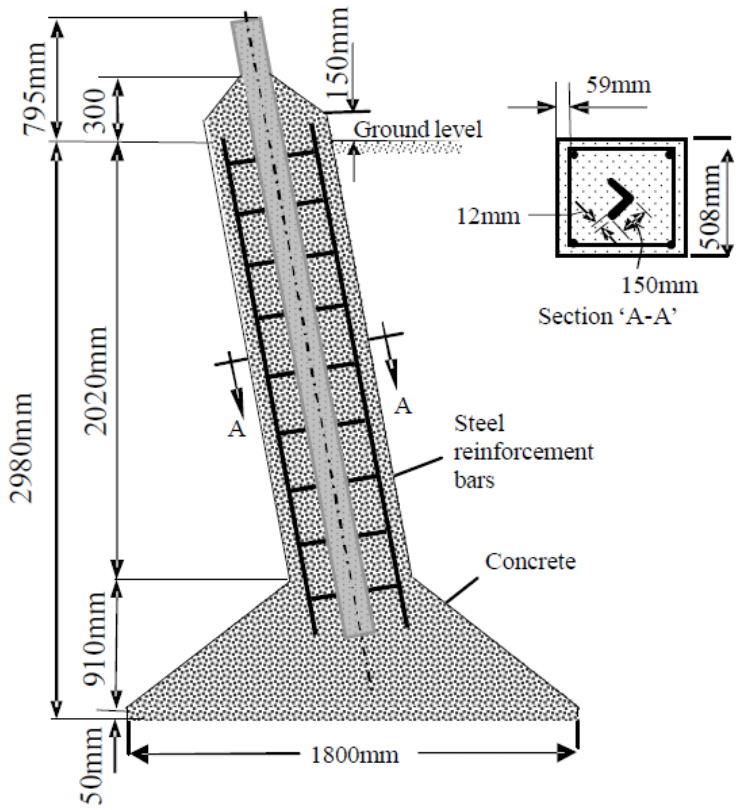

Figure 4.2 Tower footing construction of one leg of tower base

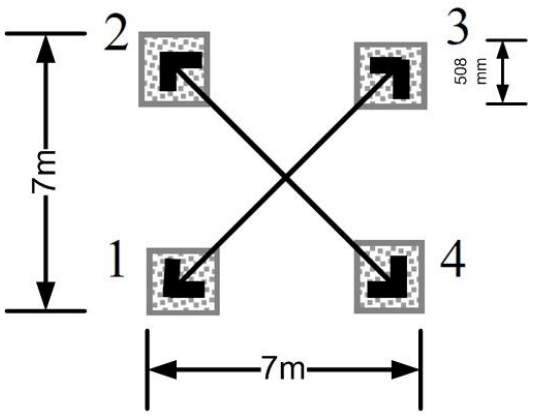

Figure 4.3 Plan view of the four legs of the Tower base

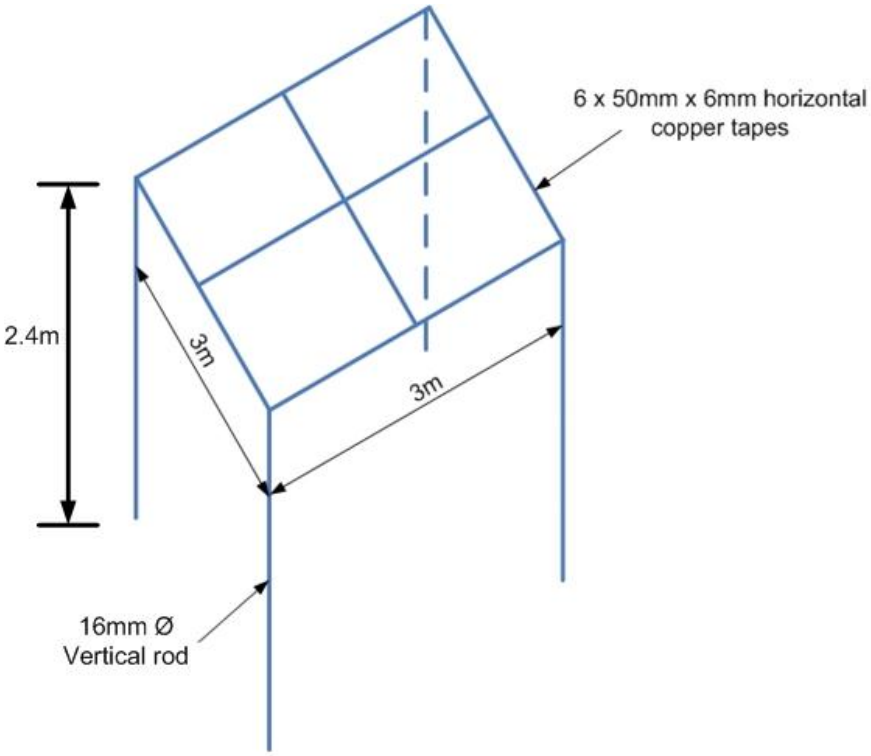

Figure 4.4 Isometric view of 3m x 3m grid

The Ring Earthing system is made up of 8 rods having 16mm Ø and 1.2m long vertical rods installed along the periphery of the circle with a 58m diameter. The plan view of ring earthing system is shown in Figure 4.5.

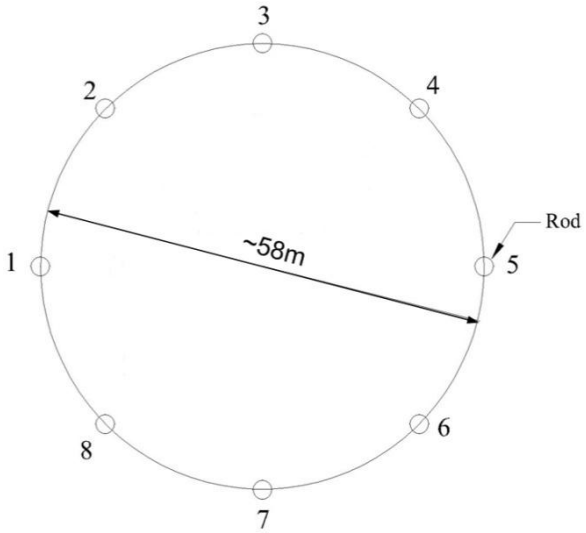

Figure 4.5 Plan view of ring earthing system

A combination of concentrated and extended earthing systems can be realised from the individual earthing electrode components at Llanrumney test field. This provides the opportunity to measure the earth impedance of the following earthing systems

1) Single earth rod – 16 mm ø, 2.4m length
2) 3m x 3m, 4 mesh earth grid
3) 275kV purpose built tower base
4) 275kV National Grid operational tower base VP9 and extended tower line earthing system
5) Parallel combination of vertical rods connected with insulated copper cable
6) Parallel combination of vertical rods connected with the bare copper cable forming a horizontal electrode plus vertical electrode arrangement
7) Extended electrode comprising the 275kV purpose built tower base in parallel with the ring earth electrode (when all the 8 vertical rods are connected with bare copper cables)

The purpose of the tests at Llanrumney was to study the behaviour of the earthing systems under the influence of various energisation such as variable current DC / AC, variable frequency and impulse current injection.

4.2. Overview of Dinorwig test site

Earth impedance measurements performed on earthing systems buried in the soil at Llanrumney provides representative practical conditions to investigate the behaviour of the earthing systems at different energisation conditions. However, the soil medium at this test site is non-homogeneous with horizontally and vertically layered resitivities of the soil structure. It is well known that the conduction of electric current in the soil is mainly electrolytic in nature and occurs through the water molecules in the micro-pores of the soil

structure. Hence, it was decided to conduct experiments on test earth electrodes in a homogenous water medium. The lower reservoir of Dinorwig pumped hydro power station was chosen to conduct such experiments at it offered the potential of homogenous water conditions. Dinorwig pumped-storage hydro-electric power station is located in Llanberis, North Wales, UK. Figure 4.6 shows a plan view of the lower reservoir of the station, which is approximately 1.8km long and 400m wide. The reservoir is characterised by steep sides and a relatively flat bottom. The reservoir water level varies over a range of about 15m and, from power station records, the water level at any given time can be ascertained accurately.

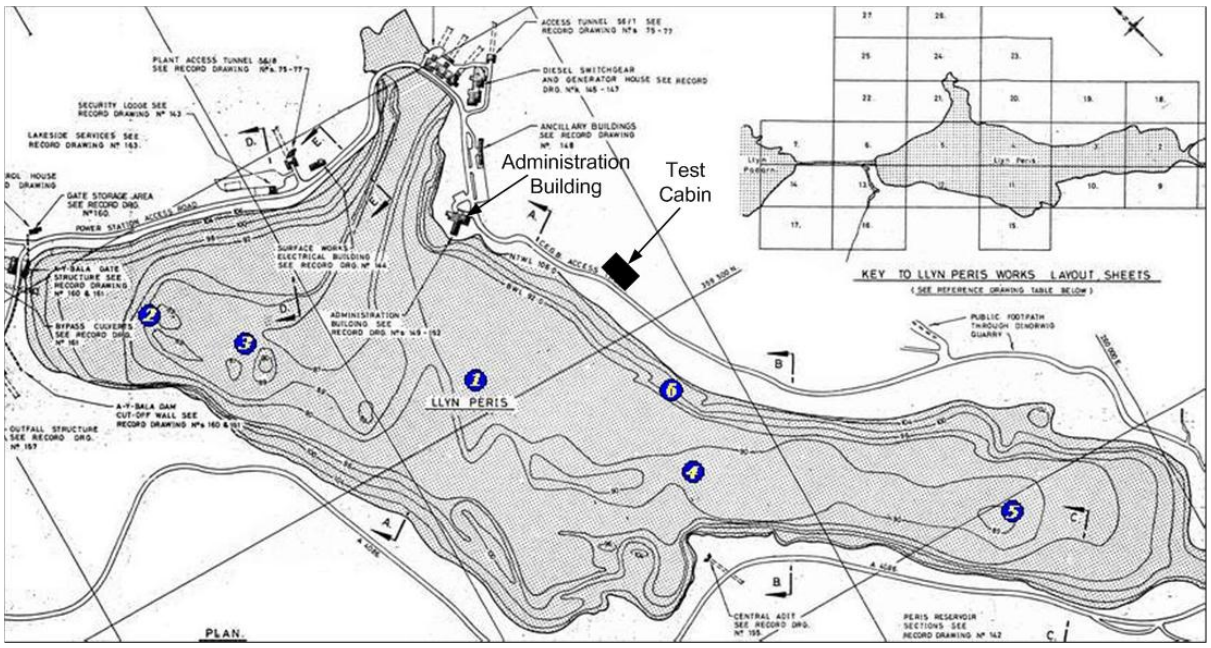

Figure 4.6 Plan of the lower reservoir at Dinorwig power station showing water resistivity test locations

4.2.1. Water resistivity measurements

Initial water resistivity measurements were carried out at positions close to the shore on 09/05/2007, 19/07/2007. Further detailed measurements were carried out on 30/07~01/08/2007 to investigate variations in water resistivity and temperature at different locations on the lake and also with water depth.

The water resistivity test locations are illustrated in Figure 4.6. Location ❶ was chosen as it corresponds to the central position of the proposed test electrode area. Location ❷ is close to the down-stream outlet while Location ❸ is inside the 'Wellington channel', the main channel for the power station. Finally, Locations ❹ and ❺ were chosen to investigate resistivity where the water may be less mixed. Location ❻ is at the end of the slip road. At Locations ❶, ❹ and ❺, detailed measurements were taken at different depths from the water surface. At the other locations, readings were taken approximately 0.5m below water surface.

4.2.2. Resistivity measurement survey on 09/05/2007

Due to the significant rise in the water level of the lake and to prevent the probe of the resistivity instrument being caught up in the rocks of the lake bed, the probe was retrieved frequently around Location ❻, according to the water level rise. As a result, all the initial measurements were restricted to the top layer of water with the probe at a depth of around 1 meter. A representative set of measurements taken on 09/05/2007 is listed in Table 4.1.

In Table 4.1, a log of measurements is shown for readings taken at 30 second intervals followed by the temperature measured (T˚C). The fourth column shows the actual conductivity results (μS/cm). The fifth column shows the temperature-corrected (to 20˚C) resistivity results (in Ωcm), based on the actual conductivity measurements. Salinity of the water and atmospheric pressure are also recorded, shown in columns 6 and 7.

Table 4.1 Typical water resistivity measurement results on 09/05/2007

Date	Time	Water Temperature (˚C)	Actual Water Conductivity (μS/cm)	Water Resistivity (Ωm)	Salinity (g/L)	Pressure (kPa)
2007/05/09	14:15:25	15.22	74	122	0.04	99.78
2007/05/09	14:15:55	15.24	74	122	0.04	99.81
2007/05/09	14:16:25	15.25	74	123	0.04	99.81
2007/05/09	14:16:55	15.26	74	122	0.04	99.81
2007/05/09	14:17:25	15.23	74	123	0.04	99.80
2007/05/09	14:17:55	15.23	74	123	0.04	99.79
2007/05/09	14:18:25	15.23	74	122	0.04	99.79
2007/05/09	14:18:55	15.25	75	122	0.04	99.79
2007/05/09	14:19:25	15.25	75	122	0.04	99.81

4.2.3. Resistivity measurement survey on 19/07/2007

A second set of lake water resistivity measurements, again at Location ❻, were taken on 19/07/2007 at the same position and depth with the first water resistivity measurement. A rise of water temperature from around 15˚C to around 19~20˚C was recorded, and the actual conductivity increased from around 74 μS/cm to 76~80 μS/cm. The water resistivity (after temperature correction), conductivity and temperature are plotted in Figure 4.7 (a) and (b) respectively.

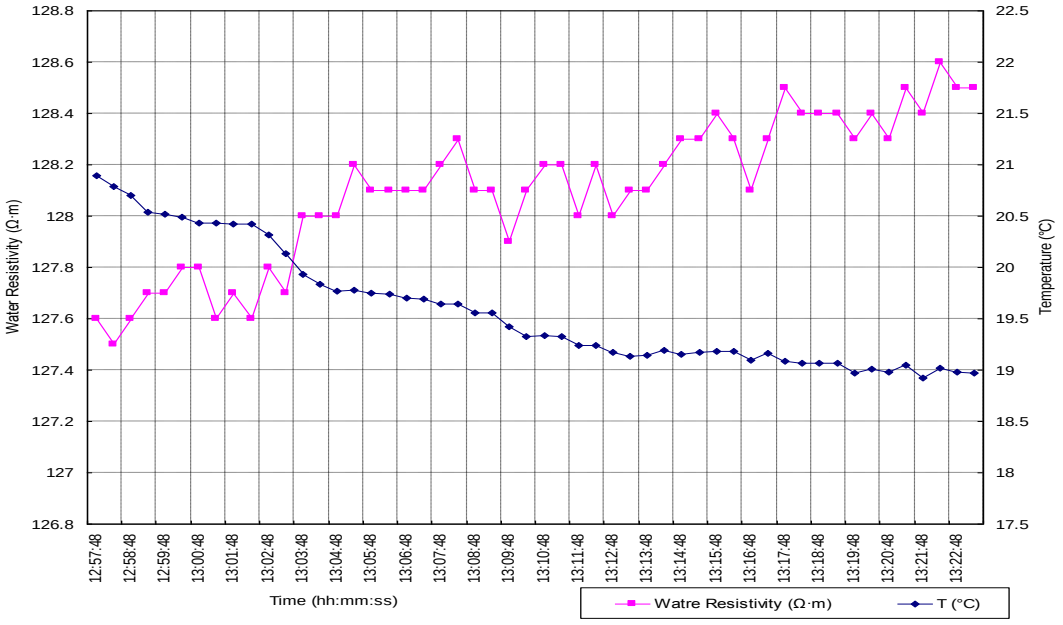

(a) Water resistivity (after temperature correction) results

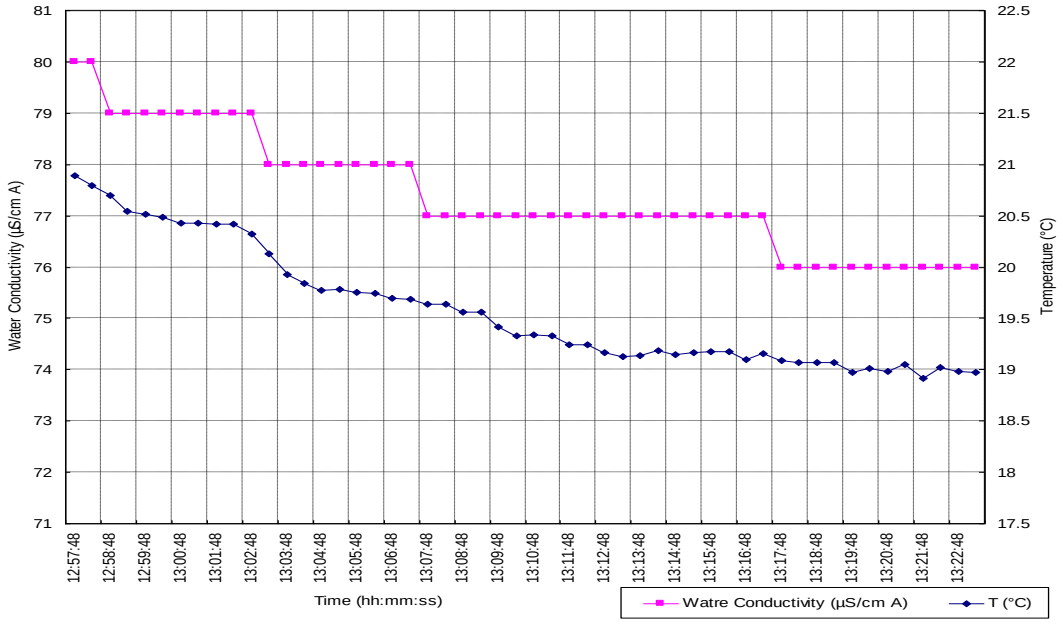

(b) Actual water conductivity measurement results

Figure 4.7 Water resistivity and conductivity measurement results on 19/07/2007

4.2.4. Resistivity measurement survey on 01/08/2007

During the site visit 30/07~01/08/2007, a comprehensive set of water resistivity measurements was carried out across the lake using the test boat. Table 4.2 lists the results obtained on 01/08/2007 at test Location ❶.

Table 4.2 Water resistivity measurement results on 01/08/2007

Date & time	Probe depth (m)	Water Resistivity (Ωm)	Water Temperature (˚C)	Actual Water Conductivity (μS/cm)
01/08/2007 15:30 onward	0.5	126	19.28	78
	1	126	19.28	78
	2	126	19.27	78
	3	126	19.22	78
	4	126	19.16	78
	5	126	19.17	78
	6	125	19.15	78
	7	126	19.16	78
	8	126	19.16	78
	9	125	19.15	78
	10	125	19.16	78
	11	125	19.15	79

The results obtained from the water resistivity measurements taken over a period of three days indicated that

- The lake water resistivity varied between 125Ωm and 130Ωm

- There was very little variation of resistivity with lake test location or with depth.
- A slight reduction in temperature with depth (up to 0.2 ˚C per 10m) was noted.

The results of water resistivity measurements at the reservoir confirm that the water resistivity and temperature on any given day is largely uniform, both depth-wise and area-wise.

4.3. Experimental set up at Dinorwig Test Site

A cabin (as test base) was set up 50m from the reservoir, to the right of the station administration building as shown in Figure 4.6. A motorboat was used to facilitate installation of the test earthing systems in the reservoir and for carrying out the water resistivity surveys. Vehicle and boat access to the water was obtained via a slip road.

To enable the test electrodes to be immersed in the lake at a fixed position, a pontoon was constructed from the shore to the electrode test position. A side view of this construction is shown in Figure 4.8. In this series of tests, two different test setups were adopted. The purpose of these comparative tests was to determine whether there are differences in results when locating the voltage sources a) in the test cabin or b) next to the test object.

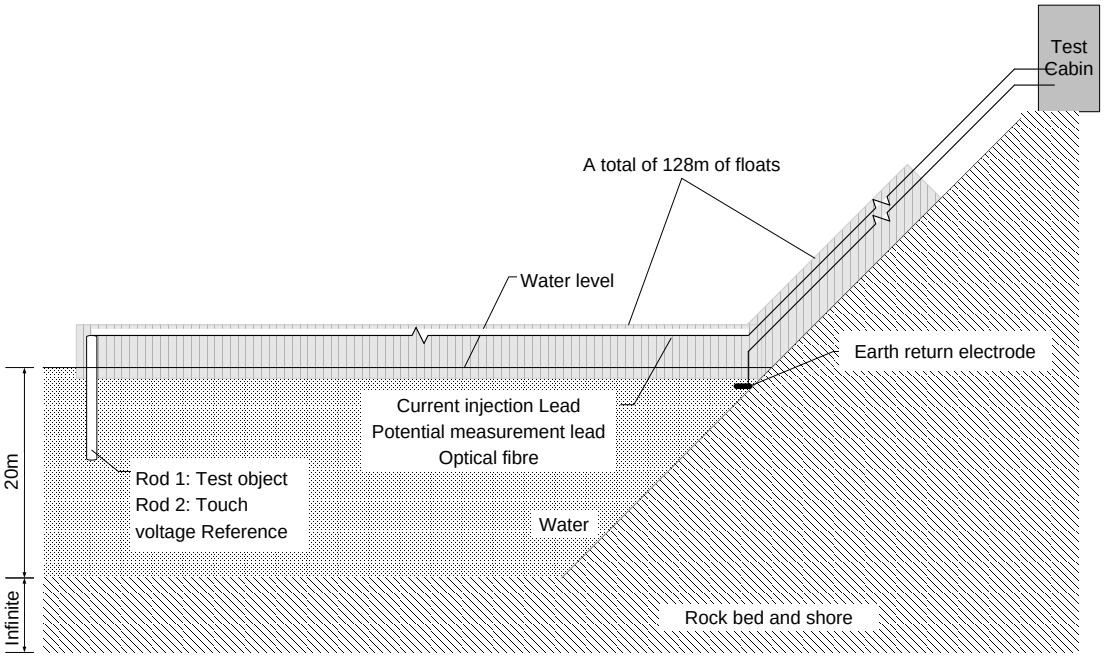

Figure 4.8 Side view of the test set up at Dinorwig

Figure 4.9 shows the plan of test set up where the test objects were (a) A 14mm diameter earth rod with 80cm immersed in water and (b) A 14mm diameter earth rod with 200cm immersed in water.

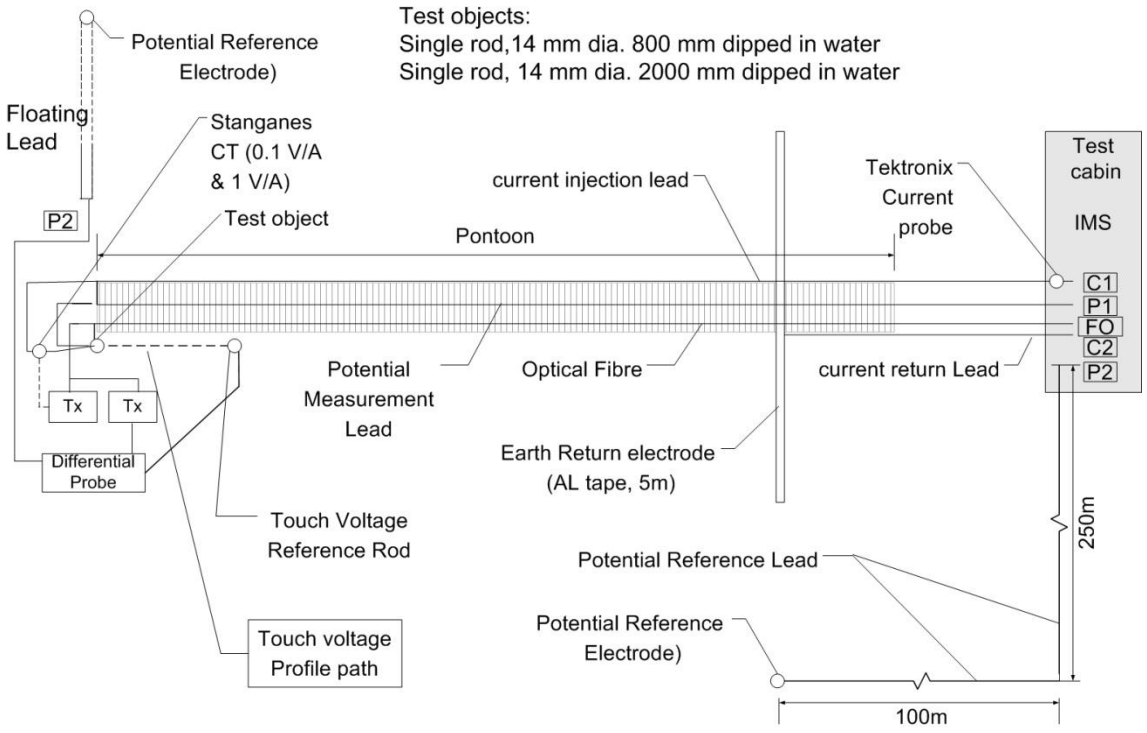

Figure 4.9 Plan view of test set up 1 (injection source placed in the test cabin 150m away from the test object)

The source (IMS, RF, Impulse generator, DET 2/2 and ABEM terrameter) were placed in the cabin. Injected current was measured with a Tektronix probe in the cabin. With all the test instruments located in the test cabin, two channels of fibre optic links were used to enable the measurement of current and touch voltage at the test electrode. The current measurement was realised by the Lilco CT and fibre channel EYE and the touch voltage was measured using DP25 (at 1/50) and fibre channel 'ABB'. The attenuation of 'EYE' channel was calibrated as 16 in lab but was recalibrated as 24.35 on site before laid out. The attenuation of channel ABB was verified to be '32', which is similar to previously obtained laboratory result.

Figure 4.10 shows the plan view of the test set up where the source (IMS, RF, Impulse generator, DET 2/2 and ABEM terrameter) were placed on the boat near the test object. In this experiment a single vertical rod (14 mm dia. and 800 mm immersed in water) and the horizontal tape (5m long and $50\times6mm^2$ at cross section) were used as test objects.

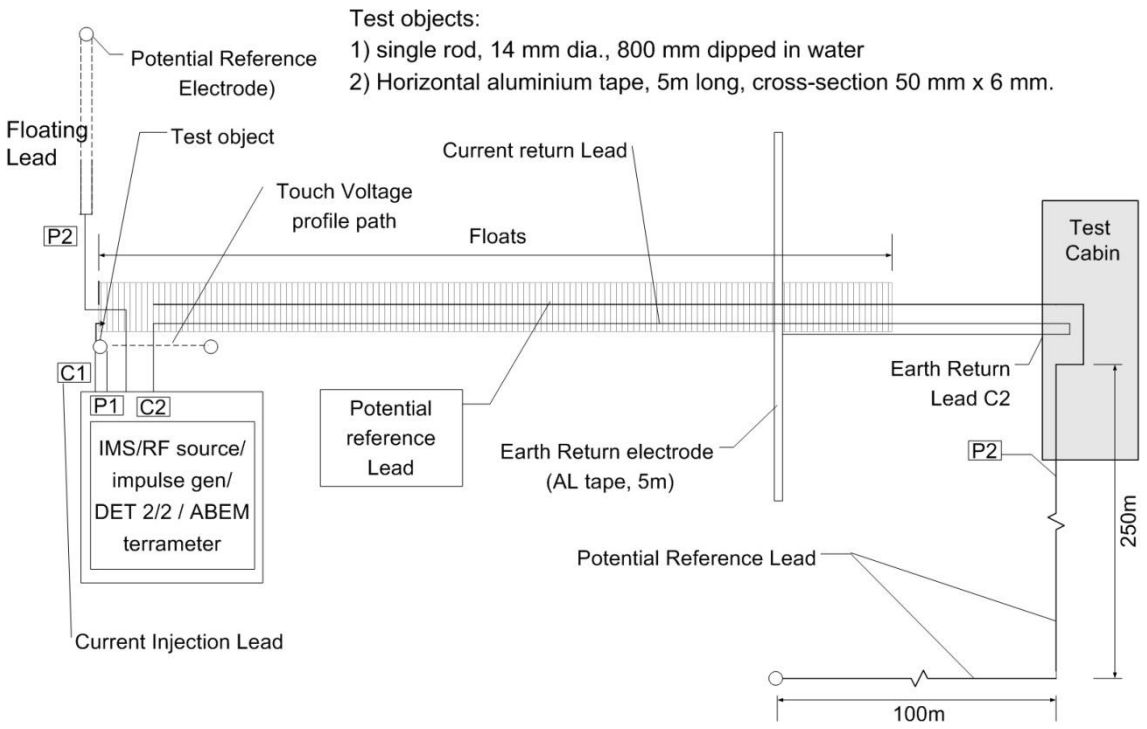

Figure 4.10 Plan view of test set up 1 (injection source placed near the test object)

Figure 4.11 shows the view from the end of the pontoon towards the test cabin. It also shows the outline of a 5m×5m grid test earth grid (diagonally oriented) beneath the water surface. The white vertical poles are used to control the depth of the test electrode. The pontoon is anchored at multiple positions to the lake bed and shore to maintain a fixed position.

Table 4.3 shows the list of earth electrodes, with dimensional details, tested at Dinorwig test site. The commonly used geometries such as single earth rod, horizontal conductor and grid earth electrodes were tested at Dinorwig to understand the behaviour of earth electrodes in homogenous medium and energised with DC / AC / impulse voltages.

Figure 4.11 View of 5m x 5m grid installed at the far end of the pontoon chain

Table 4.3 List of earth electrodes tested at Dinorwig test site

Type of earth electrode	Designation used in the experiments	Material	Dimensional details
Single rod	Rod 1	Copper	9mm dia., 80cm immersed in water
Single rod	Rod 2	Copper	14mm dia., 80cm immersed in water
Single rod	Rod 2A	Copper	14mm dia., 200cm immersed in water
Horizontal Electrode	Horizontal Electrode 1	Aluminium	5m long and $50\times6mm^2$ at cross section
Horizontal Electrode	Horizontal Electrode 2	Aluminium	15m long and $50\times6mm^2$ at cross section
5m x 5m grid	5m x 5m grid	Aluminium	5m x 5m earth grid, $50\times6mm^2$ at cross section

4.4. Description of earthing impedance measurement (IMS and Impulse) systems

4.4.1. Cardiff University Impedance Measurement System (IMS)

The Cardiff University Impedance Measurement System comprises a variable frequency signal generator (Perkin Elmer DSP lockin amplifier model 7225) coupled with power amplifier (QSC PLX 2402) used as a signal source. A Lock-in Amplifier produces a DC output proportional to the rms value of the AC measured signal. As can be seen in Figure 4.12, the input signal is amplified and then multiplied by the reference signal.

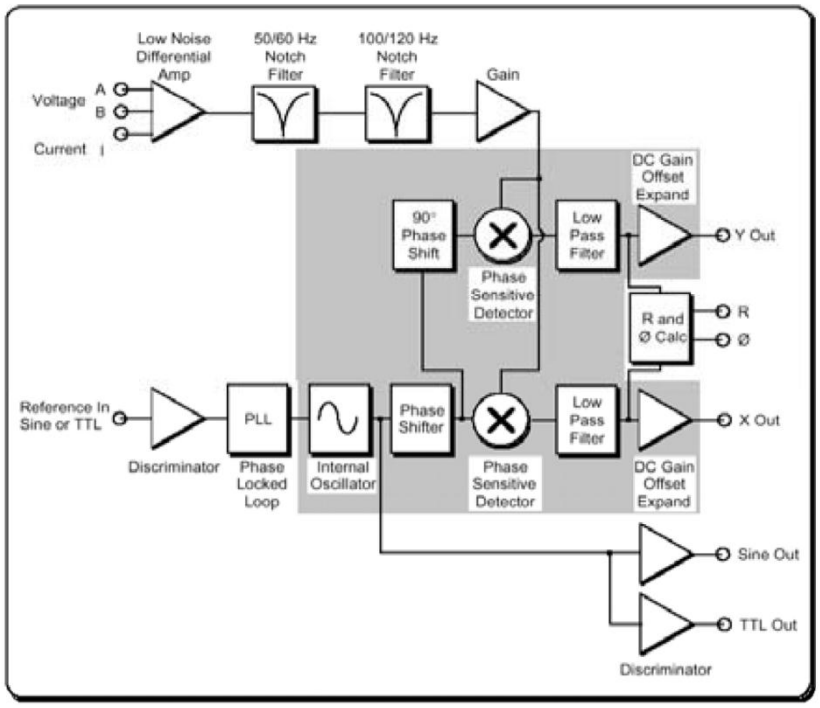

Figure 4.12 Principle of operation of lock-in amplifier

This multiplication process yields a series of signals involving the sum and difference frequencies of the input and reference signals. If the required signal frequency equals the reference signal frequency, the difference frequency component is a DC signal and can be extracted using a low-pass filter. To obtain both amplitude and phase information, two lock-in outputs are generated (X and Y). The X output is obtained from the product of the input signal and the reference oscillator signal, while the Y output is derived from the product of the input signal and the reference oscillator shifted by 90°. After filtering, these outputs provide the in-phase and quadrature components respectively of the signal phasor, from which the magnitude (R) and phase value (Φ) can be obtained. The power amplifier has maximum output power of 2.4kW and, in bridge mode, provides an open circuit voltage of

120V. The output of the power amplifier drives the current into the earthing electrode under test. Both the current injected into the system and the resulting earth potential rise are measured with transducers and fed into the inputs of two lock-in amplifiers to calculate the amplitude of the measured signals at a frequency of the reference signal. The lock-in amplifiers also compute the phase of the current and Earth Potential Rise (EPR) signals with respect to the reference signal.

Figure 4.13 shows the assembly of the Impedance Measurement System. A wide band current transformer model (Lilco 58MH100) was used as the current transducer for field tests.

Figure 4.13 Impedance Measurement System

It has an output rating of 0.1V/A, frequency response 1.5Hz to 20MHz, a capacity to measure RMS current of 100A, and 20ns response time. The minimum current measured during the experiments was of the order of few mA. At the minimum current measured during the experiments it provided a voltage output of few mV. It is to be noted that the IMS system has a resolution to measure accurately the single level of few hundred microvolts. Differential probe (SI9000) was used as the potential transducer. It has attenuation settings for 20 or 200, an accuracy of 2%, an input impedance of 2MΩ, an input capacitance of 2.5pF, a frequency

range DC to 15MHz and a maximum voltage measurement capability of 700V DC / 500V RMS.

4.4.2. Radio Frequency System (RF)

A Marconi Instruments signal generator 2019A was used as an input to the 25Watts CW, 10kHz to 250 MHz power amplifier to constitute a RF system. The Marconi make signal generator 2019A has an output frequency range of 10kHz to 1040MHz with a resolution of 10Hz over a frequency range 10kHz to 520MHz and a resolution of 20Hz over a frequency range of 520MHz to 1040MHz.

4.4.3. Impulse current injection system

A Haefley recurrent surge generator model RSG 481 is used as the signal source used for impulse tests. The maximum impulse charging voltage of this surge generator is 500V on open circuit which leads to a maximum test output voltage of approximately 400V. The components of the impulse generator such as impulse and load capacitances, front and tail resistors as well as inductances are adjustable in steps. The wave shape can thus be adjusted over a wide range (depending on the load (earthing system under test) RLC parameters). The maximum current injected into the earthing system under test depends on the energy stored in the impulse capacitance and the load RLC parameters. The typical maximum current obtained in the field with the recurrent surge generator was more than 5A with Test Tower Base as load.

4.5. Measurement of resistivity at test site locations with ABEM Terramer

4.5.1. Measurement of Resistivity at Llanrumney fields

Based on previous extensive soil resistivity surveys performed along the survey lines as shown in Figure 4.16, considerable data on soil resistivity for the Llanrumney test site has been obtained.

In addition, two surveys were carried out during the present project. The soil resistivity measurement results are shown in Figure 4.17 and Figure 4.18. The Wenner test set up as shown in the Figure 4.14 was used to map the soil resistivity along the survey line R7 as shown in Figure 4.16. Measurement of the ground resistivity was carried out by injecting a controlled current (I) between two electrodes into the ground, while measuring the potential (V) between two other electrodes. Direct current (DC) or an alternating current (AC) of very low frequency is used, and the method is often called DC-resistivity. The resistance (R) is calculated using Ohm's law: R = V / I. The Wenner configuration is a case where the four electrodes are equally spaced with a separation distance ‘a’. Using the ABEM Terrameter LUND Imaging System, multi-electrode gradient surveying was carried out by injecting current with a separation (s+2)a and simultaneously or sequentially picking up all the potential differences between the potential electrodes with the spacing a (Figure 4.15). Here, ‘s’ is an integer, which means the maximum number of potential readings for a current injection. Generally, the bigger the separation of the current electrodes is, the deeper is penetration of the injected current will be. With the smaller spacing of potential electrodes, the more details of potential variation are obtained. In practical applications, the selection of spacing ‘a’ and separation ‘s’ will be a trade-off between noise sensitivity, horizontal detail and depth penetration. In a multi-electrode gradient survey, a large number of current electrode combinations are used, scanning across the electrode layout with several different spacings ‘a’ and separations ‘s’.

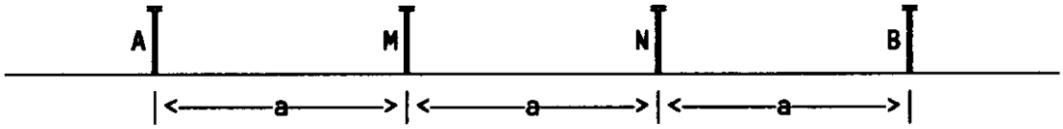

Figure 4.14 Electrodes spacing in Wenner configuration

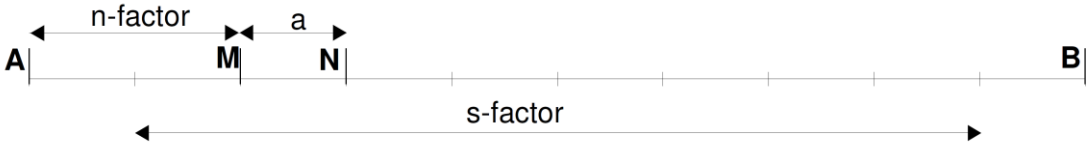

Figure 4.15 Gradient array layout showing the position of electrodes for a measurement of Wenner configuration with s factor of 8 and n factor of 2.

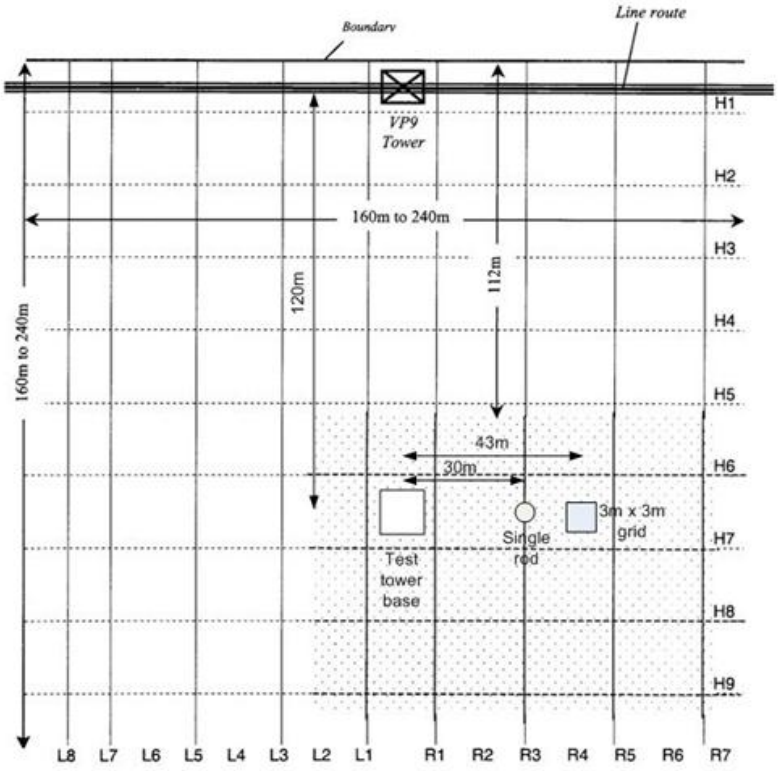

Figure 4.16 Soil resistivity survey lines at Llanrumney

Figure 4.17 and 4.18 were obtained using the computer program called RES2DINV. RES2DINV is a computer program which determines a two-dimensional (2-D) resistivity model for the subsurface, by inversion method, for the data points obtained from electrical imaging surveys using the ABEM Terrameter. The 2-D model used by the inversion program consists of a number of rectangular blocks. The arrangement of the blocks is loosely tied to

the distribution of the data points in the pseudo-section. The distribution and size of the blocks is so generated by the program, that, the number of blocks usually do not exceed the number of data points. The depth of the bottom row of blocks is set to be approximately equal to the equivalent depth of investigation of the data points with the largest electrode spacing. The survey using ABEM Terrameter, was carried out with a system where the electrodes were arranged along a line with a constant spacing between adjacent electrodes. A forward modelling subroutine was used to calculate the apparent resistivity values, and a non-linear least-squares optimisation technique was used for the inversion routine.

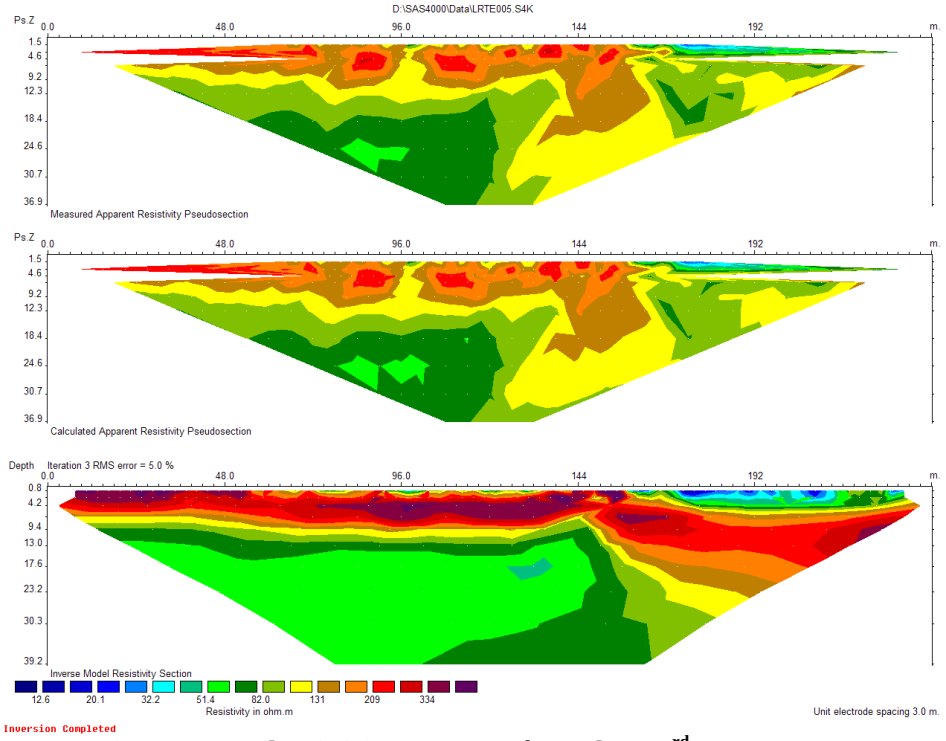

Figure 4.17 Soil resistivity survey performed on 23rd January 2009

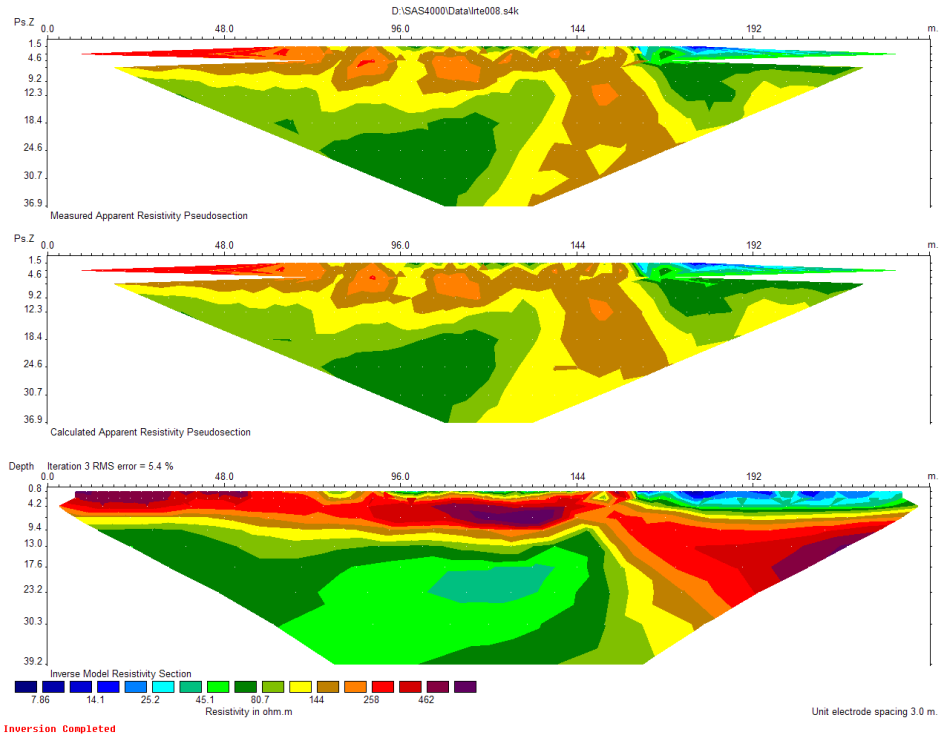

Figure 4.18 Soil resistivity survey performed on 1st April 2009

The soil resistivity results data shows that there is considerable variation in soil resistivity both according to the position in the field and also with depth. An illustration of the extent of such horizontal and vertical variation in soil resistivity can be seen in Figure 4.17 and Figure 4.18. Furthermore, experience has shown [66] that significant seasonal variations in soil resistivity occur. Accordingly, there is not one one representative simplified model for the entire test site. In order to obtain more representative simulation models, data from survey lines as close as possible to each test electrode have been used to construct simplified two-layer soil models. Table 4.4 shows the details of such models which were obtained for the single rod, 3mx3m grid, test tower base.

Table 4.4 Two layer soil model used for simulation

Earth Electrode	Resistivity of upper layer (Ωm)	Thickness of upper layer (m)	Resistivity of lower layer (Ωm)	Thickness of lower layer (m)
Single rod	250	9	70	infinite
3m x 3m grid	250	9	70	infinite
Test tower base	300	9	100	infinite

4.5.2. Measurement of Resistivity at Dinorwig

The resistivity survey was performed at the Dinorwig test site using an ABEM Terrameter LUND Resistivity Imaging system. Two consecutive measurements were performed. The test current values were fixed at 200 and 5mA in these two tests respectively. The obtained apparent resistivity values against Wenner spacing are plotted in Figure 4.19 (a) and (b). Two-dimension cross-section resistivity distributions obtained from the Lund system are shown in Figure 4.20. Comparing Figure 4.20 and Figure 4.21 and examining carefully the depth of the resistivity boundaries indicates that the water level changes (from 4.3m to 5.3m) between the times of the two measurements. On the 2D resistivity inversion result plots, the resistivity of water is shown heterogeneous and the values lie between 80 and 200Ωm. The readings from Hanna resistivity meter were 117Ωm. As can be seen in the Figure 4.19 the measured apparent resistivity shows a value of 104-135Ωm at the minimum Wenner spacing. As a result, the readings of Hanna meter will be used to represent the resistivity of water. Apart from the change of water level, the condition of the resistivity measurements has been kept the same. A detailed comparison between two sets of measurements can be made by the plot in Figure 4.21. The two sets of results are quite similar, although the results from the later test tend to have lower resistivity values with more variations in layer distribution.

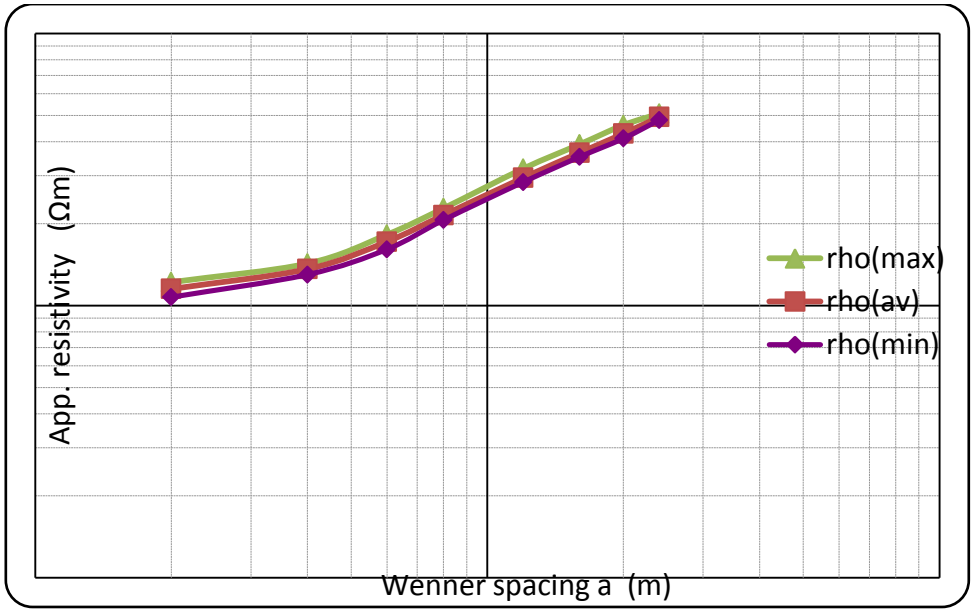

(a) Measurement at 200mA

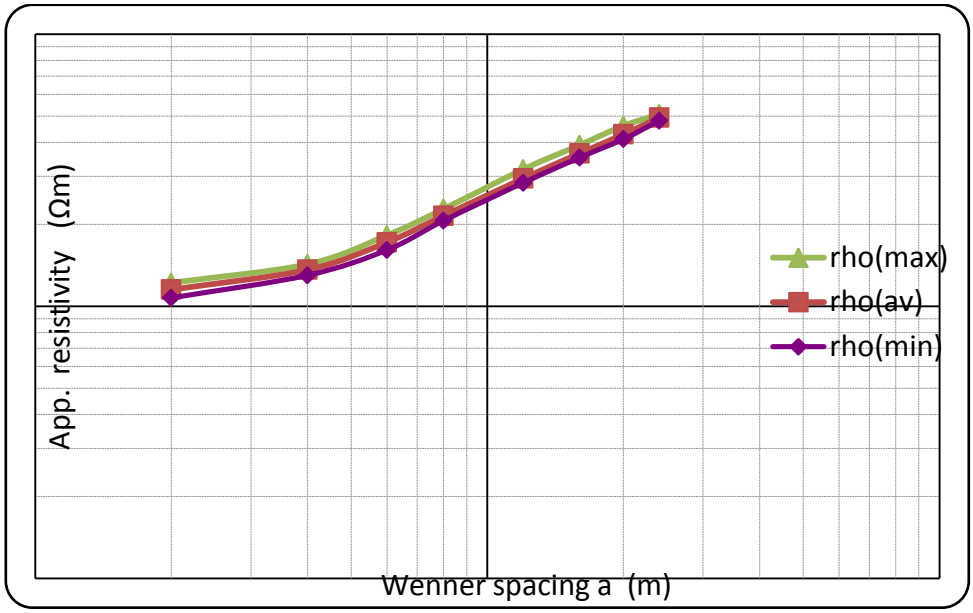

(b) Measurement at 5mA

Figure 4.19 Measured apparent resistivity against Wenner spacing

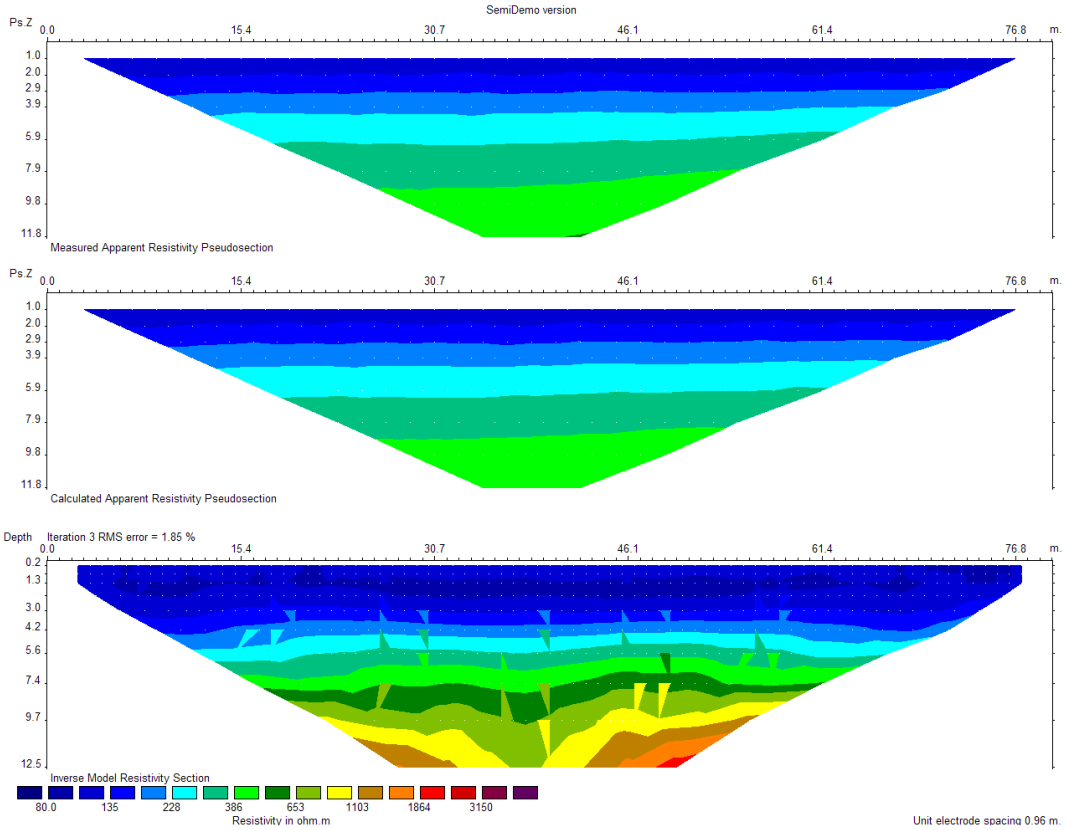

(a) Measurement at 200mA

Based on the results of the water resistivity survey, Dinorwig test site was represented as two layer model as shown in Table 4.5.

Table 4.5 Resistivity model of Dinorwig test site

Depth of layer (m)	Resistivity (Ωm)
5.5	115
Infinite	600

These resistivity values were subsequently used for CDEGS simulation purposes by substituting the actual depth of low resistivity water level at the time of measurements of test electrodes: Rod 2A (Rod having dimensions 14mm diameter and 96cm immersed in water) and 5m x 5m grid. Unlike the Llanrumney test site, there is relative ease of the representation of the resistivity of the conducting medium in the form of horizontally layered model for Dinorwig test site. The measured resistivity pattern of Dinorwig test site is shown in Figure

4.21. As seen from the inverse model resistivity section of the figure (lower part of Figure 4.21), the upper layer of water (up to about 5m depth) is of fairly uniform resistivity close to 100Ωm. The water level measured at the start of the resistivity measurement was 3.7m. The resistivity of the bottom layer is gradually becoming higher. The bottom of the lake at the Dinorwig test site is rocky. The seepage of water through the porous rock may be the cause of the gradual increase in the resistivity of the lake bottom below 5m depth.

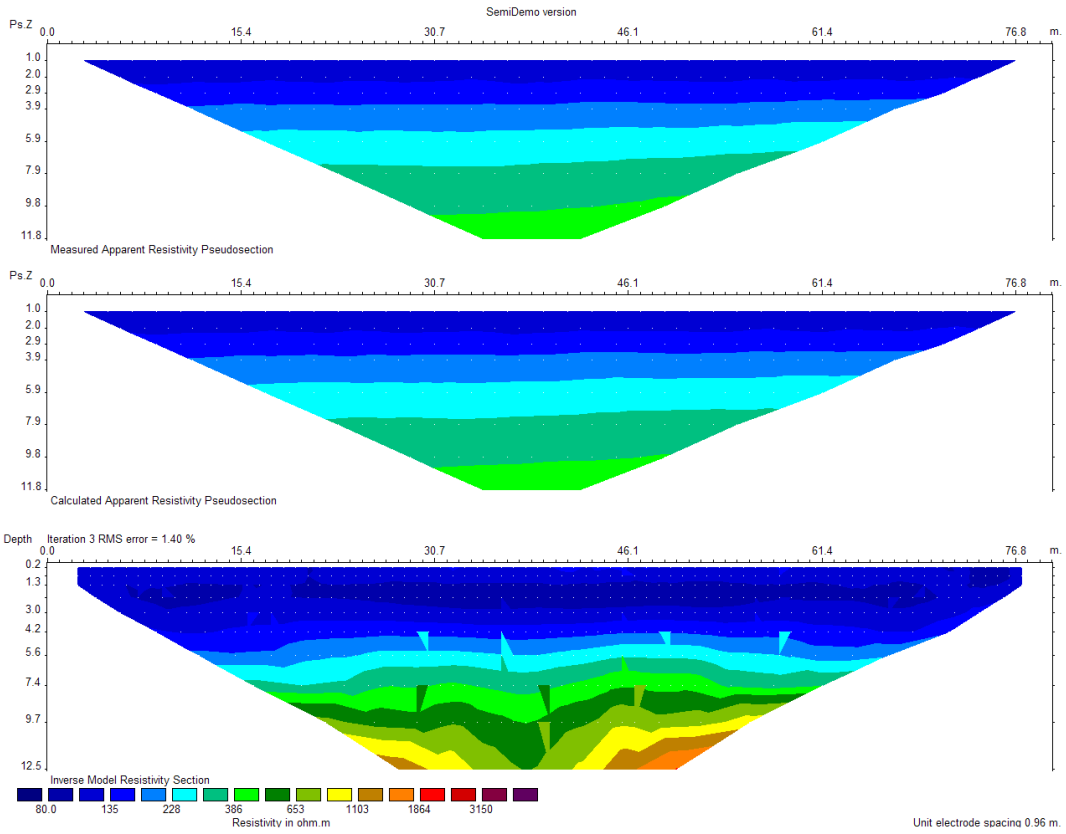

(b) Measurement at 5mA

Figure 4.20 Two dimension resistivity distributions

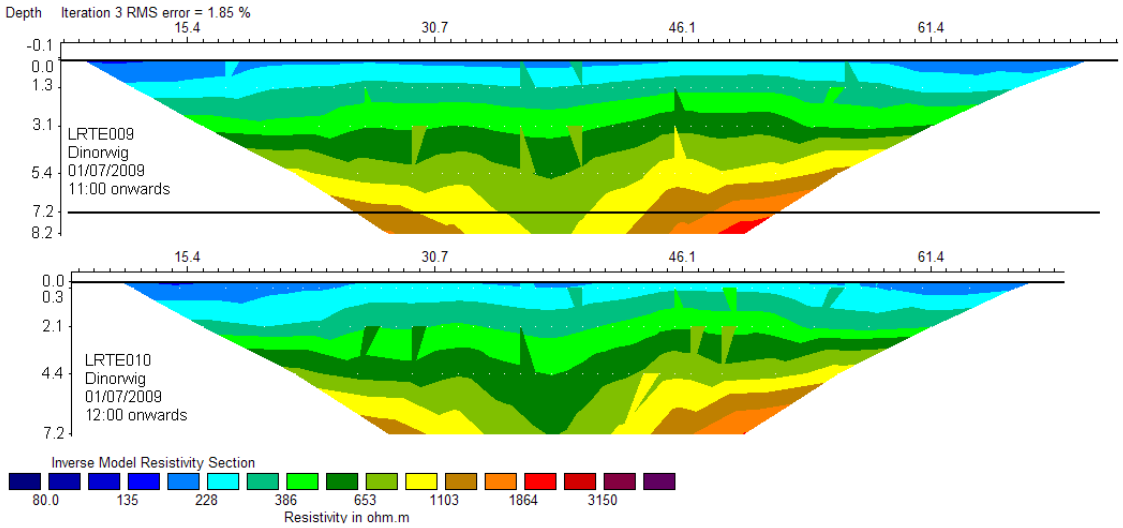

Figure 4.21 Resistivity of lake bed in two measurements

4.6. Summary

As described in this chapter Llanrumney test site has various practical earthing systems such as single rod, cluster of rods, horizontal electrode, ring earthing system, 3m x 3m grid, test tower base and National Grid 275kV operational tower base VP9. The soil resistivity measurements at Llanrumney test site have shown that there is considerable variation in soil resistivity both according to the position in the field and also with depth. Furthermore it has also been observed that the significant seasonal variations in soil resistivity occur.

The Dinorwig test site had a scope of testing the practical earthing systems such as single rod, horizontal electrode and 5m x 5m earthing grid in the relatively uniform medium as lake water of the pumped hydro power station. The water resistivity measurements conducted at various locations of the lower lake Lynn Peris of the Dinorwig pumped hydro power station indicated that the water resistivity is fairly uniform over a given day. There are some seasonal variations in the resistivity of water which may be attributed to the difference in temperatures.

Cardiff University Impedance Measurement System (IMS), Radio Frequency System, Impulse Current Injection System and ABEM Terrameter soil resistivity systems were also introduced in this chapter.

Chapter 5: Characterisation of earth electrodes under variable frequency and impulse energisation using full scale field tests

The earth resistance/impedance of operational power system installations is normally measured using test equipment generating low injection current magnitudes [11] [31]. For earth impedance measurements, a sinusoidal signal is injected into the earth electrode and by measuring the earth potential rise at the point of injection, the earth impedance is calculated by taking the ratio of the measured voltage to injected current. Such ac tests are normally performed at frequencies away from the power frequency [8] [24] [25] [32]. Many commercial 'composite' earth testers are available and these use a variable frequency switched DC energisation and measure the test electrode earth resistance [24]. Previous work [32] has indicated that quite different values of earth resistance/impedance are obtained when using test equipment producing different current magnitude, wave shape and frequency.

The high frequency behaviour of earthing systems is of interest in applications where high frequency currents are to be effectively dissipated in the earth, such as lightning currents or transient surges. The earthing systems are also expected to keep the step, touch and transferred earth potentials within the limits specified by the standards [11] [31]. If the safety voltages and transferred earth potential magnitudes are within the specified limits, it provides human safety as well as protection to the neighbouring communication circuits during lightning faults, transient faults and power frequency fault conditions on the electrical power systems.

The staged fault test employs a test current injection of magnitude similar to the fault current level into the earthing system under test and then measuring the resulting earth potential rise (EPR). The ratio of the RMS value of the Earth Potential Rise (EPR) to the RMS value of the injected current gives the value of earth impedance. This method is rarely used [16] due to two main drawbacks;

a) It involves disconnecting the earthing system from the circuit which it is protecting, which may in turn result in the protected system to be cut off from power supply for the duration of testing.

b) The injection of high current levels similar to the fault current magnitudes is not economical particularly if the earthing systems to be tested are large such as substation earthing systems, where the magnitudes of fault currents are high.

Other methods of measuring earth impedance involve the use of relatively smaller magnitudes of sinusoidal test currents at different frequencies of interest. The ratio of RMS value of resulting earth potential rise to the RMS value of injected current gives the value of measured earth impedance of the system. Some instruments use impulse signals to test the earth impedance. The ratio of the FFT (Fast Fourier Transform) of the resulting EPR impulse signal to the FFT of the injected current impulse signal will give the values of measured earth impedance in frequency domain [33] [43].

In order to measure the earthing impedance at variable frequency and current magnitudes, a series of earth tests were performed at the Cardiff University test site in Llanrumney and at the Dinorwig Power station test site (lower lake Lynn Peris). The test results were obtained with different energisation sources such as switched DC/variable frequency, AC/variable current AC/low voltage impulse. Tests were carried out on earthing systems including an operational 275kV transmission tower VP9, the test tower base, a small grid (3m x 3m size), single earth rod, ring earthing, cluster of rods and various Dinorwig test setups. The measured voltages and currents together with calculated impedance / resistance values are presented here.

5.1. Tests on single earth rod at Llanrumney test site

5.1.1. Earth resistance / impedance tests on single earth rod

Figure 5.1 shows the test set up for measuring the earth impedance of a single rod with the Cardiff University Impedance Measurement System (IMS) [32]. The test object was a single copper rod (Rod 1 of ring earthing system shown in Figure 5.1) with a 16 mm diameter and buried at 2.4m depth. The test current was injected in the test object (single earth rod) and the return current was extracted from the test tower base (shown in Figure 5.1), which was 30m away from the test object. The earth potential rise at the point of current injection in the test object was measured with respect to a remote reference electrode, as shown in Figure 5.1 which was placed at a distance of 100m from the test object and at 90° to the return current lead. The test sources were fed from a 240V A.C. power supply via an isolation transformer.

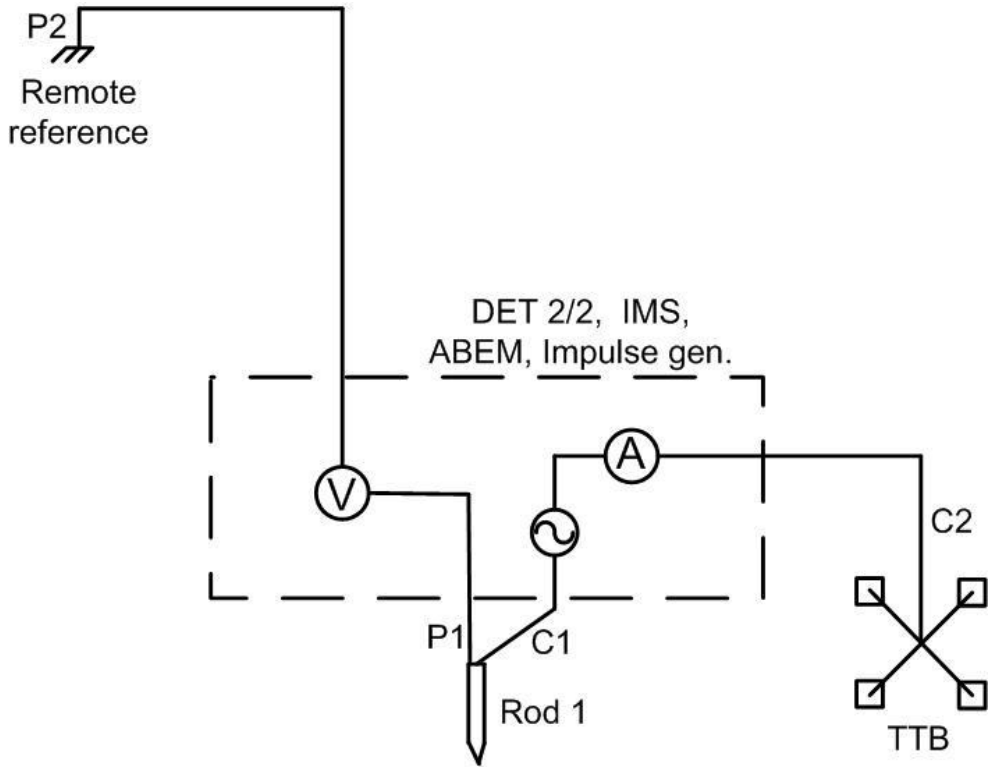

Figure 5.1 Test set-up for measurement of earth impedance of single earth rod

The measured values of the rod earth impedance at different frequencies obtained using the IMS are shown in Figure 5.2. The earth impedance of a single rod was measured at varying current magnitudes (few tens of mA to few amperes) although for these initial tests, the current was not kept constant over the entire frequency range. At any given current

magnitude, there is a reduction of about 10% in the measured earth impedance of a single rod over the frequency range from 20Hz to 100kHz. It is to be noted that the phase angle of the measured earth impedance of single earth rod was observed to be less than 5° and capacitive in nature. This small capacitance effect will result into marginal decrease of the measured earth impedance. However, the reduction in the measured earth impedance of 10% is found to be a decrease in the resistive nature, which can be explained by the following statement. It was calculated that, in order for the capacitive effect to result in the reduction of 10% impedance, the phase angle should have been more than 30°.

In addition at low frequencies (< 100Hz), there is a pronounced frequency effect for currents lower than 50mA. This finding has important implications for low current test systems. All the curves tend to converge at the same point at a frequency of around 100 kHz. It is to be noted that the IMS (Impedance Measurement System) filters the noise in the measured EPR signal with the help of a suitable filter. The current was measured with the help of a LILCO CT with an output of 0.1V/A. The minimum current measured was 13.6mA. At the minimum measured current during this experiment it provided a voltage output of 1.36mV. It is to be noted that the IMS system has a resolution to measure accurately the single level of few hundred microvolts.

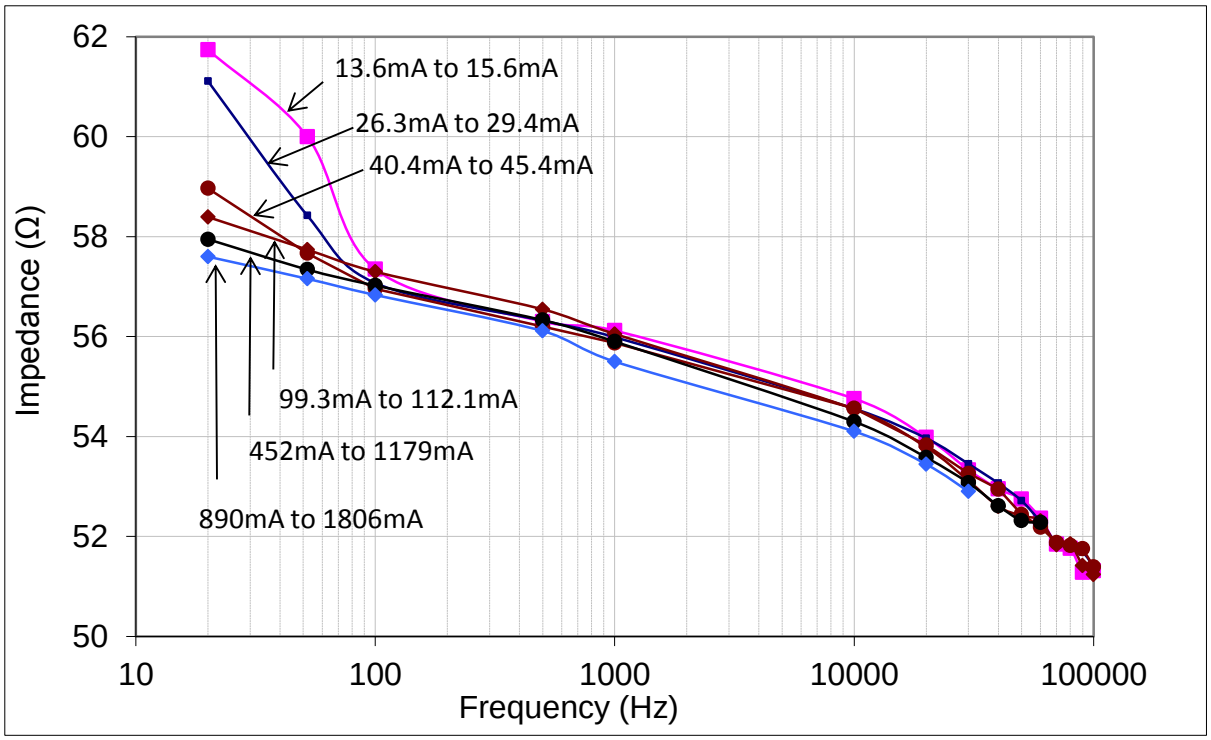

Figure 5.2 Earth impedance tests with IMS on a single 2.4m earth rod

Figure 5.3 shows the variation of earth impedance with current for the same set of test results. As can be seen from the figure the effect of current on earth resistance / impedance is more significant at low frequency e.g. when the measurement is performed with the ABEM Terrameter (switched DC frequency of 0.5Hz) and using the IMS at 20Hz. Figure 5.3 also shows the earth resistance of the single earth rod measured with the DET 2/2 (switched DC frequency of 128Hz). The earth impedance at frequencies above 100Hz have negligible variation with current. The effect of current magnitude on the impulse resistance is also shown in the figure. The impulse earth resistance was calculated from the ratio of the impulse earth potential rise at the instant of peak impulse current and the peak value of the impulse current waveform. It was observed that the peaks of the earth potential rise and the current waveforms occurred almost at the same instant for slow (rise time greater than few hundreds of μs) and fast (rise time of few μs) impulse waveforms for the single earth rod as shown in Figure 5.4 and Figure 5.5 respectively.

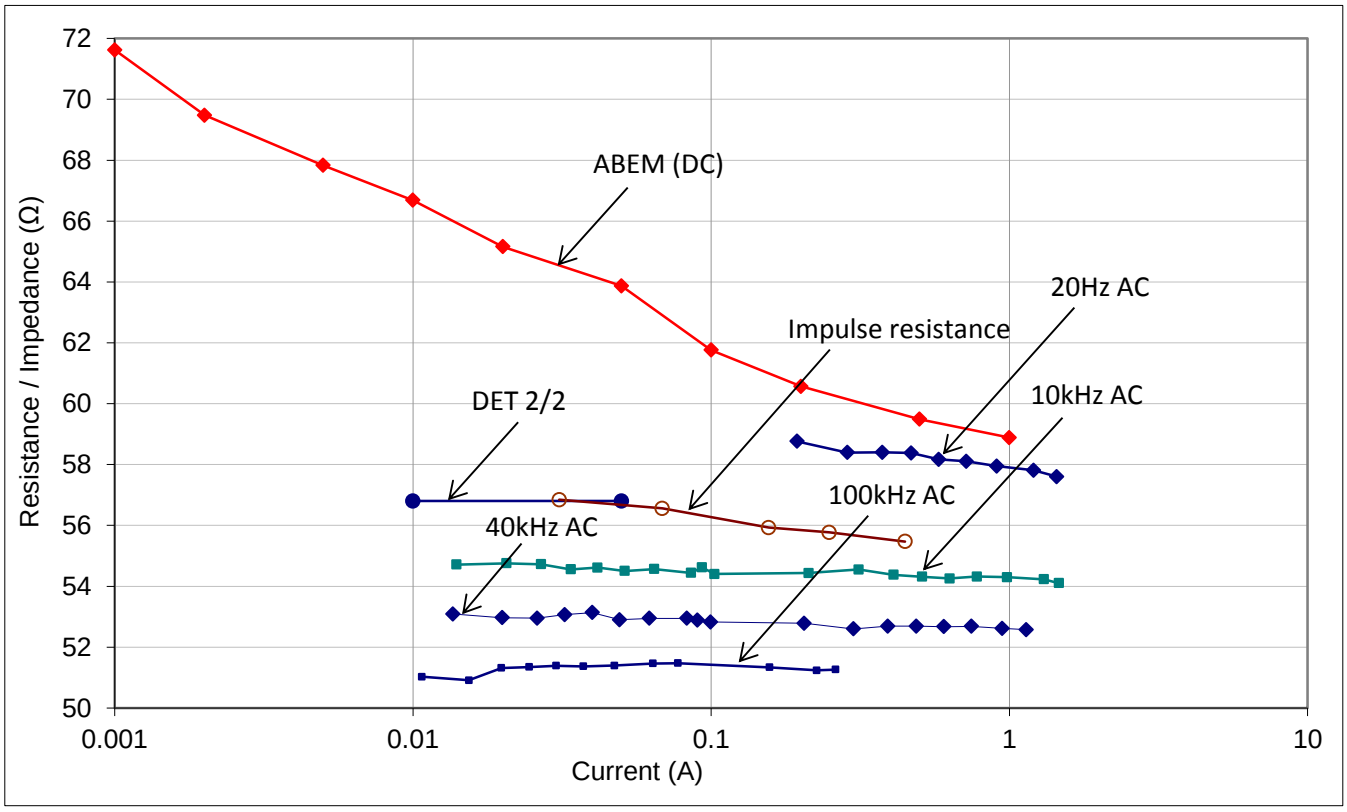

Figure 5.3 Variation of impedance with current

5.1.2. Low Voltage Impulse Tests on Single Earth Rod

Slow and fast low voltage impulse tests were performed on the single earth rod to investigate the behaviour of the earth impedance under various impulse conditions. Typical results of the injected current and the measured earth potential rise for the slow and fast impulse tests are shown in Figure 5.4 and Figure 5.5 respectively. The peak values of the injected current and the earth potential rise recorded during the low voltage impulse tests are also shown in Figure 5.4 and Figure 5.5. The Fast Fourier transformed response of the impulse tests is shown in Figure 5.6. As can be seen from the figure, the earth impedance is seen to be decreasing as

the frequency content in the impulse signal increases. Comparing Figure 5.2 and Figure 5.6 we can infer that the response of single earth rod to the variable frequency tests closely resembles to that of the response of the single earth rod to the low voltage impulse tests.

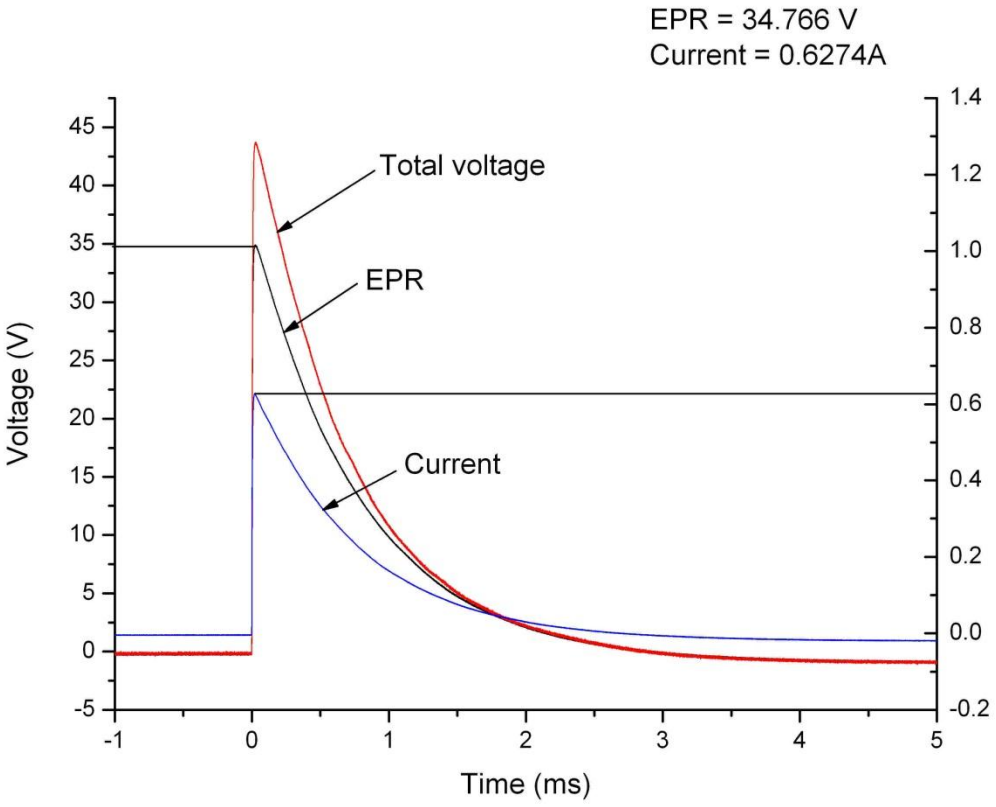

Figure 5.4 Low voltage impulse (LVI1) test waveforms

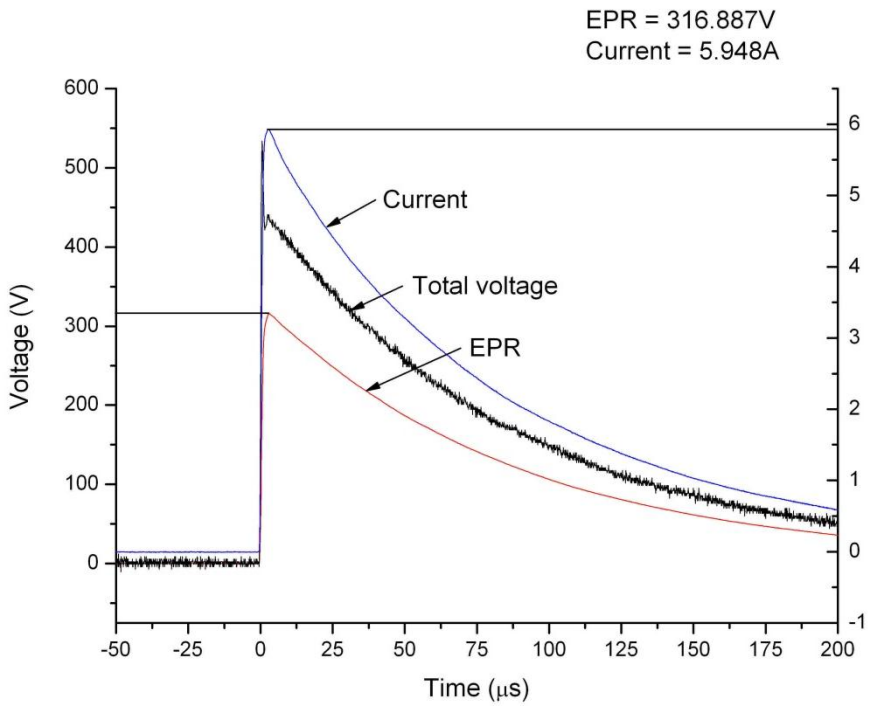

Figure 5.5 Low voltage impulse (LVI2_B) test waveforms

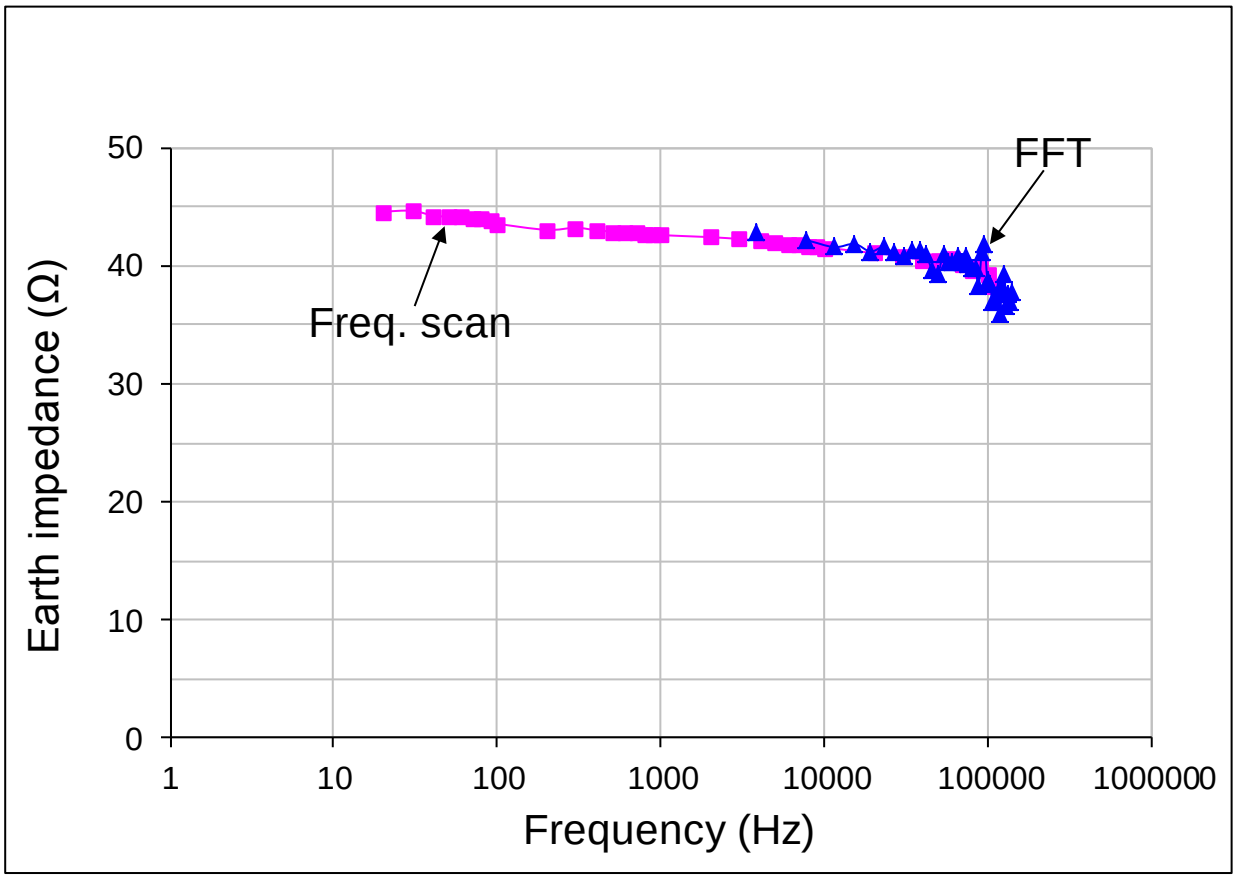

Figure 5.6 Comparison of FFT of impulse waveforms and frequency scan of earth impedance for single rod

5.2. Tests on single earth rod at Dinorwig test site

Figure 5.7 shows the set up for testing a single earth rod at Dinorwig test site. As can be seen in the figure, the test rod electrode was located at the end of the pontoon. A potential reference electrode with a floating lead was placed 70m away and perpendicular to the pontoon. The current return electrode was immersed in the lake towards the shore-end of the float system. The test electrode comprised a single copper earth rod, 14mm in diameter and 1.2m long. The top end of the rod was fixed to the end section of the floating pontoon in a vertical orientation. The length of the test rod immersed in water was 0.8m. A single rod, 0.15m long and 9mm in diameter, was used for the '90°' potential reference electrode. A 5m long aluminium tape, 50mm×6mm, 0.6m below water surface, was used as the current return electrode.

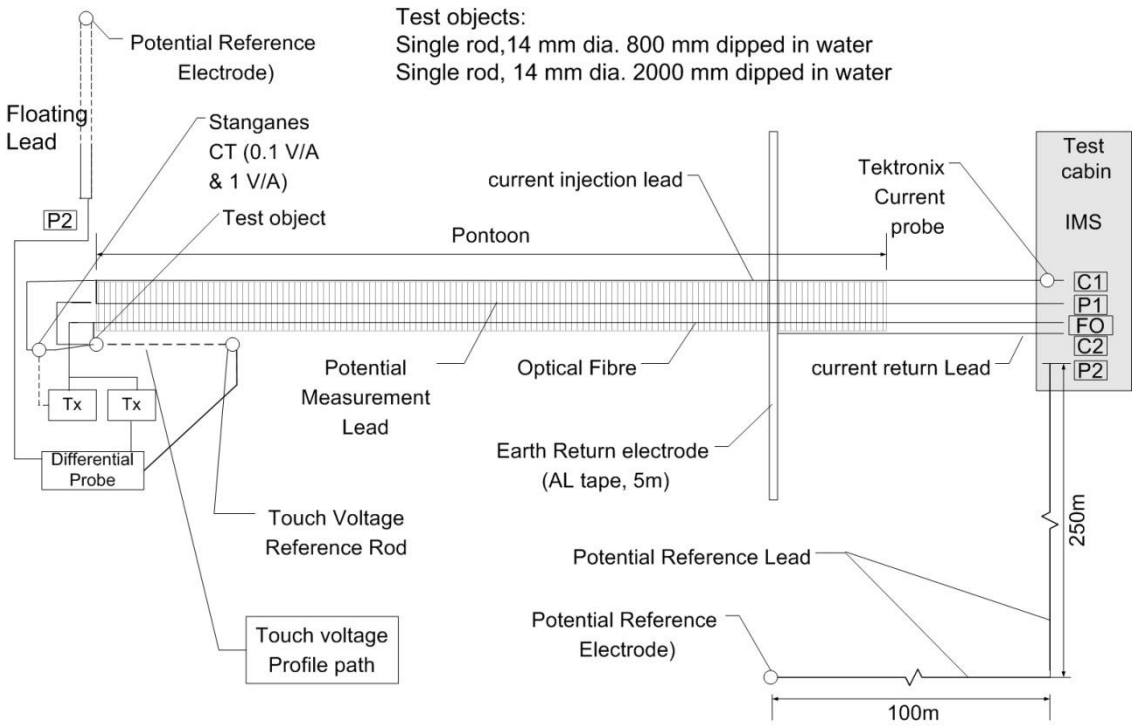

Figure 5.7 Plan view of test set up for testing single rod at Dinorwig test site

In previous preliminary tests [43], the voltage sources were located in the test cabin and the test electrode was energised using a transmission line located along the pontoon. However, for this particular series of tests, the voltage sources and measuring instruments were located in the boat adjacent to the test electrode. This arrangement was chosen in order to minimise the effects of coupling between the test leads. The test sources and instrumentation were fed from a low-voltage supply installed along the pontoon via an isolation transformer. A short lead from the boat to the pontoon was used to inject current from the source into the test object. The current return electrode placed in the water at the shore-end of the pontoon was connected back to the source using an insulated line laid along the pontoon. An additional lead was used to obtain potential measurements between the test electrode and the '90°' reference electrode. Optically-isolated differential voltage probes and current probes were used for voltage and current measurements respectively. The voltage sources comprised; i) two DC sources: a 'composite' commercial earth resistance tester (DET 2/2) and a geo-physical resistance meter (ABEM Terrameter), (ii) two AC sources: a variable AF impedance measurement system (IMS) [42], an RF measurement system, and (iii) a HAEFELY recurrent surge generator.

A DC resistance of 117.6Ω was measured using the 'composite' tester and 118.2Ω was obtained with the geo-physics earth tester at its highest current setting of 500mA. The calculated 'earth' resistance of the rod using Equation (5.1) [1] is 95.4Ω, assuming a water resistivity measured at 93.5Ωm.

$$R_{rod} = \frac{\rho}{2\pi l}\left(\ln\left[\frac{2l}{r}\left(1+\sqrt{1+(r/2l)^2}\right)\right]+\frac{r}{2l}-\sqrt{1+(r/2l)^2}\right) \tag{5.1}$$

The 'earth' resistance calculated using a commercial earthing software (CDEGS) [67] is 100.3Ω, based on a simplified two-layer medium with a 9m upper-layer of 93.5Ωm, εr=80

(water) and a lower layer of about 600Ωm, εr=1 (lake bed rock). Using the same software, with the electrode modelled in a single-layer medium having the properties of the water, a resistance of 98.2Ω is calculated.

It was observed that the measured resistance changes with current magnitude. Figure 5.8 shows the reduction in earth resistance over the range 1mA to 500mA for DC tests using the geo-physics meter. Although current dependence of earth impedance has been studied previously, the focus has been on soil ionisation phenomena at very high current magnitudes. Current dependence of earth resistance at pre-ionisation levels was reported in [14] in the range 130 to 1300A. However, commercial earth testers usually operate at current magnitudes below 10A and some instruments generate currents as low as of the order of 100mA. These results suggest that low current magnitude tests may over-estimate the earth resistance of electrodes compared with the resistance seen at higher current magnitudes of the levels seen under the fault conditions.

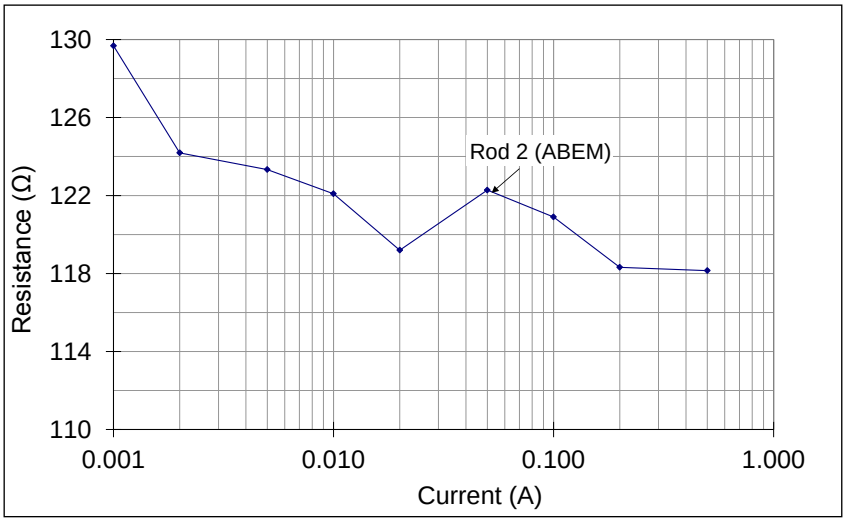

Figure 5.8 Effect of current magnitude on measured earth resistance

5.2.1. Rod 'earth' impedance

Using the same test setup as for the earth resistance tests, the 'earth' impedance of the rod was measured using the IMS system. At 50Hz, the measured value was 122.2Ω with a current injection of 400mA. For this particular electrode, the value is close to the measured DC 'earth' resistance. The comparison of the measured impedance of the single earth rod at 50Hz with the DC earth resistance and the calculated / simulated values of earth rod impedance is shown in the Table 5.1.

Table 5.1 Comparison of measured earth resistance / impedance with analytical impedance

Test object: Single rod 14mm Ø, 80cm immersed in water	Resistance / Impedance
DC resistance measured with DET 2/2	117.6Ω
DC resistance measured with ABEM	118.2Ω @ 500mA
Impedance @ 50 Hz	122.2Ω @ 400mA
Calculated value of impedance	95.4Ω
Simulated value of impedance with CDEGS software	100.3Ω

As can be seen from the table, the measured earth resistance / impedance at 50Hz are in fair agreement. However, the analytical calculations show lesser value of the impedance. This could be attributed to the constraint in accurately estimating the lower layer rock bed resistivity. The simulation results are further discussed in Chapter 6.

5.2.2. Variable frequency earth impedance measurement

The AC tests were extended to determine the earth impedance over the frequency range 20Hz to 10MHz and the results are plotted in Figure 5.9. The IMS system was used to test over the range 20Hz to 40kHz and the source was maintained at a constant current magnitude of 400mA throughout, to eliminate the effect of current magnitude on impedance. The RF system was employed above 30kHz. As can be seen in Figure 5.9, there is a close overlap in

the results for the common frequencies tested by both systems (IMS and RF) for a frequency range 30kHz to 40kHz.

Using a lumped-parameter circuit model for a rod-type electrode, as shown in Figure 5.9, the frequency response of the system was calculated using P-SPICE. The calculated values of R, L, and C are shown in Figure 5.10 using the previously defined geometric dimensions of the rod (14mm Ø, 80cm immersed in water) and the water resistivity and permittivity (ρ=93.5Ωm and εr=80). R, L and C for the vertical rod were calculated using equations (5.2), (5.3) and (5.4) given by [68]

$$R = \frac{\rho}{2\pi\ell}\left[\log\frac{4\ell}{a} - 1\right](\Omega) \quad \text{------ (5.2)}$$

$$C = 2\pi\varepsilon\ell\left[\log\frac{4\ell}{a} - 1\right](\mathrm{F}) \quad \text{------ (5.3)}$$

$$L = \frac{\mu_0\ell}{2\pi}\left[\log\frac{2\ell}{a} - 1\right](\mathrm{H}) \quad \text{------ (5.4)}$$

The calculated frequency response of the rod obtained from the circuit model is also shown in Figure 5.9 together with values calculated using the CDEGS model with the 2-layer model (9m upper-layer of 93.5Ωm, εr=80 (water) and a lower layer of about 600Ωm, εr=1 (lake bed rock)).

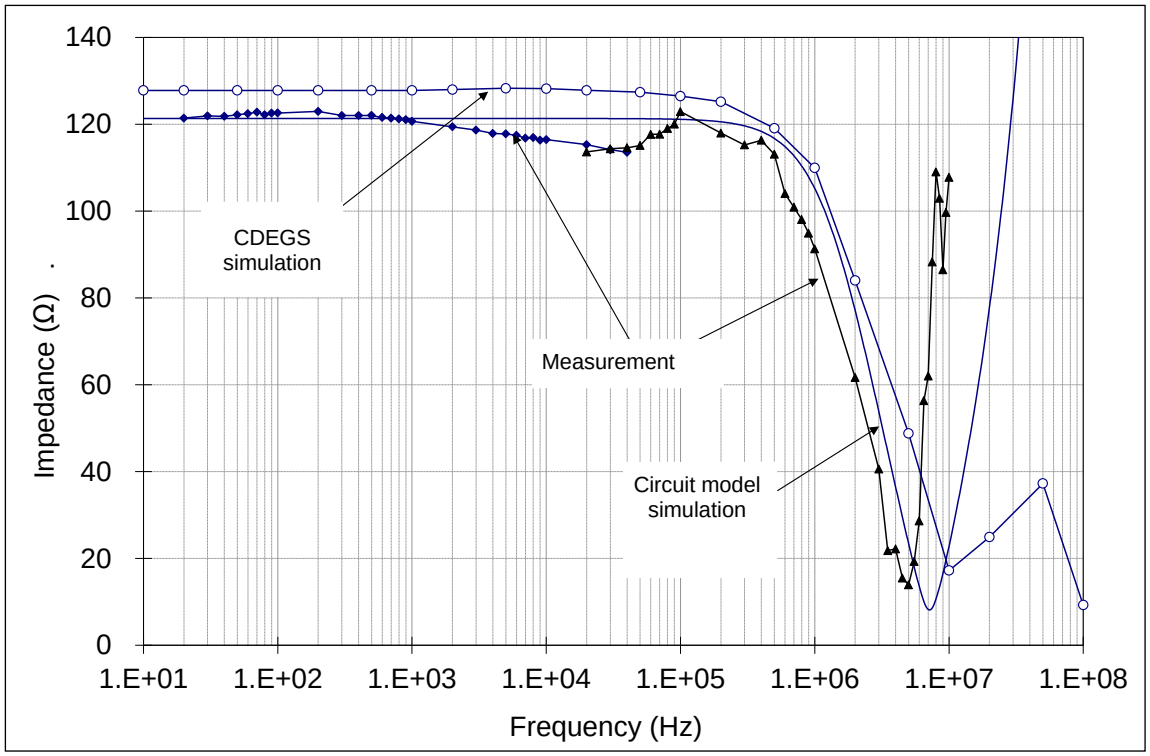

Figure 5.9 Plots of measured and simulated earth impedance magnitude with frequency

As can be seen in Figure 5.9, the overall shape of the three curves (one measured and two simulated) is similar. The shape of the curves is characterised by a relatively flat region of impedance from low frequency up to the region of 200Hz to 500kHz. Over this lower frequency range, the measured earth impedance (resistance) is about 20% higher than the simulated values. However, in the frequency range 20Hz to 40kHz, there is an indication of a reduction in measured impedance that is not predicted using the conventional earthing system model that assumes constant resistivity and relative permittivity. Above the 500kHz frequency, the measured earth impedance falls rapidly. This trend is also observed with the simulation models which may indicate an increasing capacitive effect.

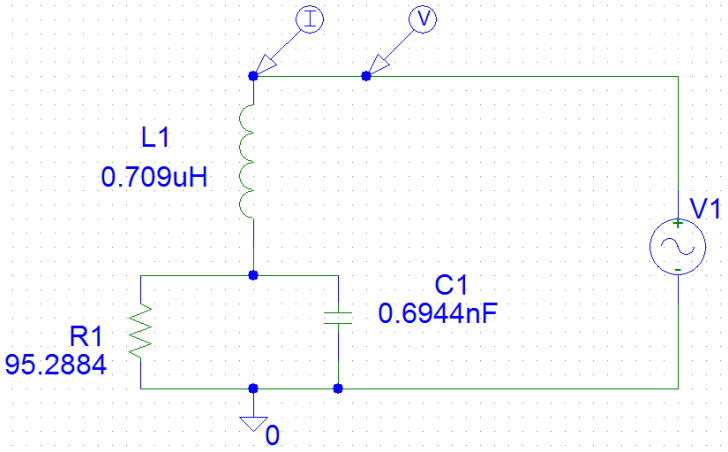

Figure 5.10 Lumped parameter circuit model for a rod electrode

5.2.3. Low voltage impulse tests

Low voltage impulse tests with different magnitudes and impulse shapes were carried out on the test rod. The transient 'earth' potential rise of the rod was measured with respect to the '90°' reference electrode for a 20/80 current impulse, and the results are shown in Figure 5.11. From the figure, it can be seen that the voltage peak occurs at the same time as the current peak for this electrode and impulse shape, indicating a mainly resistive behaviour. The parametric details of the voltage and current impulse recordings are shown in Table 5.2. With the voltage and current traces in phase, the impulse resistance was calculated as 118.1Ω by dividing the peak voltage by peak current. This impulse resistance value is very close to the measured resistance values using the DC earth testers as shown earlier in Table 5.1.

The results of water resistivity measurements at the reservoir (as discussed in section 4.2) confirm that the water resistivity and temperature on any given day is largely uniform, both depth-wise and area-wise. However, seasonal variations are evident. Figure 5.12 and Figure 5.13 show the variation of measured earth impedance of various single earth rods (Rod 2: 14mm Ø, 80cm immersed in water, Rod 2A: 14mm Ø, 96cm immersed in water and Rod 3: 14mm Ø, 200cm immersed in water) with frequency and current magnitude of the injected current.

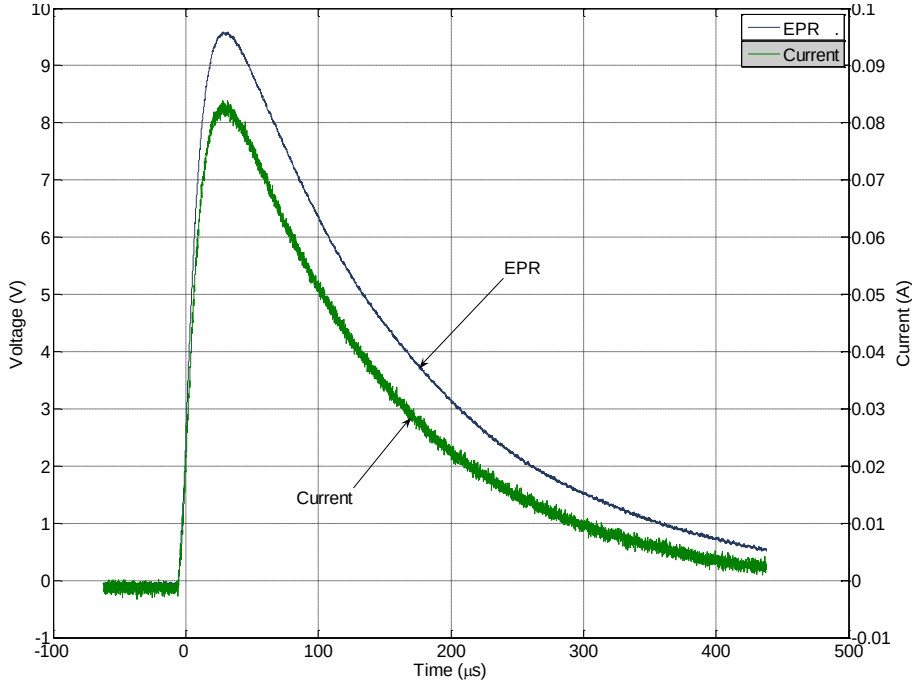

Figure 5.11 Low voltage impulse test results on a 0.8m rod

Table 5.2 Parameters of the impulse waveforms

Wave shape of current trace	Impulse rise time	Impulse fall time
	18.92μs	82.71μs
Current (A)	0.082	
EPR (V)	9.68	
R (Ω)	118.1	

5.2.4. Effect of current magnitude on measured earth impedance of signle rod at Dinorwig

The effect of current magnitude on the measured earth impedance is pronounced for the DC and low frequency AC energisation experiments conducted at Dinorwig test site. It was observed that the earth impedance of a single rod showed a reduction of about 10% with increase in frequency (over the range 20Hz to 100kHz) when the measurement was performed with the injection source placed next to the test object for the case of Rod 2 shown in Figure 5.13.

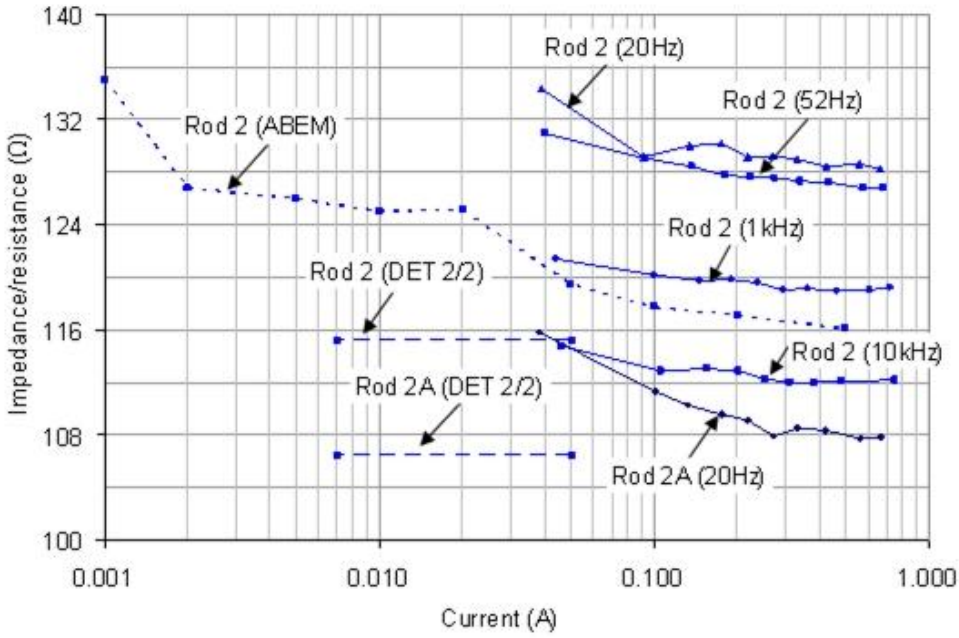

Figure 5.12 Effect of current magnitude on earth impedance of single rod at Dinorwig test site

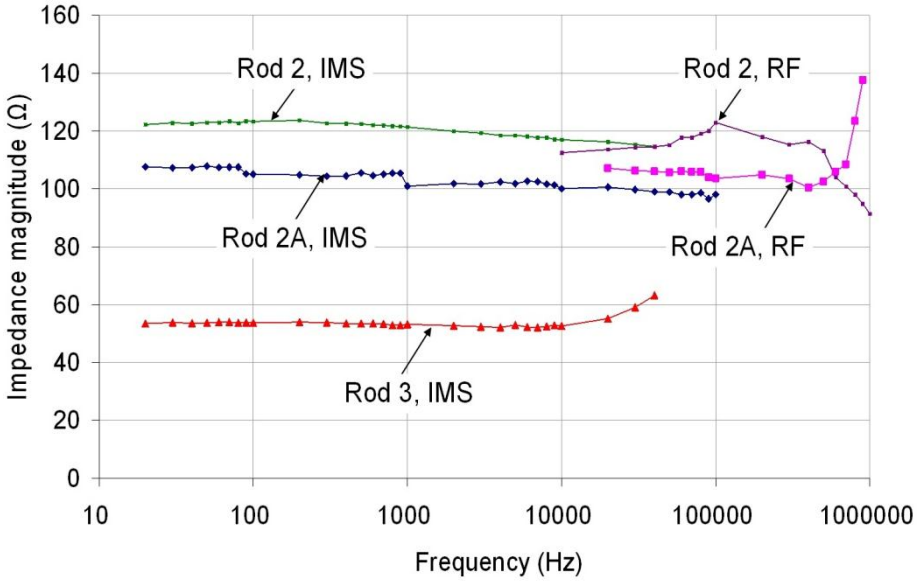

Figure 5.13 Effect of frequency on earth impedance of single rod at Dinorwig test site

As can be seen from Figure 5.12, the effect of DC current is more pronounced on the measured earth impedance when the measurement is performed with ABEM Terrameter as compared to that performed by the DET 2/2. In the case of ABEM Terrameter, the current is

varied from 1mA to 500mA while the DET 2/2 injects 7mA and 50mA DC currents at low and high settings of the current.

5.3. Tests on 3m x 3m grid at Llanrumney test site

Figure 5.14 shows the test set up for the experiments on the 3m x 3m earth grid at the Llanrumney test site. DC / Variable frequency AC / variable current AC / low voltage impulse injection tests were performed on the 3m x 3m earth grid. The test current was injected into the 3m x 3m grid and the return current was collected from the Test Tower Base (TTB) which is 43m away from the 3m x 3m grid.

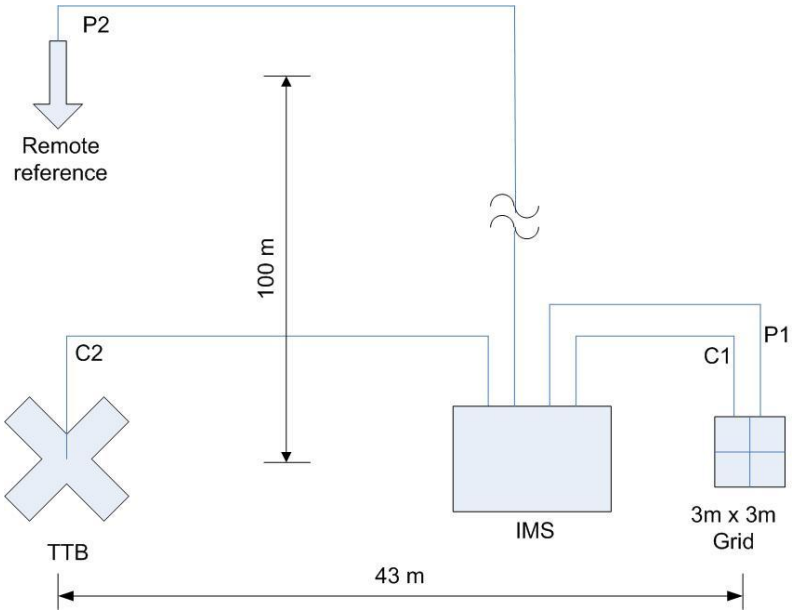

Figure 5.14 Experimental setup for tests on 3m x3m grid at Llanrumney test site

The variable current test results are shown in Figure 5.15. The effect of current magnitude on measured earth impedance was investigated by varying test current in both ascending and descending order. The test results indicate that the direction of change in current magnitudes does not have any significant effect on the trend. It was also observed that, the effect of current magnitude on earth impedance is more pronounced at lower frequencies and that, as

the frequency of injected current increases, the grid response in terms of earth impedance to injected current tends to become flat. It should be noted that the similar effect of current was observed on the measured earth impedance of the single earth rod as shown in Figure 5.3, where it is shown that the effect of current is more pronounced at DC and low frequencies and that, as the frequency increases, the effect of current tends to reduce.

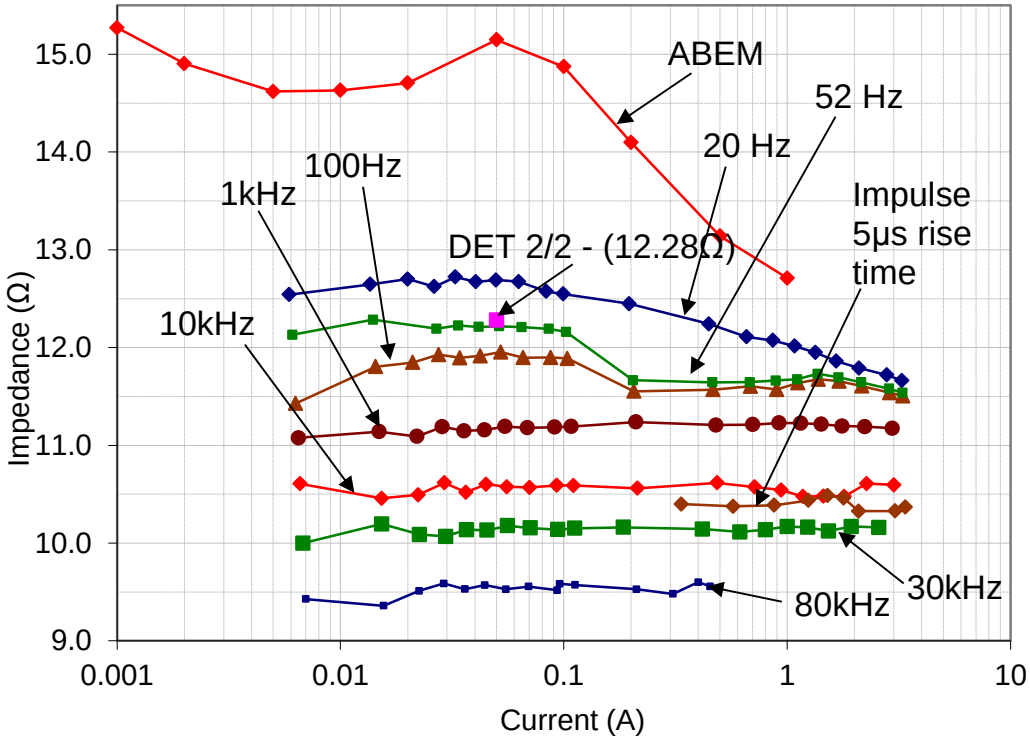

Figure 5.15 Effect of current on earth impedance of 3m x 3m grid

Figure 5.17 shows the variation of earth impedance with a variable frequency test and when computed from the FFT of measured impulse current and EPR signals shown in Figure 5.16. For the frequency scan part of the experiment, for investigation of the effect of frequency on the measured earth impedance, the frequency of the injected current signal was varied from 20 Hz to 100kHz. In other part of the experiment, the impulse current was injected and the EPR signal was acquired. The impulse current and EPR signals were captured with a Lecroy

waverunner 64Xi oscilloscope. The sampling interval was 200 ns and the sampling depth was 100 ksamples. The time for which the signal was acquired was 200 ns x 100 ksamples = 10 ms. So, the lowest frequency obtained in the computed FFT results is 1/10 ms = 100 Hz and the FFT plot is in 100 Hz steps up to the highest frequency component of the impulse current signal. The rise time of the impulse current signal was 8 μs. The results from this analysis show a reduction of 15% in the magnitude of the earth impedance with frequency (100Hz to 30kHz). The FFT analysis of the impulse tests results, shown in Figure 5.16, gives a similar trend of reduction of measured earth impedance with frequency increase as that obtained with the variable frequency test on the 3m x 3m earth grid. It should be noted that the measured earth impedance with frequency scan and that computed from the FFT from impulse signals show close agreement over the range 100Hz to 60kHz.

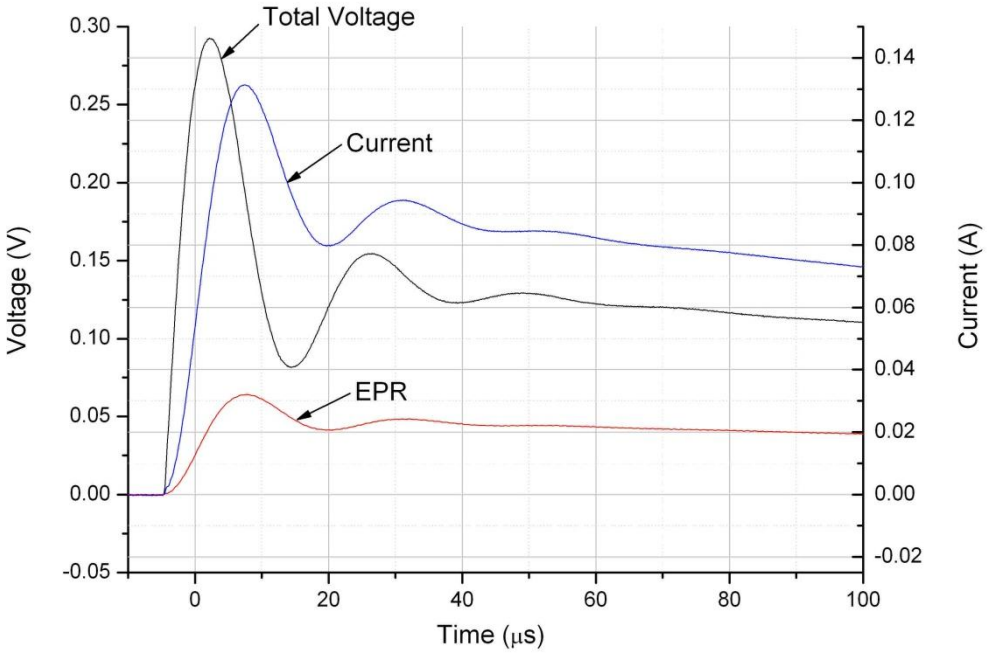

Figure 5.16 Impulse waveforms

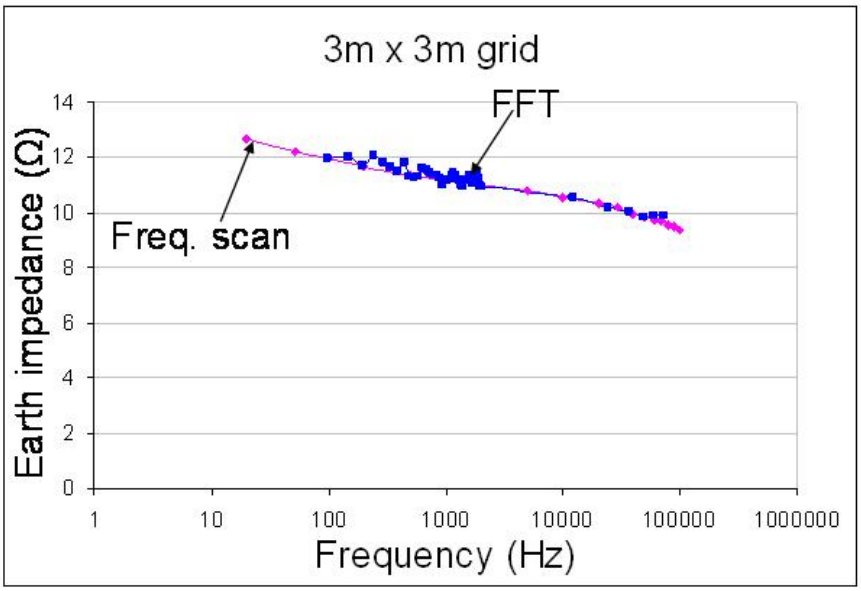

Figure 5.17 Variation of impedance with frequency scan and that computed from the FFT of impulse

5.4. Tests on 5m x 5m grid at Dinorwig test site

The plan view of the test set up for measuring the impedance of the 5m x 5m grids and the horizontal electrode 5m and 15m long is shown in Figure 5.18 (Please refer to Table 4.3 showing details of the various test electrodes used at Dinorwig test site).

5.4.1 Tests on the electrode Grid 1

The first grid (Grid 1) measures 5m×5m and comprises 25 equal meshes (each measured 1m×1m). The grid is made up of 12 pieces of aluminium strip, and each strip measures 5m×50mm×6mm. The grid was suspended from a specially constructed floating structure and was positioned 0.2m below water surface. Grid 2 is dimensionally the same as Grid 1 but positioned 0.4m below water surface. Figure 5.18 shows the test setup for the measurement of the earth impedance of Grid 1. The injection sources were placed in the boat next to the test object. The frequency dependence of earth impedance of Grid 1 was measured with the 'IMS' and 'RF' system. Figure 5.19 shows the effect of 20Hz AC and 52Hz AC current magnitude on the measured earth impedance of Grid 1. As can be seen from Figure 5.21, the

impedance is flat up to about 50 kHz for Grid 1 and 100 kHz for Grid 2 and increases significantly with frequency beyond this value.

5.4.2 DC earth resistance of Grid 1

The DC earth resistance was measured using DET2/2 (10.46Ω at low current setting and 10.44Ω at high current setting) and DET 4TC (10.53Ω for both 25V and 50V settings).

5.4.3 Current magnitude dependence of the impedance of Grid 1

The current magnitude dependence of the earth impedance was measured at 52Hz using the IMS and the results are shown in Figure 5.19. Comparing Figure 5.19 with Figure 5.12 and Figure 5.15, it can be said that a similar trend of the effect of current magnitude on the measured earth impedances is found for the 5m x 5m grid, 3m x 3m grid and the single earth rod. Figure 5.20 shows the current dependence of earth resistance of Grid 1 when measured with the geophysical meter (ABEM Terrameter). As can be observed from the figure, the variation of impedance with current is more pronounced at DC currents less than 10mA.

5.4.4 Low voltage impulse tests on Grid 1

Figure 5.22 shows the comparison between the measured impedance with the impedance computed with the FFT-based on one low voltage impulse test. The 'FFT' method produces values very close to the results obtained from the swept-frequency AC tests.

5.4.5 Tests on the electrode Grid 2

The same grid (i.e. Grid 1) was lowered to 0.4m below water surface and was tested. The new configuration is referred to as 'Grid 2'. The swept frequency response of the impedance of Grid 2 is also shown in Figure 5.21 (designated as curve C). The measured earth

impedance of Grid 2 is lower than the measured earth impedance of Grid 1 as the depth of Grid 2 is larger than the Grid1. There is negligible effect of frequency on the measured earth impedance for Grid 1 and Grid 2 over the frequency range 20Hz to 10kHz and 20Hz to 50kHz respectively. The measured earth impedance of Grid 1 and Grid 2 increases sharply above the frequency of 100kHz. DC earth resistance was measured by DET2/2 (9.26Ω at low current setting and 9.27Ω at high current setting) and DET 4TC (9.51Ωfor both 25V and 50V settings).

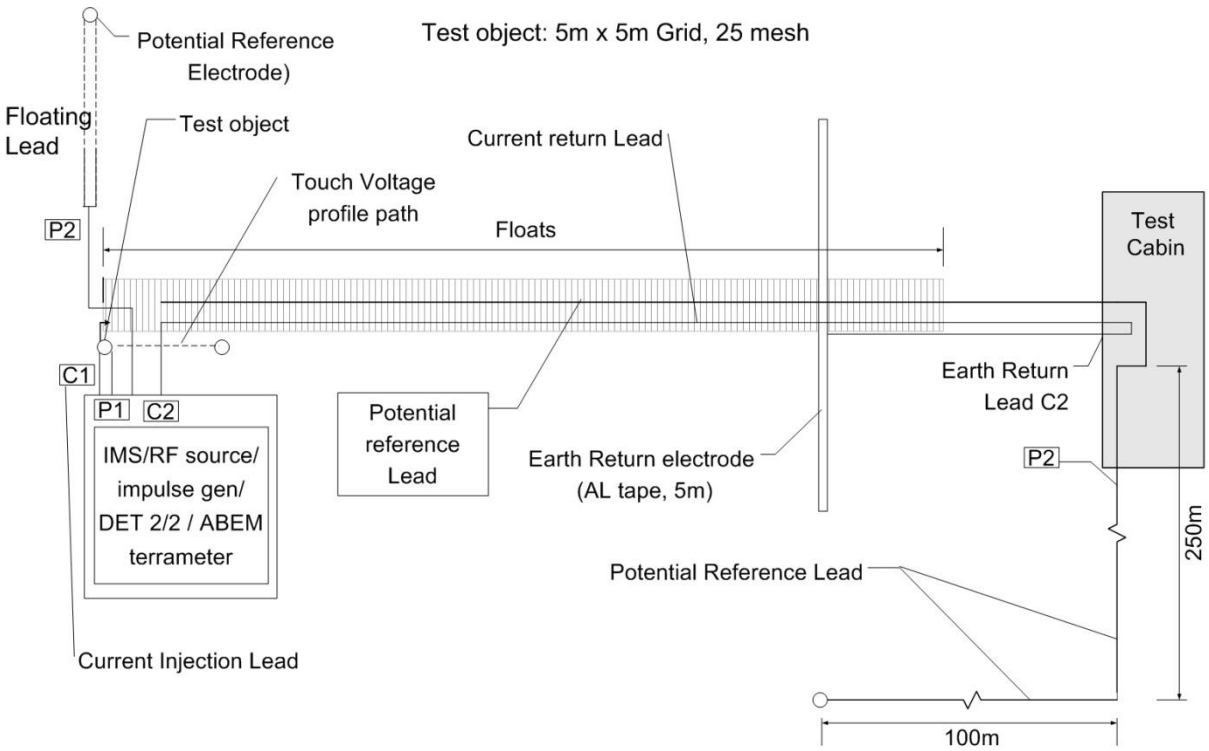

Figure 5.18 Plan view of test set up for testing 5m x 5m earth grid and horizontal electrode at Dinorwig

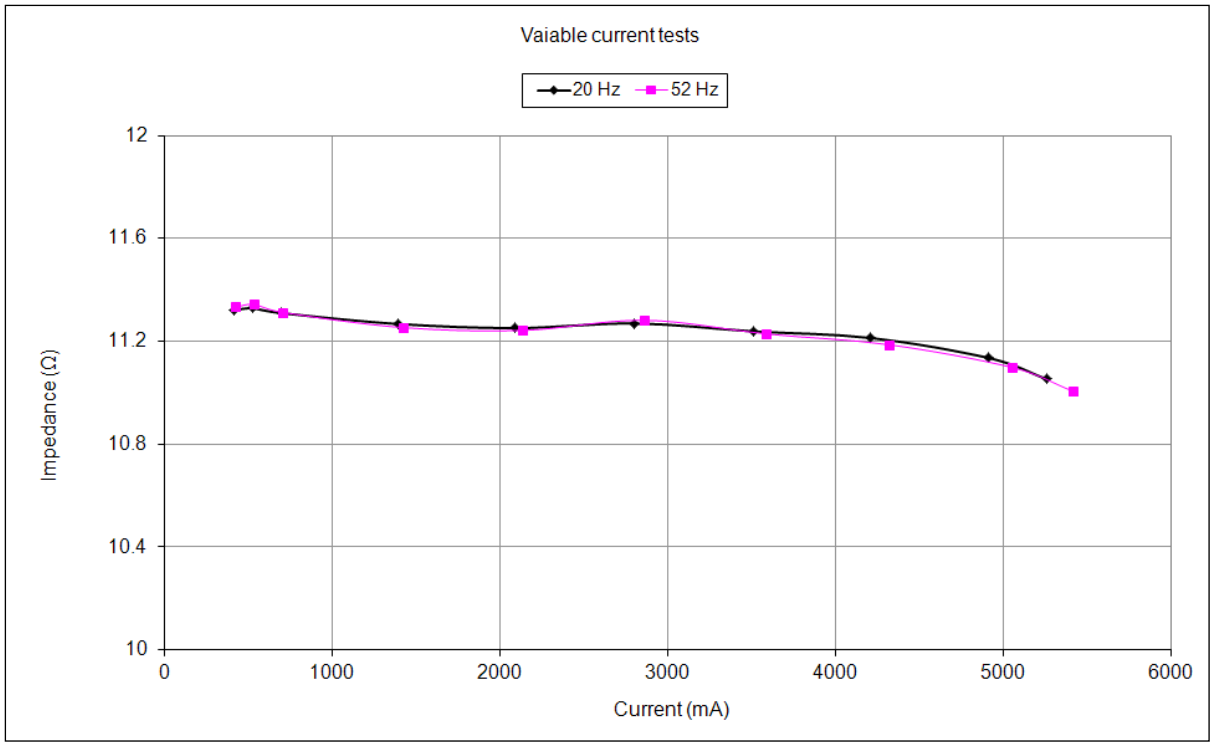

Figure 5.19 Current dependence of earth impedance of a Grid 1 at 20Hz and 52Hz

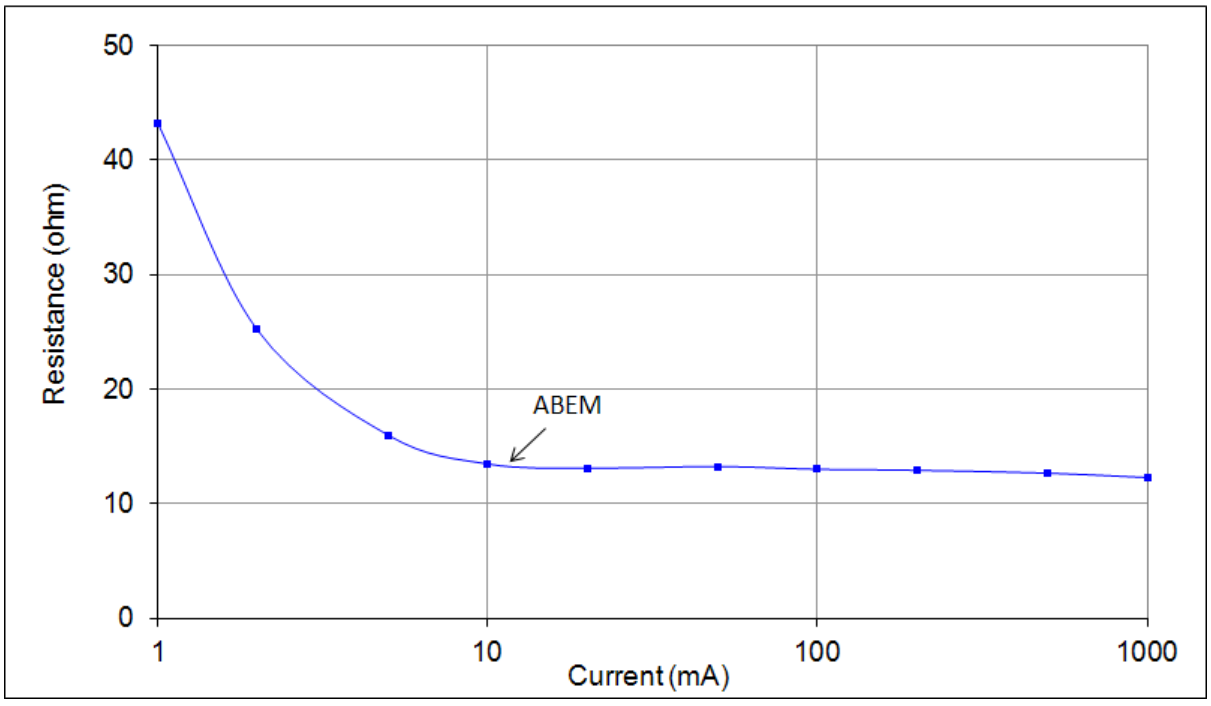

Figure 5.20 Current dependence of earth impedance of a Grid 1 at DC current (ABEM)

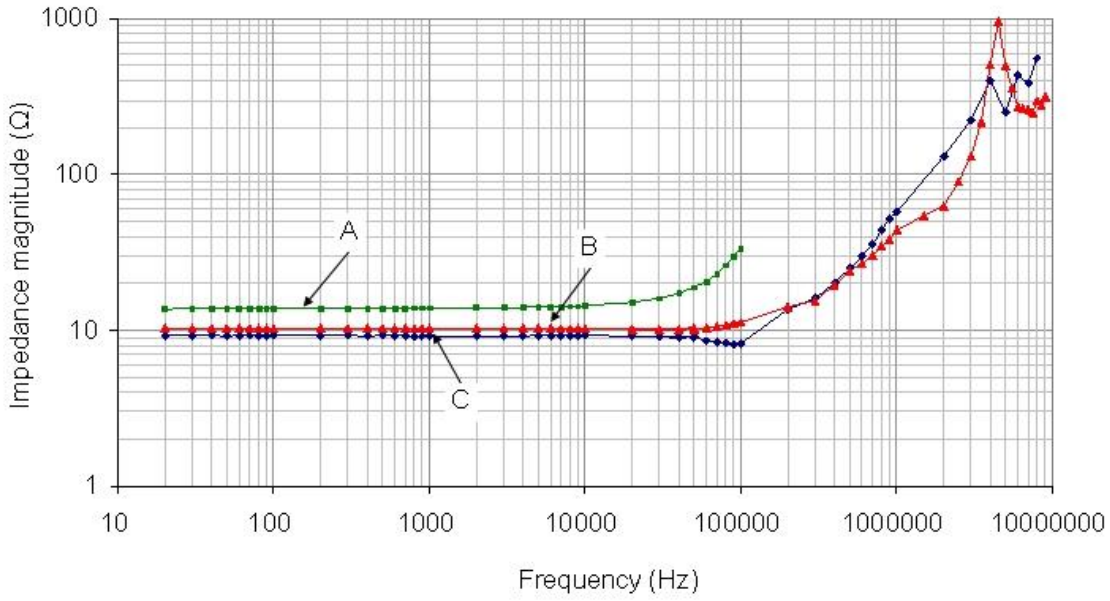

A: 5m x 5m grid, 40cm deep, 12/12/08, source @ cabin, water level = 5m, ρ =123Ωm, injection at centre
B: 5m x 5m grid, 20cm deep, 24/06/09, source @ grid, water level = 8.5m, ρ =128Ωm, injection at centre
C: 5m x 5m grid, 40cm deep, 25/06/09, source @ grid, water level = 10m, ρ =125Ωm, injection at centre

Figure 5.21 Effect of frequency on earth impedance of 5m x 5m grid at Dinorwig test site

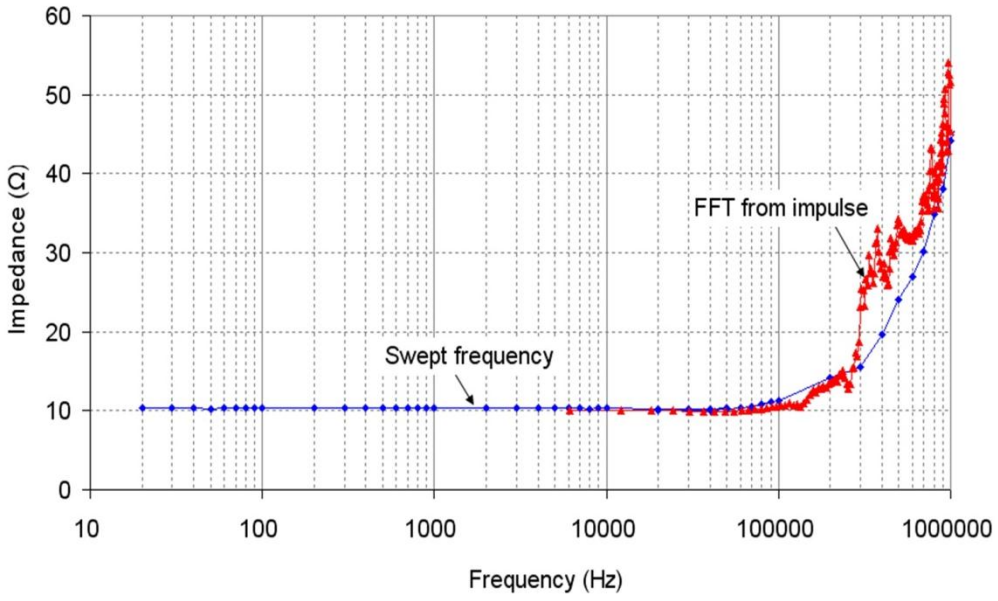

Figure 5.22 Comparison of Swept frequency and FFT from impulse methods of measurement of earth impedance of 5m x 5m earth grid.

5.5. Tests on the horizontal electrode

A horizontal electrode of dimensions 5mx50mmx6mm suspended at 0.20m below water surface is referred to as Horizontal Electrode 1. A horizontal electrode, made up of 3 pieces of 5m×50mm×6mm aluminium strips and suspended at 0.25m below water surface is referred to as Horizontal Electrode 2. The injection and measurement point was at the centre of the horizontal electrodes. The test set up for measurement of impedance of horizontal electrodes is shown in Figure 5.18. The results of the swept frequency on the horizontal electrode are shown in Figure 5.23. As can be seen from Figure 5.23, the earth impedance is marginally falling with frequency up to a frequency of around 100 kHz. Above 100kHz, an increasing trend of earth electrode impedance with increase in frequency can be seen for the Horizontal Electrode 1.

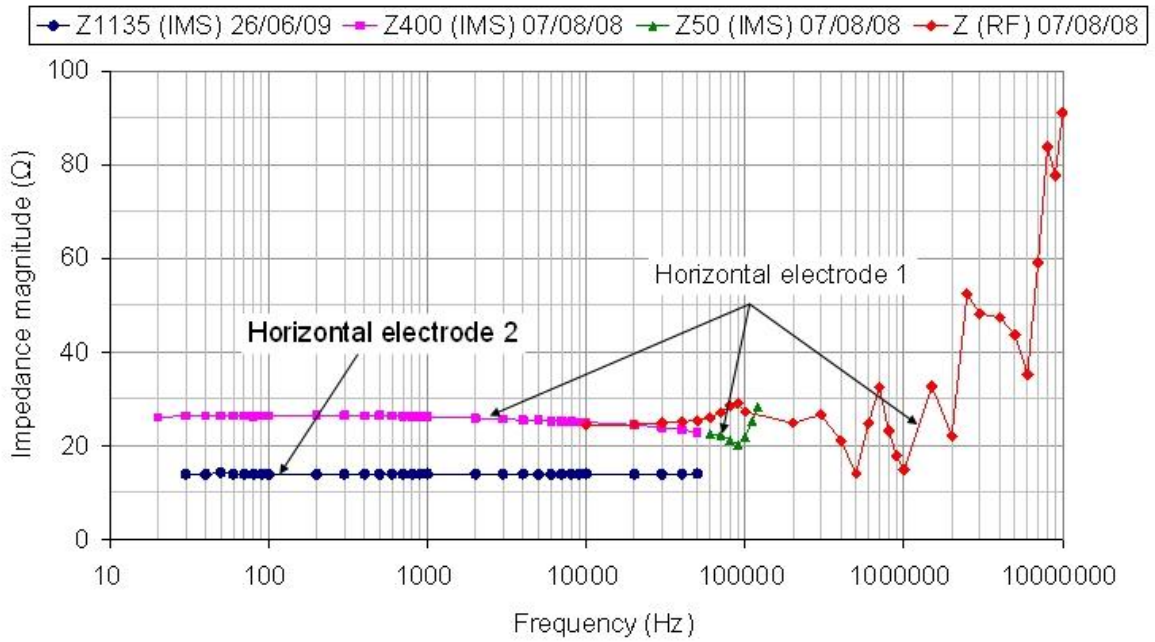

Horizontal electrode 1 (Aluminium tape 50mm x 6.25mm cross-section, 5m long), injection at one end, 20cm deep in water, 7th Aug 08, ρ = 95Ωm
Horizontal electrode 2 (Aluminium tape 50mm x 6.25mm cross-section, 15m long), injection at centre, 25cm deep in water, 26th Jun 09, ρ = 130Ωm

Figure 5.23 Effect of frequency on earth impedance of horizontal electrode at Dinorwig test site

5.5.1 DC earth resistance of Horizontal Electrode 2

The DC earth resistance of Horizontal Electrode 2 was measured using the DET2/2 (14.63Ω at low current setting and 14.62Ω at high current setting) and the DET 4TC (14.57 and 14.59Ω for 25V and 50V settings respectively).

5.5.2 The current magnitude dependence of impedance of Horizontal Electrode 2

Figure 5.24 shows the current magnitude dependence of earth impedance of Horizontal Electrode 2 measured at 20Hz using the IMS. It can be seen that there is a small increase in the measured earth impedance of the horizontal electrode with the increase in current magnitude from few mA to about 5A. This trend is opposite to that observed for the other electrodes tested during the field tests. It is shown in the Chapter 7.7 (Figure 7.10) that with the current density in the range of $0.003A/m^2$ to $0.01A/m^2$ the measured earth impedance exhibited a rising trend with the increase in injected current magnitude. The current density in the horizontal electrode is low as the area of horizontal electrode is sufficiently large. It is to be noted that the low current injection into the grids / other electrodes with large surface area will result in low current densities into the earthing electrode under test. It is believed that this condition will tend to exhibit increasing trend in the measured earth resistance with the increase in the current magnitude.

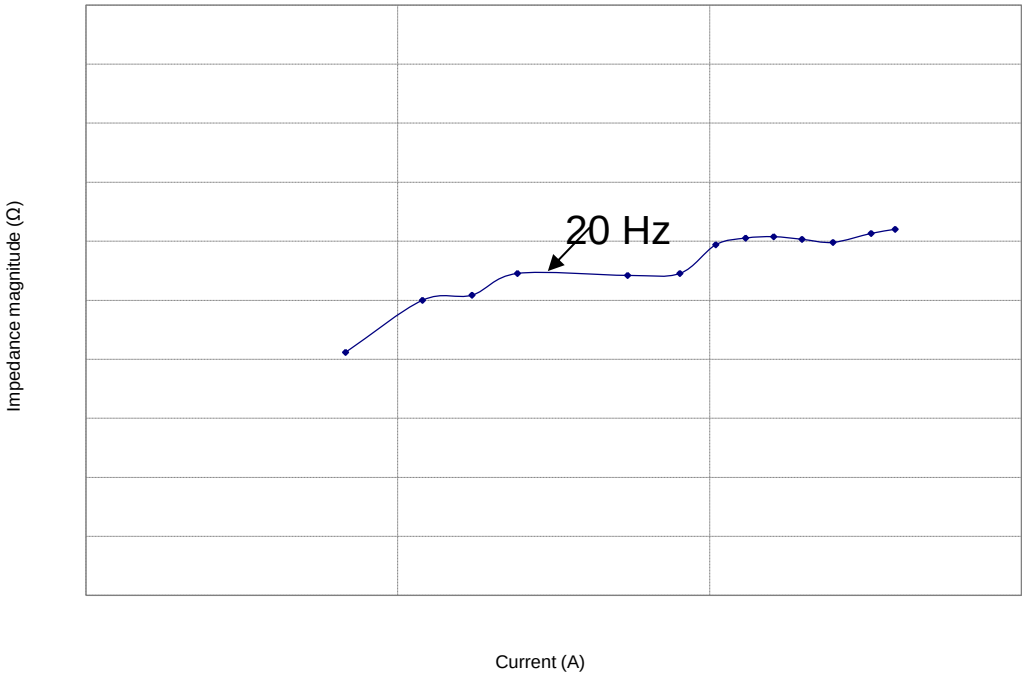

Figure 5.24 Current magnitude dependence of earth impedance of a horizontal electrode

5.6. Tower base tests at Llanrumney

5.6.1. Purpose built test Tower base (TTB)

With a low voltage variable frequency AC applied to the test tower base (TTB), its earth impedance was measured. DC and impulse tests were also conducted on the same electrode. The test setup is shown in Figure 5.25. It was observed that the earth impedance decreased with increase in frequency as shown in Figure 5.26. This trend was also seen from tests on the small grid and the other test electrodes at Llanrumney. The tests carried out on the single rod immersed in the lake at Dinorwig also showed a similar trend.

An AC test with current varying from 10mA to 2.5A was also performed on the same day, and as can be seen from Figure 5.27, the measured earth impedance decreased by about 7% at different tested frequencies. The reduction in earth impedance of test tower base with increase in current magnitude was most prominent of all the electrodes tested so far. Figure 5.27 also shows that the reduction of earth impedance with current is observed above a current magnitude of 100mA for the AC tests. The values of impulse resistance (EPR peak

divided by injected current peak) are also shown in Figure 5.27 together with selected results from the DC and variable frequency AC tests. (Note that the peaks of voltage and current in these tests occurred at the same time). From the figure, it can be observed that the earth resistance values from the impulse tests lie between the earth impedance values obtained at 10kHz and 60kHz respectively from the variable frequency tests.

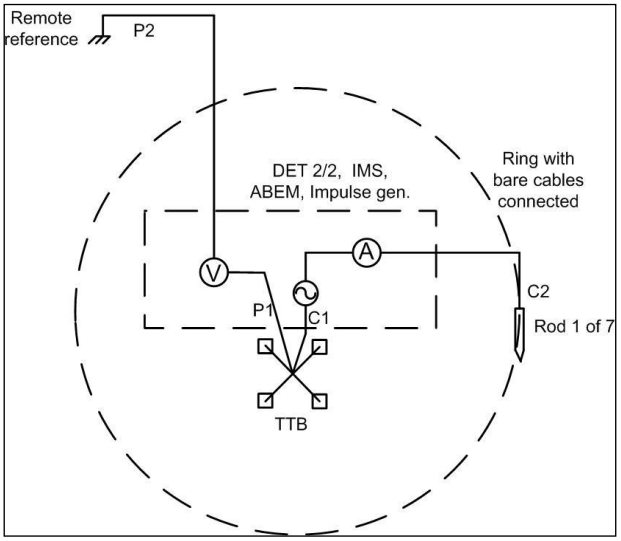

Figure 5.25 Set up for measuring earth impedance of test tower base at Llanrumney

The impulse signals with rise times of 5.1μs and 2.2μs also show a similar trend of reduction of measured earth resistance with increase in the current magnitude. It should be noted that the relatively lower frequency components are present in the 5.1μs rise time signals compared with the 2.2μs rise time signals. Hence, the measured earth resistance with 5.1μs rise time signals is greater than that measured with the 2.2μs rise time signals.

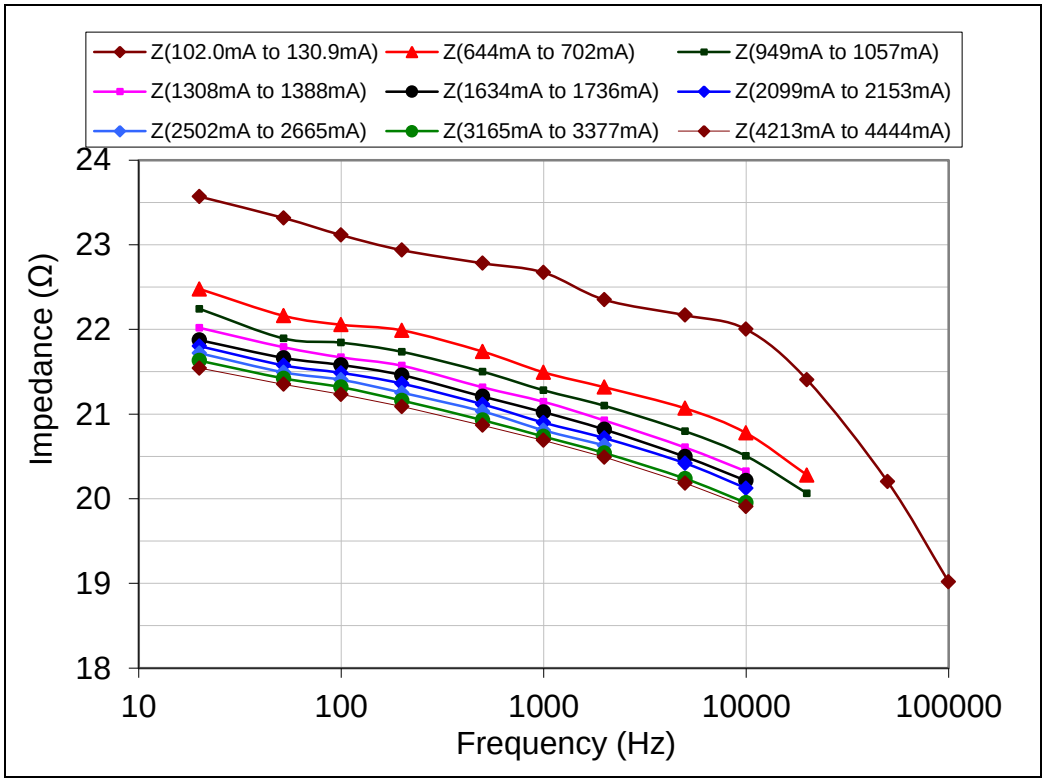

Figure 5.26 Effect of frequency on tower earth impedance tested at Llarumney

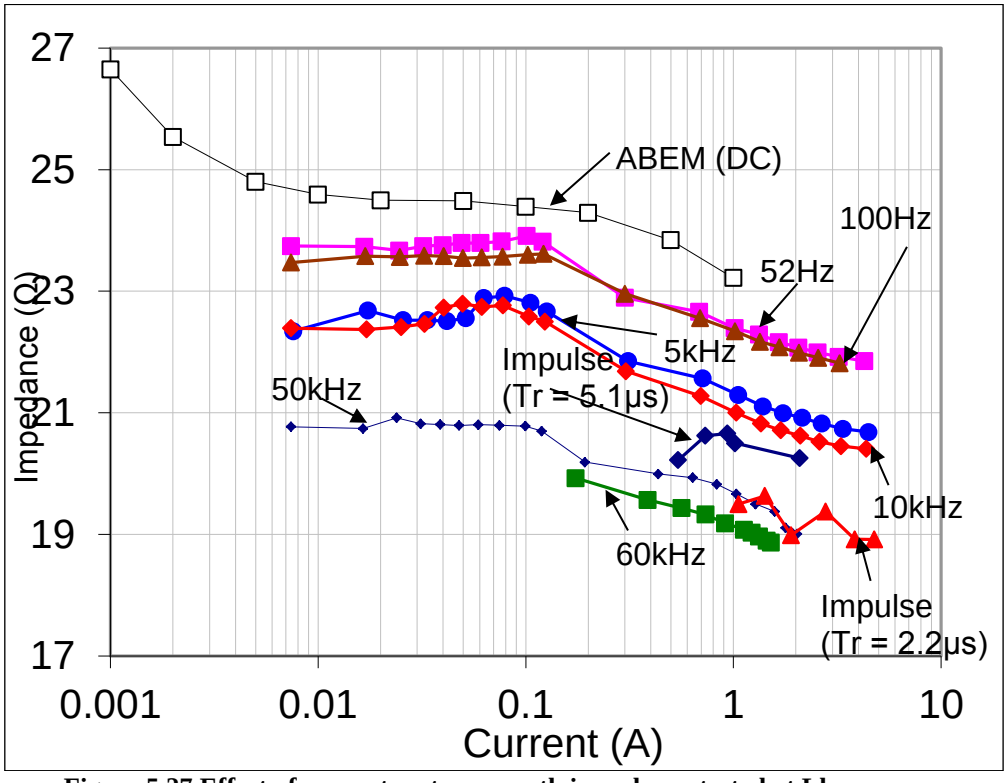

Figure 5.27 Effect of current on tower earth impedance tested at Llanrumeny

5.6.2. Operational tower (VP9) tests

Variable frequency tests were performed on the earthing system of the National Grid 275 kV operational transmission tower (VP9) at Llanrumney test site. The tests carried out on 2nd and 12th June 2008 were made with the overhead earth wire (OEW) connected. Variable frequency current was injected in one of the leg of VP9 tower base, and the isolated tower base was used as current return. Further tests were carried to investigate the effect of disconnecting the earth wire from tower VP9 using a purposely installed pneumatic switch.

Figure 5.28 shows the variation of measured earth impedance with the frequency during these tests. The measured impedance of the 275kV transmission tower represents the parallel summation of the chain impedances on both sides of VP9 and the earth impedance of the individual tower. As the frequency is increased, the earth impedance increases and tends towards a constant value of about 11.5Ω above 30 kHz.

With the overhead earth wire (OEW) disconnected, the measured earth impedance of VP9 tower is about 15Ω at low frequencies (20 Hz to 40 Hz). As the test frequency increases, the magnitude of impedance reduces. At higher frequencies, (>2 kHz and up to 70kHz) the measured earth impedance of VP9 tower is close to 12Ω. With the overhead earth wire connected, the measured earth impedance of VP9 tower is about 0.2 Ω at low frequencies (20 Hz to 40 Hz). The low value of measured earth impedance of VP9 tower at frequencies (20Hz to 40Hz) is due to the parallel summation of the chain impedances of the operational National Grid towers on both sides of VP9. As the test frequency increases, the magnitude of impedance increases up to about 11Ω over the frequency range 30kHz to 70kHz. The increase in impedance is the result of inductive effects at higher frequencies. It should be noted that the measured earth impedance of the VP9 tower at higher frequencies is in close agreement for both cases of overhead earth: wire connected and disconnected. Figure 5.28

also shows the effect of frequency on the measured earth impedance of the Test Tower Base (TTB) (case 1 to case 3) for the ease of comparison with the trend of the measured earth impedance of VP9 tower.

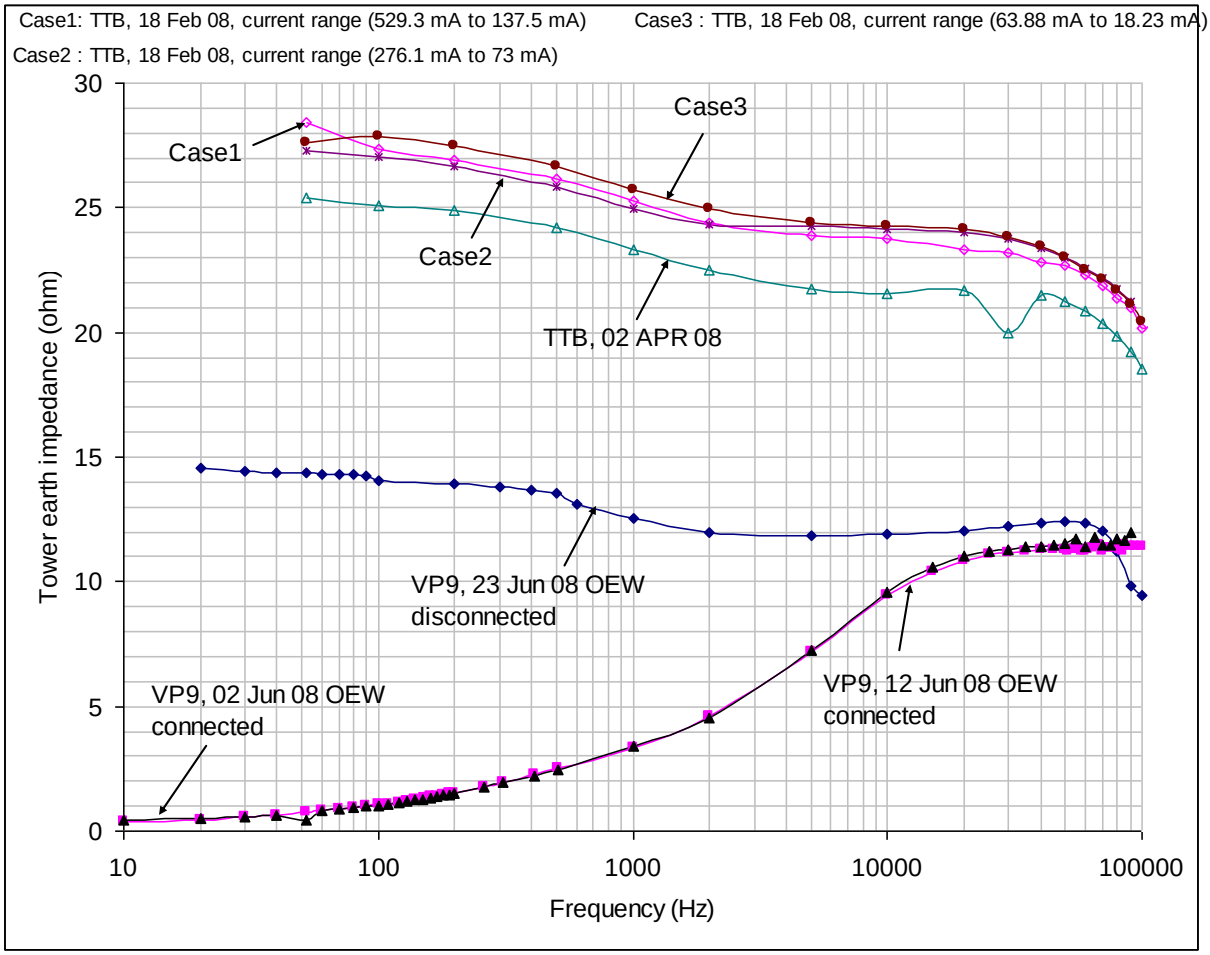

Figure 5.28 Comparison of effect of frequency on earth impedance of tower base tested at Llanrumney

5.7. Large area earthing system at Llanrumney

5.7.1 Ring Earthing System connected with Test Tower Base

AC and DC tests were conducted on a large area earthing system comprising all rods of the ring earth electrode system connected with bare cables and also connected to the test tower base (Figure 5.29 (a)). In line with previous tests, there is a marked reduction of about 20% in

measured DC resistance (ABEM meter) over the range 1mA to 1A and an 8% reduction in measured AC impedance at 20Hz over the range 200mA to 3A.

A decreasing trend in impedance with frequency was observed over the frequency range of 20Hz to 2kHz, as shown in Figure 5.29 (b). However, for this more extensive earth electrode, the earth impedance rises sharply above 10kHz. A sharp rise in earth impedance was also observed from tests on the extended tower earthing system at tower VP9, but in this case, the upturn in earth impedance occurred at a much lower frequency which attributed to the greater inductance of the tower line earthing system.

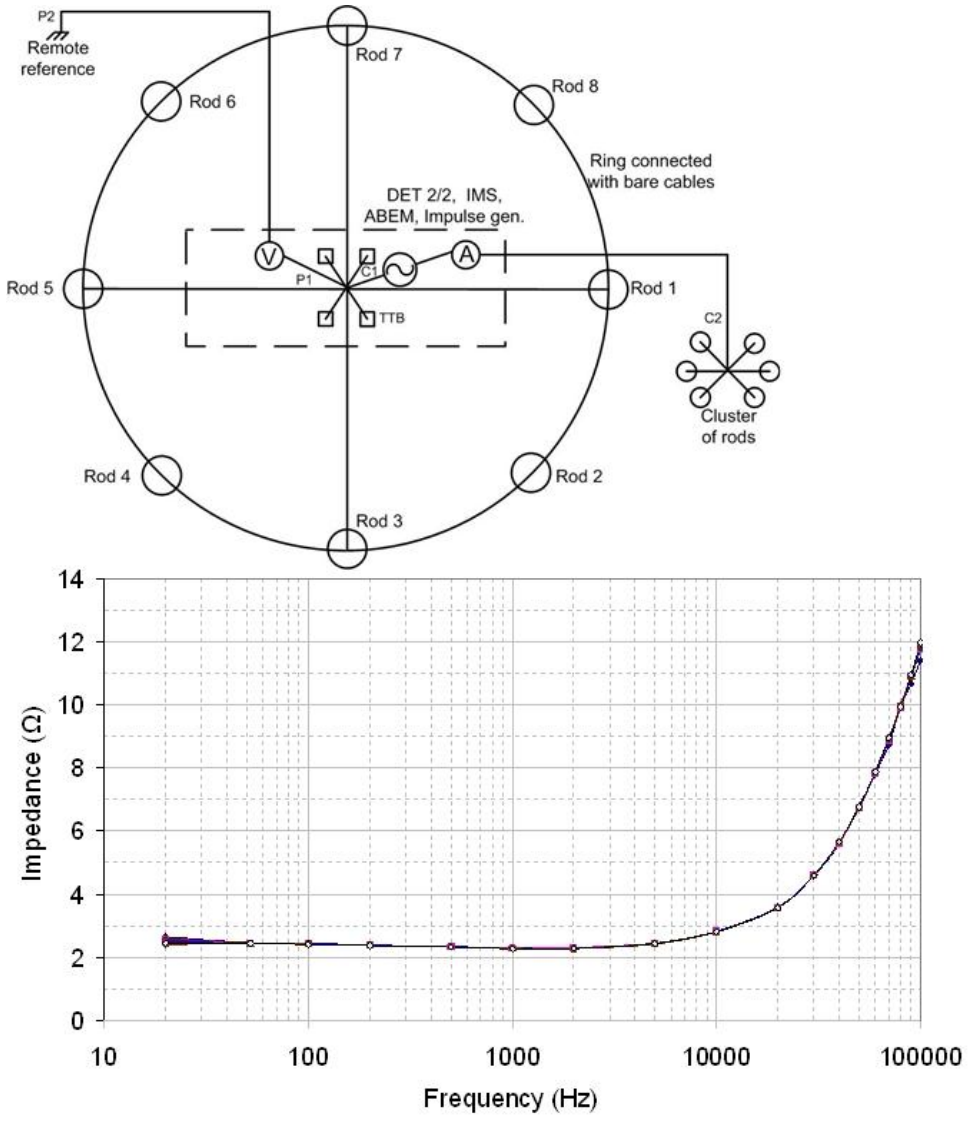

Figure 5.29 Effect of frequency on large area earthing system at Llanrumney

5.7.2 Cluster of Three Rods connected with Horizontal Electrode at Llanrumney

Variable frequency AC tests were carried out on a cluster of three rods connected with horizontal electrode at the Llanrumney test site. The test set up is shown in Figure 5.30.

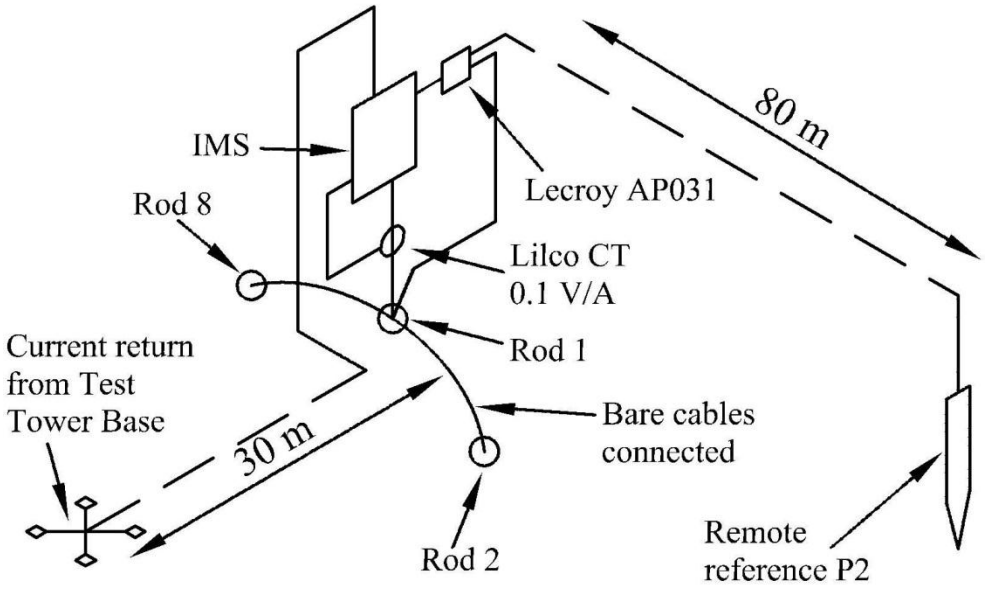

Figure 5.30 Test set up for Cluster of Three Rods with Horizontal Electrode

The test results are shown in Figure 5.31. As seen from the figure, the overall decreasing trend of measured earth impedance is observed over the frequency range 20Hz to 100kHz.

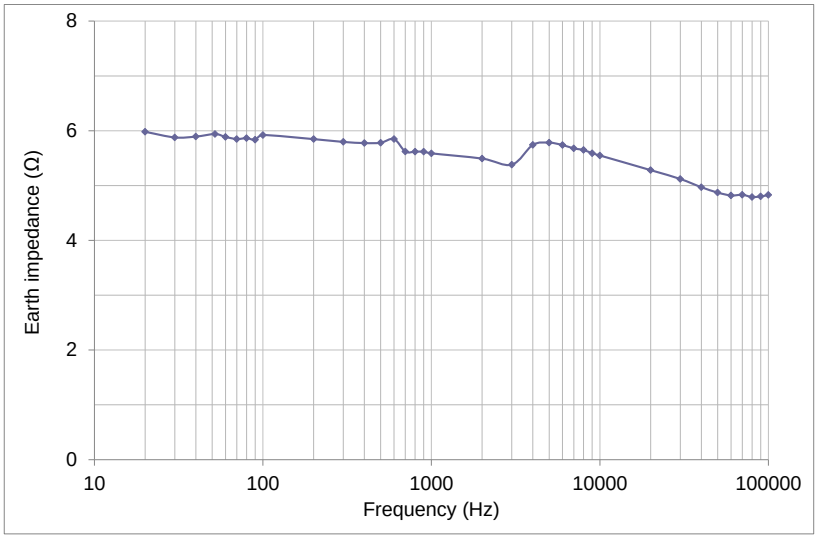

Figure 5.31 Variation of impedance with frequency (Cluster of Three Rods with Horizontal Electrode)

5.7.3 Cluster of Three Rods at Llanrumney

Variable frequency AC tests were carried out on a cluster of three rods at the Llanrumney test site. The test set up is shown in Figure 5.32, and the test results are shown in Figure 5.33. The overall decreasing trend of measured earth impedance observed over the frequency range 20Hz to 100kHz is similar to the other electrodes tested at Llanrumney and Dinorwig test site.

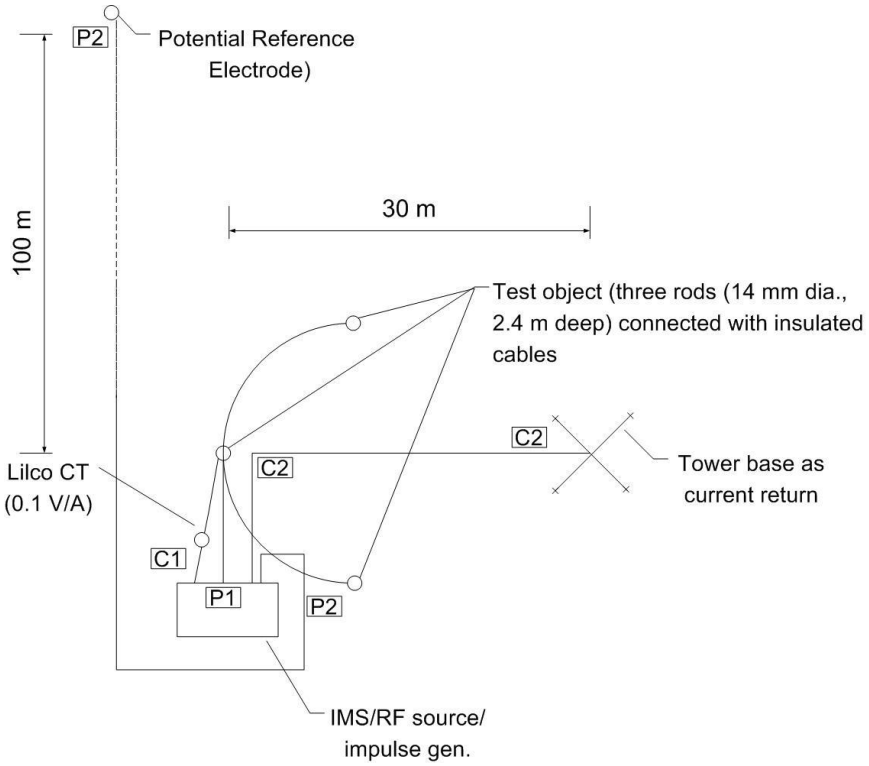

Figure 5.32 Plan view of test set up (Cluster of Three Rods)

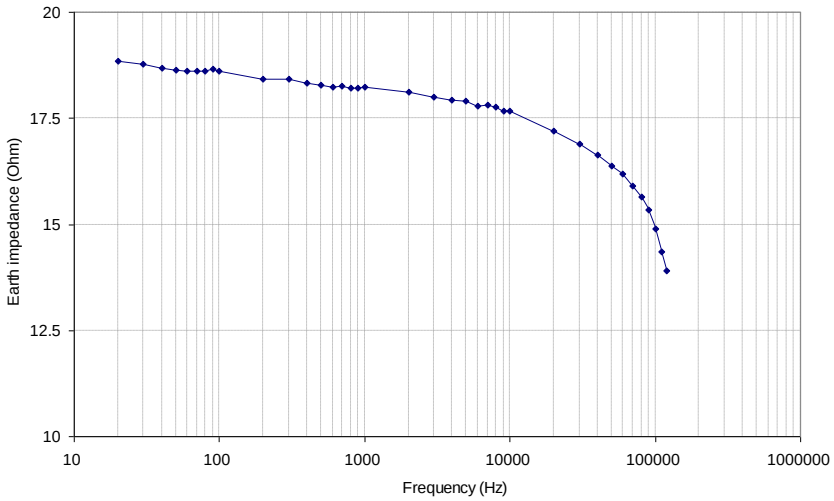

Figure 5.33 Variation of impedance with frequency (3 rod cluster)

5.8. Discussion of test results

5.8.1 Comparison of FFT from impulse and swept frequency results

The fast Fourier Transform of the impulse waveform provides the frequency spectrum of the impulse waveform. The Fast Fourier Transforms of the measured injected current and earth potential rise (EPR) signals were performed to obtain the magnitudes of these signals in the frequency domain. The ratio of the EPR to injected current in the frequency domain provides the earth impedance in the frequency domain. The so-obtained earth impedance in the frequency domain was compared with the frequency scan measurements of the earth impedance carried out with the Impedance Measurement System (IMS).

5.8.1.1. Effect of windowing functions on the FFT output of impulse waveforms

To study the effect of windowing function on the FFT output, the slow and fast impulse waveforms were transformed using FFT function of Origin 7 waveform analysis software. It was observed that the rectangular windowing function (which is the same as applying no window function) gives the better results in our case as compared to the results of other windowing functions. It was observed that the results obtained with the FFT processing showed the reduction of impedance of earth electrodes with increase in applied frequency, and the trend was similar to those observed in the field tests with the variable frequency scan on the earth electrodes tested in the field. FFT analysis of the impulse waveform can be used to obtain the measured earth impedance values at different frequencies. FFT analysis of the impulse signal waveforms of injected current and earth potential rise to obtain earth impedance values can save considerable amount of time and equipment costs as compared to the frequency scan procedure in the field. The comparison of earth impedance values obtained from the FFT outputs of the slow/fast impulse signal waveforms using different windowing functions are shown in Figure 5.34 and Figure 5.35. It was observed that the

Welch windowing function for the slow impulse waveform and the rectangular windowing function for the fast impulse waveform provided better results for the FFT analysis of the impulse test results.

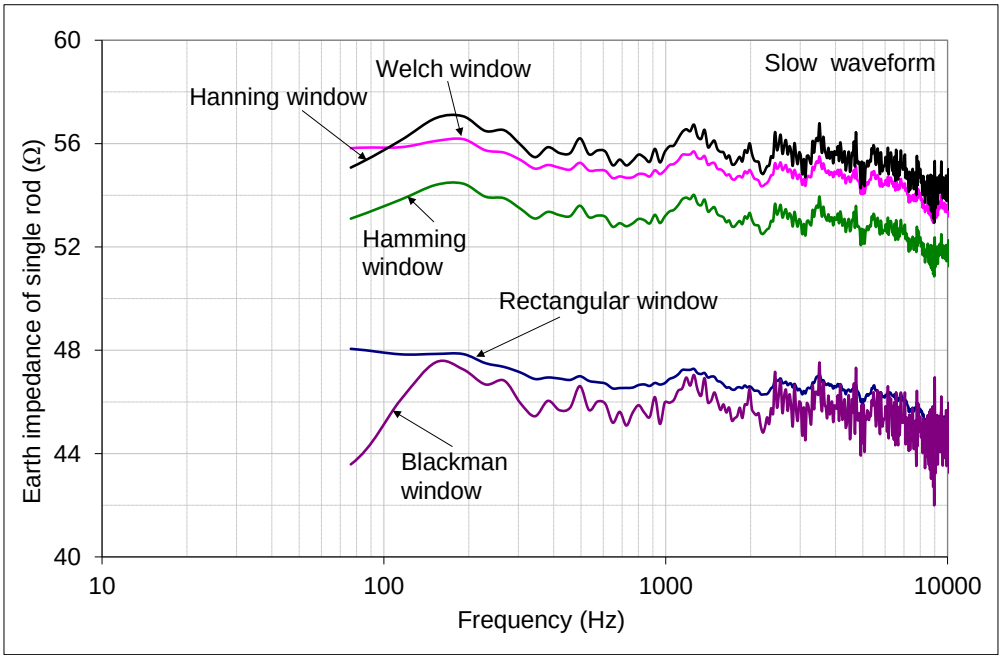

Figure 5.34 FFT of slow impulse waveform with different windowing functions

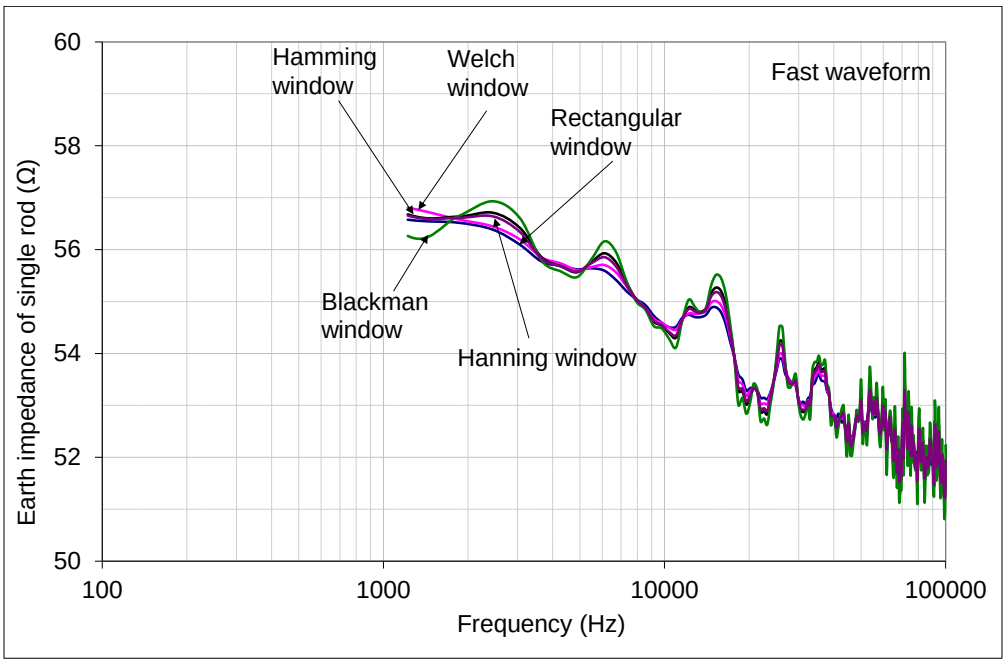

Figure 5.35 FFT of fast impulse waveform with different windowing functions (enlarged view)

5.8.1.2. Comparison of FFT of the results obtained at Llanrumney test site

The measured impulse signals of voltage and current obtained from the field tests on the test earth electrodes at Llanrumney were analysed using FFT and to obtain earth impedance values as a function of frequency. The FFT results are shown in Figure 5.36, together with the results of the measured impedance values obtained with the University's IMS system. For the single rod, 3m x 3m grid and the test tower base, the results show reasonably close agreement between the earth impedance obtained with the FFT analysis and the frequency scan over a restricted frequency range. In the case of the operational tower base VP9, the FFT results showed a significant variation about the values obtained from the frequency scan. Preliminary FFT analysis of impulse test results show reasonable agreement with swept-frequency earth impedance measurements over a restricted frequency range.

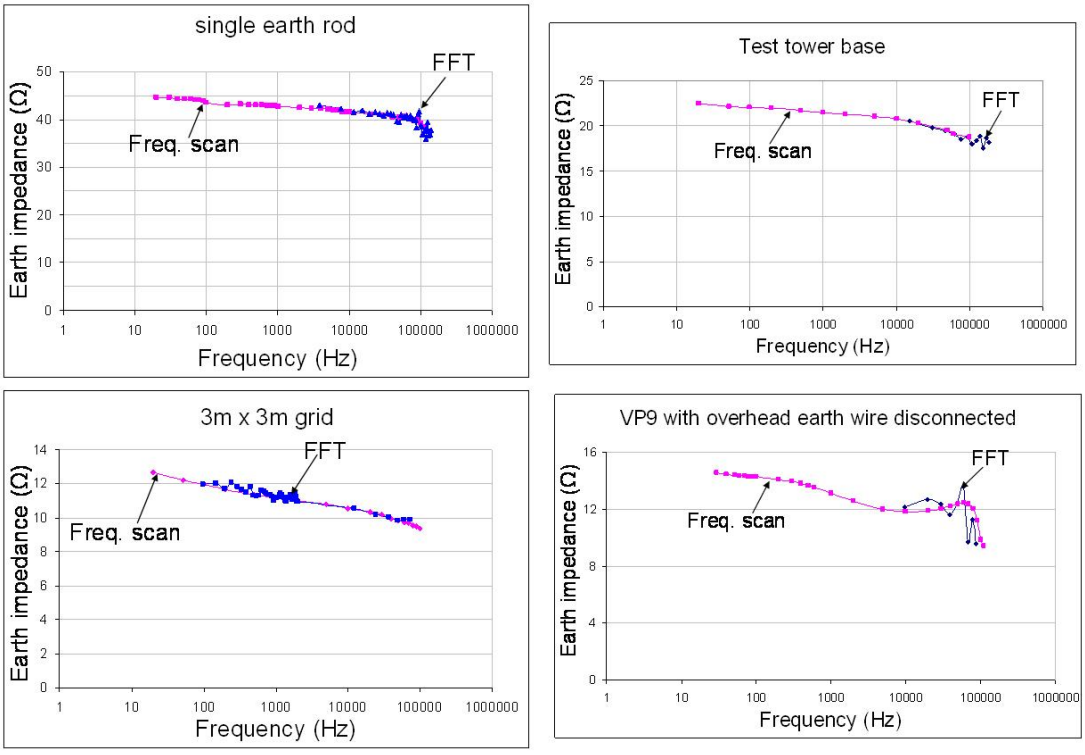

Figure 5.36 Comparison of measured earth impedance obtained from frequency scan with the earth impedance computed from FFT of measured impulse signals

5.8.1.3. Comparison of FFT of the results obtained at Dinorwig test site

Further analysis of experimental results of Dinorwig tests (conducted in June 2009) was carried out. The comparison of the results of swept frequency and FFT from impulse for Rod 2A and 5m x 5m grid are shown in Figure 5.37. As seen from the figure, there is a close agreement between the results for Rod 2A and 5m x 5m grid except for some intermediate frequencies above 1MHz and up to 7MHz in the case of 5m x 5m grid.

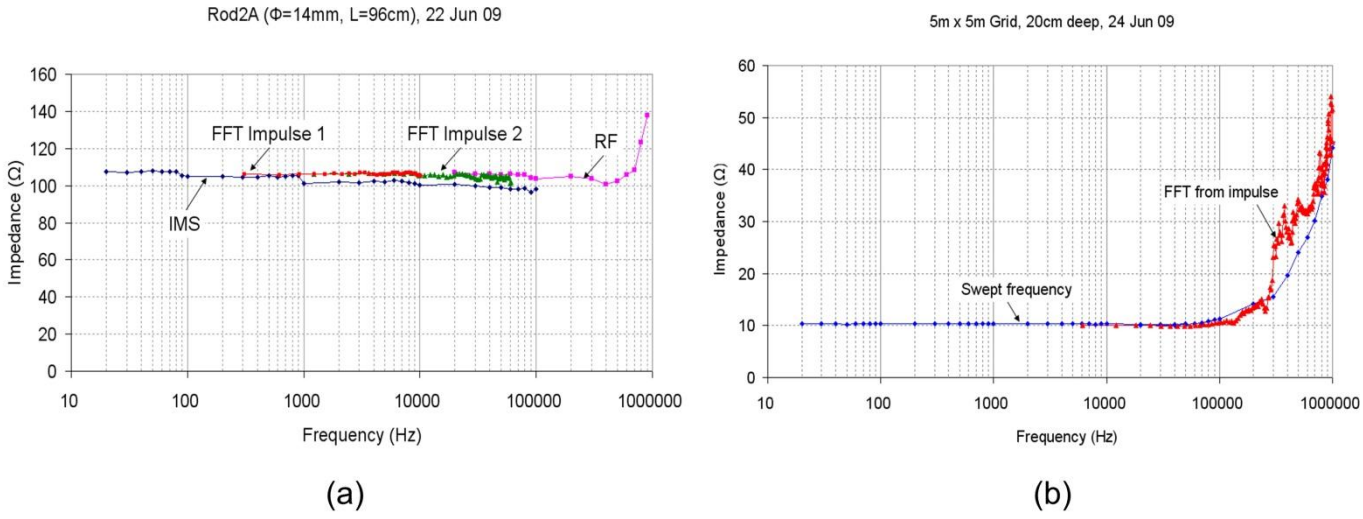

Figure 5.37 Comparison of AC steady state measurements with impulse

5.8.2 Frequency dependence of earth electrode impedance

The extensive tests carried out with variable frequency AC and impulse signals, on various practical earth electrodes showed that, the measured earth impedance decreases with increase in frequency over the range 20 Hz to 120kHz. The reduction of earth impedance with frequency is larger with the electrodes embedded in the soil than the electrodes immersed in water. The overall reduction in the measured earth impedance was in the range of 10% to 30% over the frequency range 20Hz to 120kHz. The phase difference angle between the measured earth potential rise (EPR) and the injected current was less than 5° over the range 20Hz to 120kHz. It is therefore understood, that the measured earth impedance was

dominantly resistive in nature. The resistivity of the soil surrounding the earth electrodes was found to be decreasing with the frequency of the injected current.

5.8.3 Dependence of earth electrode impedance on injected current magnitude

A series of tests conducted on the various practical earth electrodes with the variable current AC/DC/impulse signals showed that there is an effect of the current magnitude on the measured earth impedance of the earth electrodes. The effect of DC current was found to be larger than the effect of AC/impulse current. Moreover, it was also observed that the effect of AC current magnitude above the frequency of 100Hz is lesser than that at the frequencies below 100Hz for the various earth electrodes. There was a reduction of up to 15% in measured earth impedance of the various electrodes with the increase in DC current magnitude from 1mA to 500mA. This aspect is worth noting as various commercially available earth testers inject currents at current magnitudes close to few tens of mA.

5.8.4 Impulse response of earth electrode impedance

Various practical earth electrodes were tested with slow and fast impulse current signals to determine the behaviour of earth electrodes with impulse currents. It was observed that the FFT of impulse provided close agreement of impulse test results with the variable frequency AC test results. This confirmed that there is a reduction of earth impedance with increase in frequency over the range 20Hz to 120kHz. The impulse tests carried out with the variable impulse current magnitudes also confirmed that the effect of increase in impulse current magnitude is similar to the effect of current magnitudes at the corresponding high frequency contents in the impulse signal.

5.9. Conclusion

Extensive variable frequency AC/DC and impulse tests have been conducted on the several full scale earth electrodes at the University test site at Llanrumney and the Dinorwig power station earthing test facility. The tests results have shown the important aspects of the reduction of the measured earth impedance with the increase in frequency and current magnitude. An attempt is made to further investigate the cause of these effects, and is reported in Chapter 7.

Chapter 6: Comparison of experimental results with simulation

6.1. Computer modelling

Computer modelling was performed with the commercially available software for earthing analysis, CDEGS [67] which models different earthing systems under multi-layered resistivity soil conditions. Computer modelling is a useful tool to predict the earth impedance of the electrode provided that the soil resistivity and geometry of the earth electrodes is known. By computer modelling, the impedance of the electrode can be calculated before the actual measurements are performed in the field. If the computer models are made sufficiently accurate to calculate the earth impedance then this process could help in optimising the geometry of the earth electrode for a given soil resistivity pattern during the earthing system design phase. The computer modelling is most often preferred to the actual field measurements due to the ease of achievement of the desired results.

6.1.1 Concentrated earthing systems

Two layer soil models for the Llanrumney test electrodes were constructed from the soil resistivity survey results as shown in Chapter 4. The representative two layer soil models for the single earth rod, 3m x 3m grid and the test tower base and Dinorwig Test Site were shown in Table 4.4 and Table 4.5 respectively. The soil models are reproduced here in Table 6.1 and 6.4 for ease of reference. Using numerical earthing system simulation software, the geometry of the earthing systems was represented along with the soil models to compute the earth impedance of the electrodes at various frequency conditions. The computed values of earth impedance of a single electrode are shown in Figure 6.4, for frequencies ranging from 20Hz to 100kHz.

Table 6.1 Two layer soil model of Llanrumney test site used for simulation

Earth Electrode	Resistivity of upper layer (Ωm)	Thickness of upper layer (m)	Resistivity of lower layer (Ωm)	Thickness of lower layer (m)
Single rod	250	9	70	infinite
3m x 3m grid	250	9	70	infinite
Test tower base	300	9	100	infinite

The geometry of the single rod used for the simulation purpose was taken as 16mm in diameter and 2.4m long as mentioned in Chapter 4. The geometry of the 3m x 3m earth grid was used from the Figure 4.4 and is reproduced here in Figure 6.1 for ease of reference. The geometry for the test tower base was used from the Figure 4.2 and 4.3 and reproduced here in in the Figure 6.2 and Figure 6.3 for ease of reference.

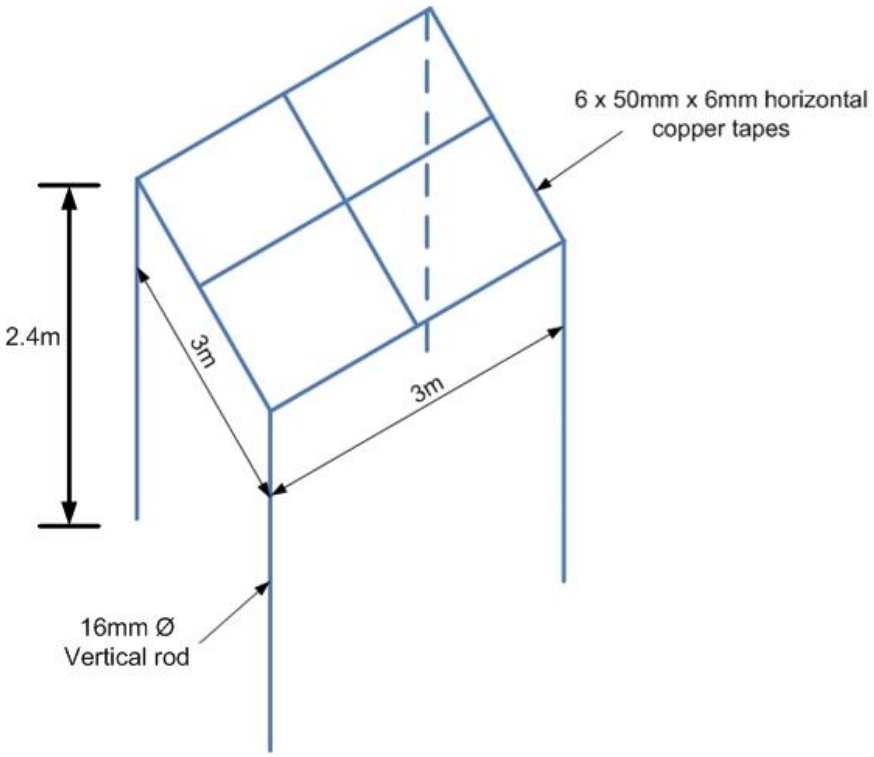

Figure 6.1 Isometric view of 3m x 3m grid

The measured values of earth impedance of single rod as a function of injection frequency are also plotted for comparison in Figure 6.4. From several earlier tests, a measure of the seasonal variation in the '50Hz' impedance values has been obtained, and this is illustrated in the figure by the vertical bar.

Similarly the comparison of the computed values of earth impedance of the 3m x 3m grid for frequencies ranging from 20Hz to 100kHz with the measured earth impedance is shown in Figure 6.5 along with the seasonal variation of the measured earth impedance represented by the vertical bar.

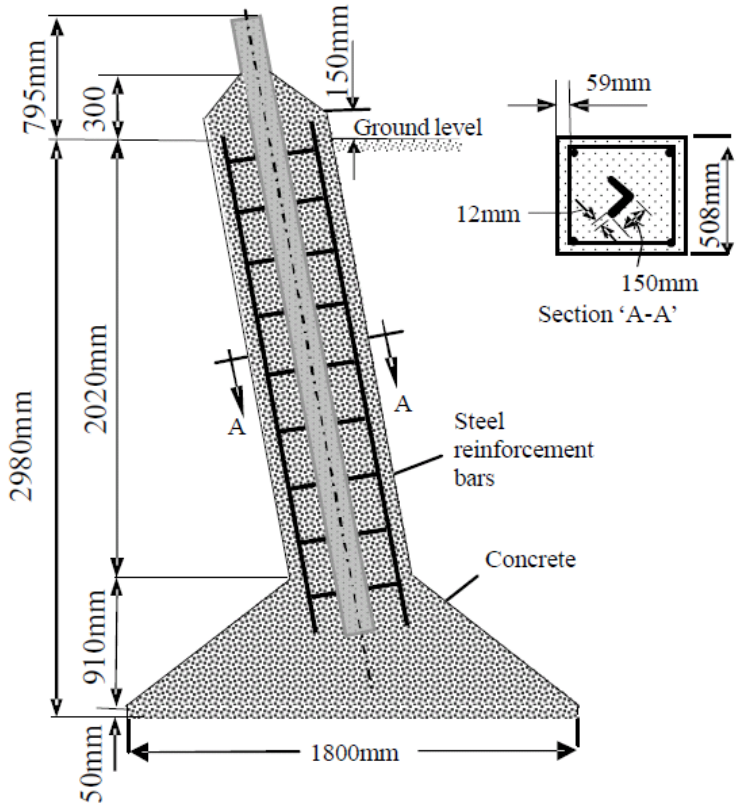

Figure 6.2 Tower footing construction of one leg of tower base

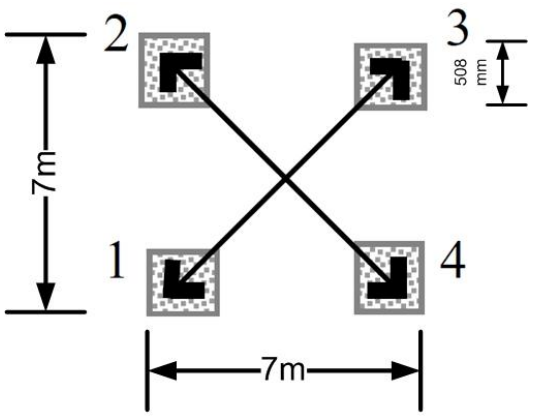

Figure 6.3 Plan view of the four legs of the Tower base

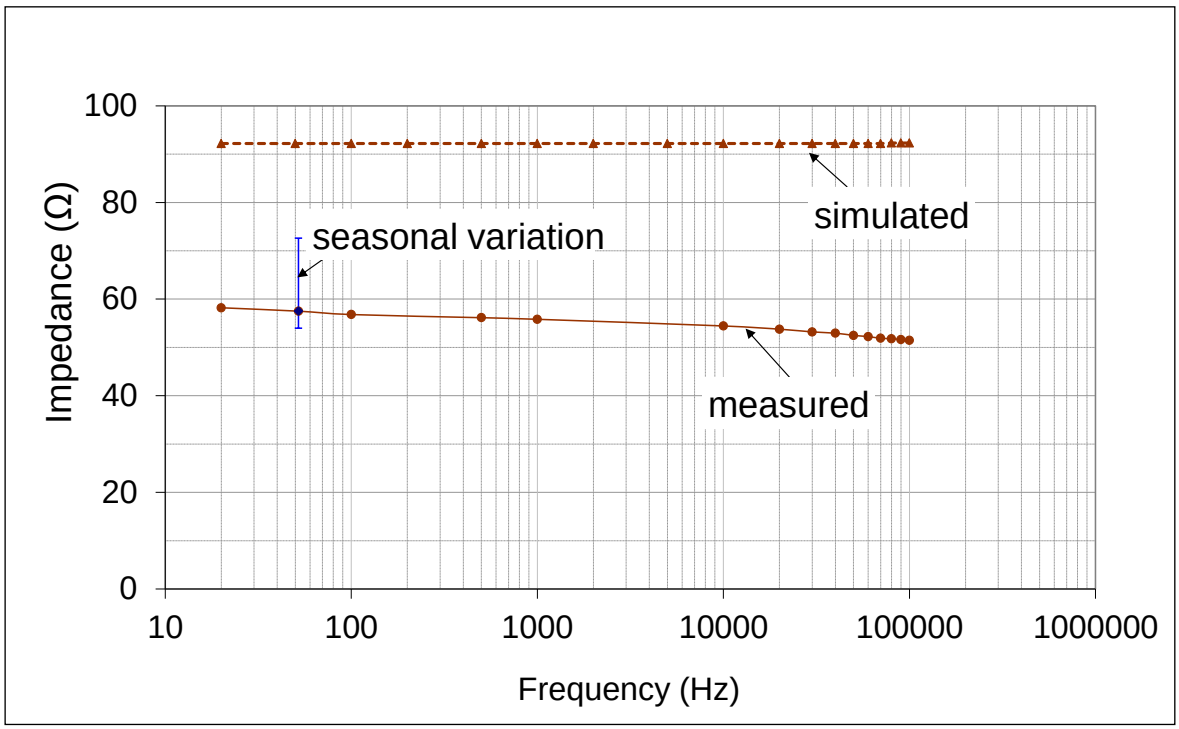

Figure 6.4 Comparison of simulated and measured earth impedance of single rod

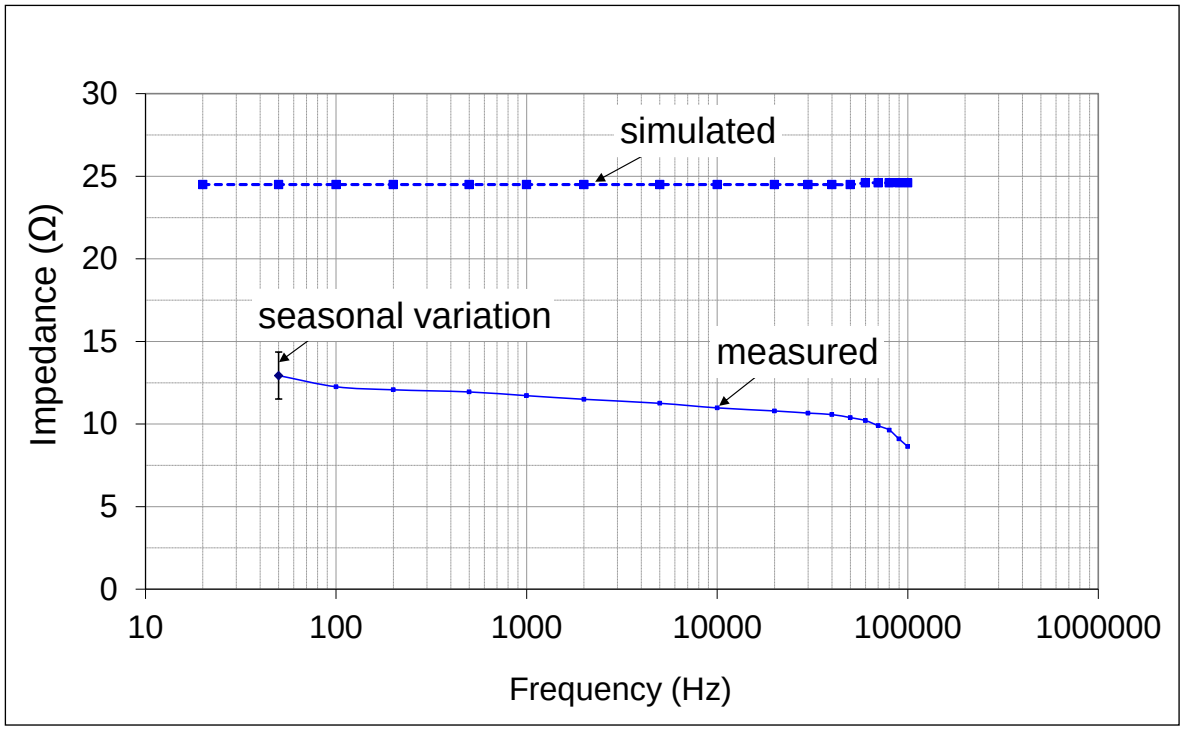

Figure 6.5 Comparison of simulated and measured earth impedance of 3mx3m grid

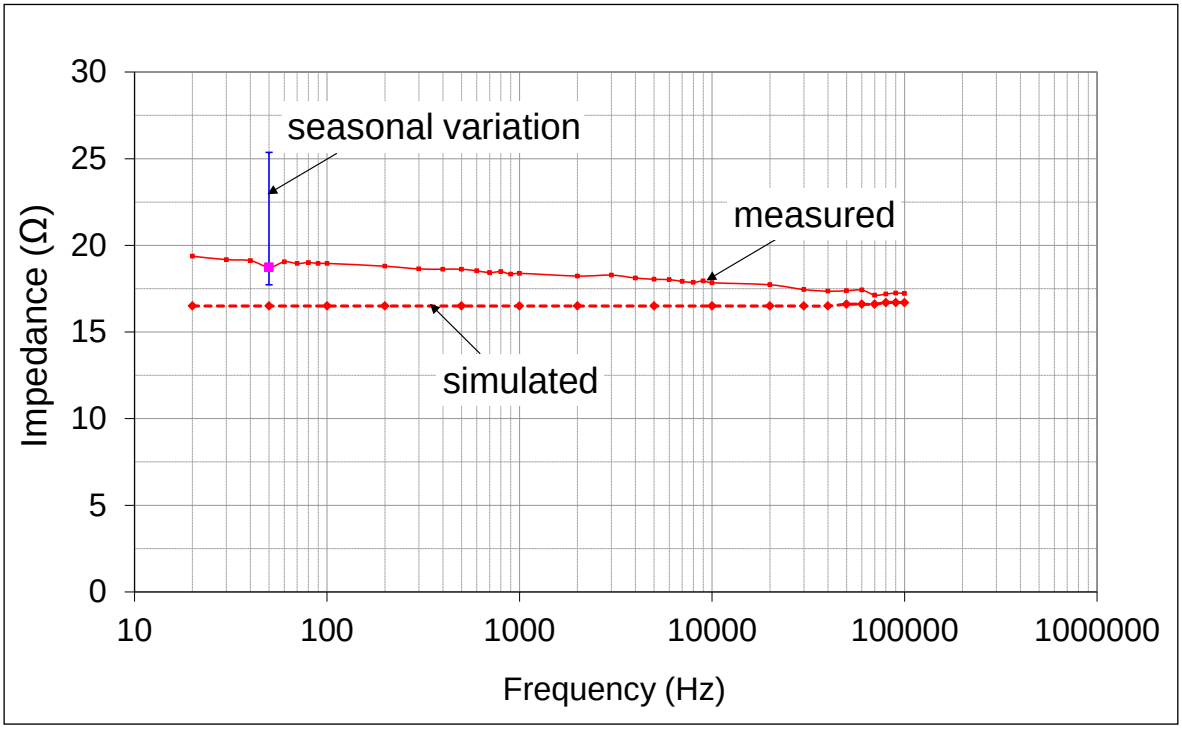

Figure 6.6 Comparison of simulated and measured earth impedance of test tower base

The comparison of the computed values of earth impedance of the test tower base for frequencies ranging from 20Hz to 100kHz with the measured earth impedance is shown in Figure 6.6 along with the seasonal variation of the measured earth impedance represented by the vertical bar.

From consideration of the measurements and simulations for the single rod, 3m x 3m grid and the test tower base, the following points are noted;

i) The simulated frequency response of the test electrodes is flat over the range of frequency, unlike the measured results that exhibit a falling trend of earth impedance with frequency.

ii) Although a significant seasonal variation is evident in the measured 50Hz impedance, the simulated impedance values for the rod and grid lie outside this range and are significantly higher than the maximum measured value. The measured and simulated values of earth impedance for the tower base are closer.

The falling trend of reduction of the measured earth impedance with frequency is not reproduced in the simulations. This may be explained by the fact that the simulation software assumes constant values of soil resistivity and permittivity with frequency. For two out of three of the test electrodes, the simulations predict much higher values of earth impedance. This may be due to the fact that a) the positions of the soil resistivity survey lines do not correspond exactly with the positions of the test electrodes and were taken at different times which could have resulted in the difference due to the seasonal variations. b) the soil structure is highly complex and exhibits a wide range of resistivity and, hence, it is difficult to translate this into a representative simplified two-layer simulation model.

The seasonal variation in the measured impedance of earth electrodes at Llanrumney test site is shown in the Table 6.2

Table 6.2 Seasonal variation in the measured earth impedance

Type of Electrode	Earth resistance measured by DET 2/2 @ high current (Ω)	Earth impedance measured by IMS @ indicated current @ 50/52Hz	Date of measurement
Rod 1 of ring earthing system	60.5	----	29th Aug 07
	72.6	----	15th April 09
	54.0	42.69Ω @ 520mA	22nd Aug 08
	56.8	57.65Ω @ 477mA	15th Dec 08
Test tower base	23.9	25.37Ω @ 411mA	2nd April 08
	19.0	18.74Ω @ 190mA	14th July 08
	24.6	----	11th Feb 08
	25.7	28.4Ω @ 443mA	18th Feb 08
	17.70	17.72Ω @ 492mA	29th May 08
	21.6	21.22Ω @ 474mA	4th Nov 08
	----	22.39 Ω @ 301mA	27th Nov 08
3m x 3m grid	12.28	11.54Ω @ 329mA	2nd Dec 08
	14.36	----	11th Feb 08
	14.13	13.81Ω @ 492mA	14th Feb 08
	13.7	----	14th Jan 09
	12.8	13.35Ω @ 273mA	29th Nov 07
	11.51	10.78Ω @ 230mA	8th Oct 08
	----	12.34Ω @ 345mA	30th Apr 08

	----	11.98Ω @ 430mA	2nd May 08

6.1.2 Cluster of rods of the ring earthing system at Llanrumney

The computer simulation of the cluster of rods with two different electrode configurations was also carried out. These electrode configurations were

a) a cluster of 3 earth rods interconnected with a 44m long bare horizontal ring electrode, (the test setup and the experimental results are shown in the Figure 5.30 and Figure 5.31) and b) cluster of 3 earth rods interconnected with 44m long insulated horizontal ring electrode (the test setup and the experimental results are shown in the Figure 5.32 and Figure 5.33).

The calculated and measured values of the earth impedance of the electrodes are shown in Figure 6.7 and 6.8 for frequencies ranging from 20Hz to 100kHz. The following observations were made from the comparison of simulated results with the measured earth impedance of the cluster of rods,

i) The measured earth impedance at the point of injection decreases with frequency over the range 20Hz to 100kHz for the cluster of rods with the bare horizontal electrode; while the simulated results show a flat frequency response up to 20kHz, above which there is an increase in earth impedance.

ii) In the case of the cluster of rods connected with insulated cables, the measured earth impedance shows a reduction of 26% over the frequency range 20Hz to 100kHz. The calculated values of earth impedance show a marginal reduction in earth impedance in the higher frequency range.

iii) The magnitude differences between measured and calculated values of earth impedances at 50Hz for both electrode configurations may be attributed to the

accuracy in estimating equivalent bulk values of earth resistivity used in the computer model.

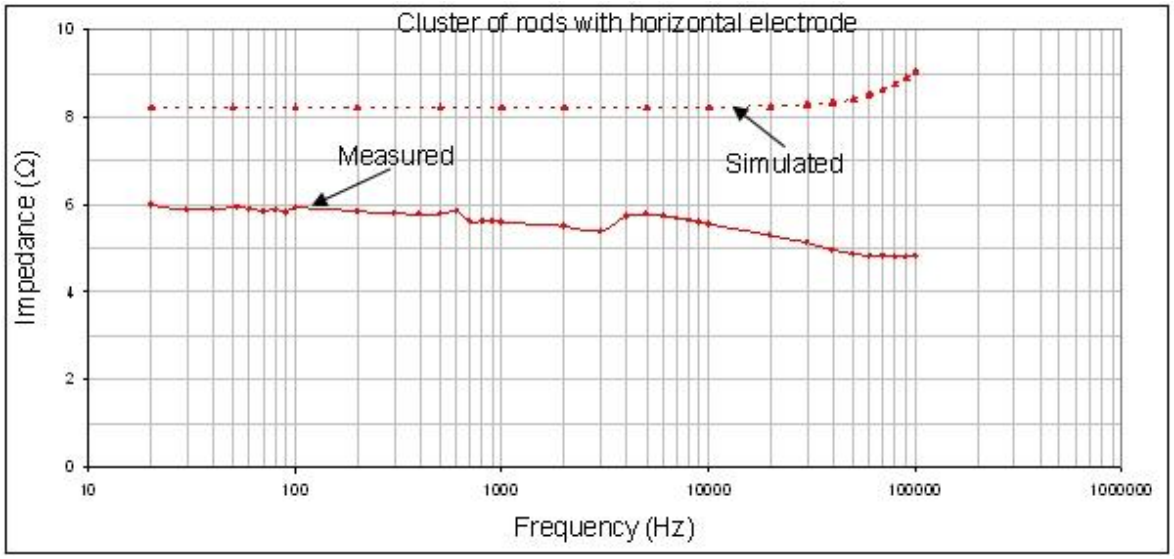

Figure 6.7 Comparison of simulated and measured earth impedance of cluster of rods

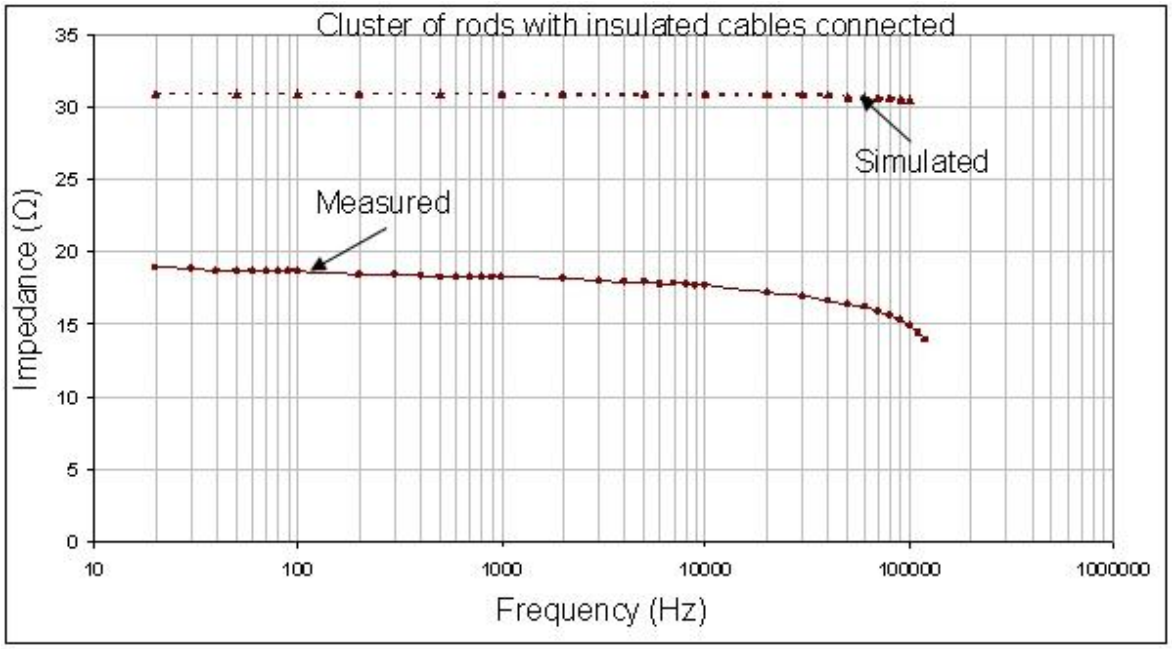

Figure 6.8 Comparison of simulated and measured earth impedance of cluster of rods

6.1.3 Operational 275kV tower base (VP9)

The geometry used for the operational 275kV tower base (VP9) was similar to that shown in the Figure 6.2 and 6.3. The soil model used for the simulation of the impedance of the operational 275kV tower base (VP9) is shown in the Table 6.3

Table 6.3 Two layer soil model of operational 275kV tower base at Llanrumney test site

Earth Electrode	Resistivity of upper layer (Ωm)	Thickness of upper layer (m)	Resistivity of lower layer (Ωm)	Thickness of lower layer (m)
Operational 275kV tower base (VP9)	250	9	70	infinite

The comparison of simulation and measurement test results for the 275kV operational tower base (VP9) at Llanrumney shows that

1) In the case of current injection at VP9 with the overhead earth wire connected, there is a close agreement between the measured and simulated values of earth impedance over the low frequency range as shown in Figure 6.9. At 100 kHz, the measured earth impedance of this arrangement is close to the measured earth impedance of the isolated VP9 (with the overhead earth wire disconnected).

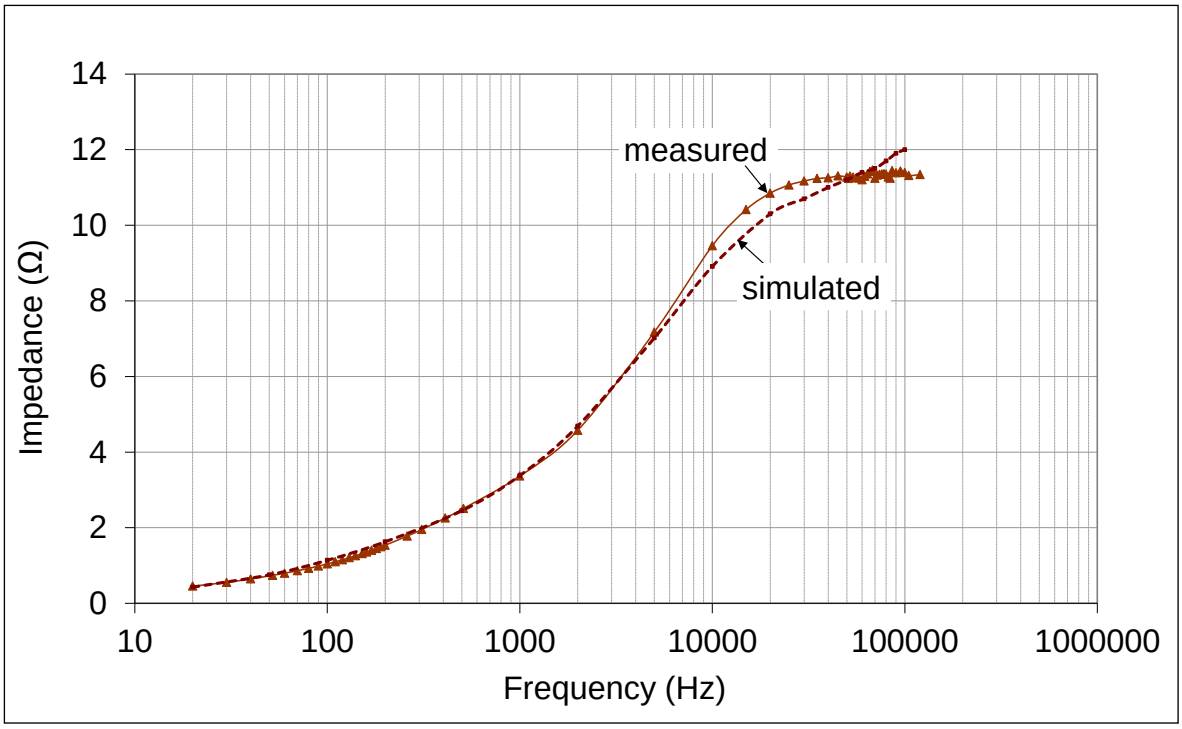

Figure 6.9 Comparison of simulated and measured earth impedance of operational 275kV tower base VP9 with overhead earth wire connected

2) In the case of the isolated VP9 tower (with the overhead earth wire disconnected), the simulated earth impedance is constant up to a frequency of 20kHz as shown in Figure 6.10. Between 20kHz and 100kHz, the simulated results show a slight increase in impedance. The measured earth impedance, however, shows a reducing trend over the frequency range 20Hz to 100kHz.

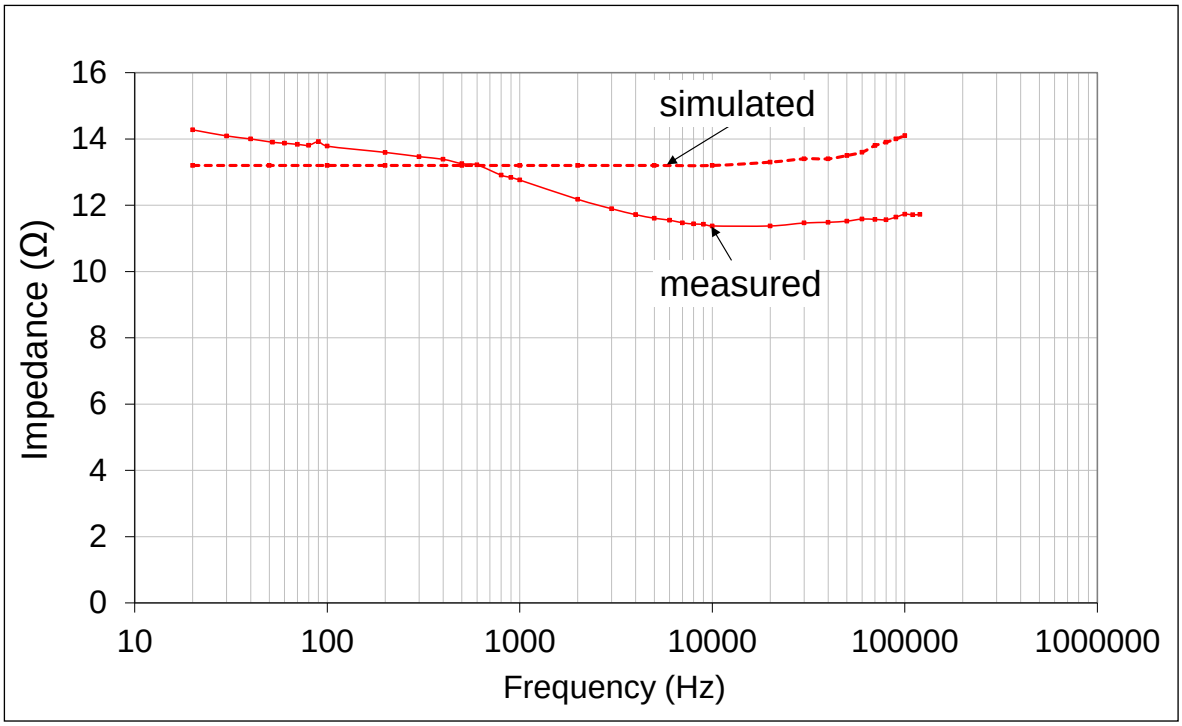

Figure 6.10 Comparison of simulated and measured earth impedance of operational 275kV tower base VP9 with overhead earth wire dis-connected

6.1.4 Comparison of simulation with experimental test results (Dinorwig test site)

The two layer soil resistivity model used for the simulation of impedance of test electrodes used at Dinorwig test site is shown in the Table 6.4. The electrode geometries simulated for the Dinorwig test site were Rod 2A, Grid 1 and Grid 2 as shown in the Table 6.5..

Table 6.4 Resistivity model of Dinorwig test site

Depth of layer (m)	Resistivity (Ωm)
5.5	115
Infinite	600

Table 6.5 List of earth electrodes tested at Dinorwig test site

Type of earth electrode	Designation used in the experiments	Material	Dimensional details
Single rod	Rod 2A	Copper	14mm dia., immersed 200cm deep in water
Grid 1	5m x 5m grid	Aluminium	5m x 5m earth grid, $50\times6mm^2$ at cross section, immersed 20cm deep in water
Grid 2	5m x 5m grid	Aluminium	5m x 5m earth grid, $50\times6mm^2$ at cross section, immersed 40cm deep in water

Unlike the Llanrumney test site, there is a close agreement between the simulated and measured earth impedances at Dinorwig test site for Rod 2A and two depths of 5m x 5m grid over the frequency range 20Hz to 1MHz as shown in Figure 6.11, Figure 6.12, Figure 6.13 and Figure 6.14. This is due to the relative ease of the representation of the resistivity of the conducting medium in the form of horizontally layered model for Dinorwig test site. It was also noted that there are contradictory trends between measurements and simulations above a frequency of few MHz for both the electrodes. This may be due to the significant electromagnetic coupling between current injection and potential measurement leads at high frequencies above few MHz.

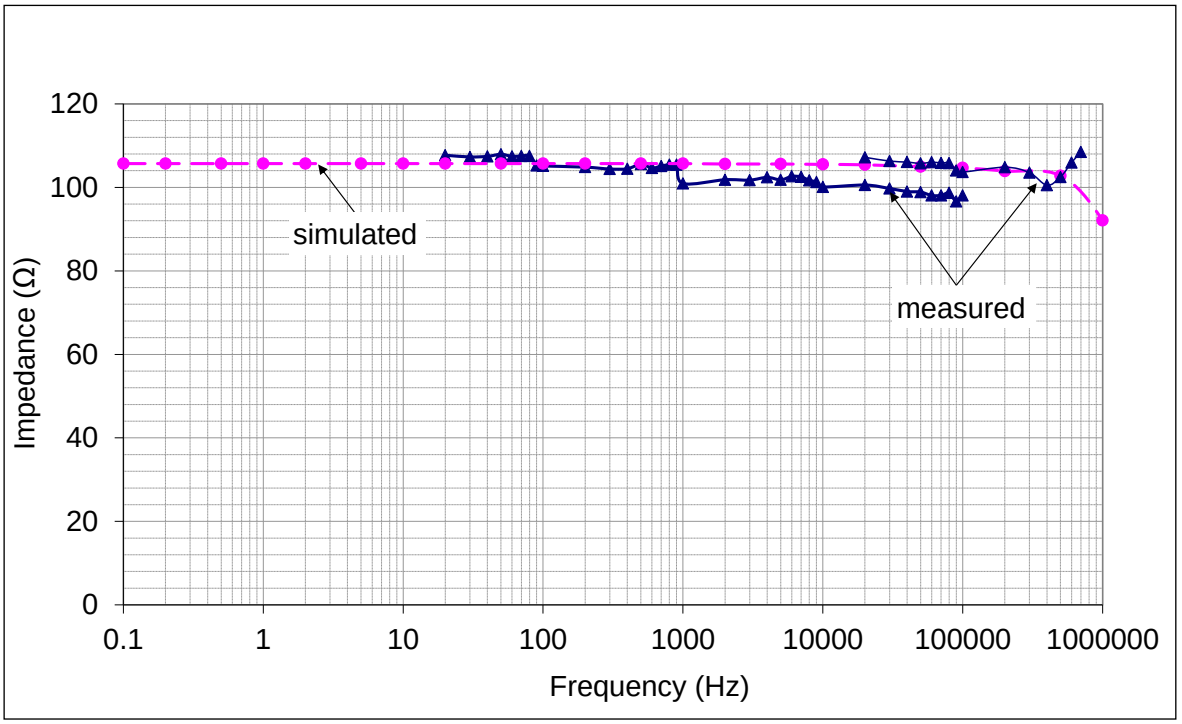

Figure 6.11 Comparison of simulated and measured earth impedance of Rod 2A

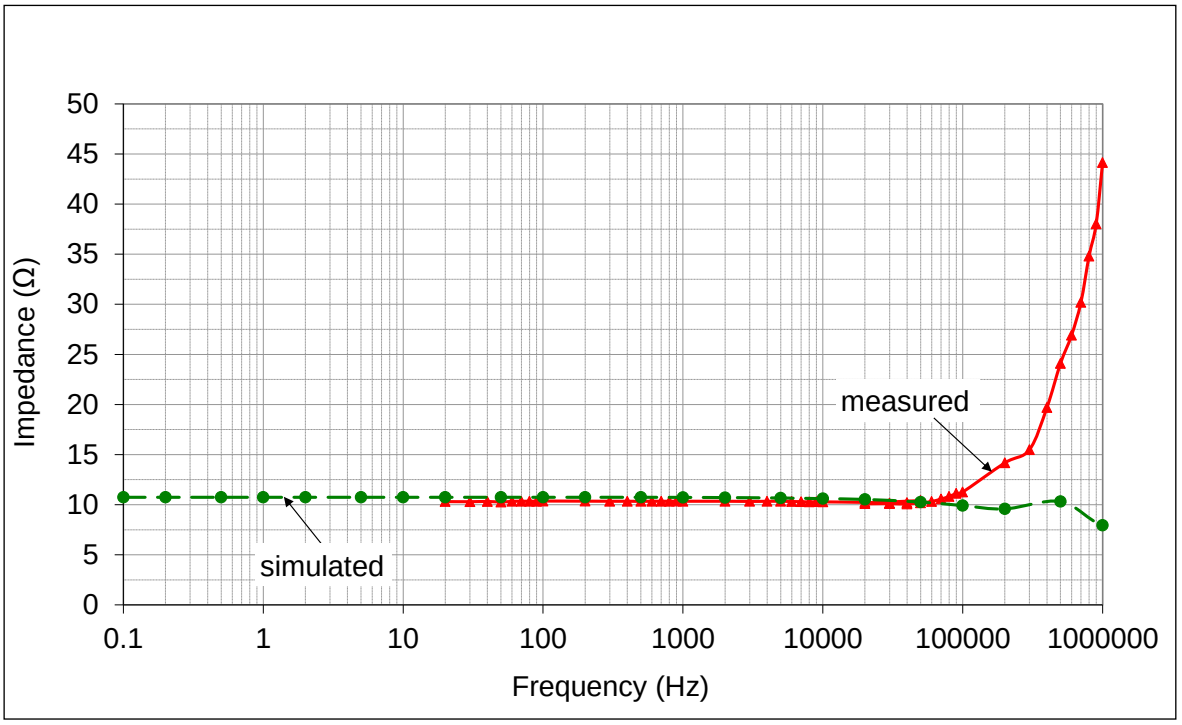

Figure 6.12 Comparison of simulated and measured earth impedance of Grid 1

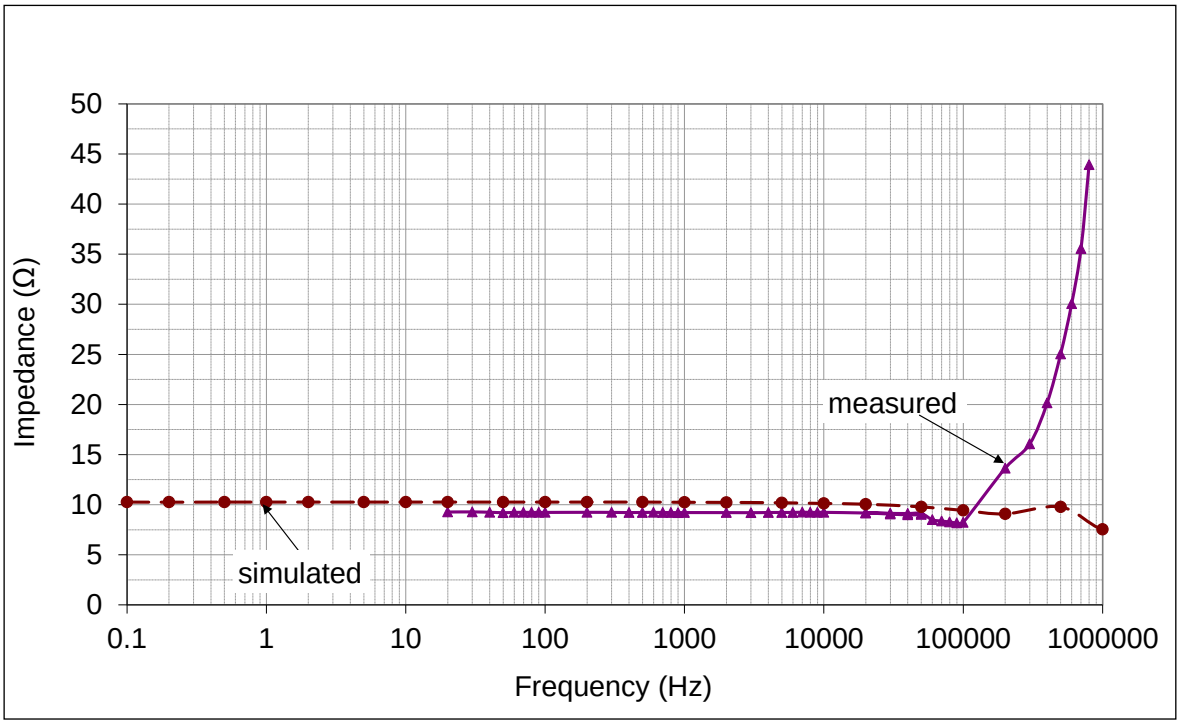

Figure 6.13 Comparison of simulated and measured earth impedance of Grid 2

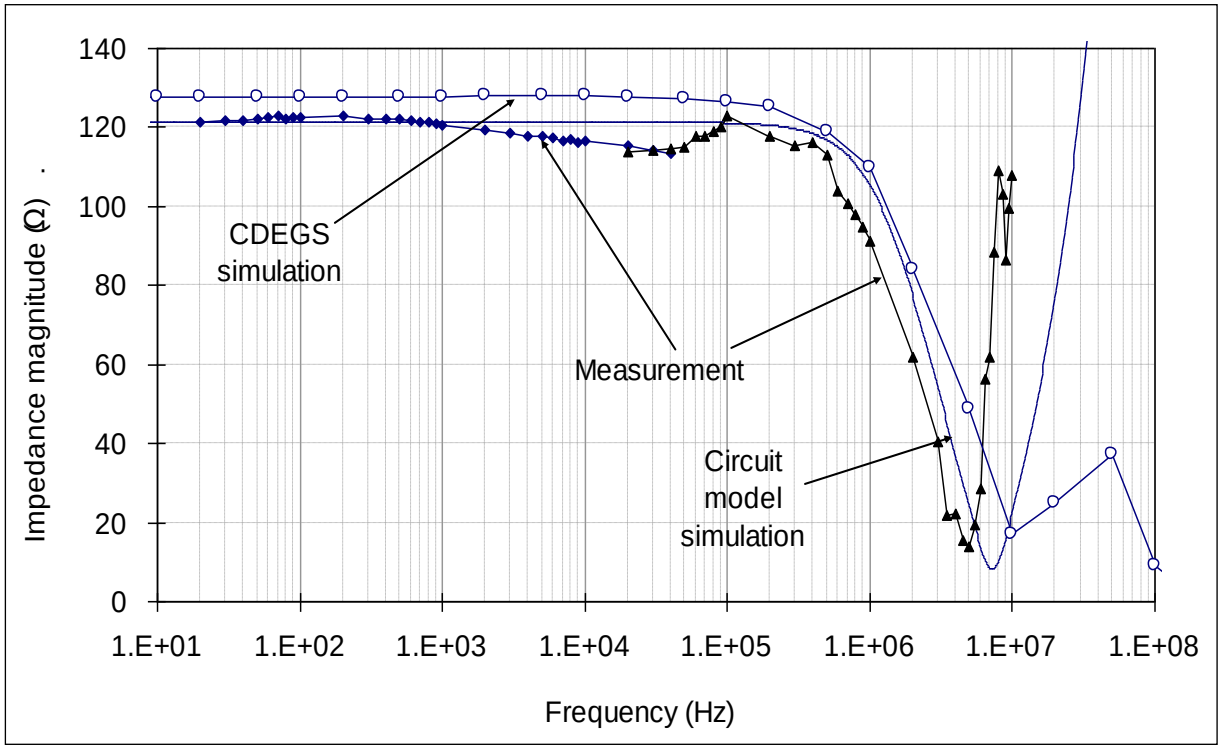

Figure 6.14 Comparison of simulated and measured earth impedance of single rod at Dinorwig

6.2. Conclusion

The extensive experimental data has been compared with numerical modelling of the test electrodes. It was observed that the numerical modelling of the test electrodes does not exhibit the reducing trend of earth electrode impedance with increase in frequency over the range 20Hz to 120kHz. However the numerical modelling does show sharp reduction in the earth impedance of earth electrodes above a frequency of few mega-hertz which is mainly attributed to the capacitive effects in the soil getting dominant above few mega-hertz. It was also observed that the measured earth impedance of earth electrodes at Llanrumney test site is different in magnitude to that predicted by the numerical modelling. This was attributed to the difficulty in representing the heterogeneous soil model in two layer model. However the measured earth impedance of earth electrodes at Dinorwig test site show a good agreement which is due to the fact that the homogenous water resistivity is easier to represent in two layer model.

Chapter 7: Analysis of current and frequency effects on earth resistance and earth impedance

7.1. Introduction

The results from AC, DC and impulse tests reported in Chapter 5 revealed important frequency and current magnitude effects on earth resistance and impedance of the various earth electrodes considered. The calculated and simulated values of earth resistance and impedance (Chapter 6), however, did not replicate the observed experimental trends showing a reduction in resistance / impedance over a low frequency and low current range. In order to explore these findings a more detailed literature search was carried out and an attempt is made to explain the phenomena involved.

7.2. Soil conduction review

The literature review on soil conduction revealed that there is an increase in the conductivity of the soil samples tested in the laboratory when the frequency is increased from 1 to 10^8 Hz [49]. This effect has been observed by several experimentalists, and this phenomenon is termed as conductivity dispersion [49] [52] [54] [55]. Figure 7.1 shows a model of electrical conduction in the soil. As can be seen from Figure 7.1 there are three possible paths of conduction in the micro-pores of the soil as follows,

a) Solid liquid pathway: Some of the electrical current flows over the soil solid particles surfaces combined with the electrolytic current flow in the moisture content of the soil micro-pores.
b) Solid pathway: A small amount of the electrical current flows through the complete solid pathway.
c) Liquid pathway: A majority of the electric current flows through the liquid pathway.

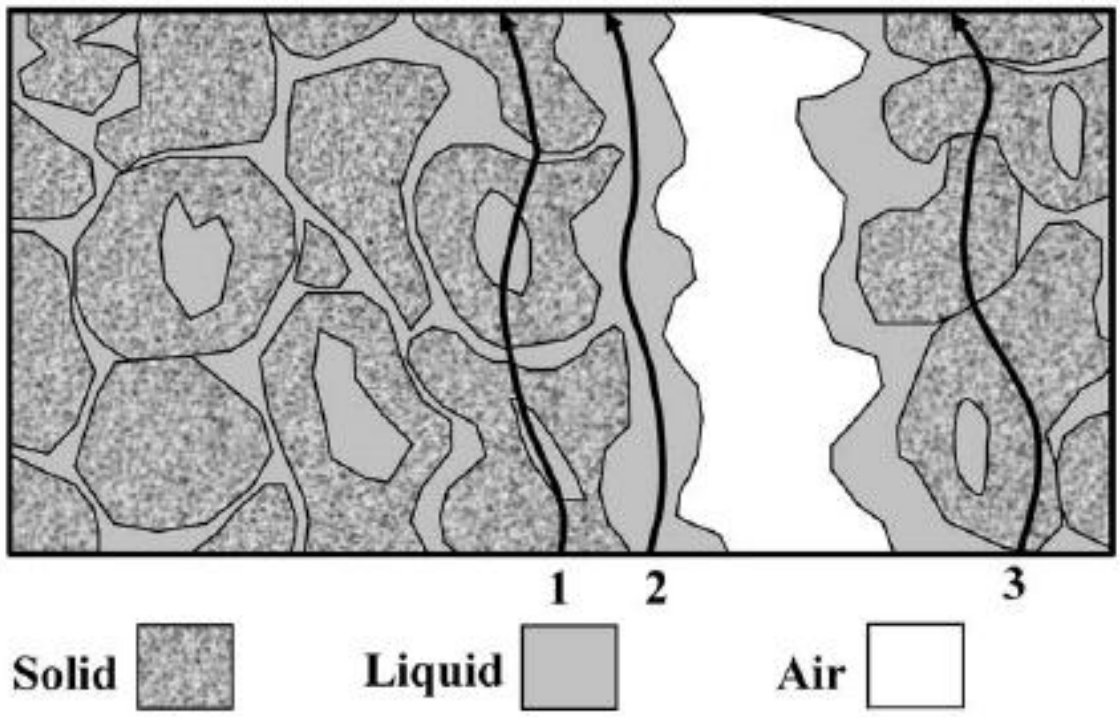

Figure 7.1 Model of conduction of electric current through soil micro-pores reproduced from [44]

7.3. Analysis of measured effect of frequency on impedance of earth electrode

With reference to the experimental results, Figure 7.2, groups all plots of earth impedances over frequency of injected current for the various electrodes tested in the field. As can be seen from the figure, all the electrodes tested show a reduction in measured earth impedance with increase in frequency over the range 20Hz to 100kHz. To visualise more clearly the effect of reduction of the measured earth impedance over frequency, the normalised values of the measured earth impedances were plotted in Figure 7.3. As can be observed from the figure, there is a decrease of between 10% and 30% in the measured earth impedances of various electrodes tested in the field.

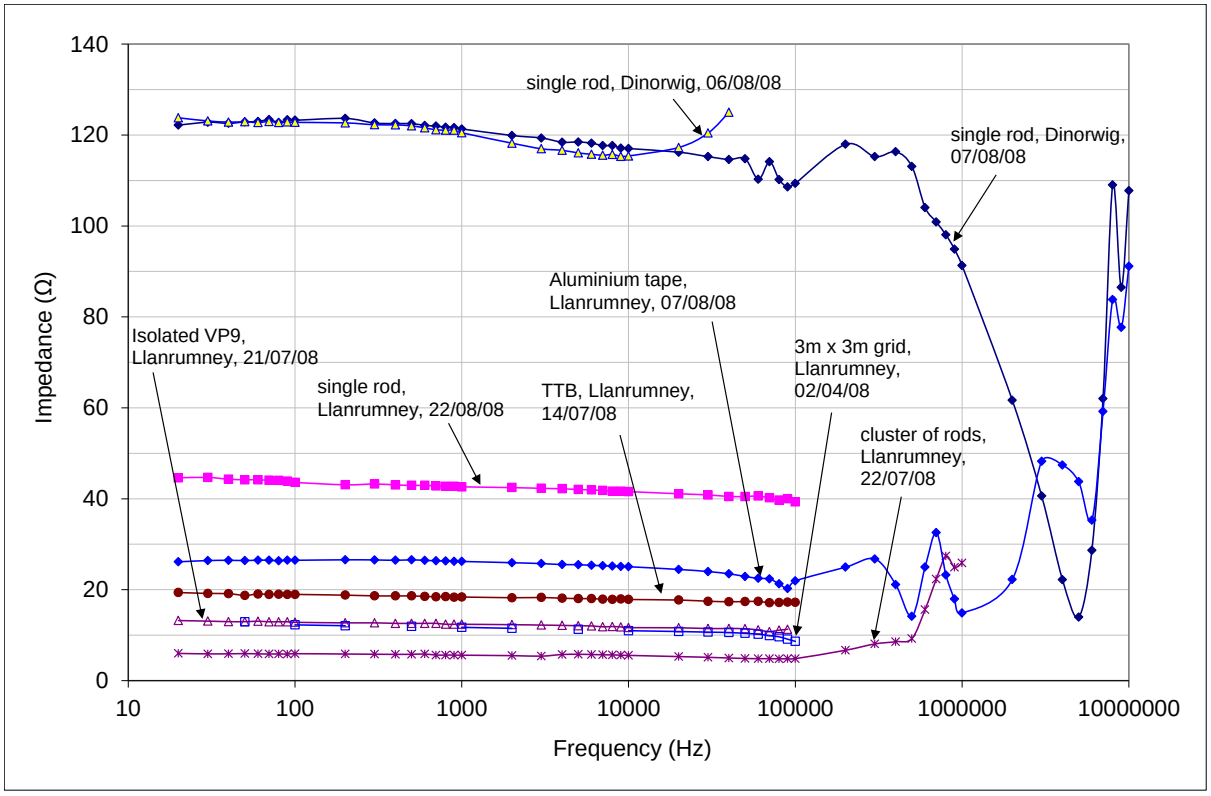

Figure 7.2 Effect of frequency on earth impedance for various electrodes

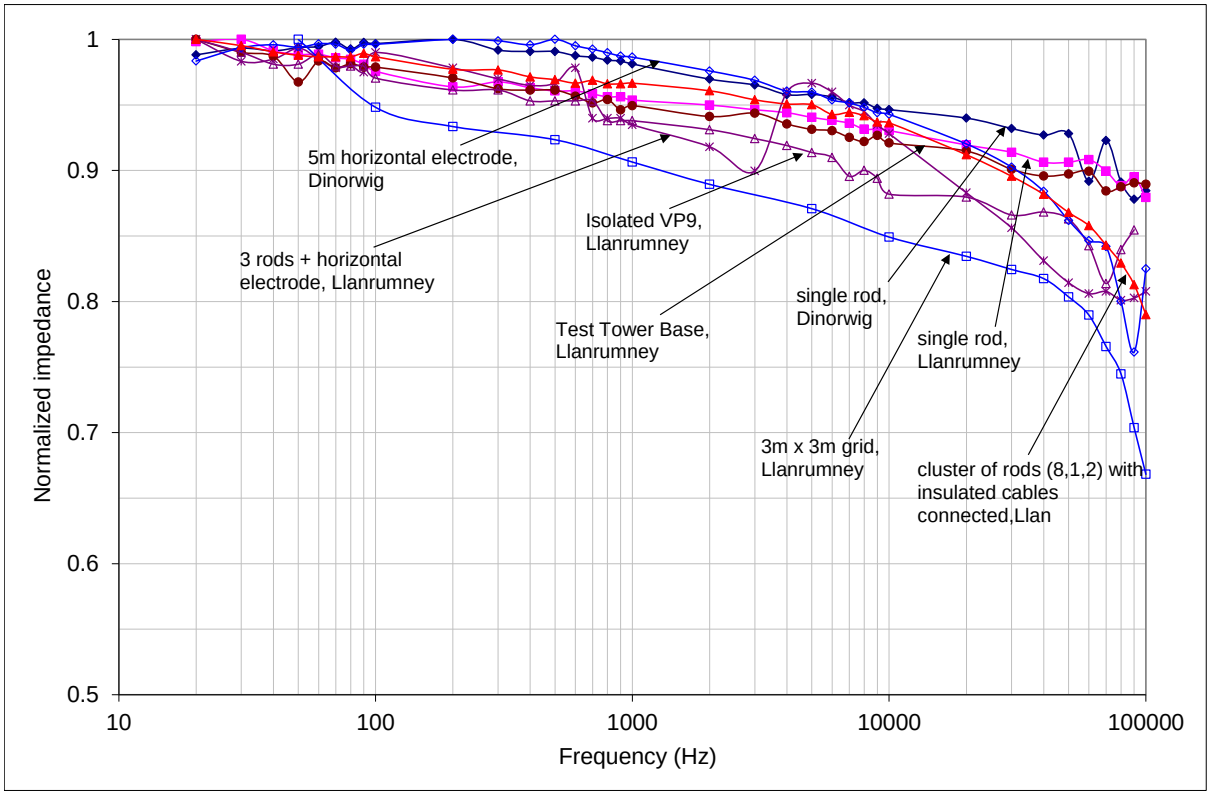

Figure 7.3 Normalized effect of frequency on earth impedance

7.4. Frequency dependence of clay water electrolyte properties: an overview

Arulanandan [46] conducted experiments on saturated kaolinite clay-water-electrolyte systems and found that there are two distinct dispersions, one in the low frequency range (0 to 100 kHz) and the other in the high frequency range (1 MHz to 100 MHz). An increase in electrical conductivity has also been experimentally observed for clays by [47], [48], [49], mineralised rocks [50], polymers [51], synthetic membranes [52], ion exchange resins [53] and polystyrene spheres [54]. The conductivity dispersion characteristics were experimentally observed in the frequency range of either 0 to 100 kHz or 1 MHz to 100 MHz.

Arulanandan [46] suggested two different mechanisms for these low frequency and high frequency conductivity dispersions; The increase in conductivity with an increase in frequency in the low frequency range is due to the increase in the surface conductance of the soil. The application of the alternating current sets the ions in an oscillatory motion. In clays and other ion exchangers, the positive counter-ions required to balance the negative fixed charges on the solid particles are in majority, and hence they impart more momentum to the water than the co-ions. Thus, there is a net water transfer in the direction of counter-ion movement. When a current is flowing in the system, there is a net water movement to accompany the flow. If a low frequency current is passing, there is enough time available for any pressure gradient to build up. Such a pressure gradient will tend to oppose the flow of the fluid. Thus, in D.C. steady state, there is an electro-osmotic counter pressure which prevents the volume flow in the clay water electrolyte solution. The hydraulic flow in the clay water electrolyte solution is caused by the passage of electric current. The electro-osmotic counter pressure opposes the hydraulic flow of clay water electrolyte solution, thereby, introducing the electrical resistivity. At high frequency, when the frequency of the alternating current is large enough, a stage could be reached when sufficient time is not available for the build up

of a pressure gradient. This stage represents the condition when there is more flow of fluid and corresponding higher electrical conductivity.

Oliver de Lima et al. [45] developed models for conductivity dispersion and compared it with the experimental observations of K. Arulanandan [46] for a sodium kaolinite sample (Hydrite R with 38.8 % water content). It was observed that the conductivity dispersion of sodium kaolinite sample (Hydrite R with 38.8 % water content) is approximately 0.018 Siemens/m at 100 Hz to 0.025 Siemens/m at 1 MHz. The conductivity dispersion of sodium kaolinite sample (Hydrite R with 59.5 % water content) is approximately 0.0135 Siemens/m at 100 Hz to 0.021 Siemens/m at 100 kHz, as shown in Figure 7.4. It was also observed that the mechanism causing the conductivity dispersion is significantly affected by the size of particles in clay water electrolyte systems.

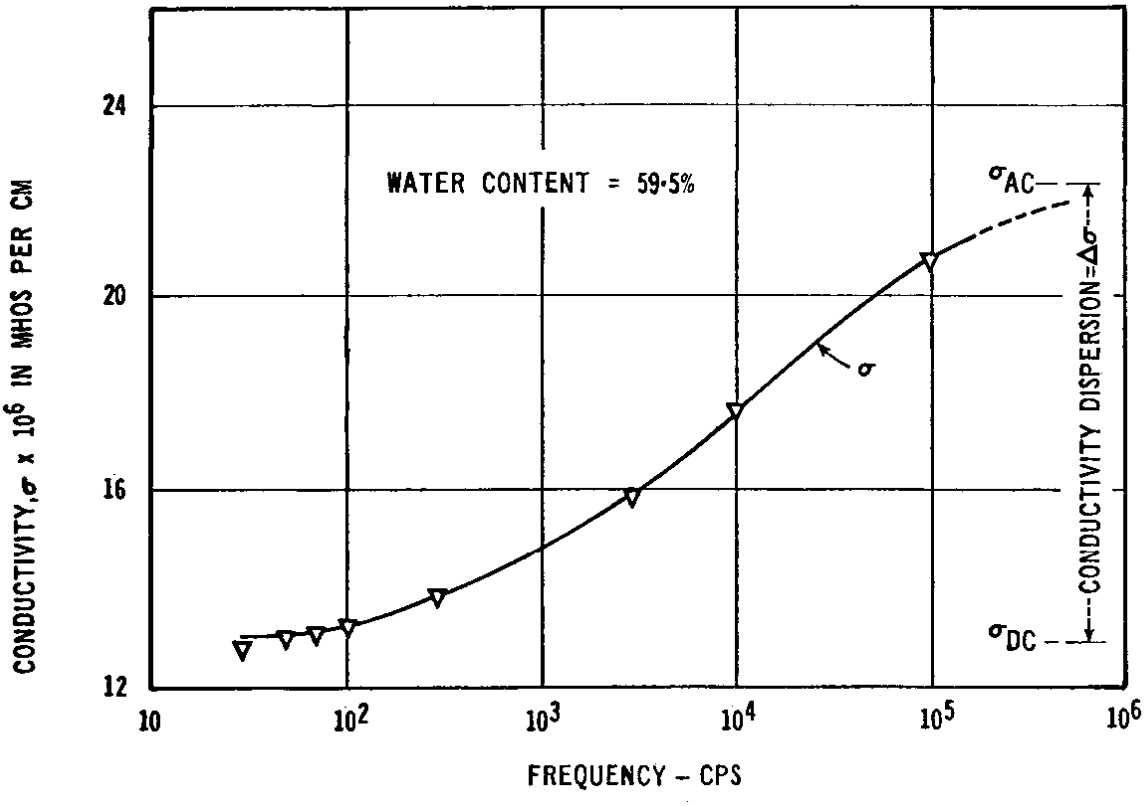

Figure 7.4 Conductivity dispersion in soil sample [46]

As seen from Figure 7.4, the increase in conductivity over the frequency range of 20Hz to 100kHz is about 33% of the value at 100kHz. The experimental results for the earth impedance measurement tests over a frequency range of 20Hz to 100kHz as shown in Figure 7.3, indicate a fall in the impedance value of 10% to 33%. The mechanism of conductivity dispersion in the soil seems to be the cause of the reduction in the measured earth impedance with increase in frequency.

Systematic experimental measurements of the electrical properties of shaly materials have shown that both their conductivity (σ) and permittivity (ϵ) are dispersive in the frequency domain. Although, individually for water and most silicate minerals, these properties are almost independent of frequency (ω), the composite properties are appreciably frequency dependent [55]. If, instead of using a DC source for measurement of resistivity, a variable low frequency AC source is used, it was found that the measured apparent resistivity of the subsurface decreases as the frequency is increased [56]. This is because the capacitance of the earth inhibits the passage of direct currents but transmits alternating currents with increasing efficiency as the frequency increases [56]. When using a standard four electrode resistivity spread in a DC mode, if the current is abruptly switched off, the voltage between the potential electrodes does not drop to zero immediately. After a large initial decrease the voltage suffers a gradual decay and can take a longer time to reach a zero value. A similar phenomenon is observed as the current is switched on. After an initial sudden voltage increase, the voltage increases gradually over a certain time interval to a steady state value. The earth, thus, acts as a capacitor and stores electric charge and it becomes polarised. The capacitance property of the earth causes both the transient decay of a residual voltage and variation of apparent resistivity as a function of frequency.

Laboratory experiments indicated that the electrical energy is stored in rocks mainly by an electrochemical process [50]. The passage of electric current through a rock as a result of an externally imposed voltage is accomplished mainly by electrolytic flow in pore fluid. Most of the rock forming minerals have a net negative charge on their outer surfaces in contact with the pore fluid and attract positive ions onto this surface. The concentration of the positive ions extends about 100 μm into the pore fluid, and if this distance is of the same order as the diameter of the pore throats, the movement of the ions in the fluid resulting from the impressed voltage is inhibited [52]. Negative and positive ions build up on either side of the blockage and, on removal of the voltage, the ions return to their original locations over a finite period of time causing gradually decaying voltage. This effect is known as membrane polarization or electrolytic polarization [45]. It is most pronounced in clay minerals where the pores are particularly small. The effect decreases with the increasing salinity of the pore fluid. When the metallic minerals are present in a rock, an alternative electronic path is available for current flow.

7.5. Effect of current on the measured earth impedance

As indicated in Chapter 5 the DC tests carried out on earth electrodes at Llanrumney and Dinorwig have revealed that there is a decrease of more than 20 % in the measured earth resistance when the injected current is varied from 1mA to 1A. Figure 7.5 shows the plots of measured earth impedance over the current range 50 mA to 3A for the various electrodes tested. In general, for the AC tests on the earth electrodes, the reduction in the measured value of earth impedance was less than 4% as shown in Figure 7.6, when the injected current was increased from 50 mA to 3A. The reduction in measured earth impedance was less than 1% between 500mA and 3A. However, for one particular electrode viz, the test tower base (VP9) as shown in Figure 7.6, a more noticeable reduction of up to 7 % was measured over

the current range 50mA to 3A. In order to check the repeatability of the measured values of tower earth impedance, the AC tests on tower base were repeated; the results of this test confirmed the previous findings. The decrease of earth resistance with the increase in magnitude of the DC current is found to be higher than that of the reduction of the earth impedance with the increase in the magnitude of AC current. It is also observed that the effect of current on the earth impedance is lower at higher frequency (1 kHz and above) compared with a lower frequency range (20 Hz to 52 Hz).

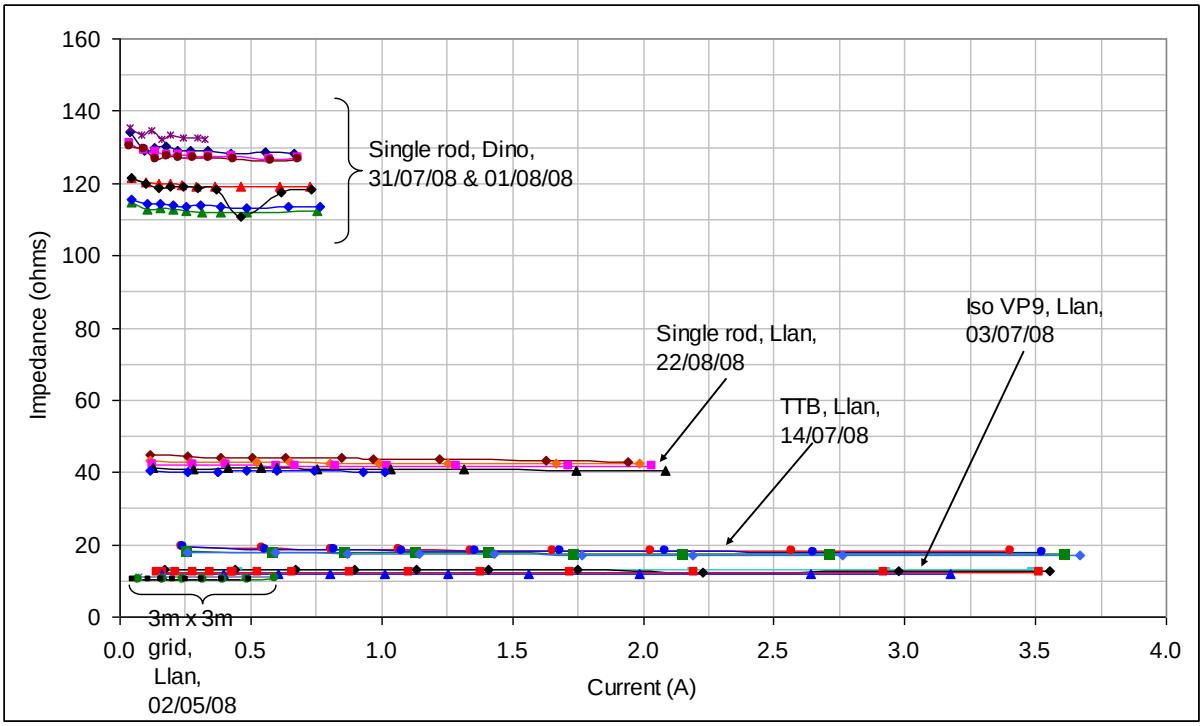

Figure 7.5 Effect of current on earth impedance

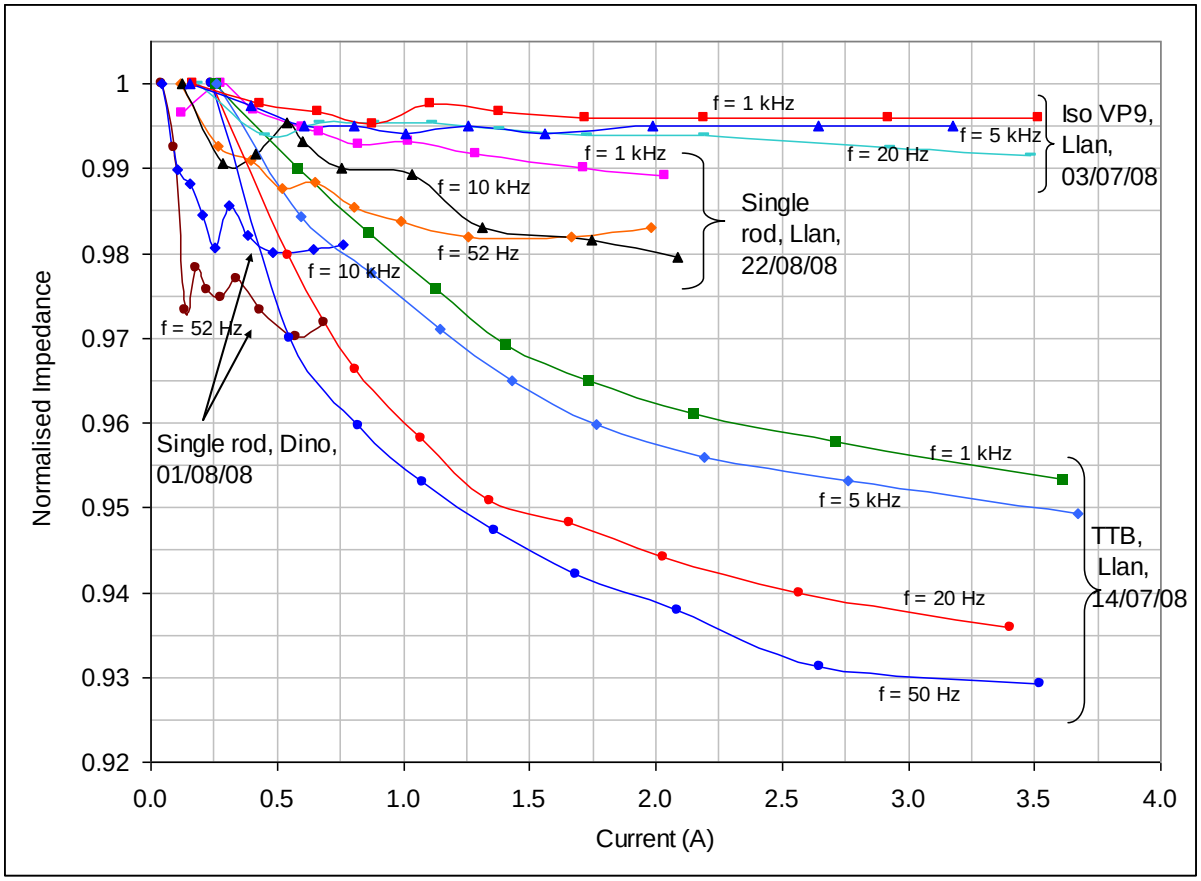

Figure 7.6 Normalized effect of current on earth impedance

7.6. Nonlinear current effect

In an attempt to explain the effect of current density on earth impedance, it was shown that the measured earth impedances exhibited an increasing trend with increase in current density in the range of 0.002A/m^2 to 0.1A/m^2 and a falling trend above 1A/m^2. It is suggested that the polarization effect, which is dominant at DC and low frequency AC (up to 50Hz), could be a possible cause of this current effect. Geo-physical literature survey [50] [56] revealed that the polarization effect occurs a) inside the micro-pores of the soil where the electric current transmits between the surface of the soil particles and the pore moisture content, and b) the interface between metallic electrodes and the soil.

The polarization impedance of metal electrodes and electrolyte interface (Z_p) operated at low current density (0.025mA/cm^2) can be calculated as given in [59] using the following equation,

$$Z_p = \left(\frac{0.005}{S}\right)\sqrt{\left(Af^{-\alpha}\right)^2 + \left(Bf^{-\beta}\right)^2} \qquad \text{---------- (7.1)}$$

Where S is the surface area of the electrode in cm^2 and Z_p is kΩ

A review of literature by Geddes [59] showed that β ranged from 0.38 to 0.78 for several common electrode metals. Table 7.1 shows the values of constants A, B, α and β for the common electrodes tested by Ragheb et al. [59] at 100Hz to 100kHz, at current density of 0.25A/m^2 [59].

Table 7.1 Values of constants for different electrode metals tested

Electrode metal	A	B	α	β
Stainless steel	989	1849	0.760	0.734
Copper	44.3	45.2	0.487	0.482
Aluminium	2427	10814	0.899	0.874

Table 7.2 shows the calculated values of polarization impedance for different electrodes tested at Llanrumney and Dinorwig for the range of current densities below 0.25A/m^2 calculated form the Equation (7.1)

As can be seen from Table 7.2, the polarization impedance for the electrodes tested in the field is negligible when compared with the measured values of earth impedances above 50Hz and the low frequency (ABEM 1Hz) measurements show noticeable polarization effects.

The non-linear effect of current magnitude has been observed by Katsube et al. [61] on dry rock samples and conductive minerals and by Ragheb and Geddes [62] on metallic electrodes in electrolytes. Katsube et al. [61] have shown that the specimen of rock samples

(serpentinite, asbestos) and conductive minerals (pyrite - FeS_2, Cubanite – $CuFe_2S_3$, galena PbS) exhibit the nonlinear current effect. They observed that the nonlinear phenomena occurred in the serpentinite and galena samples above a critical current density of 3.1 x 10^{-10}A/cm^2 at 10^{-2}Hz and 3.1 x 10^{-7}A/cm^2 at 10Hz as shown in Figure 7.8. At the test frequency of 52Hz (used in the field), the extrapolated nonlinear density would be above 3.1 x 10^{-6}A/cm^2 (above 0.03A/m^2). This is in close agreement with the field tests results which indicate nonlinearity above a current density of 0.04A/m^2, as shown in Figure 7.9. The frequency response and current dependence of the electrode-electrolyte interface resistance observed by Ragheb and Geddes [62], shown in Figure 7.8 qualitatively agrees with the test results of earth impedance measurements for electrodes tested at Llanrumney at different current magnitudes over the frequency range 20 Hz to 100kHz. The conduction of current in the soil is mainly electrolytic in nature. The combination of soil water content in the pores and the soil particles (clay particles) forms an interface through which conduction of electrical current occurs. Katsube et al. [61] suggested that the electrical non-linear phenomena occur at the micro-fractures of the soil of less than 1.0 micron thickness or at the moisture levels that have accumulated thickness of 80 microns. Their calculation was based on the assumption that the dielectric constant of water is 80.

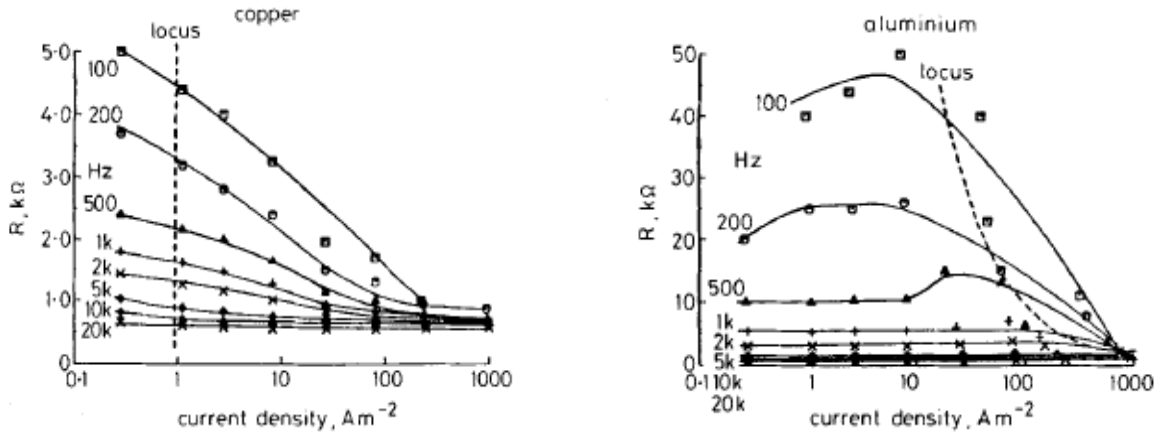

Figure 7.7 Current dependence of electrode electrolyte interface observed by Ragheb and Geddes Polarization effect observed in the literature (reproduced from Katsube et. al., "Electrical nonlinear phenomenon in rocks", Geo-physics Vol. 38, No.1, February 1973, P. 106-124

Table 7.2 Calculated values of polarization impedance

Electrode type	Surface area (m^2)	Electrode material	Frequency (Hz)	**Polarization impedance (Ω)**	Measured earth impedance (Ω)
3 m x 3m grid, Llanrumney	2.0160	Aluminium	1	**2.75**	18.64
			52	**0.087**	12.22
			100000	**0.00012**	9.39
Test tower base, Llanrumney	7.7760	Steel	1	**0.135**	23.39
			52	**0.0073**	21.22
			50000	**7.2E-03**	19.26
Isolated VP9, Llanrumney	7.7760	Steel	1	**0.135**	14.80
			52	**0.0073**	13.61
			10000	**1.5E-04**	11.84
Rod 2, Dinorwig	0.0335	Copper	1	**0.945**	123.33
			52	**0.14**	122.89
			100000	**0.0036**	109.38
Rod 1, Llanrumney	0.0605	Copper	1	**0.523**	63.87
			52	**0.078**	57.65
			100000	**0.002**	51.26
Grid 5m x 5m, Dinorwig	6.7200	Aluminium	52	**0.026**	10.27
			100000	**3.5E-05**	11.26

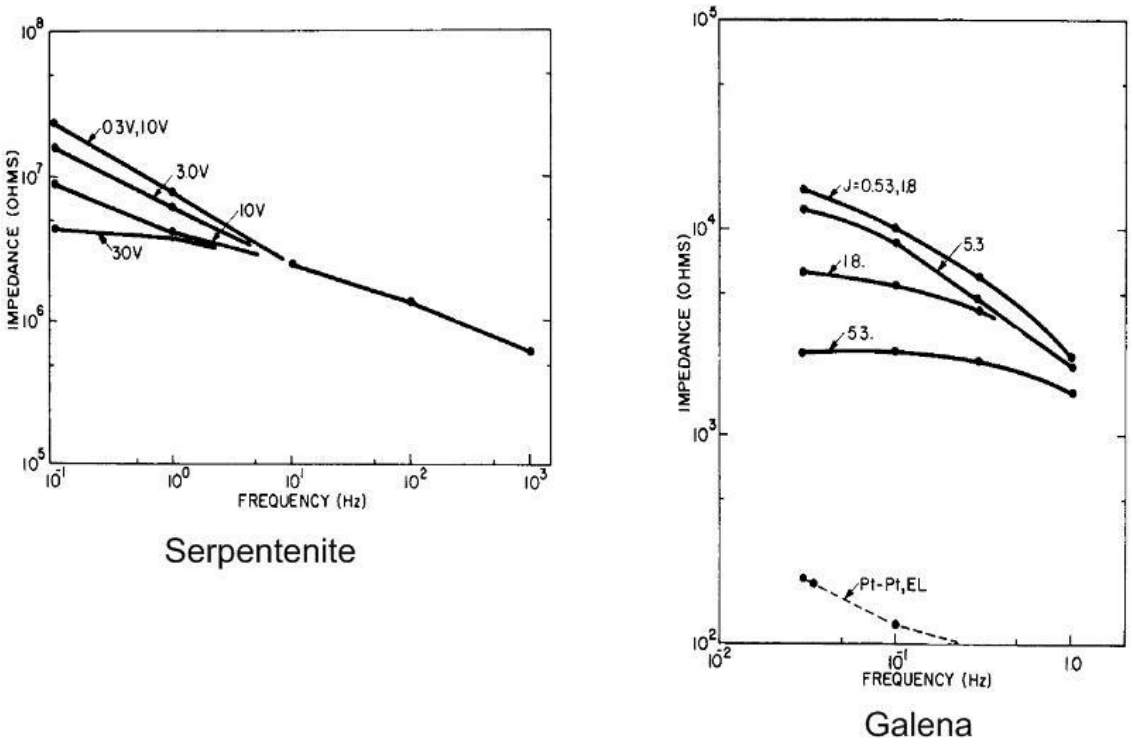

Figure 7.8 Frequency response and current dependence of the electrode-electrolyte interface resistance observed by Ragheb and Geddes [62]

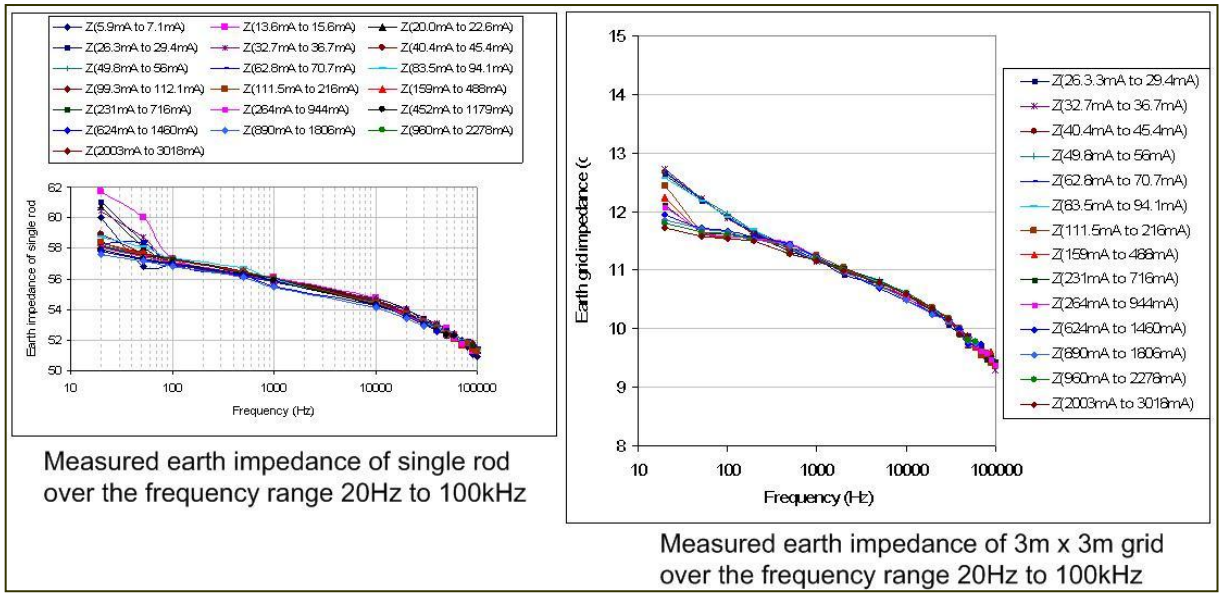

Figure 7.9 Polarization effect observed during field tests (Effect is pronounced at lower frequencies ~20Hz to 100Hz)

7.7. Comparison of variation of normalized impedance with current density

Previously reported field and laboratory a.c. tests have shown a trend of reduction of resistance/impedance of the test electrode of between 2% and 9% over the current range of between 10mA to about 5A. However, different rates of reduction in earth resistance with current were observed for different electrodes. Further calculations were carried out so that the values of earth resistance could be expressed as a function of current density at the electrode surface. The calculation of current density was achieved by dividing the total injected current by the total earth electrode surface area in the earth medium. It should be noted that the current density, as calculated, is an approximate average value. The current density at a particular point on the electrode varies according to the local surface area and position relative to the centre and extremity of the electrode. Figure 7.10 (a) to (d) show the earth resistance of rod, rods cluster, grid, TTB, isolated VP9 and resistance of laboratory test cell as a function of current density over the range 0.01 to 30A/m^2. From the results shown in the figures it can be said that the electrode resistance is relatively constant up to a current density of 1A/m^2. Between a current density of 1 and 30A/m^2, the earth resistance falls. This trend applies for all rods, rods clusters, grids horizontal electrodes at both Llanrumney and Dinorwig. However, there is one exception relating to the test tower base at Llanrumney. For this particular electrode, the reduction in earth resistance is much greater and it occurs over a range of much lower current density.

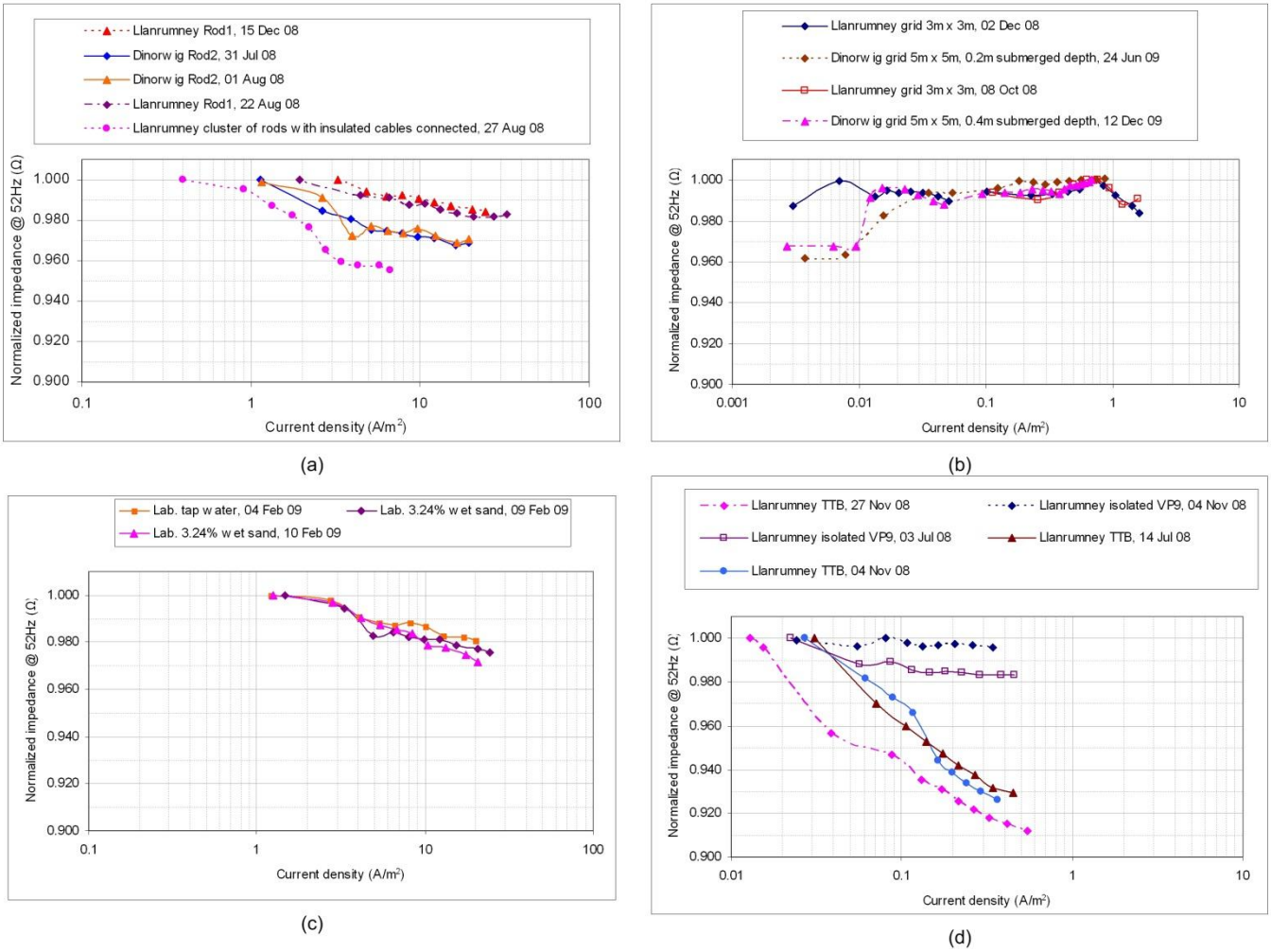

Figure 7.10 Comparison of normalized effect of current density on earth impedance

7.8. Conclusion

The geological literature survey revealed that there is conductivity dispersion in the clay water electrolyte solution when it is subjected to higher frequency electrical current. The conductivity dispersion is a phenomenon by virtue of which the conductivity of the clay water electrolyte increases to about 33% over the frequency range 20Hz to 100kHz. This phenomenon seems to be responsible for the reduction of earth electrode impedance with the increase in frequency. The geological literature survey also showed that the polarisation effect in the soil electrolyte tends to be pronounced at low frequency. The non-linear effect of current magnitude as a result of the polarisation effect in the soil seems to be responsible for the pronounced effect of DC current magnitude on the impedance of earth electrodes. It was

observed in the geological literature survey that the nonlinear phenomena occurred in the serpentinite and galena samples above a critical current density of 3.1 x 10^{-10}A/cm^2 at 10^{-2}Hz and 3.1 x 10^{-7}A/cm^2 at 10Hz. At the test frequency of 52Hz (used in the field), the extrapolated nonlinear density would be above 3.1 x 10^{-6}A/cm^2 (above 0.03A/m^2). This is in close agreement with the field tests results which indicate nonlinearity above a current density of 0.04A/m^2. The frequency response and current dependence of the electrode-electrolyte interface resistance observed by Ragheb and Geddes [62] qualitatively agrees with the test results of earth impedance measurements for electrodes tested at Llanrumney at different current magnitudes over the frequency range 20 Hz to 100kHz.

Chapter 8: Conclusion and Future Scope of Work

The survey of various earthing measurement techniques revealed that the Smart Ground Meter which operates at a maximum frequency of 400Hz would underestimate the earth of transmission tower connected with the overhead shield earthing wire. As seen from the experiments performed on the tower earth measurements of VP9 transmission tower shown in Chapter 5.6.2 (Figure 5.28) the frequency required to measure the local earth resistance of the tower base connected with the shield wires is about 30kHz. This aspect shows that the variable frequency and impulse measurements are important tool during the field tests. It was also seen during the field tests that measuring the earth resistance of various test electrodes at low DC currents (DC currents ranging from 1mA to 10mA) overestimates the value of the earth resistance. Moreover, it was observed that, the current density in the earthing electrodes during the tests plays an important role in connection with the measured value of the earthing resistance. A care has to be taken to inject the current such that a sufficient current density is achieved during the tests to achieve the appropriate value of the measured earth resistance of the test object.

8.1. Advantages and limitations of different earthing measurement techniques

A number of approaches have been used during the course of this project to measure/calculate the earth resistance / earth impedance of a variety of earth electrode systems. These are as follows

1) Switched DC for earth resistance measurement
2) Variable frequency AC for earth impedance measurement
3) Impulse

a. Calculation of impulse resistance from instantaneous voltage at peak current over the value of peak current V@Ipeak/Ipeak

b. FFT analysis to obtain frequency response

The main findings in this area including the advantages and limitations of these techniques are summarized as follows:

i) <u>Switched DC Technique</u>:

In this technique, the injected current is typically supplied from a battery driven inverter as a symmetric square wave DC source (typically 90 to 130Hz for commercial 'earth testers' and around 1Hz for 'geo-physical' meters). Such instruments have an output voltage limited to 50V and delivering currents ranging from 1mA to 1A. However, the magnitude of earth resistance measured with this type of instrument may not be representative of the value of the earth impedance under a.c. power frequency (depending on the size of earthing system) nor the characteristics of the electrode under impulse conditions. Experimental tests in this project have demonstrated that both the magnitude of injected current and switching frequency affect the measured value of the resistance. The current magnitude effect is greater at lower switching frequencies and the measurement results have shown that, over this relatively low-current range, the effect of current is quite small above 100mA. Therefore, the use of a higher DC switching frequency (e.g. between 90 to 130Hz), above the power frequency, is beneficial in reducing polarisation effects and mitigating the effects of power frequency noise. However, over this range of frequency, the inductive component of large area earthing systems may be significant and this will affect the measurement such that the reading may neither represent the earth resistance nor the earth impedance of the system.

ii) <u>Variable frequency AC Technique</u>:

The Cardiff University impedance measurement system, IMS, injects variable frequency current and, with suitable measurement of earth potential rise at the point of current injection, the frequency response of the earthing system is obtained. Moreover, the frequency selective lock-in amplifiers provide rejection of noise. Experience has shown that the impedance at

50Hz can be determined by linear interpolation when using test injection frequencies as close as 2Hz either side of 50Hz, i.e. 48Hz and 52Hz. AC tests at higher frequencies can be used to measure the earth resistance of an individual transmission tower while connected to its overhead earth wire (when the injection frequency is set higher than 50kHz). It should be noted that the time taken for acquiring the required current and EPR data using the current setup is significant, although this limitation can be overcome if the process of data acquisition is automated. Under AC tests, care is required to ensure that there is sufficient distance between the main and auxiliary earth electrodes to avoid coupling between the current injection and potential measurement leads, and the potential reference electrode is located sufficiently far away to obtain a reliable earth reference point.

iii) FFT from impulse and calculating the impulse resistance from the waveforms:

In this technique, the plot of impedance over a desired frequency range is obtained from the FFT of the impulse signals (injected current and EPR). The results obtained with this technique have shown good agreement with those obtained from variable AC tests. The frequency components obtained from the FFT of the impulse signals are limited by the sampling rate and the sampling depth (time period over which the signal is acquired). Therefore, in this investigation, two separate impulse waveforms were used; one with a fast rise time ~ 1μs, and the other with long tail (~ 50ms). In this way, frequency components ranging from 20Hz to more than 100kHz could be obtained from the FFTs of the impulse signals. This approach may be susceptible to error if the signal to noise ratio is not sufficiently high.

Another method related with impulse injection is to calculate the value of impulse resistance as V@Ipeak / Ipeak. At the instant when the injected current waveform reaches its peak value in an inductive circuit, the rate of rise of current becomes zero, and the ratio of EPR to

current is a representative of impulse resistance. The effect of current magnitude (although lower compared to low frequency currents) was observed for the impulse waveforms. Moreover, the magnitude of the impulse resistance was also affected by the rise time of the impulse (i.e. lower value of resistance in the case of faster rise time)

In summary the investigations carried out in this work have allowed to reach practical conclusions on the suitability and limitations of existing / available earth testing measurement techniques and instrumentation. These conclusions are as follows,

Switched DC test techniques to measure electrode earth resistance should be limited to small area earthing systems.

For low-current test instruments, a certain minimum current may be required e.g. 100mA.

Variable frequency AC tests require very good noise rejection capability in order to allow injection close to the power frequency and hence accurate determination of power frequency earthing impedance.

Impulse tests may be used to determine the impulse resistance with relatively low source power requirements, although the use of FFT to determine the power frequency impedance will require further investigation under conditions of realistic background noise.

8.2. Validity range of earthing measurement techniques

From an analysis of measurement results from the project test programme, consideration has been given to determine a feasible range of test current magnitude and a frequency range under DC / AC test conditions. In this work it was clearly shown that the non-linear effect of current is greater at lower frequencies.

The switched DC test instrument such as ABEM Terrameter (approx. 1Hz) has shown the highest reduction in measured resistance (up to 20%) over the range 1mA to 1A. Further reduction in measured resistance may occur above 1A. Switched DC tests carried out over a

higher frequency range (105Hz and 160Hz) using the DET2/2 did not reveal any significant change in measured resistance for any of the test electrodes at the two different current magnitude settings (7mA and 50mA).

For a.c. tests, in the 48-52Hz frequency range, the phenomenon of resistance reduction with current is less pronounced (7% over the current range 10mA to 3.5A). The variable frequency a.c. tests indicated that the current magnitude effect reduces appreciably over the frequency range 20Hz to 1kHz, above which frequency the reduction of resistance with current magnitude is negligible. Generally, there was close agreement between the a.c. test using the Cardiff University IMS system at about 50Hz and the DET2/2 results for the tested electrodes at Llanrumney and Dinorwig (excluding the VP9 operational tower earthing system). It is possible that by adopting relatively higher switched DC frequencies (up to 1kHz) for small earth electrodes, an overestimation of earth resistance due to the non-linear effect of current can be minimised. However, this would only be applicable to small-area earthing systems with low inductive reactance at the test frequency.

Impulse tests allowed investigation of earth resistance at higher currents up to 8A. It was found that by using currents with impulse rise-times in the range 2-60μs, the measured resistance values (impulse resistance) for the tested electrodes were up to 10% lower than those obtained at the power frequency a.c. tests. However, FFT analysis of impulse recordings gave values very close to those obtained using the variable frequency a.c. tests, including promising close agreement with the '50Hz' resistance values.

8.3. Feasible current and frequency ranges for earth impedance measurement

With the ABEM Terrameter, DC currents within the range of 1mA to 1A have been used in the past to measure the earth resistance. Extensive testing revealed that there is a pronounced non-linear behaviour within the DC current range 1mA to 100mA (reduction of measured

earth impedance with increase in current magnitude). The performance of earth impedance within this current range has not yet been fully explored and clarified. However, it was established experimentally that the earth impedance readings for current magnitudes above 100mA DC were within the acceptable range (within 5% of the measured values by DET 2/2).

For the case of AC currents used in the field (few tens of mA to few amperes), the earth impedance measurements (20Hz) was seen to exhibit a maximum reduction of 4% for different electrodes tested (except for the test tower base where it was up to 7%). It was also noted that the effect of current magnitude falls appreciably as the test frequency is increased above 1kHz. Hence, it would be useful to use current magnitudes of 50mA to 100mA at frequencies above 1kHz to measure earth impedance. Moreover, the use of higher frequency levels would reduce the effect of power frequency background noise.

The use of test frequencies of 20Hz to 100kHz in the field tests have shown that there is up to 30% reduction in the measured earth impedance over this frequency range. It would be useful to use the swept frequencies of this range in the practical earthing impedance measurement instrument to evaluate earth impedance values at the frequencies of interest.

The set-up of the injection system near the test object is helpful to reduce electromagnetic coupling, and the test results obtained with this set up have provided comparable results for different earth electrodes tested. As seen from the experiments conducted so far, the input voltage requirement for impedance measurement increases as the frequency of injected current is increased. This is because when the injection system is placed near the test object, the return current lead (typically 50 to 100m long) will contribute to the inductance which increases linearly with injected current frequency. This means that the input voltage required to inject the desired magnitude of current at higher frequency is larger compared with the

input voltage required to drive the same amount of current in the earthing system at lower frequency. If a low inductance lead is used for the return current circuit, then the input voltage requirement of the injection system may be reduced.

The impulse current injection tests have been conducted on various earthing electrode systems. An approach to obtain the FFT spectrum from the time domain impulse signals of current and EPR (earth potential rise) has been introduced in this work. This investigation demonstrated that the highest frequency under which the response of an earthing system can be computed by FFT analysis is the frequency component of the initial rise of the impulse current signal. The rise time of the injected current signal is also influenced by the total inductance of the earthing measurement circuit. If the inductance of the measurement circuit is reduced, by selecting low inductance return lead, then the highest frequency under which the response of an earthing system is computed can be increased. The lowest frequency component under which the response of an earthing system impedance can be computed is given by the inverse of the product of the sampling time interval and the sampling depth. For e.g. if the (10 % to 90%) linear rise time of the current signal is 1μs, the sampling interval is 200ns and the sampling depth is 500ksamples, then the lowest and highest frequency range under which the response of the earthing system can be computed is 100 Hz to 1 MHz in steps of 100 Hz each. This analysis will yield a frequency domain response which is comparable to that obtained from variable frequency test results. It is planned to adopt these findings in the future impulse current injection tests.

8.4. Future scope of work

In the present project, the effect of current magnitude has been analysed to a fair extent. It was observed that the current density into the earth electrode during the tests has important correlation to the effect of current on the measured earth impedance. In future, it would be

useful to further investigate the effect of current density, taking into consideration the materials such as copper, aluminium and steel. It could be useful to find a critical current density point in the earth electrode beyond which the current magnitude effects on the measurements could be reduced.

It would be useful to explore the possibility of developing the computer models that can accommodate the soil polarisation effects leading to the nonlinear current effect phenomenon and the conductivity dispersion effects exhibiting the frequency dependence of the earth impedance measurements.

It is well known that the impulse measurement tests have performed by several experimentalists in the hundreds of amperes range already and such results could be analysed using the proposed FFT analysis introduced in this work.

Similarly, the effect of frequency on the measured earth impedance was investigated up to a frequency of 100 kHz. Above 100 kHz the electromagnetic coupling effect is expected to be significant which may distort the measurement. A possible solution is to use low inductance co-axial cables for measurement purposes whenever possible. If the effect of frequency is to be studied beyond 100 kHz range, and up to 1 MHz range, it would be useful to characterise the behaviour of earthing systems for the lightning characteristic frequency.

References

[1] Leonid D. Grcev, "Transient Electromagnetic Fields Near Large Earthing Systems", IEEE Transactions on Magnetics, Vol 32. No. 3 , pp. 1525-1528, May 1996

[2] C. F. Dalziel, "Electric shock hazard", IEEE Spectrum, pp. 41-50, February 1972.

[3] C. F. Dalziel and W.R.Lee, "Re-evaluation of lethal electric currents", IEEE Transactions on Industry Applications, vol. IA-20, No. 4, pp. 1089, July 1984.

[4] P. G. Beigelmeier and W.R.Lee, "New considerations on the Threshold of Ventricular Fibrillation for AC shocks at 50-60 Hz", IEE Proceedings, Physical Science, Measurement and Instrumentation, Management and Education - Reviews, Vol. 127, No. 2, pp. 103-110, March 1980.

[5] "IEEE guide for safety in AC substation earthing", IEEE Std. 80-2000, pp. i-192, 2000.

[6] L. D. Grcev and M. Heimbach, "Frequency dependent and transient characteristics of substation earthing systems", IEEE Transactions on Power Delivery, Vol. 12, No. 1, pp. 172-178, January 1997.

[7] M. Heimbach and L. D. Grcev, "Grounding system analysis in transients programs applying electromagnetic field approach", IEEE Transactions on Power Delivery, Vol. 12, No.1, pp. 186-193, January 1997.

[8] Z. Rong, H. Jinliang, and G. Zhicheng, "Novel Measurement system for Grounding Impedance of Substation," IEEE Transactions on Power Delivery, Vol. 21, No.2, pp. 719 - 725, April 2006.

[9] A. P. S. Meliopoulos, G. Cokkinides, H. Abdallah, S. Duong, and S. Patel, "A PC based ground impedance measurement instrument", IEEE Transactions on Power Delivery, Vol. 8, No.3, pp. 1095-1106, July 1993.

[10] P. J. Higgs, "An Investigation of Earthing Resistances", Journal of the Institution of the Electrical Engineers, Vol. 68, No.402, pp. 736-705, June 1930.

[11] "IEEE Guide for measuring earth resistivity, earth impedance and earth surface potentials of a ground system, Part I - Normal Measurements", IEEE Std. 81-1983.

[12] Hideki Motoyama, "Experimental and analytical studies on lightning surge characteristics of ground mesh", Electrical Engineering in Japan, Vol. 160, No.4, pp. 16-23, September 2007.

[13] Sunde ED, "Earth conduction effects in transmission systems", Dover Publications Inc.; New York edition, 1968, ISBN-10: 0486618919, ISBN-13: 978-0486618913.

[14] Portela C, "Soil electromagnetic behaviour", International conference on Grounding and Earthing, Proceedings, pp 53-58, Belo, Horizonte, Brazil, April 1998.

[15] Leonid Grcev, "Improved design of power transmission line earthing arrangements for better protection of against effects of lightning, Proceedings of the International Symposium on Electromagnetic Compatibility (EMC'98 ROMA), Paper C1-7, pp. 100-103, Rome, Italy, 1998.

[16] H Griffiths and N Pilling, Chapter 8, "Earthing", "Advances in High Voltage Engineering", IEE Power and Energy Series 40, Edited by A. Haddad and D. Warne, The Institution of Electrical Engineers, UK, 2004, ISBN# 0 85296 158 8

[17] Dawalibi F and Mukhedkar D, "Resistance measurement of large grounding systems", IEEE Power Engineering Society Meeting, IEEE paper F79656-0, Vancouver, 1979.

[18] Tagg G F, "Earth Resistances", George Newnes Ltd., London, 1964, ISBN 003210

[19] Tagg G F, "Measurements of the resistance of an earth electrode system covering a large area", Proceedings of the Institution of Electrical Engineers, Vol. 116, No.3, pp. 475-479, March 1969.

[20] Curdts E B, “Some of the fundamental aspects of ground resistance measurements", AIEE Transactions, Vol. 77, No.1, pp 760, 1958.

[21] Dawalibi F and Mukhedkar D, “Ground electrode resistance measurement in non-uniform soils”, IEEE Transactions on Power Apparatus and Systems, Vol. PAS-93, No. 11, pp. 109 – 116, January 1974.

[22] Dawalibi F and Mukhedkar D, “Modelling of potential distribution around a grounding electrode”, IEEE Transactions on Power Apparatus and Systems, Vol. PAS-92, No. 5, pp. 1455-1459, 1973.

[23] Tagg G F, “Measurements of earth electrode with particular reference to earth electrode systems covering a large area", Proceedings of the Institution of Electrical Engineers, Vol. 111, No.12, pp. 2118 - 2130, Dec 1964.

[24] “Getting Down to Earth, A Practical Guide to Earth Resistance Testing”, by Megger, 1-866-254-0962, www.megger.com

[25] Liwei Li, Jiyan Zou, Hui Sun, “Research on the New Clamp-on Grond Resistance On-line Tester Based on AC Variable Frequency”, Proceedings of the 6th World Congress on Intelligent Control and Automation, Vol. 2, pp. 5286-5289, Dalian, China, June 21 - 23, 2006.

[26] Kruger M, “Measurement of overhead line and cable impedance values, earth impedance of large substations and electromagnetic interference between overhead lines and signal cables using a new technology”, International Conference on Developments in Power System Protection, Vol.1, pp. 240-243, April 2004.

[27] A.P.Meliopoulos, George Cokkinides, Hanna Abdallah, Steven Duong, Shashi Patel, “A PC Based Ground Impedance Measurement Instrument” , IEEE Transactions on Power Delivery, Vol.8, No.3, pp.1095-1106, July1993

[28] A.P.Meliopoulos, Shashi Patel, G. J. Cokkinides, “A New Method and Instrument for Touch and Step Voltage Measurements", IEEE Transactions on Power Delivery, Vol.9, No.4, pp. 1850-1860, October 1994.

[29] Jinxi Ma and Farid P. Dawalibi, “Grounding Analysis of a Large Electric Power Station”, International Conference on Power System Technology, pp.1-6, 2006.

[30] A.J. Surtees, F.D. Martzloff and A. Rousseau, “Grounding for Surge Protective Devices Ground Resistance versus Ground Impedance”, IEEE Power Engineering Society General Meeting, 2006.

[31] "ENA Power System Earthing Measurement Guide", EG0, Part - I, Management Principles, Draft Issue, August 2009.

[32] H. Griffiths, P. Jones, D. Tomlin, N. Harid, A. Haddad, “Proposal for Measurement of Earth Impedance at High Voltage Electricity Installations Using Variable Frequency Injection", International Conference on Grounding and Earthing and 2nd International Conference on Lightning Physics and Effects, Brazil, November 2006.

[33] Jong-kee Choi, Yong-ho Ahn, Sun-guen Goo, Kijun Park, Jin-yul Yoon and Gil-jo Jung, “Direct Measurement of Frequency Domain Impedance Characteristics of Grounding Systems”, International Conference on Power System Technology, Vol. 4, pp. 2218-2221, 2002.

[34] L. Bellaschi, “Impulse and 60 cycle characteristics of driven grounds”, Transactions of the American Institute of Electrical Engineers, Vol. 60, No. 3, pp. 123-128, 1941

[35] L. Bellaschi, “Impulse and 60 cycle characteristics of driven earths”, in II Trans. AIEE, vol. 61, 1941

[36] R. Verma, D. Mukhedkar, “Impulse impedance of buried ground wire”, IEEE Transactions on Power Apparatus and Systems, Vol. PAS-99, No. 5, pp. 2003-2007, 1980.

[37] B.R. Gupta, B. Thapar, “Impulse impedance of grounding grids”, IEEE Transactions on Power Apparatus and Systems, Vol. PAS-99, No. 6, pp. 2357-2362, 1980.

[38] M. Loboda, R. Kostzaluk, “Model Tests of Surge Properties of Grounding Systems in Lightning Protection”, 16th International Conference on Lightning Protection, R-5.03, Szeged, Hungary, 1981.

[39] A. L Vainer, “Impulse characteristics of complex earth grids”, Electrical Technology, USSR, Vol. 1, 1966

[40] R. Kostzaluk, M. Loboda, D. Mukhedkar, “Experimental Study of Transient Ground Impedances”, IEEE Transactions on Power Apparatus and Systems, Vol. PAS-100, No. 11, pp.4653-4660, 1981.

[41] Carlo Mazzetti, Giuseppe M. Veca, “Impulse behaviour of ground electrodes”, IEEE Transactions on Power Apparatus and Systems, Vol. PAS-102, No. 9, pp. 3148-3156, 1983.

[42] Ulrich Hauser-Ehninger,"A measurement system for the monitoring and measurement of earthing grid performance at large high voltage substations", PhD Thesis, Cardiff University, September 2007.

[43] D. Guo, D. Lathi, N. Harid, H. Griffiths, A. Haddad, A. Ainsley, "Large-scale Earthing Test Facilities at Dinorwig Power Station", International Conference on Condition Monitoring and Diagnosis, pp.808-811, Beijing, China, April 21-24, 2008.

[44] D. L. Corwin, Leesch, S.M., "Apparent Soil Electrical Conductivity Measurements in Agriculture," Computers and Electronics in Agriculture, Vol. 46, No. 1-3, pp. 11-43, 2005.

[45] A. L. Olivar de Lima and M. M. Sharma, "A Generalised Maxwell Wagner Theory for Membrane Polarization in Shaly Sands," Geophysics, Vol. 57, No.3, pp. 431-440, 1992.

[46] K. Arulanandan, "Hydraulic and Electrical Flows in Clays," Clays and Clay Minerals, vol. 17, No.2, pp. 63-76, 1969.

[47] V. Vacquier, C. R. Holmes, P. R. Kitzinger, and M. Lavergne, "Prospecting for ground-water by Induced Effect Polarisation," Geophysics, Vol. 22, No.3, pp. 660-687, 1957.

[48] H. W. Oslen, "Hydraulic Flow Through Saturated Clays," Clays and Clay Minerals, Vol. 9, No. 1, pp. 131-161, 1960

[49] J. K. Mitchell and K. Arulanandan, "Electrical Dispersion in Relation to Soil Structure," Journal of Soil Mechanics and Foundations Division, Vol. 99, No. 12, pp. 1113 -1133, 1973.

[50] T. R. Madden and D. J. Marshall, "Induced Polarisation - A Study of its Causes and Magnitudes in Geological Materials," U.S. Atomic Energy Commission Report, RME-3160, 80, 1959.

[51] W. Juda and W. A. McRae, "Ion Exchange Material and Method of Making and Using the Same", US patent 2,636,851, 1953.

[52] K. S. Spiegler and K. Arulanandan, "Radio Frequency Measurements of Ion Exchange Membranes," Research and Development Report No. 353, U.S. Government Printing Office, Washington D.C., Report to office of Saline Water, U.S. Department of the Interior, Washington D.C., 1968.

[53] S. B. Sachs and K. S. Spiegler, "Radio Frequency Measurements of Porous Conductive Plugs. Ion-Exchange Resin-Solution Systems," Journal of Physical Chemistry, Vol. 68, No. 5, pp. 1214-1222, 1964.

[54] H. P. Schwan, G. Schwarz, J. Maczuk, H. Pauly, "On the Low Frequency Dielectric Dispersion of Colloidal Particles in Electrolyte Solutions," Journal of Physical Chemistry, Vol. 66, No.12, pp.2626-2635, 1962.

[55] G. R. Olhoeft, "Low Frequency Electrical Properties," Geophysics, Vol. 50, No.12, pp. 2492-2503, 1985.

[56] M. Brooks, P. Kaerey, Ian Hill "An Introduction to Geophysical Exploration", 3rd Edition, Wiley-Blackwell Publishing, 2002, ISBN: 978-0-632-04929-5.

[57] H. P. Schwan, "Alternating Current Electrode Polarisation," Biophysik, Vol. 3, No.2, pp. 181-201, 1966.

[58] H. P. Schwan, "Linear and Non Linear Electrode Polarisation and Bilogical Materials," Annals of Biomedical Engineering, Vol. 20, No.3, pp. 269-288, 1992.

[59] T. Ragheb and L. A. Geddes, "The Polarisation Impedance of Common Electrode Metals Operated at Low Current Density," Annals of Biomedical Engineering, vol. 19, No.2, pp. 151-163, 1991.

[60] H. H. Sun and B. Onaral, "A Unified Approach to Represent Metal Electrode Polarization," IEEE Transactions on Biomedical Engineering, Vol. BME-30, No.7, pp. 399-406, 1983.

[61] T, Katsube, R. Ahrens, L. Collett, “Electrical Nonlinear Phenomenon in Rocks”, Geophysics, Vol. 38, No. 1, pp. 106-124, 1973.

[62] Ragheb and Geddes, “Electrical Properties of Metallic Electrodes”, Medical and Biological Engineering and Computing, Vol.28, No.2, pp.182-186, 1990.

[63] R.D. Southey and F.P. Dawalibi, “Improving the reliability of power systems with more accurate grounding system resistance estimates”, IEEE International Conference on Power System Technology, Vol. 1, pp. 98-105, Kumning, China, 2002

[64] K. Arulanandan, "Hydraulic and Electrical Flows in Clays," Clays and Clay Minerals, vol. 17, No.2, pp. 63-76, 1969.

[65] V. Vacquier, C. R. Holmes, P. R. Kitzinger, and M. Lavergne, "Prospecting for ground-water by Induced Effect Polarisation," Geophysics, Vol. 22, No.3, pp. 660-687, 1957.

[66] Harid N, Griffiths H, Haddad A, Walker K, "Soil Resistivity Mapping of Non-Homogeneous Soils", 13th International Symposium on High Voltage Engineering, pp. 554, Paper P.03.31 Delft, Holland, 2003.

[67] The CDEGS software package (Current Distribution, Electromagnetic Fields, Grounding and Soil Structure Analysis), Integrated Software for Power System Grounding/Earthing, Electromagnetic Fields and Electromagnetic Interference Safe Engineering Services & Technologies Ltd. Canada

[68] Leonid Grcev and Marjan Popov, "On High-Frequency Circuit Equivalents of a Vertical Ground Rod", IEEE Transactions on Power Delivery, Vol. 20, No. 2, pp. 1598-1603, 2005

[69] CIGRE Working Group C4.2.02: 'Methods for measuring the earth resistance of transmission line towers equipped with earth wires', CIGRE Publication, 2005.

Appendix A1

A1.1 Specifications of the voltage transducers

The specifications of the voltage transducers used during the measurement of earthing impedance are given in TableA1.1 and Table A1.2

Table A1.1 Technical specifications of SI 9000

Technische Daten

Eingangsbereiche 1:20 1:200	 70VDC / 50Vrms 700VDC / 500Vrms
Maximale Eingangsspannung 1:20 1:200	 1000VDC / 700Vrms 1000VDC / 700Vrms
Eingang impedanz Empfindlichkeit Genauigkeit Bandbreite isolationsspannung	 2MOhm / 2.5pF (7-9pF mit Kabel) symmetrisch differentiell, beidseitig gegen Masse 100mV for 1:20 Abschwächung 2% DC bis 25MHz 4000Veff 1min
Gleichtakt Eingang Gleichtaktunterdrückung	max. 500Vrms 50Hz -80dB 1kHz -70dB 100kHz -59dB 1MHz -47dB
Anstiegszeit 1:20 1:200	 24ns 24ns
Ausgang maximale Ausgangsspannung Ausgangsoffset	 massebezogen, Standard BNC-Anschluss + 3.5V (ab dieser Grenze tritt Verzerrung auf) < ± 5mV bei -10°C .. +45°C
Versorgung	4 St. 1.5V oder 1.25V Baterien Größe AA or UM-3 or power adaptor 6 VDC/50 mA
Arbeitstemperaturbereich	-10°C .. +40°C
Abmessungen Höhe Länge Breite Kabellänge Masse	 20mm (0.8") 170mm (6.7") 63mm (2.5") 90cm (35") 270g

Table A1.2 Technical specifications of DP25

Differential Voltage: 1,300 V (AC peak to peak + DC) max.
Input Voltage to ground: 600 Vrms max.
Attenuation: x20, x50, x200
Bandwidth: DC to 25 MHz @ -3db DC to 15 Mhz (X20)
Accuracy: 2%
Input R: 4 MΩ
Input C: 1.2 pF
Common Mode Rejection Ratio (CMRR): 60 Hz: > 90 dB 100 Hz: > 60 dB 1 MHz: > 50 dB
Noise: ≤ 2 mVrms, ≤ 4 mVrms @ x20
Rise Time: x200, x50: 14 ns x20: 23.4 ns

A1.2 Specifications of the current transducers

The specifications of the current transducers used during the measurement of earthing impedance are described in the following sections. The specifications of the current transducers are shown in the Table A1.3 and Table A1.4

A1.2.1 LILCO BROADBAND CURRENT TRANSFORMER

These current transformers are designed for use as general laboratory instruments where band width and high-frequency response are to be combined with ease of use.

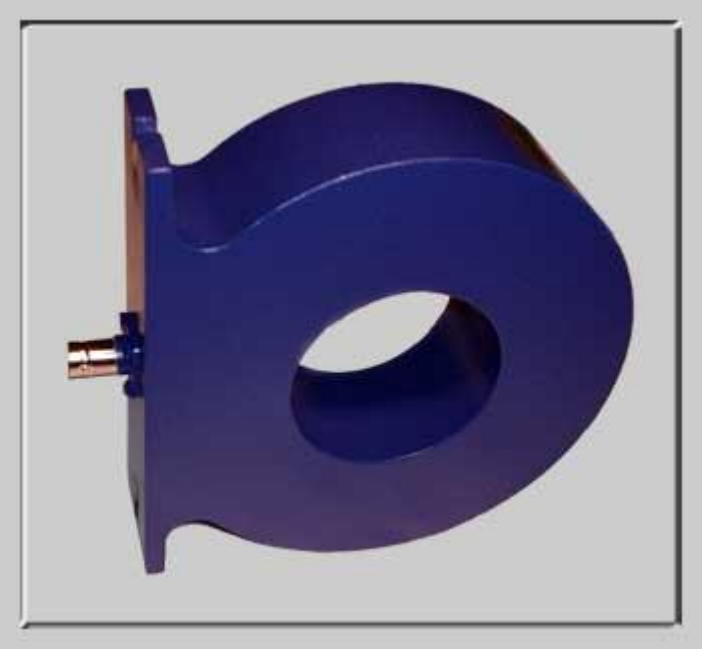

Model 58MH100

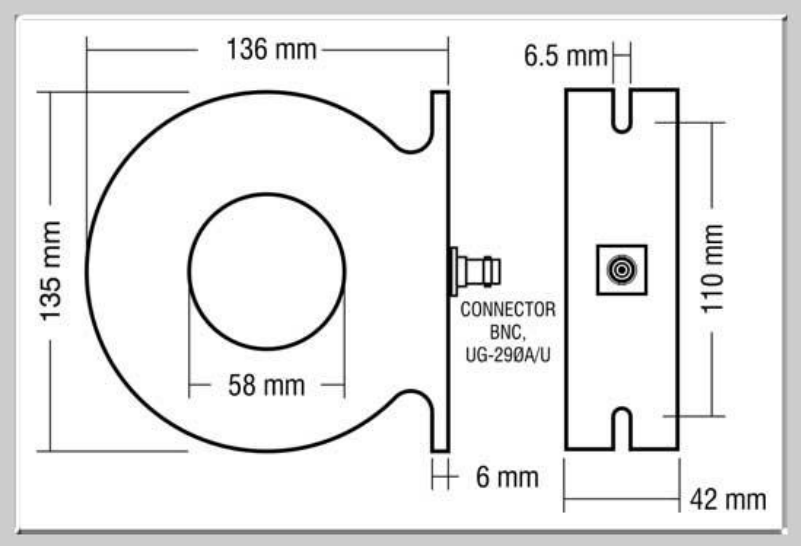

Dimensional Details of LILCO Current Transformer Model 58MH100

Table A1.3 Specifications of LILCO current transformer

Model number	Output V/A(1)	RECTANGULAR PULSE				SINEWAVE			DC saturation current Isat A	Max. rms current Irms A	Peak current Ipeak A
		Droop %/ms	Rise time ns	I-t Capability		3dB Bandwidth		Ipeak/f A/Hz			
				No bias mA s	With bias mA s	lf Hz	hf MHz				
58MH100	0.10	1	20	300	500	1.5	20	2.0	2.0	100	5000

NOTES:

Source impedance - All models have a source impedance of 50R

Load impedance - In the above tables this is assumed to be >50k

50R load - With a 50R load I-t capability is increased by between 20% and 80% and droop and lf cut-off point are reduced by a factor of 0.6 to 0.85. A 50R load at the receiver and a 50R line should be used where long cables are employed or where the highest frequency response is required.

Output – Accuracy +/-0.5% at mid-log frequency point, +/-2% within one decade of 3dB cut-off points. The use of a 50R load will halve the sensitivity

I-t No bias – Lilco broadband current transformers do not require the application any biasing current to achieve this level of I-t. The use of a 50R load will enhance the I-t capability significantly.

I-t with bias – these levels are achieved with a dc off-set current equal to Isat. The use of a 50R load will enhance the I-t capability further

58M0020 and 58D0020 – these broadband current transformers have been introduced to satisfy the measurement demands of EN61000-4-11

A1.2.2 Stangenes Pulse Current Transformer

These current transformers were mainly used for accurately measuring fast impulse currents. The placement of conductor carrying fast impulse currents in the centre of the axis of the core was maintained during measurements.

Stangenes Pulse Current Transformer

Table A1.4 Specifications of Stangenes current transformer

Model No.	Output (volt/amp) Accuracy ±0.5%	Inner Diameter (inches)	Max. Current (amperes) Peak	Max. Current (amperes) Rms	Square Pulse Rise Time (nanosec)	Square Pulse Droop (%/µsec)	Square Pulse IT max. (amp.sec)
3-0.1A	0.1	2.87	5 k	30	20	0.015	0.03